

Lingjun Li

Simulation and Control of Servo Hydraulic Actuators for Test Applications

Doctor's Thesis

Graz University of Technology

Institute of Electronics

Head: Univ.-Prof. Dipl.-Ing. Dr.techn. Bernd Deutschmann

Supervisor: Univ.-Prof. Dipl.-Ing. Dr.techn. Wolfgang Pribyl

Co-Supervisor: Ass.Prof. Dipl.-Ing. Dr.techn. Bernd Eichberger

Co-Supervisor: Dipl.-Ing. Dr.techn. Thomas Thurner

Graz, February 2015

Statutory Declaration

I declare that I have authored this thesis independently, that I have not used other than the declared sources/resources, and that I have explicitly marked all material which has been quoted either literally or by content from the used sources.

Graz, _____
Date Signature

Eidesstattliche Erklärung¹

Ich erkläre an Eides statt, dass ich die vorliegende Arbeit selbstständig verfasst, andere als die angegebenen Quellen/Hilfsmittel nicht benutzt, und die den benutzten Quellen wörtlich und inhaltlich entnommene Stellen als solche kenntlich gemacht habe.

Graz, am _____
Datum Unterschrift

¹Beschluss der Curricula-Kommission für Bachelor-, Master- und Diplomstudien vom 10.11.2008; Genehmigung des Senates am 1.12.2008

Abstract

A common problem encountered in mechanical engineering is the fatigue failure of mechanical components hence fatigue lifetime assessment of mechanical components becomes one of the research hotspots in mechanical engineering at present. Fatigue test is one of the most effective methods to validate fatigue lifetime of mechanical components. Test rigs with electro-hydraulic servo control system are the commonly used loading system for such fatigue tests. This dissertation focuses on research of solutions for some practical dominant problems related to robust and accurate control of electro-hydraulic servo systems.

Firstly a novel system modeling and identification method for electro-hydraulic servo systems is proposed so as to obtain accurate models of electro-hydraulic servo systems which are essential for controller design and system simulation. The effectiveness of the developed methods is verified by experimental results.

Secondly the exact linearization method based on differential geometry is applied in electro-hydraulic servo position control systems. Since the traditional approximate linearization method based on Taylor expansion is commonly used in engineering, performance of the two linearization methods is compared and discussed. Furthermore robustness of the control system based on the exact linearization method is discussed. Additionally on the basis of exact linearization a sliding mode variable structure control method is proposed to effectively attenuate disturbances within the control loop.

Finally many fatigue test applications are based on cyclic loading of sinusoidal signal or arbitrary functions. In those cases the method of iterative learning control can be utilized as an effective tool to obtain and ensure

accurate and robust control performance of such fatigue test systems. Consequently three types of iterative learning control methods are investigated for fatigue test applications throughout this dissertation, including the discussion on the convergence conditions of these methods. The control performance of the three iterative learning control methods in uni-axial fatigue test applications is compared and discussed with respect to robustness and control accuracy.

Simulation and experimental results indicate that the developed methodology can greatly improve the quality of fatigue tests with respect to load application and reproducibility.

Acknowledgements

I am grateful to all of my friends and colleagues who give me support and help within my doctoral study at Graz University of Technology.

Firstly I would like to express my highest appreciation and deepest gratitude to my supervisors, Dr. Thomas Thurner, Ass.Prof. Bernd Eichberger and Prof. Wolfgang Pribyl. During my doctoral study they continuously give me guidance and support. Their patience, encouragement, as well as their insightful comments help me make this a much better dissertation. They are excellent scientific researchers and will undoubtedly be the models that I should follow in my future research.

Secondly I would also like to thank all the previous and current colleagues in our laboratory throughout the past five years for their kind help in many aspects: language, life, experiment and research. I completely enjoy and greatly benefit from the communication, interaction and cooperation with them.

Finally I would like to dedicate this work to my parents. Without their continued love, encouragement and support I would never have been able to complete this dissertation.

Contents

1. Introduction	1
1.1. Background and Motivation	1
1.2. Objectives	5
1.3. Outline	6
2. Literature Review	9
2.1. Control Strategies of SISO System	9
2.1.1. Classical Control Strategy	10
2.1.2. Modern Control Strategy	10
2.1.3. Intelligent Control Strategy	15
2.1.4. Advanced Intelligent Compound Control Strategy	17
2.2. Control Strategies of MIMO System	17
2.2.1. Classical Decoupling Control Strategy	20
2.2.2. Modern Decoupling Control Strategy	21
2.2.3. Intelligent Decoupling Control	24
2.2.4. Intelligent Compound Decoupling Control	25
2.3. Control Strategies of Commercial Products	27
2.3.1. Null Pacing	27
2.3.2. Peak Valley Control	28
2.3.3. Amplitude Phase Control	29
2.3.4. Adaptive Inverse Control	29
2.3.5. Arbitrary End Level Control	30
2.3.6. Peak Valley Phase Control	31
2.3.7. Motion Isolated Load Control	32
2.3.8. Modal Control	33
2.3.9. High Order Control	33
2.3.10. Delta-P Gain Control	33
2.3.11. New Types of PID Control	34

Contents

3. System Modeling and Identification	37
3.1. System Modeling	39
3.1.1. Modeling of Cylinder	39
3.1.2. Modeling of Friction	48
3.1.3. Modeling of Servo Valve	48
3.1.4. Modeling of Position Sensor	49
3.1.5. Overall Model of the Electro-Hydraulic Servo Position Control System	49
3.2. System Identification	50
3.2.1. Experimental System Description	50
3.2.2. Design of Reference Signal	52
3.2.3. Parameter Identification with Matlab	53
3.2.4. Results Analysis	53
3.3. Summary	60
4. Exact Linearization Theory	61
4.1. Introduction	61
4.2. Literature Review of Nonlinear Control Theory	62
4.2.1. The Nonlinearity and Existing Processing Methods of Electro-Hydraulic Servo System	62
4.2.2. The Differential Geometric Control Theory of Nonlinear System	63
4.2.3. Disturbance Decoupling and Attenuation	66
4.3. Basic Conceptions of Nonlinear Control Theory	68
4.3.1. Nonlinear Coordinate Transformation and Differential Homeomorphism	68
4.3.2. Affine Nonlinear System	69
4.3.3. Vector Field	70
4.3.4. Induced Function of Vector Field	71
4.3.5. Lie Derivative and Lie Bracket	72
4.3.6. Distribution and Involution of Vector Field	75
4.3.7. Relative Degree of Nonlinear System	77
4.3.8. Normal Form of Linearization of Nonlinear System	77
4.4. Design Principles of Nonlinear Controller	79
4.4.1. Exact Linearization via State Feedback	79
4.4.2. Design Principles and Methods Based on Zero Dynamics	82

4.5.	Disturbance Decoupling and Attenuation	89
4.5.1.	Disturbance Decoupling	89
4.5.2.	Disturbance Attenuation	91
4.6.	Summary	96
5.	Design and Simulation of Control System Based on Exact Linearization	99
5.1.	Feasibility of Application of Exact Linearization via State Feedback in Electro-Hydraulic Servo System	100
5.2.	Building the Nonlinear Model	100
5.3.	Simplified Nonlinear Model	102
5.4.	Exact Linearization via State Feedback	103
5.5.	Comparison between Exact Linearization and Approximate Linearization	106
5.5.1.	Introduction	106
5.5.2.	Simulation and Comparison	107
5.6.	Robustness Analysis of the Control System	113
5.6.1.	Presentation of Robustness Problem	113
5.6.2.	Robustness of Electro-Hydraulic Servo System under Nonlinear Control	113
5.7.	Disturbance Decoupling and Attenuation	118
5.7.1.	Disturbance Decoupling	118
5.7.2.	Disturbance Attenuation	120
5.8.	Summary	124
6.	Iterative Learning Control Theory	127
6.1.	Introduction	127
6.1.1.	Background and Motivation	127
6.1.2.	Mathematical Description of ILC	129
6.2.	Literature Review of Iterative Learning Control Theory	131
6.2.1.	Algorithms	132
6.2.2.	Convergence Speed	139
6.2.3.	Initial State	140
6.2.4.	Analysis Methods	141
6.2.5.	Applications	142
6.3.	PID-Type ILC Based on Frequency Domain Filtering	144
6.3.1.	PID-Type ILC	144

Contents

6.3.2.	Convergence Analysis	145
6.3.3.	Frequency Domain Filtering	155
6.4.	Adaptive ILC	157
6.4.1.	Algorithm Description	157
6.4.2.	Convergence Analysis	160
6.5.	Inverse Model ILC	163
6.5.1.	Algorithm Description	163
6.5.2.	Convergence Analysis	165
6.6.	Summary	167
7.	Simulation and Experimental Research on Iterative Learning Control	169
7.1.	Simulation of SISO Electro-Hydraulic Servo Position Control System	170
7.1.1.	Simulation of P-Type ILC Algorithm	172
7.1.2.	Simulation of Adaptive ILC Algorithm	174
7.1.3.	Simulation of Inverse Model ILC Algorithm	177
7.2.	Experiment of SISO Electro-Hydraulic Servo Position Control System	181
7.2.1.	Experiment of P-Type ILC Algorithm	185
7.2.2.	Experiment of Adaptive ILC Algorithm	188
7.2.3.	Experiment of Inverse Model ILC Algorithm	191
7.3.	Experiment of SISO Electro-Hydraulic Servo Force Control System	196
7.3.1.	Experiment of P-Type ILC Algorithm	198
7.3.2.	Experiment of Adaptive ILC Algorithm	201
7.4.	Summary	203
8.	Conclusion and Prospect	205
8.1.	Conclusion	205
8.2.	Prospect	207
	Bibliography	209
A.	Experimental Results of P-Type ILC Algorithm with Random Signal	233

B. Experimental Results of Adaptive ILC Algorithm with Random Signal	237
C. Experimental Results of Inverse Model ILC Algorithm with Random Signal	241

1. Introduction

1.1. Background and Motivation

In mechanical engineering, a lot of mechanical components work under cyclic loading and, generally speaking, the working stress is less than the yield stress of the materials. The failure of the components, after long time operation under cyclic loading, is called fatigue failure.

Fatigue failure is the main form of premature failure of mechanical parts. According to statistics, 80% of the fracture failure of mechanical parts is fatigue fracture [1]. Since many mechanical parts have to work under severe working conditions of high temperature, high pressure, high friction, heavy load and corrosion, fatigue failure accidents emerge in endlessly. Consequently it is necessary to research on the fatigue strength and fatigue design of mechanical parts so as to improve the reliability and prolong the working life of mechanical products. At present fatigue test is one of the effective methods to validate fatigue lifetime of mechanical components.

At first researchers and engineers apply general material testing machines to complete fatigue test. Nevertheless with the development and wide application of material technology and fatigue theory, general material testing machines can not meet the requirements, therefore professional fatigue testing machines appeared. There are several types of professional fatigue testing machines. The earliest professional fatigue testing machines were mechanical ones, of which load was less than 1 kN and frequency was less than 10 Hz. With the development of electric and electronic technology, electrodynamic fatigue testing machines and electro-hydraulic fatigue testing machines appeared. Due to the different principles, the three types of fatigue testing machines have different properties. Table 1.1 introduces the main properties of the three fatigue testing machines.

1. Introduction

According to the table, it is clear that mechanical fatigue testing machines have many disadvantages such as limited maximum force, complex structure and so on. Moreover mechanical fatigue testing machines are not programmable, hence the computer technology can not be applied. Furthermore it is impossible to change the mechanical fatigue testing machines to meet the different requirements when they are manufactured. Consequently the application of mechanical fatigue testing machines is much less than before. However electro-hydraulic fatigue testing machines do not have such problems. The maximum force of electro-hydraulic fatigue testing machines is the biggest of all the three types of fatigue testing machines. Electro-hydraulic fatigue testing machines can work in both low frequency range with long stroke and high frequency range with short stroke. Furthermore the waveforms of electro-hydraulic fatigue testing machines can be modified by computer so as to realize automatic control. Moreover engineers can use several cylinders to realize parallel operation when higher force is required since electro-hydraulic fatigue testing machines have the properties of small volume and compact structure. Although the frequency range of electro-hydraulic fatigue testing machines is less wide than that of electrodynamic fatigue testing machines and waveform distortion of electro-hydraulic fatigue testing machines is more serious than that of electrodynamic fatigue testing machines, electro-hydraulic fatigue testing machines have broader applications than the other two types because the performance-price ratio of electro-hydraulic ones is higher.

Electro-hydraulic fatigue testing machine is a technology intensive system and it is relevant to hydraulics, electronics, surveying, mechanical engineering, material science and automatic control theory. Furthermore many high technologies such as closed-loop servo control, digital display, electromechanical integration and computer technology are applied in electro-hydraulic fatigue testing machines which play an important role in the field of industry and scientific research, for instance development of new material, structural design, mechanical design, ship design and research on aeronautic and astronautic technology. Electro-hydraulic fatigue testing machines can be divided into two types: static fatigue testing machines and dynamic fatigue testing machines.

1.1. Background and Motivation

Table 1.1.: Comparison of Three Types of Fatigue Testing Benches

	Mechanical	Electrodynamic	Electro-Hydraulic
Maximum Force	Small	Middle	Big
Maximum Displacement	Small	Middle	Big
Frequency Range	Narrow	Wide	Wide
Waveforms	Sinusoidal	Sinusoidal and Random	Sinusoidal, Triangular and Random
Waveform Distortion	Big	Small	Small
Programmable	No	Yes	Yes
Parameters Controllable	Displacement	Displacement, Speed and Acceleration	Displacement, Speed and Acceleration
Precision	Low	High	High
Performance-Price Ratio	Low	Middle	High

1. Introduction

The static fatigue testing machines use servo technology and can complete different tests by modifying several parameters. They can acquire, process, display and print test data and results automatically so as to decrease working strength and improve testing efficiency. They can realize static stretch test, static compress test, static bending test, static creep test, low cycle fatigue test and so on.

The dynamic fatigue testing machines are servo mechanisms composed of mechanical, hydraulic and electronic systems. They use closed-loop control rather than open-loop control so as to improve test precision. They can apply many types of signals such as sinusoidal, triangular, rectangular, sawtooth and trapezoidal signals to the specimen. Moreover they can apply alternating random load to the specimen according to the alternating load spectrum which is recorded in real world. Consequently the test results can reflect the real working condition so as to provide basis for optimal design. Now all the important project has to be tested by fatigue testing machines or no one can ensure the safety of the project design.

Furthermore according to different hydraulic control components, electro-hydraulic servo system can be divided into pump-controlled system and valve-controlled system. Moreover according to different hydraulic valves, valve-controlled system can be divided into servo valve-controlled system, proportional valve-controlled system and so on. Additionally according to different hydraulic actuators, servo valve-controlled system can be divided into cylinder system and motor system. In our laboratory the servo valve-controlled cylinder system is applied as the core component of electro-hydraulic fatigue testing system hence this dissertation focuses on solutions for some practical control problems of this kind of electro-hydraulic servo system.

The characteristics of modern electro-hydraulic servo systems are briefly described in the following [2]:

- The environment and task of electro-hydraulic servo systems is complicated, for example the parameters are time varying and the disturbances always exist.
- The electro-hydraulic servo systems have high requirements on the frequency range and test precision.

1.2. Objectives

- The influence of nonlinearity caused by throttle characteristics and flow saturation of electro-hydraulic servo valves becomes more and more serious since the requirements of the fatigue test increase.
- The stability theorems and controller design methods based on traditional discrete system theory are less useful than before because of the nonlinear sampling characteristics of many digital electro-hydraulic components.

Consequently modern electro-hydraulic servo systems have new requirements on the control strategies, some of which are [2]:

- The control strategies should improve the dynamic characteristics of the servo systems as greatly as possible under the premise of ensuring steady precision so that the controller can control the objects as fast as possible without overshoot.
- The control system should have excellent robustness to eliminate effects of parameters variation, external disturbances, cross coupling and other nonlinear factors.
- The control system should have excellent intelligence.
- The control algorithm should be as simple as possible and the function of real-time control should be as powerful as possible.
- The maximum control variable provided by controller should give full play to maximum driving capability of the power mechanism so as to improve the efficiency of the electro-hydraulic servo system.

In a word, there are a lot of influencing factors in electro-hydraulic servo systems such as strong nonlinearity, time-varying parameters, external disturbances and cross coupling which affect control performances of the systems. Therefore carrying out research on improving control performances of electro-hydraulic servo system is of significance for popularization and application of modern electro-hydraulic servo system.

1.2. Objectives

With the development of electro-hydraulic servo control technology, the application fields and ranges of electro-hydraulic servo control system are

1. Introduction

expanding constantly. However because of the high demands for modern product research and development, the requirements on electro-hydraulic fatigue testing system regarding control performance become higher and higher i.e. electro-hydraulic servo control system should operate with high control precision, strong robustness and good stability.

To realize this control target, researchers have to solve a lot of practical control problems such as accurate system modeling and identification, dealing with nonlinear factors, eliminating or attenuating effects of external disturbance, compensating time delay, decoupling and so on. Consequently in this dissertation three of these practical control problems are considered: accurate system modeling and identification, dealing with nonlinear factors and improving control precision. The specific goal of this dissertation is to research and develop solutions which are effective and feasible in practical engineering aiming at the three control problems so that electro-hydraulic servo control system can obtain optimal control performances with the valid boundary conditions of the given problems.

1.3. Outline

This dissertation focuses on solutions for some practical problems which influence the control precision of electro-hydraulic servo system. The research conducted for this work includes system modeling, system identification, exact linearization and iterative learning control.

In Chapter 2 the development of control strategies and algorithms for electro-hydraulic servo control system is reviewed.

In Chapter 3 based on the analysis of valve-controlled cylinder system, a novel system modeling method for electro-hydraulic servo position control system is presented. And then a novel system identification method is proposed to estimate the unknown parameters of the model. Finally system identification experiment is made in order to verify the effectiveness of the system modeling and identification methods.

In Chapter 4 firstly development of nonlinear control theory is introduced. Then the theory and method of the exact linearization based on differential

geometry is discussed. Finally the methods of disturbance decoupling and attenuation based on exact linearization are presented.

The application of the exact linearization method based on differential geometry in electro-hydraulic servo position control system is introduced in Chapter 5. Moreover control effects of the exact linearization method and the approximate linearization method based on Taylor expansion are compared with simulation. Additionally robustness of the control system based on exact linearization method is analyzed. Finally the methods of disturbance decoupling and attenuation are applied in electro-hydraulic servo position control system.

In Chapter 6 firstly development of iterative learning control (ILC) theory is reviewed. Then three types of iterative learning control methods are proposed: PID-type ILC, adaptive ILC and inverse model ILC. Their algorithms are introduced and their convergence conditions are discussed respectively.

The purpose of Chapter 7 is to verify the effectiveness of the three types of iterative learning control algorithms. Firstly the control effects of the three ILC algorithms in electro-hydraulic servo position control system are compared and discussed with simulation results. And then their control effects in electro-hydraulic servo position control system are further compared and discussed with experimental results. Furthermore the P-type ILC algorithm and the adaptive ILC algorithm are applied in real world electro-hydraulic servo force control system respectively to validate their control performances in force control system.

Finally conclusions are presented in Chapter 8. Moreover prospects of future work in these important research fields related to electro-hydraulic servo control system are also discussed.

1. Introduction

2. Literature Review

Electro-hydraulic servo systems can be divided into two types: single-input-single-output (SISO) systems and multi-input-multi-output (MIMO) systems. Generally speaking MIMO system is composed of several SISO systems hence MIMO system is much more complex than SISO system. The development situation of control strategies of SISO and MIMO system will be described respectively in the following. Additionally since this dissertation focuses on servo valve-controlled cylinder system, only the literatures related to this kind of electro-hydraulic servo system will be reviewed.

2.1. Control Strategies of SISO System

As far as the historical path of the research and development of electro-hydraulic servo system is concerned, the control strategies of SISO systems can be classified into four types:

- Classical control strategy (including PID control and improved PID control, linear controller and so on)
- Modern control strategy (state feedback control, nonlinear control, adaptive control, variable structure control, H_2/H_∞ robust control and so on)
- Intelligent control strategy (neural control, fuzzy control, learning control and so on)
- Advanced intelligent compound control strategy (neural fuzzy control, sliding mode variable structure control, adaptive learning control, fuzzy PID control based on evolutionary algorithm and so on)

The development of the four types of control strategies of SISO systems will be introduced in the next subsections.

2. Literature Review

2.1.1. Classical Control Strategy

In [3] Murrenhoff uses the integrated electronic technology to linearize the nonlinear valve so as to eliminate the influences of nonlinearity of flow pressure characteristics. For hydraulic servo force and torque control system, he applies force feedback and speed feedback proportional controller and obtains satisfying results of torque control. For hydraulic servo position and speed control system, he uses PID control or state feedback control and achieves good transient performance of the system.

2.1.2. Modern Control Strategy

(1) State Feedback Control

In [4], Mare and Moulaire provide the selection principles of feedback controller of electro-hydraulic servo position control system. They ignore the dynamic characteristics of the servo valve but consider the effects of nonlinear factors.

In [5], Guglielmino and Edge use a special state feedback to design the friction damping controller for the semi-active vehicle suspension system.

(2) Nonlinear Control

The disadvantages of linear control strategies of valve-controlled hydraulic position control servo system expose day by day [6]. In [7], they solve the control problem of high precision Hydraulic Die-Casting System successfully with the switch control technology. The results show that when the Die-Casting tool is close to the goal position, switch function is necessary in traditional PI controller to eliminate the negative influences of the integral action in the whole process. Furthermore the results reveal that the optimal switch point is relevant to the load pressure.

To improve the static and dynamic characteristics of position tracking of electro-hydraulic servo system, in [8, 9] they apply the switch control strategy which is switching between position control loop and speed control loop based on the actual position error as shown in Figure 2.1. In this control strategy position tracking error will be feedback to the speed control

2.1. Control Strategies of SISO System

loop so as to improve the position tracking precision. The results show that this nonlinear switch control strategy has excellent robustness against inertia load changes.

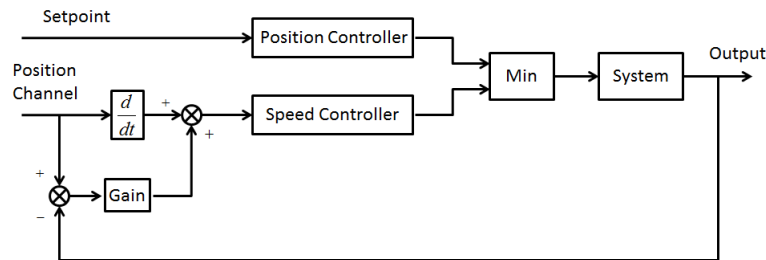


Figure 2.1.: Switch Control System based on Speed Control Loop and Position Control Loop [8, 9]

To eliminate the influences of dead zone and throttle characteristics of servo valves, in [10] a nonlinear compensation technology is proposed by Maekinen and Virvalo. The effectiveness of this technology in water hydraulic system is confirmed by the experiments. Meanwhile in [11] Whiting uses the control strategy of valve pressure/flow compensation based on local feedback. Moreover the research on the control strategies of compensation for the nonlinear characteristics of valve pressure/flow have gotten progress [12].

In [13] Garstenauer and Kurz apply the gain tuning technology of combination form of gain weight based on actual valve position in the nonlinear control of electro-hydraulic servo valve.

In [6] a nonlinear control strategy based on singular perturbation is proposed and applied in the hydraulic servodrives successfully by Manhartsgruber and Scheidl. The dynamic characteristics of the nonlinear control is better than the traditional linear control.

In [14] Alleyne solves the problem of force tracking control for hydraulic servo systems with nonlinear control strategy which has good robustness against some model errors.

2. Literature Review

(3) Adaptive Control

In [15] Edge introduces the conception of adaptive control of hydraulic servo system. The adaptive control of hydraulic servo system have two types: one is self-regulation adaptive control and the other is (direct or indirect) model reference adaptive control (MRAC).

In [16] they research the adaptive control of hydraulic servo system which is a non-minimum phase system. They use δ transform method to discretize the system. The advantage is that if the continuous system of a controlled plant is a minimum phase system then its discrete system which is gotten with δ transform method is still a minimum phase system as long as the sampling period is sufficiently small. Consequently the adaptive control theory can be applied in the hydraulic servo system directly.

In [17] Zhang and Alleyne design an indirect model reference adaptive controller for the valve-controlled servo cylinder of the active vibration isolation system to realize high performance speed tracking.

In [18] they design a model reference adaptive controller for the hydraulic excavators and the results show that this controller is better than the state feedback controller.

(4) Variable Structure Control

Utkin firstly proposed variable structure control (VSC) strategy in 1950s [19]. After 50 years development great attention has been paid to VSC. VSC is suitable for linear and nonlinear system, continuous and discrete system, deterministic and uncertain system, lumped parameter and distributed parameter system, centralized control and decentralized control system and so on. VSC is a control strategy which changes the structure of the controller according to the system state and sliding mode deviations in order to improve the performance of the system [20]. One of the advantages of VSC is that the sliding mode of VSC can keep invariant to the parameter perturbation of the system and external disturbances however this advantage is based on ideal switching condition while in real system ideal switching condition can not be realized because of the inertia of controlled object and constraint of control energy hence chattering problem of VSC always exists. Nevertheless VSC has been widely applied in electro-hydraulic servo systems.

2.1. Control Strategies of SISO System

In [21, 22] the sliding mode control of electro-hydraulic servo position control system is investigated by Handroos and Liu. They introduce the chattering problem of VSC and try to use sliding surfaces which have boundary layers to weaken chattering effects while at the expenses of the loss of system robustness.

In [23] they apply online estimator of load inertia and gaining regulator to solve the steady-state chattering problem of variable structure control of electro-hydraulic servo system. The results show that the robustness of the system can be strengthened as long as the parameters of the controller can vary with the inertia estimated.

In [24] a frequency-shaped sliding mode control based on the crossover frequency of systems with unmodeled dynamics is proposed. The principle is to use low-pass filter in the driving signal of electro-hydraulic servo systems. However this method will lead to the loss of robustness against the steady-state disturbance consequently disturbance observer is necessary to compensate it.

In [25] a variable structure control with proportional and integral compensation for electro-hydraulic servo position control system is proposed and the results show that the response speed of variable structure control with proportional and integral compensation is faster than that of variable structure control only with integral compensation. Moreover one of the advantages of VSC with proportional and integral compensation is that the system has zero steady state error under external disturbance.

Considering the influence of friction on electro-hydraulic servo position control systems, in [26] they design a sliding mode controller which has the function of nonlinear friction compensation. The principle is to use adaptive estimation of friction however they do not consider external load. The test results show that the system has good performance on friction estimation and signal tracking. Furthermore this sliding mode controller with the function of nonlinear friction compensation is applied in a low-pressure water hydraulic cylinder system and the effectiveness of sliding mode control strategy is confirmed by the test results [27].

Aiming at typical problems of variable structure control of electro-hydraulic servo systems such as chattering problem, reaching condition and reaching

2. Literature Review

law, in [28] they complete some research both in continuous and discrete time domain. They consider Slotine's boundary layer method [29], Gao's reaching law method [20, 30] and Feng's continuous integral approximation [31] comprehensively and then illustrate the contradiction between decreasing chattering and improving robustness. Moreover several new types of variable structure control strategies are proposed. They complete experimental study on variable structure control strategy with integral compensation in pump controlled hydraulic motor rotating speed system and the conclusion of theoretical analysis is verified.

To solve the tracking problems of electro-hydraulic servo systems with non-linearity and uncertainty, in [32] a second-order sliding mode control strategy based on time optimal law and Lyapunov function is proposed by Li, Yang and Zhang. They analyze the existing optimal second-order sliding mode control strategies and then an improved second-order sliding mode control algorithm with nearly time-optimal control is developed to effectively reduce chattering and enhance responding speed without losing robustness of the system. Taking the steering system model of practical transporting and lifting machinery as example, the simulation study on the algorithm is carried out, and its effectiveness is confirmed.

In [33] an optimal variable structure control with integral compensation is proposed. They use linear quadratic optimal control to determine the sliding mode switching plane however there is no quantitative relationship between weighting matrix and system performance index hence the switching plane achieved is not always ideal. Nevertheless this problem can be solved if proper pole assignment method is applied.

(5) H_2/H_∞ Robust Control

Robust control has important value in improving the robustness of electro-hydraulic servo systems. In [15] Edge researches the basic robust control problems of electro-hydraulic servo systems.

In [34] Sanada designs a force controller for a water-hydraulic servo system with robust control principle. He considers the influences of load stiffness, bulk modulus of the oil and flow characteristics of valves thus solves the parameter uncertain problem of hydraulic system nevertheless it is difficult

2.1. Control Strategies of SISO System

to determine the upper bound and lower bound of the uncertain parameters in system identification.

In [35] they develop a new type robust control for electro-hydraulic servo systems and then they compare the control results with that of traditional PID control. This control strategy can ensure the stability of the system and robustness against the variation of load stiffness and nonlinear friction.

In [36] Plummer expounds that the main factors which influence the robustness of electro-hydraulic servo systems are saturation limiting of various physical quantities, one of which is the saturation limiting of servo valve opening. To ensure the asymptotic stability of the system he then develops the evaluation theory of robustness of electro-hydraulic servo systems which have the saturation limiting of servo valve opening and moreover he proposes a new type of design method which can eliminate the effects of the saturation limiting of servo valve opening.

2.1.3. Intelligent Control Strategy

(1) Artificial Neural Network Control

In [37] they apply neural network control strategy to solve the problems caused by hydraulic system leakage and friction. The input signal of neural network controller is pressure difference and velocity while the output signal is transformed to PWM signal. The results show that the steady precision of the system is improved.

In [38] when they design the neural network controller they use both feed-forward and feedback channel signal to generate the driving signal for servo valve. Furthermore they use linear second-order transfer function as the reference model. They apply this control strategy in a servo valve controlled hydraulic cylinder system and the results show that the performance index of square error integration of neural network control is better than that of constant gain control.

In [39] when Burton designs the neural network controller, he considers the effects of nonlinear friction in the valve controlled hydraulic cylinder system. Although the performance of the system in zero velocity region

2. Literature Review

is worse than that in other regions, it can be solved by using single pulse signal in dead zone range. The results show that the performance of this control strategy is better than that of traditional PID control.

(2) Fuzzy Control

Becker research the application of forward channel fuzzy controller in hydraulic position control system [40]. The input signal of fuzzy controller is position error and its changing rate. He uses four on-off valves to control inflow and outflow of oil and determines the parameters of fuzzy controller with trial-and-error method. The results show that the dynamic characteristic of the system is better than that of sliding control system.

In [41] they design a self-organising fuzzy logic controller for water hydraulic system so as to adapt to the variation of process dynamics however the effects of adaptive control is worse than MRAC.

In [42] a self-tuning fuzzy control method is applied in the hydraulic multi-speed control system. The rapidity index of speed step response of the system is improved while the transient performance is not ideal.

(3) Learning Control

The basic principle of learning control is tuning the current control information of the system according to the past control information. To solve the position tracking problem of valve controlled hydraulic cylinder system, an iterative learning control method is proposed in [43]. The experimental results show that this control strategy is better than traditional PID control however the iteration number required is too big.

In [44] they research the application of self-learning control algorithm in an injection moulding machine and then they expound that reasonable selection of learning gain is important to decrease the iteration times.

Aiming at electro-hydraulic vibration testing machine, an iterative learning control strategy in frequency domain of acceleration control is proposed in [45]. They use the adaptive frequency response function of the system and the tracking performance achieved is almost perfect.

2.1.4. Advanced Intelligent Compound Control Strategy

Based on neural network learning algorithm, a learning control strategy of hydraulic robots is proposed in [46].

In [47] they propose a real-time adaptive learning control based on evolutionary algorithm which is introduced into the weight calculation of neural network controller in the forward channel. The experimental results show that the system has ideal robustness against the variation of external load.

A neuro-fuzzy control strategy is proposed in [48]. It is applied in the electro-hydraulic servo systems and the simulation results show that the system has ideal transient performance.

2.2. Control Strategies of MIMO System

Generally speaking, MIMO system is a multi-variable system, hence the development of control strategies of MIMO system is relevant to the the development of control strategies of multi-variable system.

The objective of multi-variable system control is to ensure that every controlled variable should follow the given value and should not be influenced by other variables while in most cases engineers only can make the influences of other variables as little as possible. Furthermore the system should has excellent static and dynamic characteristics. Hence the system need decoupling control. When engineers want to complete control design of strong coupling multi-variable system with tradition control strategies, they have to know the object parameters in advance, then design the compensator, decoupler and controller separately. It is difficult to measure the parameters of strong coupling multi-variable system, consequently design, implementation and coordination of the compensator, decoupler and controller is not so easy. In a word traditional control strategies can not realize the effective control of strong coupling multi-variable system.

2. Literature Review

The controlled systems become more and more complex hence the controlled objects have more factors such as uncertainty, nonlinearity, hysteresis, multi-disturbances, non minimum phase property and so on which influence control precision. As a result the design requirements of coupling control system is higher and higher so that the design difficulty is greater and greater. In practical engineering applications, since coupling phenomenon exists, there are several problems:

- In a multi-channel system with coupling phenomenon, different channels can not be considered separately hence the parameters of control system require many times of tuning however it is still difficult to get a satisfactory result.
- Analysis and design of coupling system requires much more information than that of decoupling system. It is convenient for engineers to design controller for decoupling system with standard design method while no one can find a universal simple design method for coupling system as yet. Especially it is difficult to realize exact decoupling design when the system has too many variables.
- It is convenient to realize on-line tuning for every channel of decoupling system which means that on-line tuning in closed-loop is possible. However it is difficult to realize on-line tuning in coupling system because there are too many relating factors in the system.

Hence the decoupling problems of multi-variable systems have caused the extensive concern.

As same as the development of other control strategies, the decoupling control theory develops from simple to complex, from primary to advanced, from classical to modern, from single to composite, from linear to nonlinear, from static to dynamic, from continuous to discrete, from non-robust decoupling to robust decoupling, from traditional decoupling to intelligent compound decoupling.

The development of decoupling control theory can be divided into six stages:

- Preliminary stage: Boksenbom and Hood proposed the irrelevant control principle based on algebraic method of multi-variable system in 1949 [49].

2.2. Control Strategies of MIMO System

- Morgan problem stage: Morgan proposed the decoupling problem of input and output of MIMO linear system based on state-variable feedback [50].
- Traditional decoupling control stage (decoupling control of linear system): there are a lot of traditional decoupling control methods which focus on deterministic MIMO linear system such as diagonally dominant matrix method [51, 52, 53, 54], relative gain analysis method [51], characteristic curve analysis method [51], state variable method [51], inverse Nyquist array method [53, 55], dyadic expansion method [56], sequential difference method [56] and singular value decomposition method [57].
- Modern decoupling control stage (decoupling control of nonlinear system): adaptive decoupling control [58, 59, 60, 61, 62], variable structure decoupling control [63, 64], robust decoupling control [65, 66, 67], state feedback decoupling control [68, 69], output feedback decoupling control [70, 71, 72, 73, 74], energy decoupling control [75, 76, 77, 78] and modern compound decoupling control [79, 80, 81].
- Intelligent decoupling control stage: neural network decoupling control [82, 83, 84, 85, 86] and fuzzy decoupling control [87, 88, 89, 90].
- Advanced intelligent compound decoupling control stage: compound decoupling control which contains adaptive control, predictive control, neural network control, fuzzy control, human-simulated intelligent control, genetic algorithm and so on [91, 92, 93].

In a word multi-variable system decoupling control theory is developing however the research on the decoupling strategy is based on traditional decoupling theory. The research results focus on the design of the decoupling controller and most of them come from trial-and-error method and its optimization. Consequently the research on the theory of decoupling stability and convergence is not yet perfect. Furthermore most of the application results of decoupling controller only can be used in lower dimension systems. In addition many of the decoupling theory can not be applied in engineering practices because the design method and algorithm is too complicated. Hence there is still a lot of work of theory research and practical application for researchers to do.

In MIMO electro-hydraulic servo system coupling means that the output signal of one channel is coupled with the input signals of other channels

2. Literature Review

while generally speaking the control signals and output signals of all the channels will influence each other especially when many actuators connect to the same load system. This is called load coupling which may cause instability of the system. Many of the MIMO electro-hydraulic servo systems can not be applied because of the coupling. Decoupling control is one of the effective means to solve the problem. Most of the MIMO electro-hydraulic servo systems have norm structure which can be called V-Norm coupling control system proposed by Mesarovic [2, 94]. Decoupling control of this kind of systems can be realized by diagonal matrix method.

Conclusively decoupling control of MIMO electro-hydraulic servo systems is worth studying. Although research results of MIMO systems are not as deep and wide as that of SISO systems, the application of MIMO electro-hydraulic servo systems is wider and the control requirements are higher than before consequently research on decoupling control of MIMO systems has caused the extensive concern and many research results have been obtained. The development of decoupling control strategy of MIMO electro-hydraulic servo systems is briefly described in the following.

2.2.1. Classical Decoupling Control Strategy

The classical control theory represented by PID control strategy are also applied widely in MIMO electro-hydraulic servo systems. In addition modern control strategy and artificial intelligence control strategy get experiences from PID control. Similarly PID control of MIMO electro-hydraulic servo systems is also based on the linear combination of current, past and future information of system error and it has many advantages such as simple structure and algorithm. However PID decoupling control can not coordinate the contradiction between rapidity and stability of the system and moreover it does not have ideal robustness against parameters variation and external disturbances because of the linear time-invariant composite structure of system error. Since the requirements on the system performance become higher and higher, traditional PID decoupling control can not meet the demands. Consequently by using the methods from adaptive control, fuzzy control and intelligent control engineers can develop adaptive PID decoupling control, fuzzy PID decoupling control, intelligent

2.2. Control Strategies of MIMO System

PID decoupling control and nonlinear PID decoupling control with computer technology so as to meet the new decoupling control requirements of MIMO electro-hydraulic servo systems.

2.2.2. Modern Decoupling Control Strategy

(1) Feedforward/Feedback Decoupling Control

Aiming at the cross-coupling effects of two-axis hydraulic manipulator, Tochizawa and Edge propose the control strategy of disturbance observer (DO) and compare it with PI controller [95]. In designing the disturbance observer, they treat the cross-coupling of two-axis hydraulic manipulator as disturbances and design the controller for each axis respectively. For small inertial load the performance of disturbance observer is as the same as that of PI controller while for the big inertial load the performance of disturbance observer is better than that of PI controller.

In [96] decoupling of the electro-hydraulic multi-variable position coupling system is designed and experimented using diagonal matrix method. The feedback decoupling and feedback complete decoupling schemes are applied respectively to eliminate the effects of structure coupling and outside disturbance force on the decoupling control. The results show that it has distinct decoupling effect. This method can be realized only with position value of two hydraulic cylinder piston, so that the algorithm is simple and easy to be applied in engineering. Nevertheless it is impossible to realize the exact decoupling because the decoupling unit structure is complicated. Furthermore there are errors in the system model hence only approximate decoupling can be realized. However the coupling effects are reduced obviously when this approximate decoupling method is applied consequently it has practical application value.

Hydraulic loading system with secondary regulation is designed based on secondary regulation technique including two parts, rotational speed control and torque control, which are connected stiffly and coupled heavily with each other. In [97], the operational principle is analyzed in detail and the coupled phenomenon in the system is studied, meanwhile, decoupling of the system is carried out and the results are effective through simulation.

2. Literature Review

The facts demonstrate that the coupled phenomenon in the system can be eliminated by using decoupling method.

In [98] the problem of compensating cross-linking disturbance and load change of multi-variable electro-hydraulic servo system is researched.

In [99] they complete the theoretical research on the coupled load in rolling mill and the dissolution of interference which provides the theory basis for further study on decoupling control of multi-variable hydraulic systems.

In [100] the influence of hydraulic and mechanical coupling on control property is analyzed in the secondary regulation load-simulation test equipment for the drive axle of heavy vehicle. Simulation results show that disturbance error caused by mechanical coupling between the speed control subsystem to simulate the drive and the torque control subsystem to simulate the loads on the secondary axle and wheel edges are comparatively large and may obviously decrease the control accuracy of the whole system. Certain decoupling control elements can be installed to the system so as to make each subsystem almost independent of each other, realize decoupling of secondary regulation load-simulation system, eliminate deteriorating effect of coupling and finally significantly improve control property. The decoupling strategy proposed provides an efficient way to realize decoupling control of the secondary regulation load simulation test equipment and to enhance its performance.

In [101], a position decoupling control strategy of electro-hydraulic servo drive system based on feedforward and feedback decoupling control is proposed and applied in the hydraulic servo control system of B2 and A340 Aircrafts and the results are satisfactory.

In [102] a novel decoupling control method is presented for multi-variable electric-hydraulic servo system. It uses only output and input signals for feedforward and feedback complex decoupling control so that the complete decoupling and poles assignment of the closed-loop system can be realized for the electric-hydraulic servo system which is a minimum phase nonlinear system. The simulation and experimental results show that the decoupling control strategy is satisfactory.

(2) Adaptive Decoupling Control

2.2. Control Strategies of MIMO System

In the process of designing decoupling control system, if some parameters or some parts of the structure of the system are unknown researchers have to estimate the unknown parameters and at the same time modify the decoupling control parameters. This method is called adaptive decoupling control strategy. Adaptive decoupling control strategy can be divided into two types: self tuning decoupling control (STDC) and model reference adaptive decoupling control (MRADC). STDC need a long time for on-line system parameters identification hence it is suitable for systems which have slowly time-varying parameters. However it can not be applied in the coupling electro-hydraulic systems with parameter jump and sudden external disturbance. Consequently in most cases engineers use MRADC or its variant in electro-hydraulic servo systems. One of the disadvantages of adaptive decoupling control strategy is that it has strict requirements on the mathematical models of the controlled system. In addition the robustness of adaptive decoupling control is not ideal.

Aiming at the hydraulic servo system of CNC pipe bending machines, in [103] Zhu applies time series modeling method, decoupling control theory and self-tuning control principle, and then analyzes the modeling and control strategy of multi-variable electro-hydraulic servo systems. He builds the low order mathematical model of the system and furthermore changes the system from a multi-variable coupling electro-hydraulic servo system to several single-variable systems which can track the reference signals and will not interfere with each other.

In [104] a novel control algorithm is developed in connection with the control of nonlinear multi-variable electro-hydraulic servo system. The new control scheme is a combination of generalized minimum variance adaptive control, predictive control and model reference control. Using this scheme, it is not necessary to identify the model of nonlinear factors. Hence it is rapid in calculation and is applicable to a quick response system. Digital simulation and real-time control showed that it acquires good results in overcoming the bad influence of nonlinear factors such as saturation, dead zone and hysteresis.

(3) Sliding Mode Variable Structure Decoupling Control

Three-axis hydraulic simulator has the characteristics of moment coupling among frames, complex friction moment disturbance and system param-

2. Literature Review

eter perturbation. In [105] they propose to equal the term of coupling to outer disturbance, and use the dynamic full-order sliding mode variable structure controller with integral compensation to make three-axis move within their own sliding modes and realize the aim of decoupling and robust to disturbance and parameter perturbation. Simulation and experimental results show that the proposed approach has a quite accuracy servo-tracking result.

(4) Robust Decoupling Control

Generally speaking the model of multi-variable system may have uncertain factors, however researchers still hope that the control system has excellent performance consequently they need robust decoupling control strategy. There are a lot of uncertain factors in multi-variable electro-hydraulic servo systems and furthermore unmodeled dynamics also exist. In recent years many robust control strategies for uncertain factors are proposed [106]. These strategies require that the upper bound of H_∞ mode of frequency response function is extreme small. They apply classical function theory and operator theory successfully and thus they solve the stabilizing compensation problems of multi-variable time-invariant systems with the limitation of H_∞ mode. H_∞ method has the advantages of state space method in calculation and moreover has the intuitional feature of frequency method. In addition, the design of controller can be completed in MATLAB. Nevertheless the problem can not be solved if it is not a small disturbance problem.

Based on the decoupling theory of state feedback, a design method is presented for the decoupling robust controller with state feedback [69]. The proposed control strategy can be effectively used to control more-link robot.

2.2.3. Intelligent Decoupling Control

Fuzzy decoupling control is suitable for the system of which the controlled parameters and their relationship can not be described accurately. Fuzzy decoupling control has excellent robustness while its control precision is

2.2. Control Strategies of MIMO System

not ideal. Hence researchers have to modify the strategy rationally so as to apply it in electro-hydraulic servo systems.

Neural network decoupling control works by imitating the working principle of sense organs and brain cells of human. It can receive, process and output mass data simultaneously. In the system the hardware is used to imitate the network of the neurons while the software imitate the working mode of the neurons. One of the advantages is that the system can process complex problem rapidly however the neural network need learning and training before processing some problem. Furthermore the neural network is a self-learning system. Nevertheless research on neural network decoupling control succeeds only in simulation and moreover convergence of the learning algorithm and stability of the whole system remains to be improved.

In [107] they research on the neural network adaptive control strategy of MIMO electro-hydraulic servo system. Firstly they decouple the MIMO electro-hydraulic servo system into two subsystems: the position control system of the driving hydraulic cylinder and the force control system of the load hydraulic cylinder so as to solve the decoupling problem of system position and system force. Secondly they use a linear second-order transfer function as the system reference model so as to complete off-line training of neural network. The performance index of the integral square error verifies the validation of the decoupling control strategy and further shows that the method is better than PID control with fixed gain. However the tracking performance of the system is not ideal when the reference signal is in high frequency range.

2.2.4. Intelligent Compound Decoupling Control

In [108] a compound control strategy of main controller combined with fuzzy controller based on wavelet transform is proposed and applied in the multi-variable control of electro-hydraulic servo system. The main controller is composed of neural network which contains PID control rules and it plays a leading role in the whole system. The fuzzy controller is used to realize compensation control so as to ensure rapid response performance of

2. Literature Review

the system. The main aim is to eliminate the mutual interference between the different closed-loops of the system and the influence of load variation and external disturbance so as to improve the precision and robustness of self-learning and adaptive decoupling control of the system.

Aiming at the control problems of multi-variable system which is time varying and has strong coupling, Liu, Yi and Tong propose a new type of neural network [109]: PID neural network which is different from the PID control system. To be specific the parameters of the PID controller can be selected and modified by neural network. PID neural network is a kind of feed-forward multilayered neural network which can select the input-output function of neurons in hidden layer according to the PID control rules so as to make them become proportion, integral and differential parts respectively. Furthermore it can complete connection weight initialization of the neural network based on PID control rules so as to stabilize the initial state of the system and improve the convergence rate of learning algorithm. Moreover it is not necessary to measure or identify the internal structure or parameters of the controlled objects when engineers use the PID neural network controller. In addition the PID neural network can complete a lot of work such as self-learning, parallel calculation, tuning network weight and decoupling control of the system by measuring the reference signal and output signal of the system so as to improve the static and dynamic performance of the multi-variable system which is time varying and has strong coupling.

Overall, the control problems of MIMO electro-hydraulic servo systems contain the control problems of both MIMO systems and SISO systems which means that researchers have to solve both the decoupling problems of the MIMO systems and the control problems of each decoupled SISO system. Particularly An effective comprehensive control scheme of MIMO electro-hydraulic servo systems has important theoretical and practical significance.

2.3. Control Strategies of Commercial Products

Although studies on the control strategies of electro-hydraulic servo systems have made progress, many of the research results have strict restrict conditions which means that they can be applied only in laboratory. However the reason why researchers do the research on the control strategies of electro-hydraulic servo systems is that they want to apply them in the practical projects rather than laboratory. When a control strategy can be applied in the practical industrial fields widely it will become a commercial product. The development situation of control strategies of commercial products will be described as follows.

2.3.1. Null Pacing

Null pacing ensures that desired levels are reached on initial cycle without over-programming. There are two types of null pacing: static null pacing and dynamic null pacing [110].

(1) Static Null Pacing

If the error is too large, static null pacing holds the command at its segment boundaries, allowing the sensor feedback more time to reach its target peak. As the error comes within the user-specified error tolerance, static null pacing resumes the command.

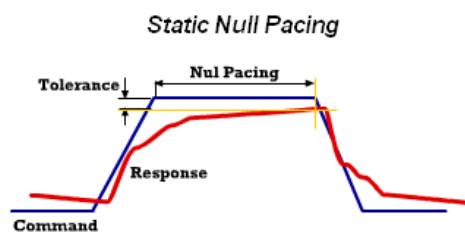


Figure 2.2.: Static Null Pacing [110]

2. Literature Review

(2) Dynamic Null Pacing

If the error is too large, dynamic null pacing reduces the command frequency allowing the sensor feedback more time to track the command. The frequency decreases until either of the following occurs:

- The error comes within the user-specified error tolerance, at which time the command frequency starts increasing towards the command frequency.
- The frequency decreases to the minimum frequency value (20% of the original frequency). The command is then held at this frequency as long as the error remains out of tolerance. This condition is also known as low cycle.

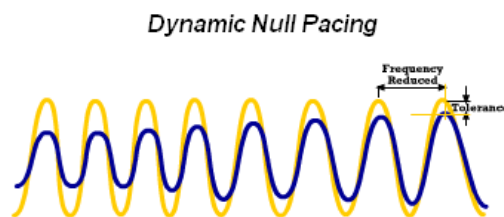


Figure 2.3.: Dynamic Null Pacing [110]

2.3.2. Peak Valley Control

Peak valley control (PVC) adapts as specimen compliance changes to ensure peaks and valleys are maintained for any constant amplitude periodic waveform. The algorithm is described as follows [110]:

- PVC boosts the command amplitude if roll-off is detected.
- PVC adjusts the commanded mean level if mean level divergence is detected.

2.3. Control Strategies of Commercial Products

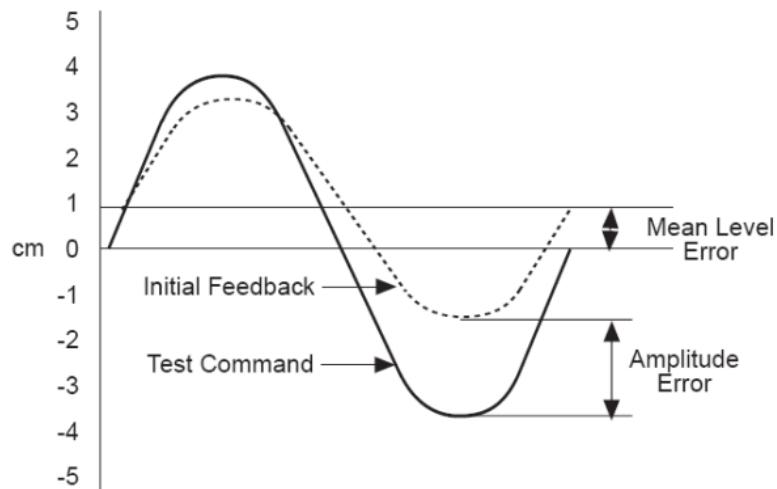


Figure 2.4.: Peak Valley Control [110]

2.3.3. Amplitude Phase Control

Amplitude phase control (APC) monitors feedback from sine and sine tapered commands for amplitude roll-off and phase lag. APC works well when engineers need to control the amplitude of the fundamental frequency component. However if engineers want to achieve peaks, particularly if the feedback is distorted, using APC is not a good choice. The algorithm is described in the following [110]:

- APC boosts the command amplitude if roll-off is detected.
- APC alters the command phase if phase lag is detected.

2.3.4. Adaptive Inverse Control

Adaptive inverse control (AIC) is a linear compensation technique that automatically adjusts a compensation filter that filters the command signal to

2. Literature Review

achieve the desired response signal. AIC is an effective digital control technique for improving tracking accuracy in mainly linear servo hydraulic test systems. AIC can be applied to any waveform, including random profiles or remote parameter control (RPC) time history files in linear systems.

The presence of dynamics in a test system can result in large tracking errors, especially at higher frequencies. The AIC compensator identifies these dynamics and actively adjusts an inverse-dynamics compensation filter between the function generator and the test system. This active adjustment pre-corrects the command signal for system dynamics, resulting in optimal tracking [110].

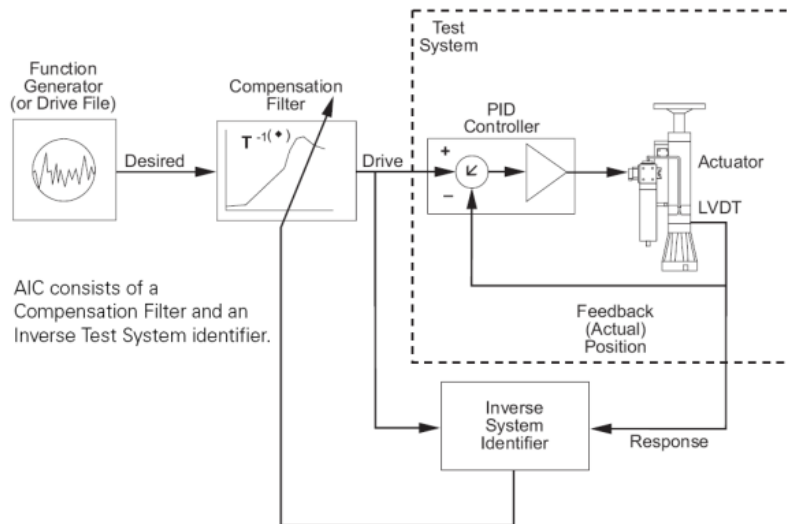


Figure 2.5.: Adaptive Inverse Control [110]

2.3.5. Arbitrary End Level Control

Arbitrary end level control (ALC) can adapt for linear or nonlinear specimens with periodic or random waveforms. ALC is an adaptive compen-

2.3. Control Strategies of Commercial Products

sation technique that improves the tracking accuracy of spectrum profiles. This technique is also known as “From-To Matrix Compensation”.

ALC compensates for peak and valley errors by building and continually updating a matrix of amplitude compensation factors. The matrix is two-dimensional, with axes mapped to either plus or minus full scale of a sub range of full scale. Each axis is divided into 16, 32 or 64 equal parts, with each part representing a fraction of the defined range. The horizontal axis is labeled “From Level” and the vertical axis is labeled “To Level”. With each pass of the spectrum, the peak/valley errors are calculated, and an estimated compensation factor is stored in the matrix. Before the command generator generates a new segment, it notes the required “From” and “To” levels, and refers to the matrix to determine how much to over-program the segment [110].

		From Level				
		- FS		0		+ FS
To Level	- FS	x1	x2	x3	x4	x5
		x6	x7	x8	x9	x10
	0	x11	x12	x13	x14	x15
		x16	x17	x18	x19	x20
	+ FS	x21	x22	x23	x24	x25

When going from 0 to + FS, ALC uses this compensation factor.

Calculated Amplitude Compensation Factors

Figure 2.6.: Arbitrary End Level Control [110]

2.3.6. Peak Valley Phase Control

Peak valley phase control (PVP) adapts for phase as well amplitude for multi-channel cyclic tests. PVP can correct for phase even with distorted waveforms. The PVP compensator combines amplitude phase compensation (APC) with peak valley compensation (PVC) algorithms to improve

2. Literature Review

the amplitude and phase tracking of the command and sensor feedback. The advantages of this technique are [110]:

- PVP compensates for phase error, unlike PVC.
- PVP provides good amplitude tracking on nonlinear specimens, unlike APC.

However the PVP compensator may have difficulty compensating command waveforms below 0.5 Hz.

The PVP is a phase compensator cascading into a peak valley compensator. The phase algorithm is similar to the one used by APC. The peak/valley algorithm is identical to the one used by PVC.

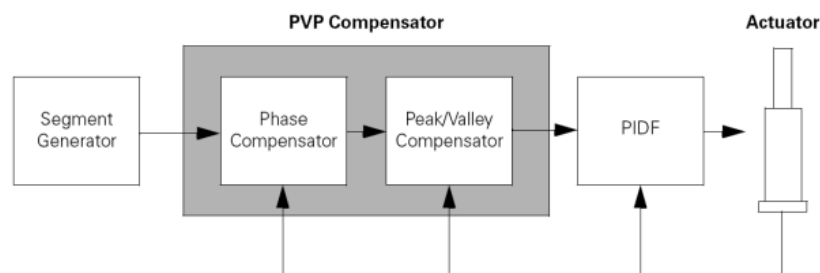


Figure 2.7.: Peak Valley Phase Control [110]

2.3.7. Motion Isolated Load Control

Motion isolated load control allows actuators which are acting typically in load control to achieve high levels of control accuracy when connected to a test piece which is subject to an external motion. This is achieved by feeding forward in the control loop, information which describes the external motion in terms of acceleration and velocity [111].

2.3.8. Modal Control

Modal control allows the direct control of user defined motions such as for example X, Y and Z pitch roll and yaw in the case of a multi-axis shake table [111]. Feedback cross-compensation allows virtual transducers to be defined from a combination of up to four real transducers. Servo valve cross compensation allows the drive for a servo valve to be compensated by the output from up to four other control channels. Both these features can be activated independently, but when they are used in combination, full modal control is achieved. As well as allowing the user direct control of deterministic command signals, modal control allows each of the virtual control loops to be independently tuned, providing increased control bandwidth.

In addition, servo valve cross compensation can be used to provide geometric compensation on a test rig by enabling the servo valve drive on one axis to be modified in sympathy with sensor information from other axes in accordance with a pre-defined compensation equation.

2.3.9. High Order Control

In addition to a conventional control loop, some products provide cascade control and a notch filter. These have the capability to achieve a much higher level of control particularly in cases where backlash or resonances are present. The inner controlled variable is (normally position), provides a robust control loop. The outer controller (normally load) contains a parallel PIDF control loop and a notch filter to compensate for system resonances. Using these techniques the control bandwidth is significantly increased and the control loop is more stable and less sensitive to changes in the dynamic behaviour of the test piece [111].

2.3.10. Delta-P Gain Control

The delta-P gain control is used with two pressure transducers, or a differential pressure transducer and an additional DC conditioner card to form

2. Literature Review

an inner feedback loop. The delta-P gain inner feedback loop is often used with compliant systems (i.e. not stiff, vibration systems with large mass, and or long thin actuator) to increase stability. Delta-P gain stabilization measures the hydraulic oil pressure difference in both chambers of the actuator by a differential pressure transducer, then feeds this signal back into the control loop. By setting up the appropriate phase and gain the signal will stabilize displacement control in the control loop by offsetting the AC feedback [112].

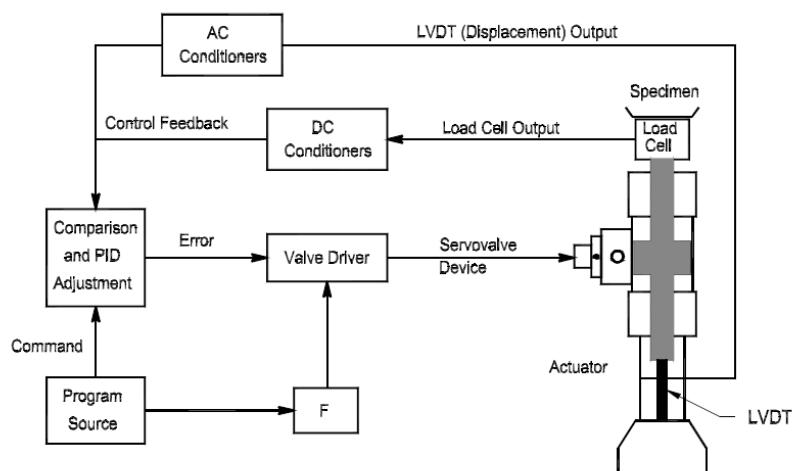


Figure 2.8.: Delta-P Gain Control [112]

2.3.11. New Types of PID Control

A combined stroke-force control method, called PIDM for mixed control, is provided by Walter and Bai AG [113]. In this mode stroke is being controlled but the force is kept within user supplied limits. As the force increases the system switches over softly from stroke to force control. This is particularly useful when setting up delicate samples. The PIDM strategy is fully parameterized.

2.3. Control Strategies of Commercial Products

Furthermore the company provide the system which is equipped with two PID based peak control algorithms. A peak controller is an adaptive strategy to ensure that peak values of a periodic output function remain constant and reach the desired value. This is extremely helpful in cases where a periodic output function suffers from severe distortions, for example due to disturbance from the mechanical setup or when the probe changes its state and hence its behaviour during the test. A conventional PID controller fails under such circumstances. The self-adjusting peak controllers can cope with such situations very well. In the background they constantly measure the transfer behaviour of the entire control loop. Based on the results they are able to automatically improve the control performance. There are two typical scenarios for using these algorithms:

- During an initial training phase the controller quickly adjusts its internal states. At the end of the training the states are frozen. From then on the optimized controller is ready for testing.
- Testing starts with a neutral or conservative initial setup of the adaptive states. During the test the adaptive controller softly adjusts its internal states to optimize the total performance. When the probe or some other component within the control loop starts to change its behavior the adaptive controller follows and compensates for the drift.

2. Literature Review

3. System Modeling and Identification

A system is a set of elements which have specific function and are mutually related and influenced. Control system is one of the typical systems in engineering. In control theory, system simulation is one of the important means to research on control system and system model is the direct object of simulation research. System model is an abstraction of the practical system and describes the essential property or other characteristics of the system. System model can be divided into entity model and mathematical model. The entity model is also called physical effect model which is built according to the similarity principle. The mathematical model includes original mathematical model and simulation mathematical model. The original mathematical model is the original mathematical description of the system while the simulation mathematical model is such a model that can be applied in computer. To be specific the simulation mathematical model is transformed from the original mathematical model by researchers according to the operation characteristics, simulation mode, calculation method and precision requirement of the computer. The mathematical model can be divided into a lot of types. For instance it can be divided into dynamic system model and static system model according to the system state. Furthermore the dynamic system model includes continuous system model and discrete system model.

Especially according to how much system information one can achieve, the system model can be divided into white box model, grey box model and black box model. If one can obtain all the system information, the white box model can be built while if one can only know part of the system information, the grey box model can be built. A black box model means that one can know little information about the system. Grey box model

3. System Modeling and Identification

and black box model can not be applied in simulation directly hence researchers need system identification to help them achieve a determined system model which is accurate enough.

System identification is a kind of theory and method to build the mathematical model of the system based on the input-output data of the system while in essence system identification is a type of optimization problem. The basic idea of the commonly used identification algorithm is to build the parameter model of the system so that the problem of system identification is converted to the problem of parameter estimation.

Particularly aiming at the electro-hydraulic servo system one can derive the mathematical model structure of the system based on the hydraulic equation and mechanical principle however there are some variables which can not be measured directly in the system therefore it is difficult to obtain the exact values of some parameters of the system model based merely on theory and experiences. One of the direct and effective methods is to apply proper identification algorithm according to the model structure so as to estimate the values of the system parameters accurately.

Hence in this chapter firstly the position control model of the electro-hydraulic servo system is built with some parameters unknown and then system identification is made with Matlab to estimate these unknown parameters so as to achieve the accurate mathematical models of the practical electro-hydraulic servo position control systems. Furthermore the contributions of this chapter are as follows:

- introducing a simple linear friction model into modeling of valve-controlled cylinder with friction which is not negligible so that the dynamic performance of friction can be described by a simple system model;
- developing a novel system identification method so that the model with unknown initial parameters can also be identified accurately.

3.1. System Modeling

A typical test rig with electro-hydraulic servo system is an integrated system composed of controller, process, sensor and the assisting components such as cabling, mechanical connections and so on where the process includes the cylinder, the servo valve and/or the unit under test (UUT). Figure 3.1 is one of the test rigs with electro-hydraulic servo system used in our laboratory. The controller compares the reference signal and system output signal and then calculates the control signal which is sent to the servo valve. The servo valve can accurately control the cylinder. With the position sensor and the force sensor the system can realize precise position control and force control respectively so that fatigue test of the UUT can be completed. Furthermore Figure 3.2 describes the control structure diagram of the test rig which uses closed-loop feedback control.

To build an accurate model of the valve-controlled cylinder system which can be applied in simulation one should derive the model of the cylinder, the servo valve and the sensor respectively. Especially in our laboratory only the double-acting double-rod cylinders are used. These cylinders can be divided into two types: the cylinders with hydrostatic bearing and the cylinders with bearing strip. The friction of the former is negligible while the friction of the latter is non-negligible. Hence when researchers want to build the model of the system which applies the cylinder with touching sealing, they have to build the friction model. Finally these sub-system descriptions can be combined to obtain the overall model of the system.

3.1.1. Modeling of Cylinder

Figure 3.3 describes the structure of the valve-controlled cylinder system composed of a four-way valve, a double-rod cylinder and a UUT. To build the model for this valve-controlled cylinder of the electro-hydraulic servo position control system three basic equations are necessary: the pressure-flow equation of the control valve, the continuity equation of fluid and the pressure-load equation.

3. System Modeling and Identification

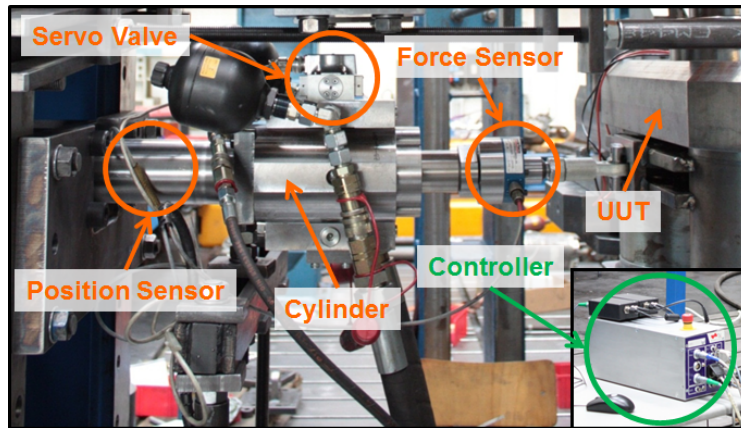


Figure 3.1.: Real World Test Rig with Electro-Hydraulic Servo System

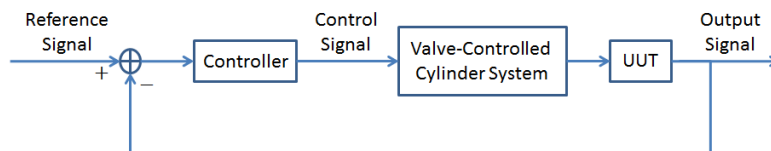


Figure 3.2.: Control Structure Diagram of Test Rig Using Closed-Loop Feedback Control

3.1. System Modeling

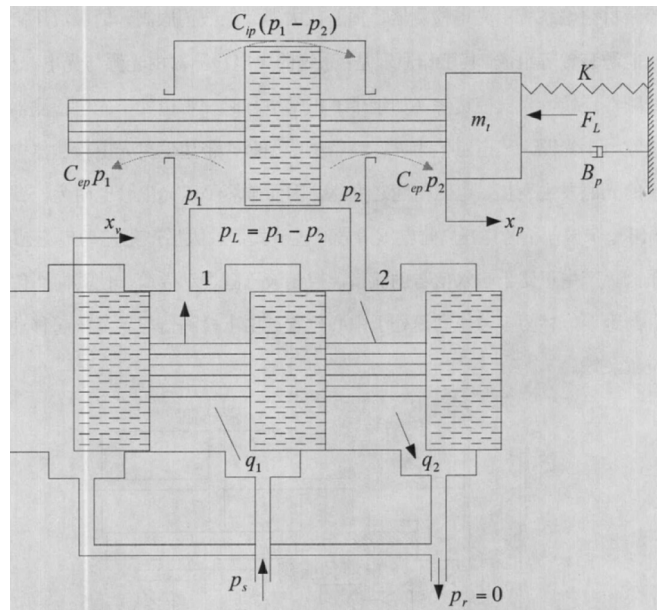


Figure 3.3.: Structure of Valve-Controlled Cylinder System [2]

3.1.1.1. Pressure-Flow Equation of the Control Valve

Before deriving the pressure-flow equation, several assumptions are made:

- The ideal constant pressure source is used which means that the supply pressure p_s is constant. In addition it is assumed that the return pressure p_r is zero. If p_r is not zero then p_s is treated as the pressure difference between the supply pressure and the return pressure.
- The pressure loss in the pipes and valve chambers can be ignored because it is much smaller than the throttle loss at the valve ports.
- The flow coefficients at each valve port are the same.
- The ideal critically centered four-way spool valve will be used which means that when the valve spool is centered all the four ports will be closed.

3. System Modeling and Identification

When the valve spool moves to the right then the displacement of the valve spool $x_v > 0$ and one can have:

$$q_1 = C_v x_v \sqrt{\frac{2}{\rho} (p_s - p_1)} \quad (3.1)$$

$$q_2 = C_v x_v \sqrt{\frac{2}{\rho} p_2} \quad (3.2)$$

with

C_v the flow coefficient,

ρ the density of the oil,

q_1 the flow of the inlet oil chamber of the cylinder,

q_2 the flow of the outlet oil chamber of the cylinder,

p_1 the pressure of the inlet oil chamber of the cylinder, and

p_2 the pressure of the outlet oil chamber of the cylinder.

If x_v remains constant, the cylinder piston will move with a steady speed. Since the symmetrical hydraulic cylinder is used, one can have $q_1 = q_2$ and furthermore one can get

$$p_s = p_1 + p_2. \quad (3.3)$$

In the dynamic process one can have $\Delta p_1 \approx -\Delta p_2$ because of the structural symmetry thus Eq. (3.3) still keeps true. The load pressure p_l is defined as

$$p_l = p_1 - p_2 \quad (3.4)$$

hence one can get

$$p_1 = \frac{1}{2} (p_s + p_l) \quad (3.5)$$

$$p_2 = \frac{1}{2} (p_s - p_l). \quad (3.6)$$

3.1. System Modeling

Substituting Eq. (3.5) into Eq.(3.1) and Eq. (3.6) into Eq. (3.2) yields the load flow q_l as

$$q_l = q_1 = q_2 = C_v x_v \sqrt{\frac{1}{\rho}(p_s - p_l)}. \quad (3.7)$$

When the valve spool moves to the left then $x_v < 0$ and Eq. (3.1) becomes

$$q_1 = C_v x_v \sqrt{\frac{2}{\rho} p_l}. \quad (3.8)$$

Substituting Eq. (3.5) into Eq.(3.8) yields

$$q_l = q_1 = q_2 = C_v x_v \sqrt{\frac{1}{\rho}(p_s + p_l)}. \quad (3.9)$$

According to Eq. (3.7) and Eq. (3.9) the load flow q_l is given by

$$q_l = C_v x_v \sqrt{\frac{1}{\rho}[p_s - \text{sign}(x_v)p_l]} \quad (3.10)$$

$$\text{where } \text{sign}(x_v) = \begin{cases} 1 & (x_v > 0) \\ 0 & (x_v = 0) \\ -1 & (x_v < 0) \end{cases} .$$

Eq. (3.10) is the pressure-flow equation of the electro-hydraulic servo valve.

3.1.1.2. Continuity Equation of Fluid of the Cylinder

Before deriving the continuity equation of fluid, several assumptions are made:

- The pipes which connect the servo valve and the cylinder are short, thick and symmetrical.

3. System Modeling and Identification

- The pressure loss in the pipes can be ignored.
- The temperature and bulk modulus of the oil keeps constant.
- The internal and external leakage of the cylinder is laminar flow.

The flow q_1 of the inlet oil chamber of the cylinder is given by

$$q_1 = A \frac{dx_p}{dt} + C_{ip}(p_1 - p_2) + C_{ep}p_1 + \frac{V_1}{K_o} \frac{dp_1}{dt} \quad (3.11)$$

with

- A the piston working area of the cylinder,
 x_p the displacement of the piston rod of the cylinder,
 C_{ip} the internal leakage coefficient,
 C_{ep} the external leakage coefficient,
 K_o the bulk modulus of oil, and
 V_1 the volume of oil in the inlet cylinder chamber, pipes and servo valve.

Similarly the flow q_2 of the outlet oil chamber of the cylinder can be written as

$$q_2 = A \frac{dx_p}{dt} + C_{ip}(p_1 - p_2) - C_{ep}p_2 - \frac{V_2}{K_o} \frac{dp_2}{dt} \quad (3.12)$$

where V_2 is the volume of oil in the outlet cylinder chamber, pipes and servo valve.

In Eq. (3.11) and Eq. (3.12), the first part on the right side of the equal sign is the flow which propels the cylinder piston, the second part is the flow of the internal leakage which passes through the piston sealing, the third part is the flow of the external leakage which passes through the piston rod sealing and the fourth part is the flow caused by oil compression and chambers transformation.

The volume of the working chambers of the cylinder is given by

$$V_1 = V_{01} + Ax_p \quad (3.13)$$

3.1. System Modeling

$$V_2 = V_{02} + Ax_p \quad (3.14)$$

with

V_{01} the initial volume of the inlet oil chamber, and

V_{02} the initial volume of the outlet oil chamber.

According to Eq. (3.11), Eq. (3.12), Eq. (3.13) and Eq. (3.14) one can derive the continuity equation of fluid as

$$\begin{aligned} q_l &= \frac{q_1 + q_2}{2} \\ &= A \frac{dx_p}{dt} + C_{ip}(p_1 - p_2) + \frac{C_{ep}}{2}(p_1 - p_2) \\ &\quad + \frac{1}{2K_o} \left(V_{01} \frac{dp_1}{dt} - V_{02} \frac{dp_2}{dt} \right) + \frac{Ax_p}{2K_o} \left(\frac{dp_1}{dt} + \frac{dp_2}{dt} \right). \end{aligned} \quad (3.15)$$

In Eq. (3.11) and Eq. (3.12) the flow of the external leakage $C_{ep}p_1$ and $C_{ep}p_2$ is so small that it can be ignored. Furthermore if the flow of compression $\frac{V_1}{K_o} \frac{dp_1}{dt}$ is equal to $-\frac{V_2}{K_o} \frac{dp_2}{dt}$ then $q_1 = q_2$. In addition it is assumed that the servo valve is symmetrical hence the flow which passes through the throttle 1 is equal to that passes through the throttle 2. Consequently $p_s = p_1 + p_2$ is approximately valid in the dynamic process. Since $p_l = p_1 - p_2$ one can have $p_1 = \frac{1}{2}(p_s + p_l)$ and $p_2 = \frac{1}{2}(p_s - p_l)$. Thus one can obtain

$$\frac{dp_1}{dt} = \frac{1}{2} \frac{dp_l}{dt} = -\frac{dp_2}{dt}. \quad (3.16)$$

To make sure that the flow of compression is the same, the initial volume V_{01} should be equal to V_{02} which means

$$V_{01} = V_{02} = V_0 = \frac{1}{2}V_t \quad (3.17)$$

where V_0 is the volume of each working chamber when the piston is in the middle position and V_t is the total volume of the cylinder chambers.

3. System Modeling and Identification

When the piston is in the middle position, the influence of the oil compression is the largest, the natural frequency of the hydraulic components is the lowest and the damping ratio is the smallest. Hence the stability of the system is the worst. Consequently when researchers analyze the system they should choose the middle position as the initial position of the piston.

Since $Ax_p \ll V_0$ and $\frac{dp_1}{dt} + \frac{dp_2}{dt} \approx 0$, Eq. (3.15) can be reduced to

$$q_l = A \frac{dx_p}{dt} + C_{tp} p_l + \frac{V_t}{4K_o} \frac{dp_l}{dt} \quad (3.18)$$

where C_{tp} is the total leakage coefficient of the cylinder, $C_{tp} = C_{ip} + \frac{C_{ep}}{2}$.

Eq. (3.18) is the continuity equation of fluid of the cylinder. The first part on the right side of the equal sign is the flow which propels the cylinder piston, the second part is the flow of total leakage and the third part is the flow caused by oil compression and chambers transformation.

3.1.1.3. Pressure-Load Equation

The dynamic characteristics of the hydraulic components are influenced by the load characteristics. The load force contains inertia force, kinetic damping force, elastic force and any external load force.

The pressure-load equation is given by

$$Ap_l = m_t \frac{d^2x_p}{dt^2} + B_p \frac{dx_p}{dt} + Kx_p + F_l \quad (3.19)$$

with

- m_t the mass (including piston and piston rod),
- B_p the kinetic damping coefficient,
- K the spring stiffness, and
- F_l the external load force.

3.1. System Modeling

Now the three important equations have been derived: the pressure-flow equation of the control valve which is given by Eq. (3.10), the continuity equation of fluid of the cylinder which is given by Eq. (3.18) and the pressure-load equation which is given by Eq. (3.19). In Eq. (3.10) q_l has a nonlinear relationship with x_v and p_l therefore one has to linearize the equation. The exact linearization method will be introduced in Chapter 4 while in this section the approximate linearization method based on Taylor series is used thus Eq. (3.10) can be linearized as [114]:

$$q_l = K_q x_v - K_c p_l \quad (3.20)$$

where K_q is the flow gain and K_c is the flow-pressure coefficient.

Applying Laplace transform to Eq. (3.20), Eq. (3.18) and Eq. (3.19) one can obtain:

$$Q_l = K_q X_v - K_c P_l, \quad (3.21)$$

$$Q_l = A s X_p + \left(C_{tp} + \frac{V_t}{4K_o} s \right) P_l, \quad (3.22)$$

$$A P_l = m_t s^2 X_p + B_p s X_p + K X_p + F_l. \quad (3.23)$$

Furthermore in position control it can be assumed that $F_l = 0$. In this case by combining Eq. (3.21), Eq. (3.22) and Eq. (3.23) one can derive the open loop transfer function of the cylinder in position control system without friction as:

$$\frac{X_p(s)}{Q_0(s)} = \frac{\frac{1}{A}}{\frac{V_t m_t}{4K_o A^2} s^3 + \left(\frac{m_t K_{ce}}{A^2} + \frac{B_p V_t}{4K_o A^2} \right) s^2 + \left(1 + \frac{B_p K_{ce}}{A^2} + \frac{K V_t}{4K_o A^2} \right) s + \frac{K K_{ce}}{A^2}} \quad (3.24)$$

where $X_p(s)$ is the Laplace transform of the displacement signal of the piston rod, $Q_0(s)$ is the Laplace transform of the no-load flow signal of the servo valve and $K_{ce} = K_c + C_{tp}$.

Considering that in position control spring stiffness is negligible i.e. $K = 0$ and Matlab will be applied to complete system identification, Eq. (3.24) is simplified to

$$\frac{X_p(s)}{Q_0(s)} = \frac{\frac{1}{A}}{s \left(\frac{s^2}{\omega_h^2} + \frac{2\zeta_h}{\omega_h} s + 1 \right)} \quad (3.25)$$

where ω_h is the natural frequency and ζ_h is the damping ratio.

3. System Modeling and Identification

3.1.2. Modeling of Friction

Eq. (3.25) is the open loop transfer function of the cylinder with hydrostatic bearing however when researchers use the cylinder with bearing strip they have to consider the influence of friction i.e. they should build a proper friction model. There are a lot of friction models nevertheless engineers should apply the friction model which is as simple as possible so that it is applicable in engineering. In our paper [114] we introduce a simple friction model which is described by

$$F_f = B_f \frac{dx_p}{dt} \quad (3.26)$$

where F_f is the friction force and B_f is the friction coefficient.

Thus the friction can be treated as part of the system damping consequently Eq. (3.25) can also be the open loop transfer function of the cylinder with bearing strip.

3.1.3. Modeling of Servo Valve

Generally speaking servo valve is a complex system since several parameters may only be estimated within some (wide) range, or even completely unknown. According to engineering practice servo valve can be described as a second order system

$$\frac{X_v(s)}{I(s)} = \frac{K_{sc}}{\omega_{sv}^2 s^2 + \frac{2\zeta_{sv}}{\omega_{sv}} s + 1} \quad (3.27)$$

where I is the input (current), X_v is the output (spool displacement of servo valve), K_{sc} is the gain of servo valve, ω_{sv} is the natural frequency and ζ_{sv} is the damping ratio.

Sometimes servo valve can also be described as a first order system

$$\frac{X_v(s)}{I(s)} = \frac{K_{sc}}{\frac{s}{\omega_{sv}} + 1} \quad (3.28)$$

3.1. System Modeling

Especially in fatigue test engineers often use low frequency signal as the reference signal thus the dynamic characteristics of servo valve can be ignored hence it can be treated as a proportional part

$$x_v = K_{sc} \times i. \quad (3.29)$$

In this chapter the G761 series of servo valves from MOOG company will be used. According to the datasheet [115] of the servo valve a first order model can describe the dynamic characteristics of the servo valve completely. Consequently the open loop transfer function of the servo valve is given by

$$\frac{Q_0(s)}{I(s)} = \frac{K_{sv}}{\frac{s}{\omega_{sv}} + 1} \quad (3.30)$$

where K_{sv} is the flow-current gain of the servo valve: $K_{sv} = K_q K_{sc}$.

3.1.4. Modeling of Position Sensor

In position control a high quality MTS Temposonics R-Series position sensor is attached inside the cylinder. This sensor has a linear position measurement uncertainty which is less than 0.01% and negligible. Moreover the dynamic non-ideality for this type of position sensor is significantly far above the bandwidth of the servo valve and the cylinder. Consequently the sensor-amplifier system can be considered ideal and thus its open loop transfer function reduces to

$$F(s) = 1. \quad (3.31)$$

3.1.5. Overall Model of the Electro-Hydraulic Servo Position Control System

The overall mathematical model of the electro-hydraulic servo position control system is achieved by combining the previously derived transfer functions of the cylinder, the servo valve, the friction and the position sensor

3. System Modeling and Identification

thus it can be written as

$$\frac{X_p(s)}{I(s)} = \frac{\frac{K_{sv}}{A}}{s\left(\frac{s^2}{\omega_h^2} + \frac{2\zeta_h}{\omega_h}s + 1\right)\left(\frac{s}{\omega_{sv}} + 1\right)}. \quad (3.32)$$

3.2. System Identification

Now the position control model of the electro-hydraulic servo system has been built with some parameters unknown. One method to build the simulation mathematical model is to estimate the values of the unknown parameters based on measurement and experiences. Nevertheless on the one hand some parameters of the system such as the flow-pressure coefficient are difficult to be measured and on the other hand some parameters such as the bulk modulus are time-varying. Consequently although the simulation mathematical model estimated can describe the time domain and frequency domain characteristics of the system to some extent, it can not meet the requirements of controller design and stability analysis. Therefore it is necessary to apply system identification to obtain the accurate mathematical model of the electro-hydraulic servo position control system.

In this section system identification will be made for the electro-hydraulic servo position control system using the test cylinder with hydrostatic bearing and the system using the test cylinder with bearing strip respectively.

3.2.1. Experimental System Description

When engineers run the experiments to acquire data for system identification, they connect the valve-controlled cylinder system of which the model is derived above to a digital control system where a state-of-the-art PID controller is implemented [116]. Thus the overall experimental system is composed of the PID controller and the valve-controlled cylinder system as shown in Figure 3.4. Moreover Figure 3.5 gives the photograph of the real world experimental system which includes the PID controller, the servo valve and the test cylinder with hydrostatic bearing and Figure 3.6 gives the photograph of the system using the test cylinder with bearing strip.

3.2. System Identification

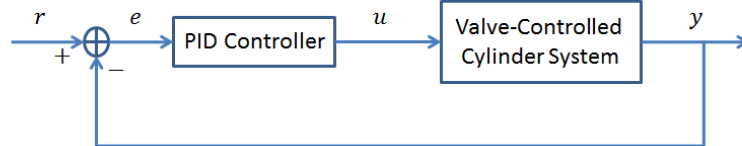


Figure 3.4.: Schematic Diagram of the Experimental System for Identification

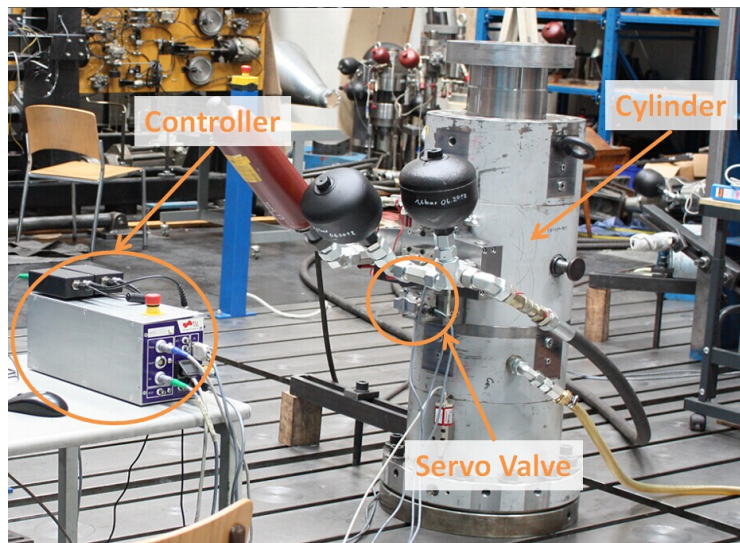


Figure 3.5.: Real World Valve-Controlled Cylinder System, Including the Cylinder with Hydrostatic Bearing, the Servo Valve and the Controller

3. System Modeling and Identification

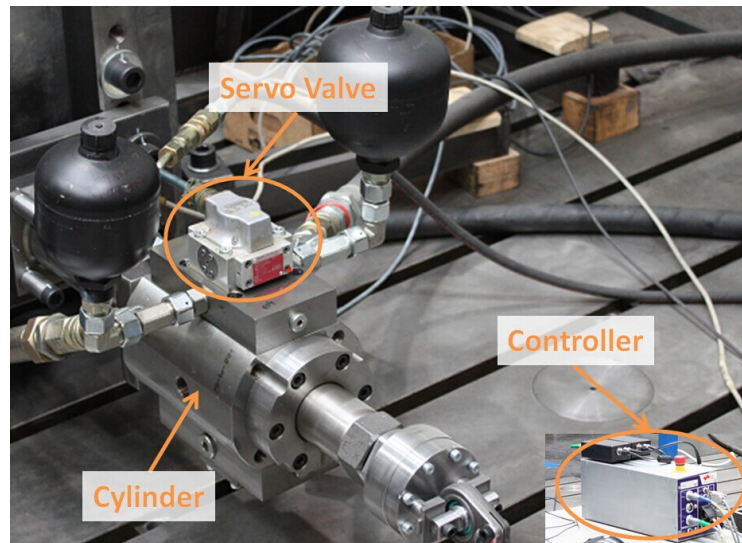


Figure 3.6.: Real World Valve-Controlled Cylinder System, Including the Cylinder with Bearing Strip, the Servo Valve and the Controller

3.2.2. Design of Reference Signal

When researchers select the reference signal for system identification they have to ensure that within the experimental time the input-output data can describe the dynamic characteristics of the system sufficiently i.e. the frequency spectrum of the reference signal should cover that of the system from the view of spectral analysis. In addition the selection of reference signal should improve the precision of system identification. There are several different types of signal which can be used as reference signal while here two kinds of proper colored noise signals are applied as the reference signals:

- zero mean white Gaussian noise which is filtered by a 1st order low-pass filter with the cutoff frequency of $f_c = 10$ Hz;
- zero mean white Gaussian noise which is filtered by a 6th order band-pass filter with the low and high cutoff frequencies of $f_l = 150$ Hz and $f_h = 450$ Hz.

Furthermore an assumption is made that the valve-controlled cylinder system can be considered linear so that the low frequency signal is superimposed on the high frequency signal for identification and verification [114].

3.2.3. Parameter Identification with Matlab

Given the grey box model of the electro-hydraulic servo system, the initial estimated values of unknown parameters and the input-output data from the experiment, one can use Matlab to complete system identification to achieve an accurate system model for controller design and system analysis. The general process is described as follows [117]:

- estimating the values of the unknown parameters based on theory, datasheet and experiences so as to provide an initial model for Matlab;
- describing the initial model of the system which need to be identified with Matlab function;
- completing system identification by using the well-known prediction error method (PEM) provided in the System Identification Toolbox of Matlab with the input-output data.

In this dissertation most parameters of the valve-controlled cylinder system are unknown i.e. all the four parameters ω_h , ξ_h , ω_{sv} and K_{sv} in the overall mathematical model of the valve-controlled cylinder system described by Eq. (3.32) are unknown. Therefore in the next section values of these parameters will be estimated with system identification.

3.2.4. Results Analysis

3.2.4.1. Results Analysis of the System Using the Cylinder with Hydrostatic Bearing

In our laboratory there is a 250kN cylinder which uses the hydrostatic bearing i.e. the friction of the cylinder is negligible. And a MOOG G761-

3. System Modeling and Identification

3005 servo valve is attached to the cylinder. Based on the datasheet of the cylinder and the servo valve and the experiences, the initial values of the unknown parameters can be estimated so that the System Identification Toolbox of Matlab can be used with the input-output data to obtain an accurate mathematical model. Table 3.1 gives the comparison of the initial values and the identified values of the unknown Parameters. Furthermore Figure 3.7 gives the comparison of the frequency response function (FRF) of the real valve-controlled cylinder system, the initial model and the identified model. In Figure 3.7 the red line is the power spectral density (PSD) curve of the real system calculated with the input-output data; the green line is the FRF of the initial system model based on the datasheet and experiences and the blue line describes the FRF of the improved system model with system identification. Observing Table 3.1 and Figure 3.7 one can find that according to the datasheet and the experiences a system model which describes the dynamic characteristics of the system roughly can be built and with system identification one can greatly improve the accuracy of the system model which is the basis of controller design and stability analysis.

Table 3.1.: Comparison of the Initial Values and Identified Values of the Unknown Parameters

Parameter	Initial Value	Identified Value
ω_h (rad/s)	891	930.8491
ζ_h	0.2	0.1966
ω_{sv} (rad/s)	500	623.35
K_{sv} (m ³ /(s · A))	0.02625	0.0368

To further verify the result of system identification, simulation is made with the identified system model, the same PID controller and the same reference signal as that used in experiment. Simulink of Matlab is used to complete simulation and the result is given by Figure 3.8 from which one can observe that the output displacement signal of the real system obtained from measurement and the signal of the identified system model obtained from simulation are basically in coincidence i.e. the identified

3.2. System Identification

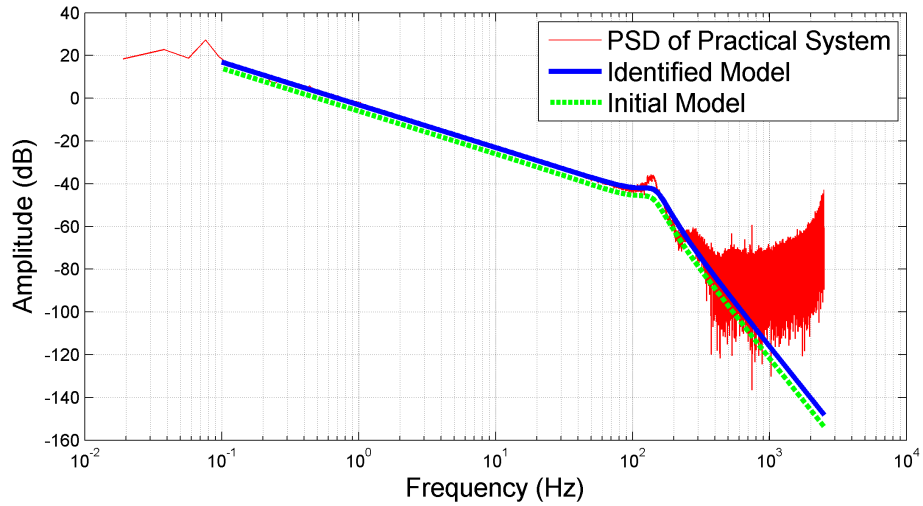


Figure 3.7.: Comparison of the Frequency Response of the Real Valve-Controlled Cylinder System, the Initial Model and the Identified Model

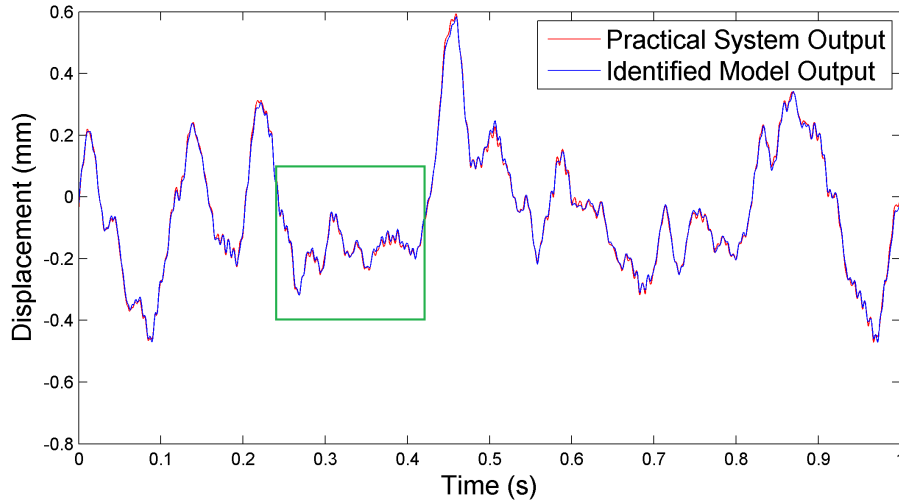


Figure 3.8.: Comparison of the Displacement Signal of the Real System Obtained from Measurement and the Identified System Model Obtained from Simulation

3. System Modeling and Identification

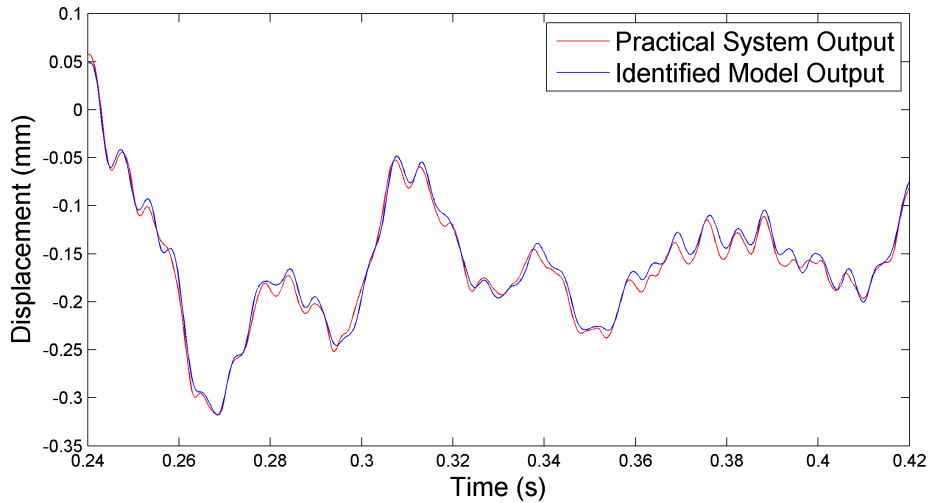


Figure 3.9.: Details of Comparison of the Displacement Signal of the Real System Obtained from Measurement and the Identified System Model Obtained from Simulation

system model can describe the dynamic characteristics of the system completely and the model accuracy is satisfying. Moreover to compare the two different system output signals more deeply, the green rectangular region in Figure 3.8 is zoomed in and the result is shown in Figure 3.9. According to Figure 3.9 it is obvious that the two different system output signals fit well while the error is mainly caused by high frequency signal. Nevertheless the result meets the accuracy requirements.

3.2.4.2. Results Analysis of the System Using the Cylinder with Bearing Strip

In our laboratory there is a 40kN cylinder which uses the bearing strip i.e. the friction of the cylinder is non-negligible. At the same time a MOOG G761-3003 servo valve is attached to the cylinder. Since there is not any information about the friction, it is difficult to estimate the initial values of the unknown parameters only on the base of the datasheet and the experi-

3.2. System Identification

ences. Consequently a novel method of system identification is developed which is called black-grey box model identification method and is introduced in [114]. The main points of this method are as follows:

- calculating the PSD of the real system with the input-output data (black box model identification);
- estimating the values of the unknown parameters based on the PSD result, the datasheet and the experiences so as to provide an initial system model for system identification;
- completing system identification with the System Identification Toolbox of Matlab so as to achieve an accurate system model (grey box model identification).

Table 3.2.: Comparison of the Initial Values and Identified Values of the Unknown Parameters

Parameter	Initial Value	Identified Value
ω_h (rad/s)	2000	2157.2
ξ_h	0.7	0.9766
ω_{sv} (rad/s)	816.814	1005.3
K_{sv} (m ³ /(s · A))	0.0079167	0.0114

Table 3.2 is the comparison of the initial values and identified values of the unknown parameters. Moreover Figure 3.10 provides a comparison of the identified system model with the real system. The red curve describes a plot of the frequency response of the real system obtained from input-output data and particularly the FRF of the real system is obtained by a non-parametric PSD estimation which can be regarded as a kind of black box model identification process. The green curve shows the FRF of the grey box model where the unknown parameters have been improved based on the prior PSD result and by utilizing this model as the initial model of the grey box model identification one can obtain an accurate mathematical model of the valve-controlled cylinder system. The corresponding FRF estimation is provided by the blue curve. By comparing the three results one can come to the conclusion that the result of black box model identification

3. System Modeling and Identification

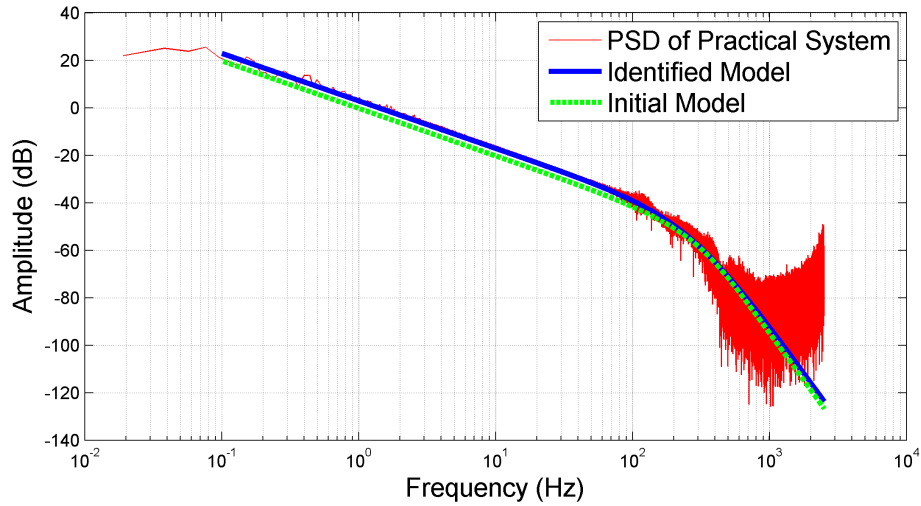


Figure 3.10.: Comparison of the Frequency Response of the Real Valve-Controlled Cylinder System, the Initial Model and the Identified Model

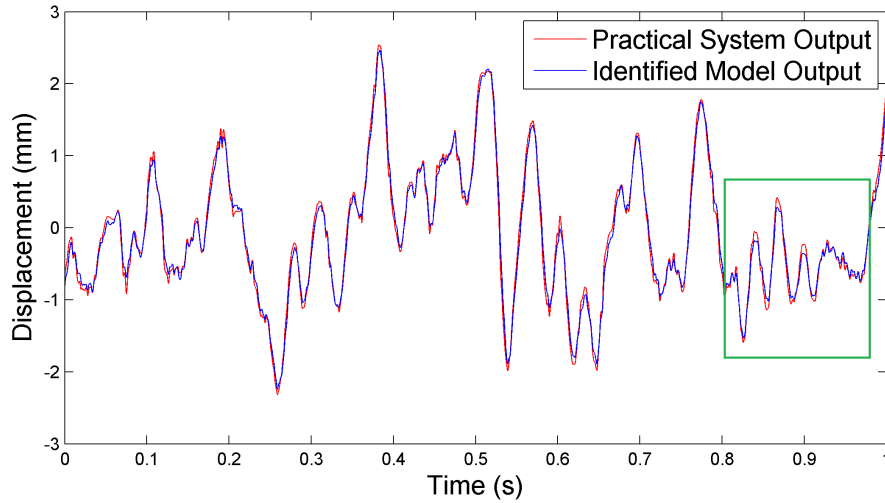


Figure 3.11.: Comparison of the Displacement Signal of the Real System Obtained from Measurement and the Identified System Model Obtained from Simulation

3.2. System Identification

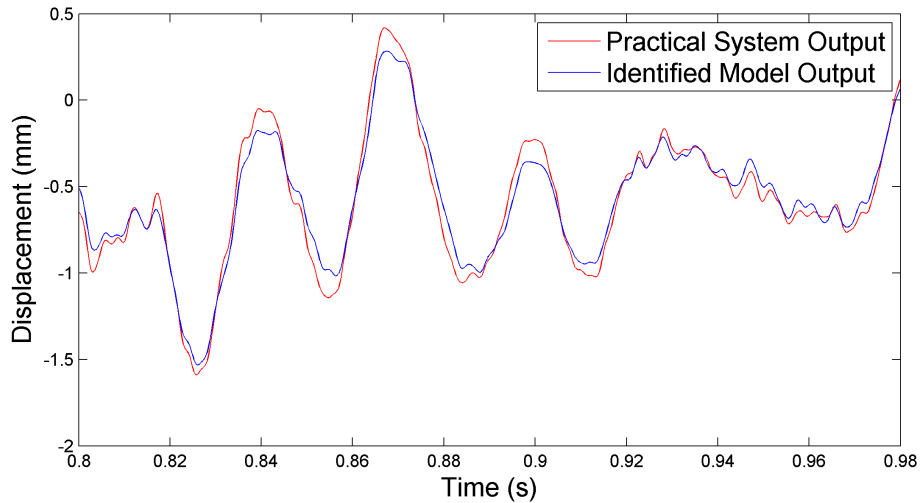


Figure 3.12.: Details of Comparison of the Displacement Signal of the Real System Obtained from Measurement and the Identified System Model Obtained from Simulation

(PSD) can improve the accuracy of the theoretical model which is then applicable as the initial model of the grey box model identification so as to achieve the mathematic model of the electro-hydraulic servo system which meets the requirements of precision.

Likewise to further test the result of system identification simulation is made once more in Simulink with the identified system model, the same PID controller and the same reference signal as that used in experiment. Figure 3.11 describes the output displacement signal measured from the experiment, to be compared with the signal obtained from the simulation. It is very obvious that the waveform of the simulated system output signal is close to that of the measured output signal which shows a nearly perfect agreement between identified model and practical system also for a comparison based on the time series. Additionally to compare the two different system output signals more deeply, the green rectangular region in Figure 3.11 is zoomed in and the result is shown in Figure 3.12. According to Figure 3.12 it is clear that the two different system output signals fit

3. System Modeling and Identification

well while the error is mainly caused by high frequency signal and friction. However the result satisfies the precision requirements.

3.3. Summary

In this chapter the position control model of electro-hydraulic servo system is built based on the characteristics of the hydraulic components and dynamic equations of the valve-controlled cylinder system. Particularly a simple friction model is proposed for practical applications. And then since some parameters of the model are unknown, the values of these parameters are estimated with system identification. Especially a novel identification method called black-grey box model identification method is presented. This method is useful when the initial values of the unknown parameters of the model are difficult to achieve for system identification. Additionally the force control model of electro-hydraulic servo system can also be built and identified with the same methods. Finally the effectiveness of the system modeling and identification methods is verified by the experimental results.

4. Exact Linearization Theory

4.1. Introduction

It is well known that the majority of the control systems in engineering are nonlinear. The traditional analysis and control method of nonlinear system is to linearize the system approximately with Taylor Series and then research into the system with linear control theory. The accuracy of this linearization method depends on the working point and the range in which the system deviate from the working point. However this linearization method cannot provide effective system model for system analysis and control when the system is strongly nonlinear and has large variation range. When researchers design controller based on the approximately linearized model, the control effect is not satisfying. Particularly there are many nonlinear factors in fatigue test rigs with electro-hydraulic servo systems. These nonlinear factors influence the control precision greatly while the requirements of fatigue tests on control accuracy becomes higher and higher. Consequently to build the new system of exact linearization theory is necessary.

The differential geometric method which can be applied in the analysis and control of nonlinear system originates in the 1970s. It uses the differential manifold theory to realize exact linearization of nonlinear system by constructing the diffeomorphism transform [118] and feedback transform. The advantages of this exact linearization are as follows [119]:

- The method does not have errors in theory and is always effective in the linearizable region hence it is called exact linearization method.
- The linearizable region is large enough even if engineers only use local linearization therefore the result from local linearization can be treated as global result in engineering.

4. Exact Linearization Theory

Consequently great attention has been paid to this problem how to realize exact linearization of nonlinear control system based on differential geometric method in both of theory and engineering in recent years. At present the differential geometric theory of nonlinear control system preliminarily forms and becomes a new branch of control theory. In this chapter first the development of nonlinear control theory is introduced, then the basic concepts of nonlinear control theory, the design principles of the nonlinear controller and the disturbance decoupling and attenuation theory are discussed, which lays a foundation of further application of differential geometric method in electro-hydraulic servo control system.

4.2. Literature Review of Nonlinear Control Theory

4.2.1. The Nonlinearity and Existing Processing Methods of Electro-Hydraulic Servo System

Nonlinearity is the difficult problem which exists universally in electro-hydraulic servo system and has not been solved effectively yet. The nonlinearity of electro-hydraulic servo system is caused by the throttle characteristics of the electro-hydraulic element and control element (servo valve, throttle valve and so on) and the inherent problems of hydraulic power mechanism such as hysteresis, dead zone, limiting properties and so on. As far as the nonlinearity caused by the latter which is called essential nonlinearity generally, researchers can achieve good results with describing function method [120] while for the nonlinearity caused by the former there is no satisfying processing method. The existing processing method is incremental linearizing method near the working point which can linearize the nonlinear part of the system dynamic equation. To be specific the nonlinear system will be transformed to a increment linearized system near the working point which researchers can analyze with linear system theory. The well known parameters of the servo valve such as flow gain and flow-pressure coefficient come from this method. The incremental linearizing method is effective for the electro-hydraulic servo system which

4.2. Literature Review of Nonlinear Control Theory

has small setpoint signals and external loads and often works near the rated point. However in modern projects the electro-hydraulic servo system should have the ability to track any curve function point by point and can endure big external disturbance. Consequently the working point of the system will change greatly in a wide range so that the incremental linearizing theory is not applicable any more. There are two methods to solve the problem. The first one is to apply the robust control strategy which has good adaptability and intelligence based on the linear model of the controlled object to deal with the uncertainty caused by the system non-linearity and the variation of the working point. The second method is to linearize the nonlinear system exactly in a wide range and design nonlinear controller with the geometric control theory for the nonlinear system.

4.2.2. The Differential Geometric Control Theory of Nonlinear System

Over the last twenty years by combining the design problem of nonlinear control system with modern differential geometric method, researchers achieve the differential geometric control theory of nonlinear system. In this theory there is one branch called the exact linearization theory via state feedback of nonlinear system which develops quickly and is applied in practical engineering systems such as manipulator, helicopter, electric power system and so on [121]. The basic principle of the exact linearization theory is to find a nonlinear feedback $u = a(\underline{x}) + b(\underline{x})v$ so that with the selected coordinate transformation $\underline{z}(t) = \underline{\phi}(\underline{x}(t))$ the original nonlinear system can be converted to a linear system which is completely controllable thus researchers can use the linear system theory to analyze and synthesize the system [122].

Some nonlinear control systems can be described by nonlinear ordinary differential equation. The development of nonlinear system theory can be divided into two stages [123]. In the first stage before 1970s researchers developed the classical theory of nonlinear system which included phase plane method, harmonic linearization method, Lyapunov direct method, the stability theory of Lur'e systems and so on. The main features of this stage are [124]:

4. Exact Linearization Theory

- All the methods are aiming at certain special and simple basic system respectively hence the conclusions achieved are not systematic.
- No effective methods are developed to solve the synthesis problem of the nonlinear system.
- The analysis of the system only focuses on the absolute stability and only the sufficient conditions are achieved.

Since 1970s the development of the nonlinear system theory enters the second stage. The outstanding characteristic of this stage is that researchers try to explore the basic characteristics and research on the synthesis methods of nonlinear system and moreover several design methods of nonlinear control system such as inverse system theory [125] are proposed. Especially when Brockett [126] found the "interface" between differential geometry and control system, the differential manifold concept and differential geometry method becomes the powerful mathematical tool to research on nonlinear system. The essential points of differential geometry method of nonlinear system are described as follows. First the nonlinear system on one differential manifold should be defined thus the state equation of the system can be described by the vector field on the manifold. And then scientists can research on the properties of the nonlinear system by exploring the properties of various submanifolds, distribution and dual distribution determined by the nonlinear system with the mathematical tool in differential geometry such as submanifold, distribution, Lie algebra and so on. Although there are still several imperfections in the study of basic properties of nonlinear system, with the differential geometry method researchers begin to research on the problems which can not be solved in the past therefore this method plays an important role in revealing the essence of nonlinear system.

When researchers design the nonlinear control system they try to simplify the system first. The general method is to convert the original system into linear system or single input system and the differential geometry method plays a key role in researching on the exact linearization problem and the decoupling problem (including disturbance decoupling control and non-interaction control) of nonlinear system. The so called exact linearization method via state feedback is to convert the nonlinear system into the linear system which is completely controllable with differential homeomorphism and state feedback linearization [122]. Fliess discusses the realization prob-

4.2. Literature Review of Nonlinear Control Theory

lem of the affine nonlinear systems and he describes the input-output relationship of the system with the Fliess expansions determined by Lie derivative [127]. In [128] Cheng gives the nonlinear system set which can be linearized only with differential homeomorphism which is a pioneering result of exact linearization theory. In [129] Cheng gives the theory and design method of exact linearization feedback control of affine nonlinear systems. Sampei and Furuta change the time scale so that the system can be linearized with the new time scale nevertheless using this method researchers have to solve several partial differential equations [130]. This method is not applicable when the system has high dimension. Arapostathic and Nam research on the linearization problem of the discrete nonlinear system respectively [131, 132]. Liu proposes the linearizable condition of nonlinear singular systems [133, 134].

Focusing on the design method of nonlinear control system based on exact linearization model, Lu proposes two design schemes of nonlinear stable control system: zero dynamics method and exact linearization method [135]. Bymes defines the concept of zero dynamics of nonlinear system so that the nonlinear system can be divided into two parts: linear part which is controllable and zero dynamics part. The zero dynamics method is to design the stable control law aiming at the linear part so that the output of the nonlinear system keeps stable. When the zero dynamics part is not stable researchers can apply exact linearization method which is to design the stable control law aiming at the exact linearization model. In [135] Lu illustrates that compared with traditional linear controller the nonlinear excitation controller of the large generator designed with the method introduced above can adapt to the state change in a wider range so as to improve the stability of the electric power system with great disturbance to a greater extent. Meyer applies the nonlinear transformation theory to the design of helicopter flight control system [136]. Here the nonlinear transformation is just the differential homeomorphism transformation designed with differential geometry method. One of the prerequisites of exact linearization of nonlinear system is that the input output map is nonsingular. When the input output map is nearly singular the system requires large control input which is sometimes not allowed. Rapidly maneuvering aircraft is one of the examples and Singh solves the problem [137]. Moreover Li [138, 139] applies the geometry control theory of nonlinear system to the

4. Exact Linearization Theory

hydraulic servo control field and then proposes the theory and method of nonlinear control and nonlinear optimal design of hydraulic servo system. In [140, 141] the nonlinear control method of electro-hydraulic servo speed control system and single-rod cylinder system has been further studied.

4.2.3. Disturbance Decoupling and Attenuation

It is well known that disturbance exists universally in practical system. Generally speaking disturbance effect means the influence of the external disturbance input on the control system output. The research on the disturbance problem is a very important part of the development history of control system. In general the disturbance problem can be divided into two types: disturbance decoupling and disturbance attenuation.

4.2.3.1. Disturbance Decoupling

The so-called disturbance decoupling means to eliminate the influence of the external disturbance on the system output completely. Disturbance decoupling method is closely related to the development of differential geometry theory of nonlinear system. Under the promotion of differential geometry theory the research on the linearization and decoupling problems of nonlinear system develops rapidly. In [142] they discuss the related problems about the control and decoupling of nonlinear system comprehensively and deeply. It is generally believed that the differential geometry theory of nonlinear system is of great theoretical significance but is not suitable for practical application in engineering. However in [143, 144] they apply the decoupling method based on differential geometry theory to the control of induction motor and achieve satisfying results. In [145] they research on the disturbance decoupling problem of a class of nonlinear SISO systems with delay based on the concept of relative degree and give the necessary and sufficient existing condition of system decoupling control. In [146] they discuss the disturbance decoupling problem of a class of SISO nonlinear systems with input and state multi-delay and give the necessary and sufficient existing condition of bicausal feedback controller and

4.2. Literature Review of Nonlinear Control Theory

the sufficient existing condition of a class of compensators. When the external disturbance is measurable, the disturbance can be considered as the feedback variable consequently Xia researches on the disturbance decoupling problem of SISO nonlinear system based on measurement feedback and gives the necessary and sufficient condition of disturbance decoupling based on static and dynamic measurement feedback [147]. In [148] they discuss the disturbance decoupling problem for a class of SISO nonlinear systems with time delays on the input and state and then give the necessary and sufficient solvable condition of the disturbance decoupling problem of nonlinear system based on the concept of relative degree.

4.2.3.2. Disturbance Attenuation

When the influence of the external disturbance on the system can not be eliminated completely, researchers try to reduce the influence of the external disturbance to the acceptable level. This is called disturbance attenuation which can also be called almost disturbance decoupling, robust disturbance decoupling, H_∞ disturbance decoupling and so on since different researchers have different emphasis points. In [149, 150] they discuss the adaptive tracking and regulation problems with almost disturbance decoupling for a class of nonlinear systems respectively. In [151] they research on the robust almost disturbance decoupling problem for a class of nonlinear systems with uncertain dynamic input. They construct the robust state feedback controller with backstepping design method so that, for any uncertain dynamic input which is allowed, the L_2 gain from disturbance to output of the closed loop system with zero initial state is arbitrarily small and the closed loop system is globally asymptotically stable in the absence of disturbance. In [152] they make the feedback design with the so-called adding one power integrator and backstepping method and then they give the design method of one smooth control law which ensures that the closed loop system can realize disturbance attenuation on the basis of internal stability. In [153] the disturbance attenuation problem of a class of affine nonlinear systems is researched with measurement feedback so that the L_2 gain from disturbance to output has minimum value and in [154] they widen the constraint condition so as to propose two different methods. The work [155] proposes a new output feedback stabilization method,

4. Exact Linearization Theory

which has L_2 disturbance attenuation, for the nonlinear system with dynamic uncertainty. When they design the output feedback they apply a new method of nonlinear processing and linear gain adjustment which is state-dependent. When the system satisfies certain conditions the influence of the disturbance on the output can be reduced to an arbitrary small level and it ensures that the system is asymptotically stable.

4.3. Basic Conceptions of Nonlinear Control Theory

4.3.1. Nonlinear Coordinate Transformation and Differential Homeomorphism

Generally speaking in linear control system researchers only consider linear coordinate transformation such as the translation and rotation of the coordinate system. Nevertheless nonlinear coordinate transformation plays a very important role in solving the control problems in nonlinear control system. Nonlinear coordinate transformation can be expressed as $\underline{z} = \underline{\phi}(\underline{x})$ where \underline{z} and \underline{x} are the vectors of the same dimension and $\underline{\phi}(\underline{x})$ is the nonlinear functional vector. $\underline{z} = \underline{\phi}(\underline{x})$ can be expanded as [119]:

$$\begin{cases} z_1 = \phi_1(x_1, x_2, \dots, x_n) \\ z_2 = \phi_2(x_1, x_2, \dots, x_n) \\ \vdots \\ z_n = \phi_n(x_1, x_2, \dots, x_n) \end{cases} \quad (4.1)$$

If the inverse transformation $\underline{x} = \underline{\phi}^{-1}(\underline{z})$ of $\underline{z} = \underline{\phi}(\underline{x})$ exists, and moreover, both of $\underline{\phi}(\underline{x})$ and $\underline{\phi}^{-1}(\underline{z})$ are smooth functions which means that their arbitrary rank partial derivative functions exist and these partial derivative functions are continuous, then the formula $\underline{z} = \underline{\phi}(\underline{x})$ is a qualified coordinate transformation and the coordinate transformation expression $\underline{z} = \underline{\phi}(\underline{x})$ is called a differential homeomorphism between two coordinate

4.3. Basic Conceptions of Nonlinear Control Theory

spaces. If the conditions of differential homeomorphism are satisfied only in the neighborhood of some specific point \underline{x}^0 , it is called local differential homeomorphism. If the conditions of differential homeomorphism are satisfied in the whole space, it is called global differential homeomorphism.

Differential homeomorphism can be used to realize the conversion from one nonlinear system to another nonlinear system which is expressed by new states hence it plays an important role in nonlinear analysis. In some condition nonlinear systems can be transformed into the systems which have the simple structures such as linear structures, triangular structures, chained structures and so on [122].

4.3.2. Affine Nonlinear System

In engineering there are a lot of nonlinear systems such as power system, hydraulic servo system, robot system, helicopter control system, chemical process control system and so on, of which the mathematical models have the same form i.e. the state equation can be expressed as:

$$\begin{cases} \dot{x}_1 = f_1(x_1, \dots, x_n) + g_{11}(x_1, \dots, x_n)u_1 + \dots + g_{m1}(x_1, \dots, x_n)u_m \\ \dot{x}_2 = f_2(x_1, \dots, x_n) + g_{12}(x_1, \dots, x_n)u_1 + \dots + g_{m2}(x_1, \dots, x_n)u_m \\ \vdots \\ \dot{x}_n = f_n(x_1, \dots, x_n) + g_{1n}(x_1, \dots, x_n)u_1 + \dots + g_{mn}(x_1, \dots, x_n)u_m \end{cases} \quad (4.2)$$

and the output equation can be expressed as:

$$\begin{cases} y_1 = h_1(x_1, x_2, \dots, x_n) \\ y_2 = h_2(x_1, x_2, \dots, x_n) \\ \vdots \\ y_m = h_m(x_1, x_2, \dots, x_n) \end{cases} \quad (4.3)$$

4. Exact Linearization Theory

According to Eq. (4.2) and (4.3) the following expression can be derived:

$$\begin{cases} \dot{\underline{x}}(t) = \underline{f}(\underline{x}(t)) + \sum_{i=1}^m \underline{g}_i(\underline{x}(t)) u_i(t) \\ \underline{y}(t) = \underline{h}(\underline{x}) \end{cases} \quad (4.4)$$

where $\underline{x} \in R^n$ is state vector, $u_i (i = 1, 2, \dots, m)$ are control variables, $\underline{f}(\underline{x})$ and $\underline{g}_i(\underline{x}) (i = 1, 2, \dots, m)$ are n-dimensional function vectors and $\underline{h}(\underline{x})$ is m-dimensional output function vector.

From the equations above it can be found that one of the characteristics of this kind of systems is that: it has a nonlinear relationship with the state vector $\underline{x}(t)$ while it has a linear relationship with the control variables $u_i (i = 1, 2, \dots, m)$. This kind of nonlinear systems is called affine nonlinear system. Electro-hydraulic servo system is one of the typical affine nonlinear systems [122].

4.3.3. Vector Field

Let $\underline{f}(\underline{x})$ be a n-dimensional function vector which means:

$$\underline{f}(\underline{x}) = \begin{bmatrix} f_1(x_1, x_2, \dots, x_n) \\ f_2(x_1, x_2, \dots, x_n) \\ \vdots \\ f_n(x_1, x_2, \dots, x_n) \end{bmatrix}. \quad (4.5)$$

Every component of $\underline{f}(\underline{x})$ is the function of the vector $\underline{x}^T = (x_1, x_2, \dots, x_n)$. Generally speaking, any definite point of the state space corresponds to a definite state \underline{x}^0 so as to corresponds to a definite vector of this point:

$$\underline{f}(\underline{x}^0) = \left(f_1(\underline{x}^0), f_2(\underline{x}^0), \dots, f_n(\underline{x}^0) \right)^T. \quad (4.6)$$

According to the analysis above it can be known that any definite point \underline{x}^0 of the state space corresponds to a vector $\underline{f}(\underline{x}^0)$ which depends on $\underline{f}(\underline{x})$, hence $\underline{f}(\underline{x})$ is called one of the vector fields of the state space [118].

4.3.4. Induced Function of Vector Field

The induced function of vector field plays an important role in the exact linearization algorithm of affine nonlinear systems.

Firstly a differential homeomorphism mapping $\underline{\phi} : \underline{z} = \underline{\phi}(\underline{x})$ from an n-dimensional space R^n with X-coordinate to another n-dimensional space with Z-coordinate is defined as:

$$\begin{cases} z_1 = \phi_1(x_1, x_2, \dots, x_n) \\ z_2 = \phi_2(x_1, x_2, \dots, x_n) \\ \vdots \\ z_n = \phi_n(x_1, x_2, \dots, x_n) \end{cases}$$

and a vector of R^n space:

$$\underline{f}(\underline{x}) = \begin{bmatrix} f_1(x_1, x_2, \dots, x_n) \\ f_2(x_1, x_2, \dots, x_n) \\ \vdots \\ f_n(x_1, x_2, \dots, x_n) \end{bmatrix}.$$

It is defined that $J_{\underline{\phi}}(\underline{x})$ is the Jacobian matrix of the space mapping $\underline{\phi}(\underline{x})$:

$$J_{\underline{\phi}}(\underline{x}) = \frac{\partial \underline{\phi}(\underline{x})}{\partial \underline{x}} = \begin{bmatrix} \frac{\partial \phi_1}{\partial x_1} & \frac{\partial \phi_1}{\partial x_2} & \dots & \frac{\partial \phi_1}{\partial x_n} \\ \frac{\partial \phi_2}{\partial x_1} & \frac{\partial \phi_2}{\partial x_2} & \dots & \frac{\partial \phi_2}{\partial x_n} \\ \vdots & \vdots & \dots & \vdots \\ \frac{\partial \phi_n}{\partial x_1} & \frac{\partial \phi_n}{\partial x_2} & \dots & \frac{\partial \phi_n}{\partial x_n} \end{bmatrix}. \quad (4.7)$$

Then the induced function $\underline{\phi}(f)$ of $\underline{f}(\underline{x})$ based on the space mapping $\underline{\phi}(\underline{x})$ can be expressed as [118]:

$$\underline{\phi}(f) = J_{\underline{\phi}}(\underline{x})\underline{f}(\underline{x})|_{\underline{x}=\underline{\phi}^{-1}(\underline{z})}. \quad (4.8)$$

4. Exact Linearization Theory

4.3.5. Lie Derivative and Lie Bracket

The research on nonlinear control systems cannot be separated from the concepts and basic principles of Lie derivative and Lie bracket which are parts of the kernel of the differential geometric method of nonlinear systems.

4.3.5.1. Lie Derivative [118]

It is defined that there is a scalar function of \underline{x} :

$$\lambda(\underline{x}) = \lambda(x_1, x_2, \dots, x_n) \quad (4.9)$$

and a vector field:

$$\underline{f}(\underline{x}) = \begin{bmatrix} f_1(x_1, x_2, \dots, x_n) \\ f_2(x_1, x_2, \dots, x_n) \\ \vdots \\ f_n(x_1, x_2, \dots, x_n) \end{bmatrix}$$

then $L_{\underline{f}}\lambda(\underline{x})$ can be defined as:

$$L_{\underline{f}}\lambda(\underline{x}) = \frac{\partial \lambda(\underline{x})}{\partial \underline{x}} \underline{f}(\underline{x}) = \sum_{i=1}^n \frac{\partial \lambda(\underline{x})}{\partial x_i} f_i(\underline{x}). \quad (4.10)$$

The new scalar function $L_{\underline{f}}\lambda(\underline{x})$ is called Lie derivative which is the derivative of the scalar function $\lambda(\underline{x})$ along the vector field $\underline{f}(\underline{x})$. Consequently Lie derivative is the change rate of scalar function $\lambda(\underline{x})$ along the direction of the vector field $\underline{f}(\underline{x})$. According to the definition of Eq. (4.10) it can be found that Lie derivative is a scalar function hence one can calculate the Lie derivative once more along another vector field $\underline{g}(\underline{x})$ which can be expressed as:

$$L_{\underline{g}}L_{\underline{f}}\lambda(\underline{x}) = \frac{\partial [L_{\underline{f}}\lambda(\underline{x})]}{\partial \underline{x}} \underline{g}(\underline{x}). \quad (4.11)$$

4.3. Basic Conceptions of Nonlinear Control Theory

Certainly the scalar function $\lambda(\underline{x})$ can be differentiated 2 times along the vector field $\underline{f}(\underline{x})$ so one can get the second order Lie derivative and with the same method one can get the Lie derivative of order k:

$$\begin{aligned} L_{\underline{f}}[L_{\underline{f}}\lambda(\underline{x})] &= L_{\underline{f}}^2\lambda(\underline{x}) = \frac{\partial[L_{\underline{f}}\lambda(\underline{x})]}{\partial\underline{x}}\underline{f}(\underline{x}) \\ &\vdots \\ L_{\underline{f}}[L_{\underline{f}}^{k-1}\lambda(\underline{x})] &= L_{\underline{f}}^k\lambda(\underline{x}) = \frac{\partial[L_{\underline{f}}^{k-1}\lambda(\underline{x})]}{\partial\underline{x}}\underline{f}(\underline{x}) \end{aligned} \quad (4.12)$$

where the Lie derivative $L_{\underline{f}}^k\lambda(\underline{x})$ of order k of $\lambda(\underline{x})$ along $\underline{f}(\underline{x})$ is still a scalar function, consequently it can be differentiated along another vector field $\underline{g}(\underline{x})$:

$$L_{\underline{g}}L_{\underline{f}}^k\lambda(\underline{x}) = \frac{\partial[L_{\underline{f}}^k\lambda(\underline{x})]}{\partial\underline{x}}\underline{g}(\underline{x}). \quad (4.13)$$

4.3.5.2. Lie Bracket [118]

It is defined that there are two vector fields \underline{f} and \underline{g} , both of them defined on the same space:

$$\underline{f}(\underline{x}) = \begin{bmatrix} f_1(x_1, x_2, \dots, x_n) \\ f_2(x_1, x_2, \dots, x_n) \\ \vdots \\ f_n(x_1, x_2, \dots, x_n) \end{bmatrix}, \quad \underline{g}(\underline{x}) = \begin{bmatrix} g_1(x_1, x_2, \dots, x_n) \\ g_2(x_1, x_2, \dots, x_n) \\ \vdots \\ g_n(x_1, x_2, \dots, x_n) \end{bmatrix}.$$

Then a new type of calculation can be defined as follows:

$$[\underline{f}, \underline{g}] = ad_{\underline{f}}\underline{g} = \frac{\partial\underline{g}}{\partial\underline{x}}\underline{f} - \frac{\partial\underline{f}}{\partial\underline{x}}\underline{g} \quad (4.14)$$

which is a new vector field called the Lie bracket of \underline{f} and \underline{g} .

From Eq. (4.14) it can be found that in fact the Lie bracket is the derivative of one vector field along another vector field. In Eq. (4.14) $\frac{\partial\underline{g}}{\partial\underline{x}}$ and $\frac{\partial\underline{f}}{\partial\underline{x}}$ are the Jacobian matrices of the vector fields $\underline{g}(\underline{x})$ and $\underline{f}(\underline{x})$ respectively.

4. Exact Linearization Theory

Similarly one can repeat bracketing of a vector field $\underline{g}(\underline{x})$ with the same vector field $\underline{f}(\underline{x})$ until the Lie bracket of order k is obtained:

$$\begin{aligned} ad_{\underline{f}}^2 \underline{g}(\underline{x}) &= [\underline{f}, [\underline{f}, \underline{g}]](\underline{x}) \\ &\vdots \\ ad_{\underline{f}}^k \underline{g}(\underline{x}) &= [\underline{f}, ad_{\underline{f}}^{k-1} \underline{g}](\underline{x}) \end{aligned} \quad (4.15)$$

4.3.5.3. Operation Rules of Lie Derivative and Lie Bracket

The main operation rules of Lie derivative and Lie bracket are introduced as follows [122]:

- Skew commutative: if \underline{f} and \underline{g} are vector fields then

$$[\underline{f}, \underline{g}] = -[\underline{g}, \underline{f}]. \quad (4.16)$$

- Bilinear: if \underline{f} , \underline{f}_1 , \underline{f}_2 , \underline{g} , \underline{g}_1 and \underline{g}_2 are smooth vector fields, a_1 and a_2 constant scalars then

$$\begin{aligned} [a_1 \underline{f}_1 + a_2 \underline{f}_2, \underline{g}] &= a_1 [\underline{f}_1, \underline{g}] + a_2 [\underline{f}_2, \underline{g}] \\ [\underline{f}, a_1 \underline{g}_1 + a_2 \underline{g}_2] &= a_1 [\underline{f}, \underline{g}_1] + a_2 [\underline{f}, \underline{g}_2] \end{aligned} \quad (4.17)$$

- Jacobi identity: if \underline{f} , \underline{g} and \underline{p} are vector fields then

$$[\underline{f}, [\underline{g}, \underline{p}]] + [\underline{g}, [\underline{p}, \underline{f}]] + [\underline{p}, [\underline{f}, \underline{g}]] = 0. \quad (4.18)$$

- If \underline{f} and \underline{g} are vector fields and λ is a scalar function then

$$L_{[\underline{f}, \underline{g}]} \lambda(\underline{x}) = L_{\underline{f}} L_{\underline{g}} \lambda(\underline{x}) - L_{\underline{g}} L_{\underline{f}} \lambda(\underline{x}). \quad (4.19)$$

All these operation rules of Lie derivative and Lie bracket above constitute a new type of algebraic operation called Lie Algebra.

4.3.6. Distribution and Involution of Vector Field

4.3.6.1. Distribution of Vector Field [118]

Given a group of smooth vector fields $\{\underline{f}_1, \underline{f}_2, \dots, \underline{f}_m\}$, then the distribution $\Delta(\underline{x})$ can be defined as:

$$\Delta(\underline{x}) = \text{span}\{\underline{f}_1, \underline{f}_2, \dots, \underline{f}_m\} \quad (4.20)$$

which means that $\Delta(\underline{x})$ is the spanned subspace which is expressed in terms of the linear combination of $\underline{f}_1, \underline{f}_2, \dots, \underline{f}_m$. The element of $\Delta(\underline{x})$ can be expressed as:

$$a_1\underline{f}_1 + a_2\underline{f}_2 + \dots + a_m\underline{f}_m \quad (4.21)$$

where $a_i (i = 1, 2, \dots, m)$ are scalars.

If $\underline{F}(\underline{x}) \in R^{n+m}$ is the matrix which is defined by $\{\underline{f}_1, \underline{f}_2, \dots, \underline{f}_m\}$ then

$$\Delta(\underline{x}) = \text{image}[\underline{F}(\underline{x})]. \quad (4.22)$$

It is defined that the rank $m(\underline{x})$ of $\underline{F}(\underline{x})$ is the rank of the distribution at \underline{x} . If the rank $m(\underline{x})$ is constant in one neighborhood of \underline{x} , then \underline{x} is called a regular point of the distribution, otherwise it is called a singular point. If all the points are regular, then the distribution is regular.

4.3.6.2. Involution of Vector Field [118]

It is defined that there are k n -dimensional vector fields:

$$\underline{g}_1(\underline{x}) = \begin{bmatrix} g_{11}(x_1, x_2, \dots, x_n) \\ g_{12}(x_1, x_2, \dots, x_n) \\ \vdots \\ g_{1n}(x_1, x_2, \dots, x_n) \end{bmatrix}, \dots, \underline{g}_k(\underline{x}) = \begin{bmatrix} g_{k1}(x_1, x_2, \dots, x_n) \\ g_{k2}(x_1, x_2, \dots, x_n) \\ \vdots \\ g_{kn}(x_1, x_2, \dots, x_n) \end{bmatrix}$$

4. Exact Linearization Theory

and then a matrix which is composed of these vector fields can be defined as:

$$\underline{G} = \begin{bmatrix} g_{11} & g_{21} & \cdots & g_{k1} \\ g_{12} & g_{22} & \cdots & g_{k2} \\ \vdots & \vdots & \cdots & \vdots \\ g_{1n} & g_{2n} & \cdots & g_{kn} \end{bmatrix} = \begin{bmatrix} \underline{g}_1(\underline{x}) & \underline{g}_2(\underline{x}) & \cdots & \underline{g}_k(\underline{x}) \end{bmatrix}. \quad (4.23)$$

The rank of the matrix is k at $\underline{x} = \underline{x}^0$. Furthermore if the rank of the augmented matrix $\begin{bmatrix} \underline{g}_1(\underline{x}) & \underline{g}_2(\underline{x}) & \cdots & \underline{g}_k(\underline{x}) & [\underline{g}_i(\underline{x}), \underline{g}_j(\underline{x})] \end{bmatrix}$ is still k at $\underline{x} = \underline{x}^0$ for any integers i and j ($1 \leq i, j \leq k$), then the set of the vector fields is involutive. From the perspectives of geometry involution means that: the new vector field from the Lie bracket calculation between any two vector fields of the set of the vector fields $\{\underline{g}_1, \underline{g}_2, \cdots, \underline{g}_k\}$ and the k vector fields of the set are linearly dependent. Involution distribution ensures the closure of Lie bracket calculation.

Several properties of involution are as follows [156]:

- Constant vector field is always involutive. In fact the Lie bracket of two constant vector fields is a zero vector which is the trivial linear combination of vector fields.
- The set which is composed of only one vector field is always involutive. Actually:

$$[\underline{g}, \underline{g}] = ad_{\underline{g}}\underline{g} = \frac{\partial \underline{g}}{\partial \underline{x}}\underline{g} - \frac{\partial \underline{g}}{\partial \underline{x}}\underline{g} = 0.$$

- Inspecting whether the set of the vector fields $\{\underline{g}_1, \underline{g}_2, \cdots, \underline{g}_k\}$ is involutive is equivalent to inspecting whether the following equality holds for any \underline{x} , i and j :

$$rank[\underline{g}_1(\underline{x}) \cdots \underline{g}_k(\underline{x})] = rank[\underline{g}_1(\underline{x}) \cdots \underline{g}_k(\underline{x}) [\underline{g}_i, \underline{g}_j](\underline{x})].$$

If $[\underline{g}_i, \underline{g}_j]$ can be expressed in terms of the linear combination of the vector fields $\underline{g}_1, \underline{g}_2, \cdots, \underline{g}_k$, the rank of the two matrices should be equivalent.

4.3.7. Relative Degree of Nonlinear System

It is assumed that there is a SISO nonlinear system:

$$\begin{cases} \dot{\underline{x}} = \underline{f}(\underline{x}) + \underline{g}(\underline{x}) u \\ y = h(\underline{x}) \end{cases} \quad (4.24)$$

where $\underline{x} \in R^n$ is state vector, $u \in R$ and $y \in R$ denote input and output signal of the system respectively, $\underline{f}(\underline{x})$ and $\underline{g}(\underline{x})$ are vector fields, which are sufficiently smooth, of the space R^n and $h(\underline{x})$ is a nonlinear function which is sufficiently smooth.

If:

- the value of the Lie derivative of the k -order Lie derivative of the output function $h(\underline{x})$ along the vector field $\underline{f}(\underline{x})$ along the vector field $\underline{g}(\underline{x})$ is zero in some neighborhood of $\underline{x} = \underline{x}^0$, that is

$$L_{\underline{g}} L_{\underline{f}}^k h(\underline{x}) = 0, \quad (0 \leq k < r - 1) \quad (4.25)$$

- the value of the Lie derivative of the $(r-1)$ -order Lie derivative of the output function $h(\underline{x})$ along the vector field $\underline{f}(\underline{x})$ along the vector field $\underline{g}(\underline{x})$ is not zero in some neighborhood of $\underline{x} = \underline{x}^0$, that is

$$L_{\underline{g}} L_{\underline{f}}^{r-1} h(\underline{x}) \neq 0 \quad (4.26)$$

then the nonlinear system expressed by Eq. (4.24) has relative degree r in a neighborhood of $\underline{x} = \underline{x}^0$ [156].

4.3.8. Normal Form of Linearization of Nonlinear System

Suppose the nonlinear system is described by Eq. (4.24) and the relative degree of the system is $r < n$. If the coordinate transformation can be

4. Exact Linearization Theory

expressed as: $\underline{z} = \underline{\phi}(\underline{x})$, then:

$$\left\{ \begin{array}{l} z_1 = \phi_1(\underline{x}) = h(\underline{x}) \\ z_2 = \phi_2(\underline{x}) = L_{\underline{f}}h(\underline{x}) \\ \vdots \\ z_r = \phi_r(\underline{x}) = L_{\underline{f}}^{r-1}h(\underline{x}) \\ z_{r+1} = \phi_{r+1}(\underline{x}) \\ \vdots \\ z_n = \phi_n(\underline{x}) \end{array} \right. \quad (4.27)$$

where $\phi_{r+1}, \phi_{r+2}, \dots, \phi_n$ satisfy the relations:

$$L_{\underline{f}}\phi_i(\underline{x}) = 0 \quad (r+1 \leq i \leq n) \quad (4.28)$$

and moreover the Jacobian matrix of $\underline{\phi}(\underline{x})$ at $\underline{x} = \underline{x}^0$ is nonsingular.

If it is set that:

$$\begin{aligned} a(\underline{z}) &= L_{\underline{f}}^r h(\underline{\phi}^{-1}(\underline{z})) \\ b(\underline{z}) &= L_{\underline{g}} L_{\underline{f}}^{r-1} h(\underline{\phi}^{-1}(\underline{z})) \end{aligned} \quad (4.29)$$

and

$$\begin{aligned} q_{r+1}(\underline{z}) &= L_{\underline{f}}\phi_{r+1}(\underline{\phi}^{-1}(\underline{z})) \\ &\vdots \\ q_n(\underline{z}) &= L_{\underline{f}}\phi_n(\underline{\phi}^{-1}(\underline{z})) \end{aligned} \quad (4.30)$$

4.4. Design Principles of Nonlinear Controller

then the original nonlinear system can be expressed as:

$$\begin{cases} \dot{z}_1 = z_2 \\ \dot{z}_2 = z_3 \\ \vdots \\ \dot{z}_r = a(\underline{z}) + b(\underline{z})u \\ \dot{z}_{r+1} = q_{r+1}(\underline{z}) \\ \vdots \\ \dot{z}_n = q_n(\underline{z}) \end{cases} \quad (4.31)$$

The system model described by Eq. (4.31) is called the normal form of linearization of the nonlinear system described by Eq. (4.24) [119].

4.4. Design Principles of Nonlinear Controller

4.4.1. Exact Linearization via State Feedback

In recent years research on nonlinear control system has gotten progress. The results show that with nonlinear state feedback and proper coordinate system one affine nonlinear system can be linearized exactly under certain conditions and furthermore the state feedback can ensure that the system will have good stability and dynamic characteristics [119]. In this part it will be introduced how to linearize the SISO affine nonlinear system exactly.

4.4.1.1. Linear Design Principles When Relative Degree r Is Equal to System Order n [119]

Given a SISO nonlinear system:

$$\begin{cases} \dot{\underline{x}} = \underline{f}(\underline{x}) + \underline{g}(\underline{x})u \\ y = h(\underline{x}) \end{cases} \quad (4.32)$$

4. Exact Linearization Theory

where $\underline{x} \in R^n$ is state vector, $u \in R$ and $y \in R$ are control input and output of the nonlinear system respectively, $\underline{f}(\underline{x})$ and $\underline{g}(\underline{x})$ are sufficiently smooth vector fields of R^n and $h(\underline{x})$ is sufficiently smooth nonlinear function.

Suppose the relative degree r of the nonlinear system is equal to the system order n i.e. $r = n$. According to the discussion in §4.3.7 one can choose the coordinate transformation as follows:

$$\underline{z} = \underline{\phi}(\underline{x}) = \begin{bmatrix} h(\underline{x}) \\ L_{\underline{f}}h(\underline{x}) \\ \vdots \\ L_{\underline{f}}^{r-1}h(\underline{x}) \end{bmatrix} \quad (4.33)$$

so as to linearize the original nonlinear system to the normal form as follows:

$$\begin{cases} \dot{z}_1 = z_2 \\ \dot{z}_2 = z_3 \\ \vdots \\ \dot{z}_{n-1} = z_n \\ \dot{z}_n = \alpha(\underline{x}) + \beta(\underline{x})u \Big|_{\underline{x}=\underline{\phi}^{-1}(\underline{z})} \end{cases} \quad (4.34)$$

where $\alpha(\underline{x})$ and $\beta(\underline{x})$ are nonlinear scalar functions of \underline{x} . In the normal form described by Eq. (4.34), the last equation $\dot{z}_n = \alpha(\underline{x}) + \beta(\underline{x})u \Big|_{\underline{x}=\underline{\phi}^{-1}(\underline{z})}$ which contains the control variable u is nonlinear while all the other equations, none of which contain the control variable u , are linearized.

In order to linearize the system described by Eq. (4.34) exactly and completely, It is defined that:

$$v = \alpha(\underline{x}) + \beta(\underline{x})u \quad (4.35)$$

and from §4.3.7 and §4.3.8 it can be known that:

$$\begin{aligned} \alpha(\underline{x}) &= L_{\underline{f}}^n h(\underline{x}) \\ \beta(\underline{x}) &= L_{\underline{g}} L_{\underline{f}}^{n-1} h(\underline{x}) \neq 0 \end{aligned}$$

4.4. Design Principles of Nonlinear Controller

Consequently two conclusions are obtained as follows:

- The completely controllable and exactly linearized system described by the new coordinate system $\underline{z} = [z_1 \ z_2 \ \cdots \ z_n]^T$ is achieved:

$$\begin{cases} \dot{z}_1 = z_2 \\ \dot{z}_2 = z_3 \\ \vdots \\ \dot{z}_{n-1} = z_n \\ \dot{z}_n = v \end{cases} \quad (4.36)$$

Eq. (4.36) is called Brunovszky normal form [156] and can be expressed as:

$$\dot{\underline{z}} = \underline{A}\underline{z} + \underline{b}v \quad (4.37)$$

$$\text{where } \underline{A} = \begin{pmatrix} 0 & 1 & 0 & \cdots & 0 & 0 \\ 0 & 0 & 1 & \cdots & 0 & 0 \\ \vdots & \vdots & \vdots & \vdots & \vdots & \vdots \\ 0 & 0 & 0 & \cdots & 0 & 1 \\ 0 & 0 & 0 & \cdots & 0 & 0 \end{pmatrix}, \underline{b} = \begin{bmatrix} 0 \\ 0 \\ \vdots \\ 0 \\ 1 \end{bmatrix} \text{ and } \underline{z} = \begin{bmatrix} z_1 \\ z_2 \\ \vdots \\ z_{n-1} \\ z_n \end{bmatrix}.$$

- The expression of the control variable u can be achieved as:

$$u = -\frac{\alpha(\underline{x})}{\beta(\underline{x})} + \frac{1}{\beta(\underline{x})}v. \quad (4.38)$$

In Eq. (4.38) only v remains to be ascertained however the value of v can be determined by a lot of methods such as pole assignment, linear optimal control, ITAE (integral of time-weighted absolute error) and so on. Since the control variable u of the system expressed by Eq. (4.32) and the control variable v of the exactly linearized system expressed by Eq. (4.37) have the relationship shown in Eq. (4.38), once the control variable v is determined then the control variable u is determined according to Eq. (4.38).

4. Exact Linearization Theory

4.4.1.2. Linear Design Principles in General Case [119]

In some cases of reality the output equation of the system is indeterminate. Sometimes the physical meaning of the output equation of the system is determinate but the relative degree r is less than the system order n . In these two cases it is difficult to write out the output equation or it is impossible to linearize the original nonlinear system into the Brunovszky normal form by utilizing the known output equation. At this time one can try to find out a new output equation of the system such that the relative degree r of the original system according to the new output equation is equal to the system order n and then the system can be linearized exactly with the method introduced in §4.4.1.1. It is proved that under certain condition this kind of output equation exists [119].

4.4.2. Design Principles and Methods Based on Zero Dynamics

The design principles based on exact linearization via state feedback is introduced in §4.4.1. This method compensates or counteracts the nonlinear characteristics of the original system dynamically so as to transform the original system into the controllable linear system which has satisfying dynamic characteristics. Nevertheless the control law designed according to this method is complicated and the solving process is tedious. Consequently in this section the design method based on zero dynamics is introduced. It is not necessary to exact linearize all the state equations with this method. Generally speaking the dynamic behavior of one system can be divided into two parts: internal dynamics and external dynamics. From an application standpoint the external state of the system is more important which means that the external states should have good stability and dynamic performance while the internal states only need to be stable. The control law based on this method is simple and practical and moreover this is the basic thinking of the zero dynamics design method [157]. The design principles and methods based on zero dynamics are introduced as follows.

4.4.2.1. The First Design Method Based on Zero Dynamics [119]

Given a SISO nonlinear system:

$$\begin{cases} \dot{\underline{x}} = \underline{f}(\underline{x}) + \underline{g}(\underline{x}) u \\ y = h(\underline{x}) \end{cases}$$

where $\underline{x} \in R^n$ is state vector, $u \in R$ and $y \in R$ are control input and output of the nonlinear system respectively, $\underline{f}(\underline{x})$ and $\underline{g}(\underline{x})$ are sufficiently smooth vector fields of R^n and $h(\underline{x})$ is sufficiently smooth nonlinear function. The relative degree r of the system according to output equation $y = h(\underline{x})$ is less than the system order n . Thus the system can be transformed into the normal form as follows with the mapping $\underline{z} = \underline{\phi}(\underline{x})$:

$$\begin{cases} \dot{z}_1 = z_2 \\ \dot{z}_2 = z_3 \\ \vdots \\ \dot{z}_r = L_{\underline{f}}^r h(\underline{\phi}^{-1}(\underline{z})) + L_{\underline{g}} L_{\underline{f}}^{r-1} h(\underline{\phi}^{-1}(\underline{z})) u \\ \dot{z}_{r+1} = L_{\underline{f}} \phi_{r+1}(\underline{\phi}^{-1}(\underline{z})) \\ \vdots \\ \dot{z}_n = L_{\underline{f}} \phi_n(\underline{\phi}^{-1}(\underline{z})) \end{cases} \quad (4.39)$$

where

$$\underline{\phi}(\underline{x}) = \begin{bmatrix} \phi_1(\underline{x}) \\ \phi_2(\underline{x}) \\ \vdots \\ \phi_r(\underline{x}) \\ \phi_{r+1}(\underline{x}) \\ \vdots \\ \phi_n(\underline{x}) \end{bmatrix} = \begin{bmatrix} z_1 \\ z_2 \\ \vdots \\ z_r \\ z_{r+1} \\ \vdots \\ z_n \end{bmatrix} = \begin{bmatrix} h(\underline{x}) \\ L_{\underline{f}} h(\underline{x}) \\ \vdots \\ L_{\underline{f}}^{r-1} h(\underline{x}) \\ \phi_{r+1}(\underline{x}) \\ \vdots \\ \phi_n(\underline{x}) \end{bmatrix}$$

4. Exact Linearization Theory

and the selected functions $\phi_{r+1}(\underline{x}), \phi_{r+2}(\underline{x}), \dots, \phi_n(\underline{x})$ satisfy the relations:

$$L_{\underline{g}}\phi_{r+1}(\underline{x}) = L_{\underline{g}}\phi_{r+2}(\underline{x}) = \dots = L_{\underline{g}}\phi_n(\underline{x}) = 0 \quad (4.40)$$

and furthermore the Jacobian matrix of $\underline{\phi}(\underline{x})$ is nonsingular.

Generally speaking one can select output equation $h(\underline{x}(t))$ such that the value of the equation at the equilibrium point \underline{x}^0 is zero. Thus the output $y(t) = h(\underline{x}(t))$ is the dynamic deviation between the actual output (dynamic response) of the system and the equilibrium point output. If one can use some control strategy to make sure that the dynamic deviation of the system output is zero at any time which means:

$$y(t) = h(\underline{x}(t)) = 0 \quad (0 \leq t \leq \infty) \quad (4.41)$$

thus from the perspectives of the external dynamics of control system, the system is highly stable so that the output remains constant with any interferences. The conditions which can ensure that the system output remains zero at any time contain two aspects:

- The external dynamics of the system are asymptotically stable.
- The system output has the optimal dynamic performance because zero is always less than or equal to the minimum value of quadratic form performance function.

Since $y(t) = z_1(t)$ is set to be zero at any time, the following can be achieved

$$z_2(t) = \dot{z}_1(t) = 0. \quad (4.42)$$

In the same way $z_3(t), z_4(t), \dots, z_r(t)$ are always zero, hence

$$\dot{z}_r = L_{\underline{f}}^r h(\underline{x}) + L_{\underline{g}} L_{\underline{f}}^{r-1} h(\underline{x}) u = 0. \quad (4.43)$$

According to Eq. (4.43) the control variable u can be calculated by

$$u = -\frac{L_{\underline{f}}^r h(\underline{x})}{L_{\underline{g}} L_{\underline{f}}^{r-1} h(\underline{x})}. \quad (4.44)$$

4.4. Design Principles of Nonlinear Controller

Consequently under this condition, the first r equations are always equal to zero and the rest dynamic equations are given by

$$\begin{cases} \dot{z}_{r+1} = L_{\underline{f}}\phi_{r+1}(0, 0, \dots, 0, z_{r+1}, z_{r+2}, \dots, z_n) \\ \dot{z}_{r+2} = L_{\underline{f}}\phi_{r+2}(0, 0, \dots, 0, z_{r+1}, z_{r+2}, \dots, z_n) \\ \vdots \\ \dot{z}_n = L_{\underline{f}}\phi_n(0, 0, \dots, 0, z_{r+1}, z_{r+2}, \dots, z_n) \end{cases} \quad (4.45)$$

Since the external dynamics of the system is identically equal to zero under the action of control law described by Eq. (4.44), the differential equations given by Eq. (4.45) describe the internal dynamic behavior of the system and are called zero dynamic equations (in short, zero dynamics) of the original system. If the zero dynamics are stable then under the action of control law described by Eq. (4.44) the whole system is stable and the output of the system remains constant with any disturbances.

4.4.2.2. The Second Design Method Based on Zero Dynamics [119]

The first design method based on zero dynamics need solve the partial differential equations

$$L_{\underline{f}}\phi_i(\underline{x}) = 0 \quad (r + 1 \leq i \leq n)$$

to obtain the solutions of $z_{r+1} = \phi_{r+1}(\underline{x})$, $z_{r+2} = \phi_{r+2}(\underline{x})$, \dots , $z_n = \phi_n(\underline{x})$. However in general case it is difficult to solve partial differential equations. Therefore to avoid solving partial differential equations one can utilize the

4. Exact Linearization Theory

incomplete normal form given by

$$\begin{cases} \dot{z}_1 = z_2 \\ \dot{z}_2 = z_3 \\ \vdots \\ \dot{z}_{r-1} = z_r \\ \dot{z}_r = L_{\underline{f}}^r h(\underline{\phi}^{-1}(\underline{z})) + L_{\underline{g}} L_{\underline{f}}^{r-1} h(\underline{\phi}^{-1}(\underline{z})) u \\ \dot{z}_{r+1} = \underline{q}(\underline{\xi}, \underline{\eta}) + \underline{p}(\underline{\xi}, \underline{\eta}) u \end{cases} \quad (4.46)$$

where

$$\underline{q}(\underline{\xi}, \underline{\eta}) = \begin{bmatrix} q_{r+1}(\underline{z}) \\ q_{r+2}(\underline{z}) \\ \vdots \\ q_n(\underline{z}) \end{bmatrix} = \begin{bmatrix} L_{\underline{f}} \phi_{r+1}(\underline{\phi}^{-1}(\underline{x})) \\ L_{\underline{f}} \phi_{r+2}(\underline{\phi}^{-1}(\underline{x})) \\ \vdots \\ L_{\underline{f}} \phi_n(\underline{\phi}^{-1}(\underline{x})) \end{bmatrix}$$

$$\underline{\xi} = [z_1 \ z_2 \ \cdots \ z_r]^T$$

$$\underline{\eta} = [z_{r+1} \ z_{r+2} \ \cdots \ z_n]^T.$$

Since the state feedback variable can force the output of the system to be identically equal to zero i.e. when one applies the state feedback expression above to control the system, the states can be forced to satisfy the constraint conditions as follows

$$\begin{cases} y(t) = h(\underline{x}(t)) = 0 \\ \dot{y}(t) = L_{\underline{f}} h(\underline{x}(t)) = 0 \\ \vdots \\ y^{(r-1)}(t) = L_{\underline{f}}^{r-1} h(\underline{x}(t)) = 0 \end{cases} \quad (4.47)$$

where r is the relative degree of the system.

4.4.2.3. Discussion of Several Problems about Zero Dynamics [119]

(1) About Control Variable

The state feedback control variables achieved by the first design method and the second design method based on zero dynamics have the same form which can be written as

$$u = - \frac{L_{\underline{f}}^r h(\underline{\phi}^{-1}(\underline{z}))}{L_{\underline{g}} L_{\underline{f}}^{r-1} h(\underline{\phi}^{-1}(\underline{z}))} \Big|_{\underline{z}=\underline{\phi}(\underline{x})}.$$

Nevertheless the coordinate transformations utilized by the two design methods are different hence actually the state feedback variables are different. The state feedback control variable above can be expressed with the coordinate system X of the original system as

$$u = - \frac{L_{\underline{f}}^r h(\underline{x})}{L_{\underline{g}} L_{\underline{f}}^{r-1} h(\underline{x})}.$$

Since this state feedback variable can force the output $y(t) = h(\underline{x}(t))$ of the system to be identically equal to zero which means that when the state feedback variable $u(\underline{x}(t))$ expressed above is used to control the system, the state $\underline{x}(t)$ can be forced to satisfy the constraint conditions in the following

$$\begin{cases} y(t) = h(\underline{x}(t)) = 0 \\ \dot{y}(t) = L_{\underline{f}} h(\underline{x}(t)) = 0 \\ \vdots \\ y^{(r-1)}(t) = L_{\underline{f}}^{r-1} h(\underline{x}(t)) = 0 \end{cases}$$

where r is the relative degree of the system.

(2) Advantages and Disadvantages of the Two Design Methods Based on Zero Dynamics

4. Exact Linearization Theory

When one uses the two design methods the selections of the coordinate transformations $z_{r+1}, z_{r+2}, \dots, z_n$ are different:

$$\begin{cases} z_{r+1} = \phi_{r+1}(\underline{x}) \\ z_{r+2} = \phi_{r+2}(\underline{x}) \\ \vdots \\ z_n = \phi_n(\underline{x}) \end{cases}$$

hence the zero dynamic equations of the system are not the same. Generally speaking when researchers utilize the first design method, they have to solve the partial differential equations

$$L_{\underline{f}}\phi_i(\underline{x}) = 0 \quad (r + 1 \leq i \leq n)$$

of which the solving process are complicated nevertheless the zero dynamic equations obtained by the first method are more simple than those obtained by the second method consequently it is much easier to analyze the zero dynamic equations with the first method. Therefore each of the two methods has its own advantages and disadvantages and one should select the proper method according to the actual system.

(3) Limitations of the Design Method Based on Zero Dynamics [157]

The design method based on zero dynamics has limitations because the control law obtained by this method can not ensure the stability of the zero dynamic equations of the system. If the zero dynamics of the system are unstable one has to modify the scheme according to the system structure or design the control law of the nonlinear system anew with other methods to make sure that the zero dynamics of the system are stable. Furthermore this method is limited by the system order such that this method is not suitable for the system which has high order state equations. When researchers utilize the zero dynamic method to obtain the control law of the high order nonlinear system it is difficult for them to achieve the ultimate zero dynamic equations which are the expression with linear equations after coordinate transformation. Hence it is difficult to verify whether the zero dynamics are stable and whether the control law is suitable.

4.5. Disturbance Decoupling and Attenuation

Strictly speaking, any practical system in the real world works under the effects of external disturbance. Consequently the study on anti-disturbance has great significance. In this section the principles when and how can one eliminate or weaken the influence of the external disturbance based on the state feedback linearization theory will be introduced.

4.5.1. Disturbance Decoupling

4.5.1.1. Disturbance Relative Degree [119]

Considering one type of SISO nonlinear system:

$$\begin{cases} \dot{\underline{x}} = \underline{f}(\underline{x}) + \underline{g}(\underline{x})u + \underline{p}(\underline{x})w \\ y = h(\underline{x}) \end{cases} \quad (4.48)$$

where $\underline{x} \in R^n$ is state vector, $u \in R$ and $y \in R$ are control input and output of the nonlinear system respectively, $w \in R$ is external disturbance, $\underline{f}(\underline{x})$, $\underline{g}(\underline{x})$ and $\underline{p}(\underline{x})$ are sufficiently smooth vector fields of R^n and $h(\underline{x})$ is sufficiently smooth nonlinear function. The objective is to find a static state feedback control as

$$u = a(\underline{x}) + b(\underline{x})v \quad (4.49)$$

where $a(\underline{x})$ and $b(\underline{x})$ are the functions of system states respectively and v is the new control input so that the output y of the system expressed by Eq. (4.48) and Eq. (4.49) is completely independent of the disturbance w .

To solve this problem one has to define the disturbance relative degree. Considering the system (4.48), it can be defined that the system has the relative degree ρ with respect to disturbance w in a neighborhood of $\underline{x} = \underline{x}^0$ if

$$L_{\underline{p}}L_{\underline{f}}^k h(\underline{x}) = 0, \quad (0 \leq k < \rho - 1) \text{ and } L_{\underline{p}}L_{\underline{f}}^{\rho-1} h(\underline{x}) \neq 0.$$

4. Exact Linearization Theory

4.5.1.2. Disturbance Decoupling [119]

Proposition 4.1. Suppose the system (4.48) has the relative degree r and the relative degree ρ with respect to disturbance w , the state feedback control $u = a(\underline{x}) + b(\underline{x})v$ can be found so that the system output y is decoupled from the disturbance input w if and only if $r < \rho$.

The proof of this proposition is given in [119]. If system (4.48) satisfies this proposition, one can choose the coordinate transformation (4.27) and then the system can be written as:

$$\begin{cases} \dot{z}_1 = z_2 \\ \dot{z}_2 = z_3 \\ \vdots \\ \dot{z}_{r-1} = z_r \\ \dot{z}_r = L_f^r h(\underline{\phi}^{-1}(\underline{z})) + L_g L_f^{r-1} h(\underline{\phi}^{-1}(\underline{z})) u \\ \dot{\underline{\eta}} = \underline{q}(\underline{\xi}, \underline{\eta}) + \underline{k}(\underline{\xi}, \underline{\eta}) w \end{cases}$$

and

$$y = z_1$$

where $\underline{\xi} = [z_1 \ z_2 \ \cdots \ z_r]^T$ and $\underline{\eta} = [z_{r+1} \ z_{r+2} \ \cdots \ z_n]^T$.

If one chooses the state feedback as follows:

$$u = -\frac{L_f^r h(\underline{\phi}^{-1}(\underline{z}))}{L_g L_f^{r-1} h(\underline{\phi}^{-1}(\underline{z}))} + \frac{1}{L_g L_f^{r-1} h(\underline{\phi}^{-1}(\underline{z}))} v \quad (4.50)$$

4.5. Disturbance Decoupling and Attenuation

then with this feedback the system can be described by:

$$\left\{ \begin{array}{l} \dot{z}_1 = z_2 \\ \dot{z}_2 = z_3 \\ \vdots \\ \dot{z}_{r-1} = z_r \\ \dot{z}_r = v \\ \dot{\underline{\eta}} = \underline{q}(\underline{\xi}, \underline{\eta}) + \underline{k}(\underline{\xi}, \underline{\eta})w \end{array} \right. \quad (4.51)$$

from which it can be found that the system output y i.e. the state variable z_1 is decoupled from the external disturbance w completely.

4.5.2. Disturbance Attenuation

When the system does not satisfy the proposition 4.1 one can not eliminate the influence of external disturbance on the system output completely. Hence one can only choose to reduce the influence of external disturbance to the acceptable level. This is called disturbance attenuation.

There are several linear control methods which can realize disturbance attenuation. Since the original nonlinear system can be treated as a linear system after exact linearization via state feedback one can use these linear control methods. Consequently in this section sliding mode variable structure control theory will be used to design the controller for the linear system after linearization so as to reduce the disturbance effects.

4.5.2.1. Sliding Mode Variable Structure Control Theory [158]

Linear system plays an important role in modern control theory and application and its theory develops quite well. Sliding mode variable structure control theory is one of the important research results. The principle of sliding mode variable structure control is to design the switching hyperplane and reaching law so that the system can reach the hyperplane. Once

4. Exact Linearization Theory

the system reaches the hyperplane and makes sliding mode motion on the hyperplane, it will have strong robustness. Hence when conventional feedback controller with variable structure control is used, one can improve the anti-disturbance ability of the system.

The basic steps of designing sliding mode variable structure controller are:

- (1) Designing switching function so that the sliding mode dynamics which is determined by this function is asymptotically stable and has good dynamic characteristics.
- (2) Selecting proper control law so that the system can reach the switching hyperplane and realize sliding mode motion on the hyperplane.

Considering the single input linear system:

$$\dot{\underline{x}} = \underline{A}\underline{x} + \underline{b}u \quad (4.52)$$

where $\underline{x} \in R^n$ is state vector, $u \in R$ is control input, \underline{A} and \underline{b} are matrix and vector with corresponding dimensions and $\text{rank}\underline{b} = 1$. The switching function is selected as $s = \underline{c}^T \underline{x}$ where \underline{c} is $n \times 1$ undetermined coefficient vector.

Since $\text{rank}\underline{b} = 1$ there exists a nonsingular linear transformation $\underline{x} = \underline{M}\underline{z}$ so that system (4.52) can be described by

$$\begin{bmatrix} \dot{z}_1 \\ \dot{z}_2 \end{bmatrix} = \begin{bmatrix} \underline{A}_{11} & \underline{a}_{12} \\ \underline{A}_{21} & \underline{a}_{22} \end{bmatrix} \begin{bmatrix} z_1 \\ z_2 \end{bmatrix} + \begin{bmatrix} 0 \\ b_2 \end{bmatrix} u \quad (4.53)$$

where $z_1 \in R^{n-1}$, $z_2 \in R$ and b_2 is non-zero real number. Furthermore one can derive:

$$\underline{M}^{-1}\underline{A}\underline{M} = \begin{bmatrix} \underline{A}_{11} & \underline{a}_{12} \\ \underline{A}_{21} & \underline{a}_{22} \end{bmatrix}; \quad \underline{M}^{-1}\underline{b} = \begin{bmatrix} 0 \\ b_2 \end{bmatrix}. \quad (4.54)$$

With this transformation, the corresponding switching surface is

$$s = \underline{c}^T \underline{M}\underline{z} = \underline{c}_1^T \underline{z}_1 + c_2 z_2 = 0 \quad (4.55)$$

4.5. Disturbance Decoupling and Attenuation

where c_2 is non-zero real number. Consequently on the switching surface one can have

$$z_2 = -c_2^{-1} \underline{c}_1^T \underline{z}_1 = -\underline{d}^T \underline{z}_1. \quad (4.56)$$

Consequently the sliding mode motion equation satisfies Eq. (4.56) and the reduced-order equation as follow:

$$\dot{\underline{z}}_1 = \underline{A}_{11} \underline{z}_1 + \underline{a}_{12} z_2. \quad (4.57)$$

Thereupon the sliding mode of the linear system can be treated as a $n - 1$ dimensional subsystem described by Eq. (4.57) with the feedback (4.56). Thus one can calculate the feedback vector \underline{d} with the usual linear feedback design methods such as pole assignment method, optimal method, eigenvector assignment method, geometric method and so on. Finally one can get the coefficient vector \underline{c} of the switching function $s = \underline{c}^T \underline{x}$. When the system realize sliding mode motion z_2 can be expressed by \underline{z}_1 linearly, therefore once \underline{z}_1 inclines to zero with proper exponential decay rate, z_2 will incline to zero with the same exponential decay rate. If it is defined that $c_2 = 1$ then $\underline{c}_1 = \underline{d}$. Consequently according to Eq. (4.55) the switching coefficient matrix, which can make sure that the sliding mode of the original linear system has good dynamic characteristics, can be calculated by

$$\underline{c}^T = (\underline{d}^T, 1) \underline{M}^{-1}. \quad (4.58)$$

When researchers design the switching function $s = \underline{c}^T \underline{x}$ and get the switching hyperplane $s = 0$, the next step is to design the reaching law so that the system can move to the hyperplane. This motion is called reaching motion.

There are four typical reaching laws:

(1) Constant reaching law

$$\dot{s} = -\varepsilon \cdot \text{sgn}(s), \quad \varepsilon > 0 \quad (4.59)$$

where ε is the reaching rate with which the system moves to the hyperplane. The smaller ε is, the lower the reaching rate is. Conversely the bigger

4. Exact Linearization Theory

ε is, the more quickly the system will move to the hyperplane nevertheless the more serious the chattering of the system will be.

(2) Exponential reaching law

$$\dot{s} = -\varepsilon \cdot \text{sgn}(s) - k \cdot s, \quad \varepsilon > 0, k > 0 \quad (4.60)$$

where $-k \cdot s$ is the exponential reaching part because the solution of the equation $\dot{s} = -k \cdot s$ is $s = s(0)e^{-kt}$. This part ensures that the system can reach the hyperplane quickly and moreover when the system is near the hyperplane the reaching rate is low. In exponential reaching law, to increase reaching rate and eliminate chattering one should increase k and decrease ε .

(3) Power reaching law

$$\dot{s} = -k|s|^\alpha \text{sgn}(s), \quad k > 0, 0 < \alpha < 1 \quad (4.61)$$

which ensures that the working point of the system can enter into the sliding mode smoothly.

(4) General reaching law

$$\dot{s} = -\varepsilon \cdot \text{sgn}(s) - f(s), \quad \varepsilon > 0 \quad (4.62)$$

where $f(0) = 0$ and when $s \neq 0, sf(s) > 0$.

Aiming at the linear system (4.52), with some reaching law the control input u can be derived as follows.

Based on the switching function $s = \underline{c}^T \underline{x}$ one can get:

$$\dot{s} = \underline{c}^T \dot{\underline{x}} = slaw \quad (4.63)$$

where $slaw$ is some reaching law.

Substituting Eq. (4.52) into Eq. (4.63) yields

$$u = (\underline{c}^T \underline{b})^{-1} (-\underline{c}^T \underline{A}x + slaw). \quad (4.64)$$

4.5.2.2. Sliding Mode Variable Structure Control Based on Exact Linearization

Considering the SISO nonlinear system (4.48), it is assumed that the system satisfies the matching condition:

$$\text{rank}[\underline{g}, \underline{p}] = \text{rank}[\underline{g}] = 1. \quad (4.65)$$

Then the design problem of the sliding mode dynamic characteristics is considered. Supposing the relative degree of the system is r , according to the matching condition (4.65) one can define

$$\underline{p} = a \cdot \underline{g}$$

where $a \in R$ is a constant. Thus one can have

$$L_{\underline{p}} L_{\underline{f}}^k h(\underline{x}) = \frac{\partial L_{\underline{f}}^k h(\underline{x})}{\partial \underline{x}} \cdot \underline{p} = a \cdot \frac{\partial L_{\underline{f}}^k h(\underline{x})}{\partial \underline{x}} \cdot \underline{g} = a \cdot L_{\underline{g}} L_{\underline{f}}^k h(\underline{x}) = 0, \quad (0 \leq k < r - 1).$$

If the relative degree of the system r is equal to the system order n , one can select the coordinate transformation (4.33) and the original nonlinear system can be expressed by

$$\dot{\underline{z}} = \underline{A}\underline{z} + \underline{b}v + \underline{e}w \quad (4.66)$$

$$\text{where } \underline{A} = \begin{pmatrix} 0 & 1 & 0 & \cdots & 0 & 0 \\ 0 & 0 & 1 & \cdots & 0 & 0 \\ \vdots & \vdots & \vdots & \vdots & \vdots & \vdots \\ 0 & 0 & 0 & \cdots & 0 & 1 \\ 0 & 0 & 0 & \cdots & 0 & 0 \end{pmatrix}, \underline{b} = \begin{bmatrix} 0 \\ 0 \\ \vdots \\ 0 \\ 1 \end{bmatrix}, \underline{e} = \begin{bmatrix} 0 \\ 0 \\ \vdots \\ 0 \\ L_{\underline{p}} L_{\underline{f}}^{n-1} h(\underline{x}) \end{bmatrix},$$

$$v = L_{\underline{f}}^n h(\underline{x}) + L_{\underline{g}} L_{\underline{f}}^{n-1} h(\underline{x})u \text{ and } \underline{z} = [z_1 \ z_2 \ \cdots \ z_n]^T.$$

Thus with the new coordinate system, one can select the switching function as:

$$s(\underline{z}) = \sum_{i=1}^{n-1} c_i z_i + z_n. \quad (4.67)$$

4. Exact Linearization Theory

Hence when the system makes sliding mode motion, one can have:

$$z_n = - \sum_{i=1}^{n-1} c_i z_i \quad (4.68)$$

and the sliding mode equation is given by

$$\begin{bmatrix} \dot{z}_1 \\ \dot{z}_2 \\ \vdots \\ \dot{z}_{n-1} \end{bmatrix} = \begin{bmatrix} 0 & 1 & 0 & \cdots & 0 & 0 \\ 0 & 0 & 1 & \cdots & 0 & 0 \\ \vdots & \vdots & \vdots & \vdots & \vdots & \vdots \\ 0 & 0 & 0 & \cdots & 0 & 1 \\ 0 & 0 & 0 & \cdots & 0 & 0 \end{bmatrix} \begin{bmatrix} z_1 \\ z_2 \\ \vdots \\ z_{n-1} \end{bmatrix} + \begin{bmatrix} 0 \\ 0 \\ \vdots \\ 0 \\ 1 \end{bmatrix} z_n. \quad (4.69)$$

Thereupon one can derive a linear subsystem described by Eq. (4.69) with the feedback (4.68). Consequently according to §4.5.2.1 one can calculate the parameters c_i ($1 \leq i \leq n-1$) and further the control input v of the linear system. Finally with Eq. (4.38) one can get the control input u of the original nonlinear system.

It is noticed that the system (4.66) satisfies the matching condition:

$$\text{rank}[\underline{b}, \underline{e}] = \text{rank} \underline{b} = 1$$

hence the sliding mode of the system will not be influenced by the disturbance [20].

If the relative degree of the system r is not equal to the system order n , one can select a new output equation of the system so as to realize exact linearization according to §4.4.1.2 and the detailed content is given in [119]. Then based on the exact linearization result one can design the sliding mode variable structure controller with the method mentioned above.

4.6. Summary

In this chapter firstly the development of nonlinear control theory is introduced. One of the core ideas of modern nonlinear control theory is to

4.6. Summary

exactly linearize or partially linearize the nonlinear system with proper coordinate transformation and state feedback. Consequently several basic conceptions of exact linearization theory are presented. These conceptions are linked closely. Moreover since affine nonlinear system is often used in practical engineering, the controller design methods of SISO affine nonlinear system are then discussed. One of the methods is based on exact linearization via state feedback and the other is based on zero dynamics. Finally since all the control systems have to work with external disturbance, the disturbance decoupling and attenuation strategies are discussed.

4. Exact Linearization Theory

5. Design and Simulation of Control System Based on Exact Linearization

In Chapter 3 the nonlinear model of the electro-hydraulic servo position control system is built and in Chapter 4 the nonlinear control theory and the design principles of nonlinear controller are introduced. In this chapter the nonlinear control theory will be applied in the SISO nonlinear electro-hydraulic servo position control system. Particularly the contributions of this chapter are as follows:

- applying exact linearization method based on differential geometry in SISO nonlinear electro-hydraulic servo position control system;
- comparing control performances of SISO nonlinear electro-hydraulic servo position control system with exact linearization method and approximate linearization method;
- analyzing robustness of the nonlinear controller of SISO nonlinear electro-hydraulic servo position control system with exact linearization method;
- combining sliding mode variable structure control method and exact linearization method so as to attenuate the influence of external disturbance.

5.1. Feasibility of Application of Exact Linearization via State Feedback in Electro-Hydraulic Servo System

In practical control system there is a class of simple and common nonlinear systems which is called affine nonlinear system. This kind of nonlinear system has a nonlinear relationship with the system state \underline{x} while has a linear relationship with the control variable u [122]. For affine nonlinear system, many research achievements about exact linearization with nonlinear state feedback and local differential homeomorphism transform are obtained so as to replace the original nonlinear system with the equivalent linear system. The control variable of the equivalent linear system can be determined based on linear control theory and then the control variable of the original nonlinear system is obtained by using coordinate transformation. Practical application shows that almost all the hydraulic servo systems are affine nonlinear system [159] therefore the application of exact linearization control via state feedback in hydraulic servo system is feasible. Furthermore the application and popularization of computer control technology lays a foundation for engineering application of exact linearization control via state feedback. Since most of the hydraulic servo systems are required that the output $y(t)$ can track the reference signal $r(t)$ with external disturbance, $y(t)$ can be selected as the output function $h(\underline{x}(t))$ of the nonlinear system. Consequently in this chapter the exact linearization method via state feedback based on the geometric control theory of nonlinear system will be applied to design controller.

5.2. Building the Nonlinear Model

Electro-hydraulic servo position control system contains many nonlinear factors hence essentially it is a type of nonlinear system. One of the important characteristics of nonlinear system is that the response of the system depends on the form and amplitude of system input. Nonlinear factors may

5.2. Building the Nonlinear Model

cause static error and self-sustained oscillation. When self-sustained oscillation happens, system precision will be influenced seriously and system energy will be consumed unnecessarily. Furthermore self-sustained oscillation will cause abrasion and deformation of mechanical components thus the life span of the system will be shorted.

The nonlinear factors of electro-hydraulic servo position control system can be divided into two types. The first type is the flow-pressure characteristics of electro-hydraulic servo valve and the second type contains several typical nonlinearities such as saturation nonlinearity, dead zone nonlinearity, backlash nonlinearity, hysteretic nonlinearity and so on. In this chapter only the first type of nonlinear factors will be analyzed.

According to the system equations built in §3.1, one can build the nonlinear model for the electro-hydraulic servo position control system.

Generally speaking the frequency width of electro-hydraulic servo valve is higher than 80 Hz while the frequency width of position control system is only 5...20 Hz. Consequently according to the simplification result in [160] the electro-hydraulic servo valve can be treated as a proportional component. Thus Eq. (3.30) can be reduced to

$$x_v = K_{sc} \times i. \quad (5.1)$$

Substituting Eq. (5.1) into Eq. (3.10) yields

$$q_l = C_v K_{sc} i \sqrt{\frac{1}{\rho} [p_s - \text{sign}(i) p_l]}. \quad (5.2)$$

According to Eq. (5.2), Eq. (3.18) and Eq. (3.19), the physical equations of the system can be written as

$$\begin{cases} A p_l = m_t \ddot{x}_p + B_p \dot{x}_p + K x_p + F_l \\ C_v K_{sc} i \sqrt{\frac{1}{\rho} [p_s - \text{sign}(i) p_l]} = A \dot{x}_p + \frac{V_t}{4K_o} \dot{p}_l + C_{tp} p_l \end{cases}. \quad (5.3)$$

5. Design and Simulation of Control System Based on Exact Linearization

It is selected that $x_1 = x_p$, $x_2 = \dot{x}_p$ and $x_3 = p_l$ thus according to Eq. (5.3) one can derive the state equation

$$\begin{cases} \dot{x}_1 = x_2 \\ \dot{x}_2 = \frac{1}{m_t}(-Kx_1 - B_p x_2 + Ax_3 - F_l) \\ \dot{x}_3 = \frac{4K_0}{V_t}(-Ax_2 - C_{tp}x_3 + \hat{K}\sqrt{p_s - \text{sign}(i)x_3}i) \end{cases} \quad (5.4)$$

where $\hat{K} = C_v K_{sc} \sqrt{\frac{1}{\rho}}$ and the output equation

$$y = x_p = x_1. \quad (5.5)$$

5.3. Simplified Nonlinear Model

According to the content in §3.1 one can have $K = 0$ and $B_p = 0$, then the state equation can be reduced to

$$\begin{cases} \dot{x}_1 = x_2 \\ \dot{x}_2 = \frac{1}{m_t}(Ax_3 - F_l) \\ \dot{x}_3 = \frac{4K_0}{V_t}(-Ax_2 - C_{tp}x_3 + \hat{K}\sqrt{p_s - \text{sign}(i)x_3}i) \end{cases} \quad (5.6)$$

and the output equation is $y = x_p = x_1$. Hence one can get

$$\begin{cases} \dot{\underline{x}} = \begin{bmatrix} x_2 \\ \frac{A}{m_t}x_3 - \frac{F_l}{m_t} \\ -\frac{4AK_0}{V_t}x_2 - \frac{4K_0C_{tp}}{V_t}x_3 \end{bmatrix} + \begin{bmatrix} 0 \\ 0 \\ \frac{4K_0\hat{K}}{V_t}\sqrt{p_s - \text{sign}(i)x_3} \end{bmatrix} i \\ y = x_p = h(\underline{x}) = x_1 \end{cases} \quad (5.7)$$

where $\dot{\underline{x}} = (\dot{x}_1, \dot{x}_2, \dot{x}_3)^T$.

5.4. Exact Linearization via State Feedback

The nonlinear model of electro-hydraulic servo position control system given by Eq. (5.7) can be expressed as

$$\begin{cases} \dot{\underline{x}} = \underline{f}(\underline{x}) + \underline{g}(\underline{x}) u \\ y = h(\underline{x}) \end{cases}$$

where $\underline{x} = (x_1, x_2, x_3)^T = (x_p, \dot{x}_p, p_l)^T$, $\dot{\underline{x}} = (\dot{x}_1, \dot{x}_2, \dot{x}_3)^T$, $u = i$, $y = x_p = h(\underline{x}) = x_1$,

$$\underline{f}(\underline{x}) = \begin{bmatrix} x_2 \\ \frac{A}{m_t} x_3 - \frac{F_l}{m_t} \\ -\frac{4AK_o}{V_t} x_2 - \frac{4K_o C_{tp}}{V_t} x_3 \end{bmatrix} \text{ and } \underline{g}(\underline{x}) = \begin{bmatrix} 0 \\ 0 \\ \frac{4K_o \hat{K}}{V_t} \sqrt{p_s - \text{sign}(i)x_3} \end{bmatrix}.$$

Based on the differential geometric method introduced in Chapter 4 the different order derivatives can be calculated as

$$\begin{aligned} h(\underline{x}) &= x_1 \\ L_{\underline{g}}h(\underline{x}) &= \frac{\partial h(\underline{x})}{\partial \underline{x}} \underline{g}(\underline{x}) = [1 \ 0 \ 0] \begin{bmatrix} 0 \\ 0 \\ \frac{4K_o \hat{K}}{V_t} \sqrt{p_s - \text{sign}(i)x_3} \end{bmatrix} \\ &= 0 \\ L_{\underline{f}}h(\underline{x}) &= \frac{\partial h(\underline{x})}{\partial \underline{x}} \underline{f}(\underline{x}) = [1 \ 0 \ 0] \begin{bmatrix} x_2 \\ \frac{A}{m_t} x_3 - \frac{F_l}{m_t} \\ -\frac{4AK_o}{V_t} x_2 - \frac{4K_o C_{tp}}{V_t} x_3 \end{bmatrix} \\ &= x_2 \\ L_{\underline{g}}L_{\underline{f}}h(\underline{x}) &= \frac{\partial [L_{\underline{f}}h(\underline{x})]}{\partial \underline{x}} \underline{g}(\underline{x}) = [0 \ 1 \ 0] \begin{bmatrix} 0 \\ 0 \\ \frac{4K_o \hat{K}}{V_t} \sqrt{p_s - \text{sign}(i)x_3} \end{bmatrix} \\ &= 0 \end{aligned}$$

5. Design and Simulation of Control System Based on Exact Linearization

$$\begin{aligned}
 L_{\underline{f}}^2 h(\underline{x}) &= \frac{\partial [L_{\underline{f}} h(\underline{x})]}{\partial \underline{x}} \underline{f}(\underline{x}) = [0 \quad 1 \quad 0] \begin{bmatrix} x_2 \\ \frac{A}{m_t} x_3 - \frac{F_l}{m_t} \\ -\frac{4AK_o}{V_t} x_2 - \frac{4K_o C_{tp}}{V_t} x_3 \end{bmatrix} \\
 &= \frac{A}{m_t} x_3 - \frac{F_l}{m_t} \\
 L_{\underline{g}} L_{\underline{f}}^2 h(\underline{x}) &= \frac{\partial [L_{\underline{f}}^2 h(\underline{x})]}{\partial \underline{x}} \underline{g}(\underline{x}) = [0 \quad 0 \quad \frac{A}{m_t}] \begin{bmatrix} 0 \\ 0 \\ \frac{4K_o \hat{K}}{V_t} \sqrt{p_s - \text{sign}(i) x_3} \end{bmatrix} \\
 &= \frac{4AK_o \hat{K}}{m_t V_t} \sqrt{p_s - \text{sign}(i) x_3} \\
 L_{\underline{f}}^3 h(\underline{x}) &= \frac{\partial [L_{\underline{f}}^2 h(\underline{x})]}{\partial \underline{x}} \underline{f}(\underline{x}) = [0 \quad 0 \quad \frac{A}{m_t}] \begin{bmatrix} x_2 \\ \frac{A}{m_t} x_3 - \frac{F_l}{m_t} \\ -\frac{4AK_o}{V_t} x_2 - \frac{4K_o C_{tp}}{V_t} x_3 \end{bmatrix} \\
 &= -\frac{4A^2 K_o}{m_t V_t} x_2 - \frac{4AK_o C_{tp}}{m_t V_t} x_3.
 \end{aligned}$$

According to the definition of relative degree of nonlinear system in §4.3.7, one can get that the relative degree of nonlinear system is $r - 1 = 2$ hence $r = 3$. Since the order of the nonlinear system is $n = 3$, the relative degree r equals to the system order n : $r = n = 3$. Consequently one can linearize the original nonlinear system with the method of exact linearization via state feedback.

Based on the theory of nonlinear coordinate transformation which is described in Chapter 4, the coordinate transformation equation is given by

$$\underline{z} = \underline{\phi}(\underline{x}) = \begin{bmatrix} z_1 \\ z_2 \\ z_3 \end{bmatrix} = \begin{bmatrix} h(\underline{x}) \\ L_{\underline{f}} h(\underline{x}) \\ L_{\underline{f}}^2 h(\underline{x}) \end{bmatrix} = \begin{bmatrix} x_1 \\ x_2 \\ \frac{A}{m_t} x_3 - \frac{F_l}{m_t} \end{bmatrix}. \quad (5.8)$$

5.4. Exact Linearization via State Feedback

Then one can get

$$\begin{cases} \dot{z}_1 = z_2 \\ \dot{z}_2 = z_3 \\ \dot{z}_3 = \alpha(\underline{x}) + \beta(\underline{x})u \end{cases} \quad (5.9)$$

where $\alpha(\underline{x}) = L_f^3 h(\underline{x})$ and $\beta(\underline{x}) = L_g L_f^2 h(\underline{x})$.

The feedback transformation can be selected as

$$u = \frac{-\alpha(\underline{x}) + v}{\beta(\underline{x})} \quad (5.10)$$

where $\beta(\underline{x}) \neq 0$.

Thus one can have

$$\begin{cases} \dot{z}_1 = z_2 \\ \dot{z}_2 = z_3 \\ \dot{z}_3 = v \end{cases} \quad (5.11)$$

Finally the original nonlinear model can be transformed to the linear model as

$$\begin{cases} \dot{\underline{z}} = \begin{bmatrix} \dot{z}_1 \\ \dot{z}_2 \\ \dot{z}_3 \end{bmatrix} = \begin{pmatrix} 0 & 1 & 0 \\ 0 & 0 & 1 \\ 0 & 0 & 0 \end{pmatrix} \begin{bmatrix} z_1 \\ z_2 \\ z_3 \end{bmatrix} + \begin{bmatrix} 0 \\ 0 \\ 1 \end{bmatrix} v \\ y = \underline{c}^T \underline{z} = [1 \quad 0 \quad 0] \begin{bmatrix} z_1 \\ z_2 \\ z_3 \end{bmatrix} \end{cases} \quad (5.12)$$

which is

$$\begin{cases} \dot{\underline{z}} = \underline{A}\underline{z} + \underline{b}v \\ y = \underline{c}^T \underline{z} \end{cases} \quad .$$

5.5. Comparison between Exact Linearization and Approximate Linearization

5.5.1. Introduction

In this section the stabilization problem of nonlinear electro-hydraulic servo system will be solved i.e. a state feedback controller will be designed so that the closed loop system is a stable system. The general method is to linearize the nonlinear system and then design the controller based on the stability theory of linear system. Generally speaking there are two different linearization methods: one is the approximate linearization method based on Taylor expansion and the other is the exact linearization method based on differential geometry. The exact linearization method is introduced in §5.4 and the exact linear model is given by Eq. (5.12). The approximate linear model of the nonlinear system $\dot{\underline{x}} = \underline{f}(\underline{x}) + \underline{g}(\underline{x})u$ can be derived by

$$\begin{bmatrix} \dot{x}_1 \\ \dot{x}_2 \\ \vdots \\ \dot{x}_n \end{bmatrix} = \begin{bmatrix} \frac{\partial f_1(\underline{x})}{\partial x_1} & \frac{\partial f_1(\underline{x})}{\partial x_2} & \dots & \frac{\partial f_1(\underline{x})}{\partial x_n} \\ \frac{\partial f_2(\underline{x})}{\partial x_1} & \frac{\partial f_2(\underline{x})}{\partial x_2} & \dots & \frac{\partial f_2(\underline{x})}{\partial x_n} \\ \vdots & \vdots & \vdots & \vdots \\ \frac{\partial f_n(\underline{x})}{\partial x_1} & \frac{\partial f_n(\underline{x})}{\partial x_2} & \dots & \frac{\partial f_n(\underline{x})}{\partial x_n} \end{bmatrix}_{\underline{x}^0} \cdot \begin{bmatrix} x_1 \\ x_2 \\ \vdots \\ x_n \end{bmatrix} + \begin{bmatrix} g_1(\underline{x}^0) \\ g_2(\underline{x}^0) \\ \vdots \\ g_n(\underline{x}^0) \end{bmatrix} \cdot u \quad (5.13)$$

where \underline{x}^0 is the equilibrium point of the system.

Hence the approximate linear model of the nonlinear electro-hydraulic servo system which is expressed by Eq. (5.7) can be written as:

$$\begin{cases} \begin{bmatrix} \dot{x}_1 \\ \dot{x}_2 \\ \dot{x}_3 \end{bmatrix} = \begin{bmatrix} 0 & 1 & 0 \\ 0 & 0 & \frac{A}{m_t} \\ 0 & -\frac{4AK_0}{V_t} & -\frac{4K_0C_{tp}}{V_t} \end{bmatrix} \cdot \begin{bmatrix} x_1 \\ x_2 \\ x_3 \end{bmatrix} + \begin{bmatrix} 0 \\ 0 \\ \frac{4K_0\bar{K}}{V_t}\sqrt{p_s} \end{bmatrix} \cdot i \\ y = x_1 \end{cases} \quad (5.14)$$

with the equilibrium point $\underline{x}^0 = [0 \ 0 \ 0]^T$.

5.5. Comparison between Exact Linearization and Approximate Linearization

One can apply the pole assignment method of linear system to design the feedback controller of the system based on the exact linear model expressed by Eq. (5.12) or the approximate linear model expressed by Eq. (5.14). The difference is that the control variable obtained by the former feedback controller is v rather than the control variable u of the original system hence one need the transformation from v to u which is given by Eq. (5.10) to control the original system while the latter feedback controller can be applied to the original nonlinear system directly and is effective in a small working range.

By comparing these two methods, one can find that the main shortcoming of the classical approximate linearization method is that it has errors and the errors will increase when the system deviates from the equilibrium point \underline{x}^0 . Nevertheless the exact linearization method can work in a large range no matter how seriously the system deviates from the equilibrium point \underline{x}^0 consequently the exact linearization method is applicable to the high precision control of nonlinear system especially when the system always deviates from the equilibrium point.

5.5.2. Simulation and Comparison

In this section two different state feedback controllers will be designed based on exact linearization method and approximate linearization method respectively and then their control performances in different conditions will be compared.

5.5.2.1. Controller Design

(1) Controller Design Based on Exact Linearization Method

According to linear system theory the state feedback controller which stabilizes the exact linear model given by Eq. (5.12) is

$$v = -\underline{k}_e^T \underline{z} = -k_{e1}z_1 - k_{e2}z_2 - k_{e3}z_3$$

5. Design and Simulation of Control System Based on Exact Linearization

and \underline{k}_e should satisfy that $s^3 + k_{e3}s^2 + k_{e2}s + k_{e1}$ is a Hurwitz polynomial. Furthermore the state feedback controller which can stabilize the original nonlinear system is given by Eq. (5.10).

(2) Controller Design Based on Approximate Linearization Method

The state feedback controller which stabilizes the approximate linear model given by Eq. (5.12) is

$$u = -\underline{k}_a^T \underline{x} = -k_{a1}x_1 - k_{a2}x_2 - k_{a3}x_3$$

and \underline{k}_a should satisfy that all the eigenvalues of the matrix $(\underline{A} - \underline{b}\underline{k}_a^T)$

must have negative real parts where $\underline{A} = \begin{bmatrix} 0 & 1 & 0 \\ 0 & 0 & \frac{A}{m_t} \\ 0 & -\frac{4AK_o}{V_t} & -\frac{4K_o C_{tp}}{V_t} \end{bmatrix}$ and

$$\underline{b} = \begin{bmatrix} 0 \\ 0 \\ \frac{4K_o \hat{K}}{V_t} \sqrt{p_s} \end{bmatrix}.$$

5.5.2.2. Simulation

The 250kN cylinder and the G761-3005 type MOOG servo valve is used in simulation with Simulink. The necessary parameters are as follows:

$$A = 8.34 \times 10^{-3} \text{ m}^2$$

$$V_t = 1.126 \times 10^{-3} \text{ m}^3$$

$$m_t = 217.8 \text{ kg}$$

$$K_o = 2 \times 10^9 \text{ Pa}$$

$$C_{tp} = 7.6042 \times 10^{-12} \text{ m}^4 \cdot \text{s/kg}$$

$$p_s = 22 \times 10^6 \text{ Pa}$$

$$\hat{K} = 1 \times 10^{-5} \text{ m}^4 / (\text{A} \cdot \text{s} \cdot \sqrt{\text{N}}).$$

5.5. Comparison between Exact Linearization and Approximate Linearization

Setting the three poles as

$$s_1 = -100$$

$$s_2 = -7.07 + 7.07i$$

$$s_3 = -7.07 - 7.07i$$

one can derive the two controllers' parameters as

$$\underline{k}_e = [10000 \quad 1510 \quad 114.1]^T$$

$$\underline{k}_a = [-7.8366 \times 10^{-4} \quad 0.1777 \quad -1.8027 \times 10^{-10}]^T.$$

Figure 5.1 and Figure 5.2 are the structure diagrams of the state feedback controllers based on exact linearization method and approximate linearization method respectively.

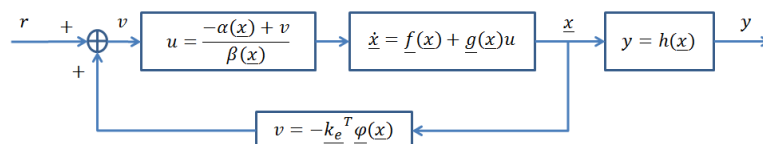


Figure 5.1.: State Feedback Controller Based on Exact Linearization Method

5.5.2.3. Result

In this section the step signal is used as the reference input r and the simulation is run in Simulink to compare the results.

(1) $F_l = 0$

5. Design and Simulation of Control System Based on Exact Linearization

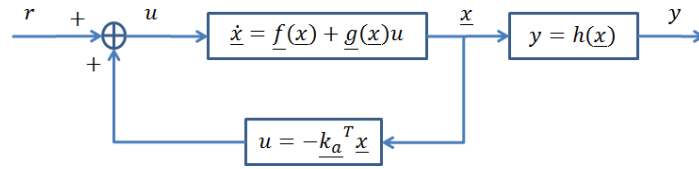


Figure 5.2.: State Feedback Controller Based on Approximate Linearization Method

With the external load force $F_l = 0$ the original nonlinear system can work near the equilibrium point \underline{x}^0 . The simulation results of the system with the two controllers are shown in Figure 5.3 and Figure 5.4 respectively.

From Figure 5.3 and Figure 5.4 it can be found that when the system works in a small range of the equilibrium point, both of the two controllers are satisfying.

(2) $F_l = -8.34 \times 10^3 N$

When the system has a large external load force, the value of the state x_3 ($= p_l$) will increase according to Eq. (3.19) which means that the system has to work far away from the equilibrium point \underline{x}^0 . The simulation results of the system with the two controllers are shown in Figure 5.5 and Figure 5.6 respectively.

Figure 5.5 shows that the state feedback controller based on exact linearization method is still effective. However Figure 5.6 shows that the state feedback controller based on approximate linearization method can not work and the whole system is not stable when it deviates from the equilibrium point \underline{x}^0 . The results prove the conclusion in §5.5.1.

5.5. Comparison between Exact Linearization and Approximate Linearization

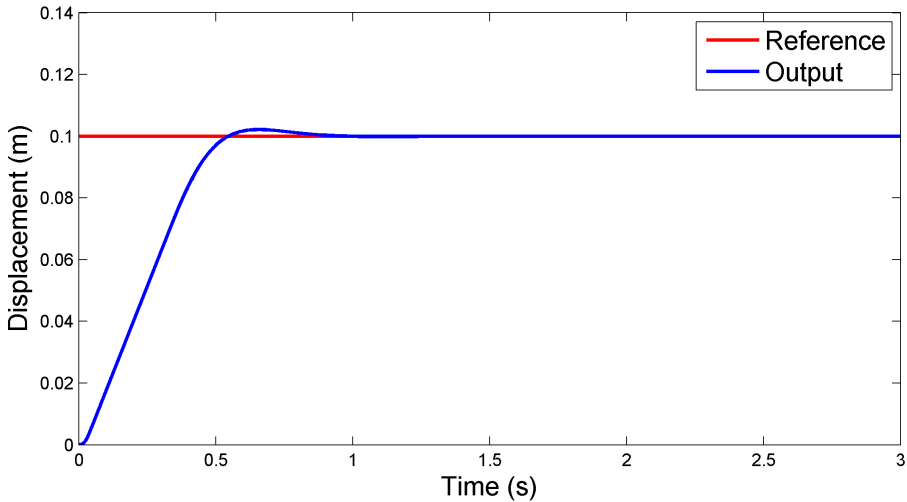


Figure 5.3.: System Output with State Feedback Controller Based on Exact Linearization Method When $F_l = 0$

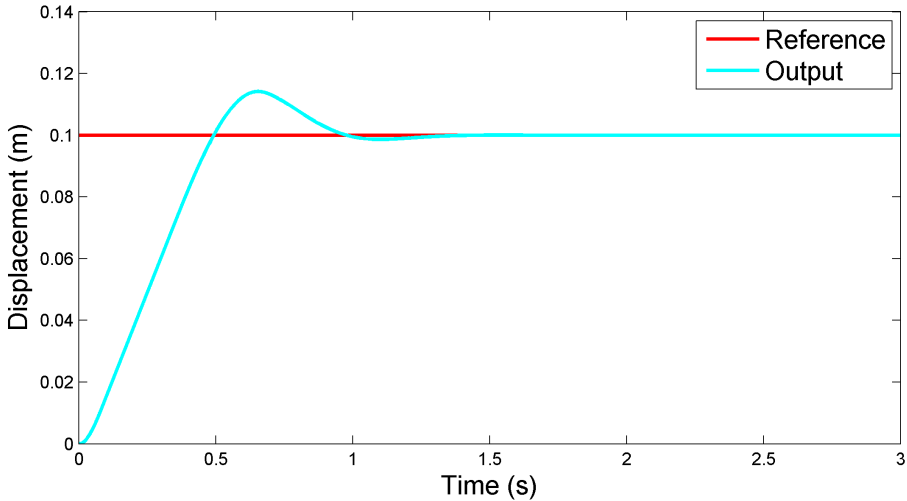


Figure 5.4.: System Output with State Feedback Controller Based on Approximate Linearization Method When $F_l = 0$

5. Design and Simulation of Control System Based on Exact Linearization

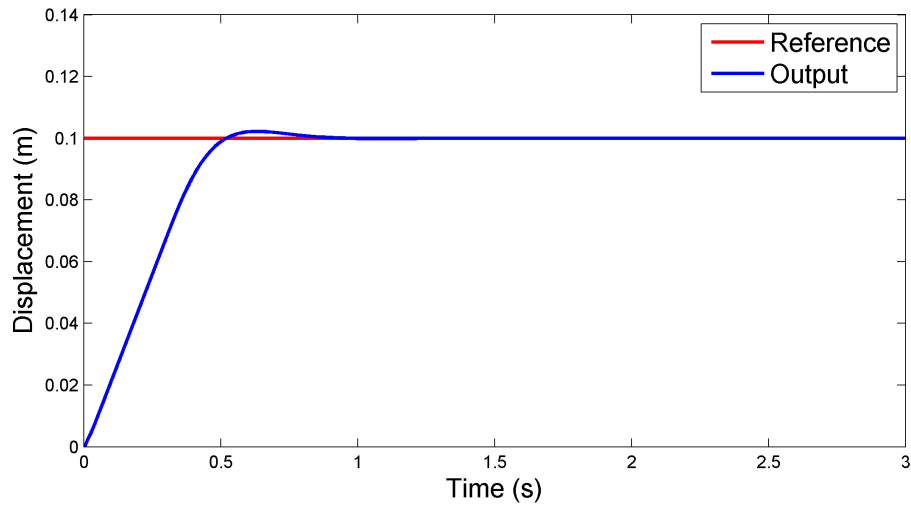


Figure 5.5.: System Output with State Feedback Controller Based on Exact Linearization Method When $F_l = -8.34 \times 10^3 N$

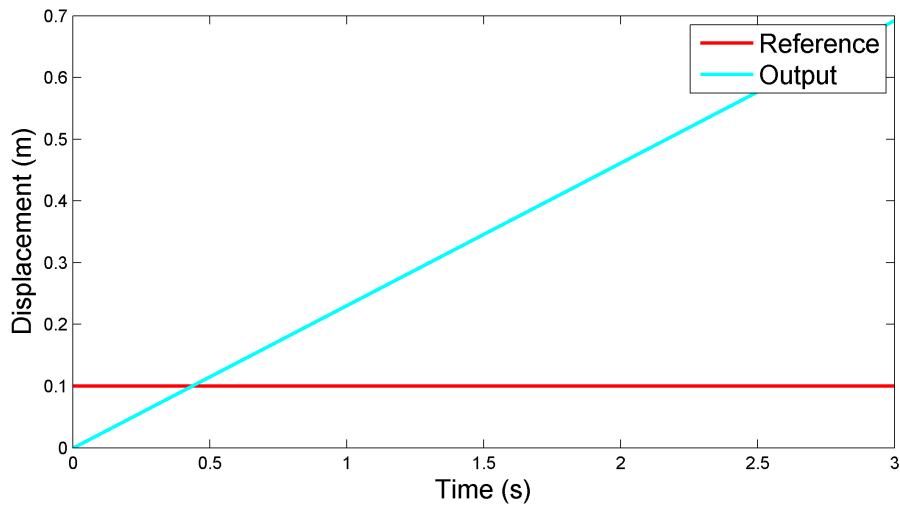


Figure 5.6.: System Output with State Feedback Controller Based on Approximate Linearization Method When $F_l = -8.34 \times 10^3 N$

5.6. Robustness Analysis of the Control System

5.6.1. Presentation of Robustness Problem

Generally speaking when researchers build the system model and estimate the values of the model parameters based on datasheet or system identification, they can not make sure that the values of the model parameters are completely identical to the real values. Furthermore the industrial control system has to work in the harsh environment and various disturbances will enter the system through the input and output channels. Moreover most of the controlled systems are time variant which means that even if the real values of the system parameters are achieved, they will change with the time. All these cases are called model uncertainty. The control system is based on the system model $G(s)$ while the closed-loop stability and the closed-loop performance index is on the premise of the assumption $G(s) = G_0(s)$ where $G_0(s)$ is the real controlled object. Nevertheless the model uncertainty i.e. the case when $G(s) \neq G_0(s)$ is not negligible. Supposing $G(s) \neq G_0(s)$ or there exists the external disturbance, the ability of the control system to keep closed-loop stability is called stability robustness and the one to keep closed-loop performance index is called performance robustness. Thus whether the control system designed with model uncertainty can operate stably and has anticipant performance index is called robustness problem which has received great concerns recently. In addition robustness of the system is closely related to the control algorithm which means that robustness of the same system will change with the different control strategies. Consequently researchers should research robustness of the system under certain control algorithm.

5.6.2. Robustness of Electro-Hydraulic Servo System under Nonlinear Control

In practical electro-hydraulic servo system some parameters such as total leakage coefficient are difficult to estimate and in addition some parameters such as bulk modulus of oil are time variant. Therefore one only can

5. Design and Simulation of Control System Based on Exact Linearization

achieve the comparatively accurate estimated value (nominal value) rather than exact value of these parameters through system analysis and identification. When the parameters deviate from the nominal value, the system will also deviate from the nominal mathematical model. Hence it should be known whether the control law based on the ideal model still works well when the system deviates from the ideal model i.e. whether the non-linear control strategy derived has robustness. Now this problem will be discussed with simulation results when bulk modulus K_o , total leakage coefficient C_{tp} , flow coefficient \hat{K} and load mass m_t change. Figure 5.5 (with $F_l = -8.34 \times 10^3 N$) is used as the reference simulation result while the results with modified parameters are shown from Figure 5.7 to Figure 5.11.

5.6.2.1. Influence of Modified Bulk Modulus

Bulk Modulus K_o depends on the air content in oil and changes frequently. Here it is assumed that the value of K_o decreases by 50% (from 2000 MPa to 1000 MPa) and the simulation result is given by Figure 5.7. Bulk Modulus embodies the relationship between volume variation and pressure change. The decrease of bulk modulus means that one can achieve more volume variation with the same pressure and thus in dynamic system it is possible that the oscillation increases. Nevertheless comparing Figure 5.7 with Figure 5.5 one can find that there is no significant change.

5.6.2.2. Influence of Modified Total Leakage Coefficient

From theoretical point of view, when total leakage coefficient C_{tp} increases, leakage of the whole system will increase which means that the practical working flow of servo valve with the same current will decrease so that the overshoot will be reduced and the response time will be prolonged. Here it is assumed that the total leakage coefficient C_{tp} increases by 100% and the simulation result is shown in Figure 5.8 from which one can see that the response curve has no obvious changes compared with Figure 5.5.

5.6. Robustness Analysis of the Control System

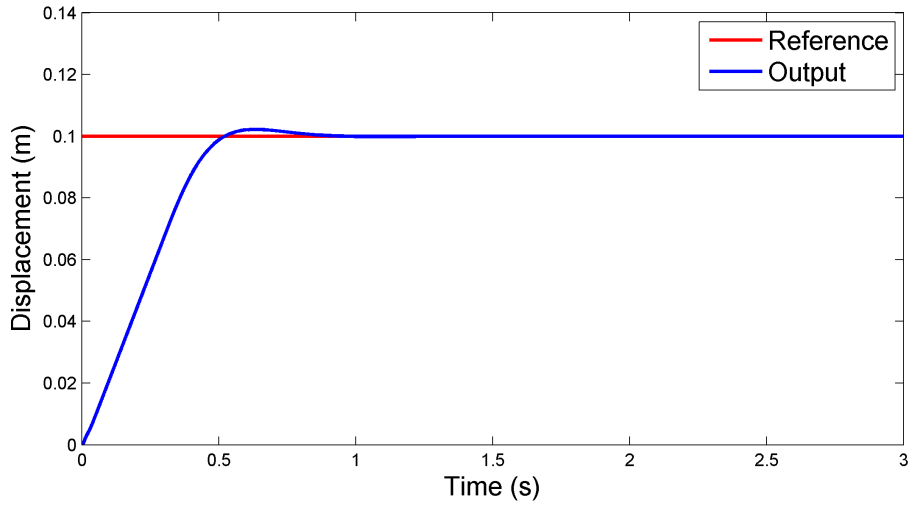


Figure 5.7.: System Output with State Feedback Controller Based on Exact Linearization Method When Bulk Modulus Changes

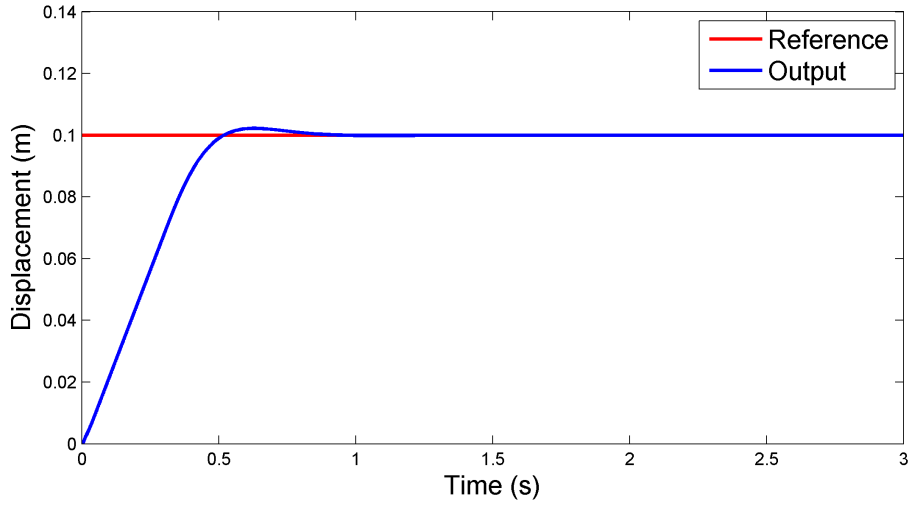


Figure 5.8.: System Output with State Feedback Controller Based on Exact Linearization Method When Total Leakage Coefficient Changes

5. Design and Simulation of Control System Based on Exact Linearization

5.6.2.3. Influence of Modified Flow Coefficient

Generally speaking when flow coefficient decreases, the output flow of servo valve with the same current will decrease so as to reduce the overshoot and prolong the response time. Now it is assumed that the flow coefficient K decreases by 25% and the result is given by Figure 5.9 from which one can find that the overshoot of the response curve is reduced a little and the response time is prolonged by 0.2 s compared with Figure 5.5. However this variation is acceptable.

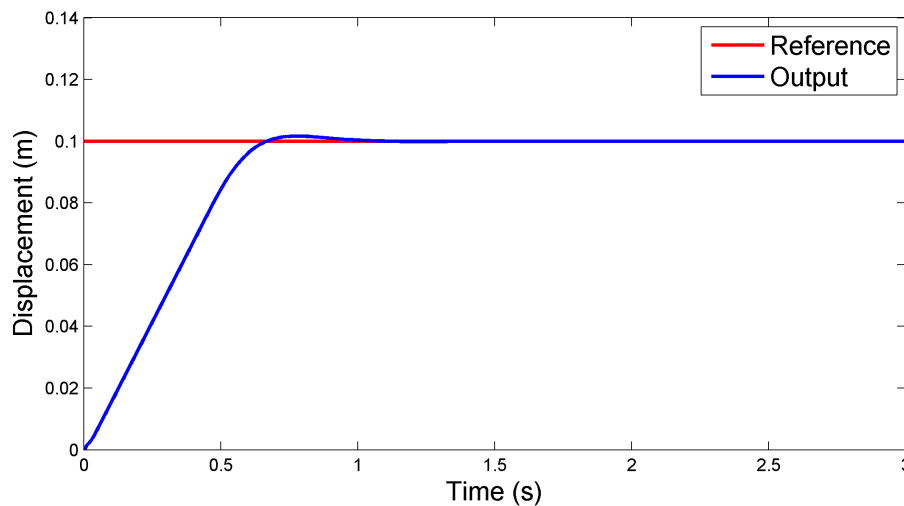


Figure 5.9.: System Output with State Feedback Controller Based on Exact Linearization Method When Flow Coefficient Changes

5.6.2.4. Influence of Modified Load Mass

When load mass increases the inertia of the system load will also increase so that the response time will be prolonged. Supposing that the load mass m_t increases by 50% one can get the simulation result as shown in Figure 5.10. It can be observed that the response curve does not change significantly compared with Figure 5.5.

5.6. Robustness Analysis of the Control System

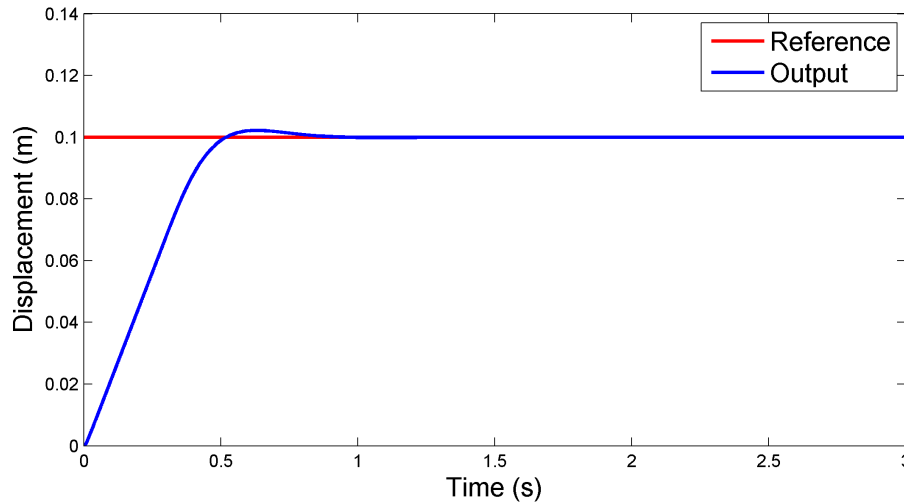


Figure 5.10.: System Output with State Feedback Controller Based on Exact Linearization Method When Load Mass Changes

5.6.2.5. Influence of Multi Modified Parameters

Now it can be assumed that all the four parameters change simultaneously according to the content above and the simulation result is given by Figure 5.11 from which one can notice that the overshoot of the response curve is reduced a little, the response time is prolonged by 0.2s and the regulating time of the modified system increases slightly compared with Figure 5.5. Nevertheless the result is satisfying.

All the analysis shows that when the system parameters change, not only can the modified system keep stable but also have good dynamic and static performance. Consequently in summary the electro-hydraulic servo system has good robustness with the state feedback controller after exact linearization.

5. Design and Simulation of Control System Based on Exact Linearization

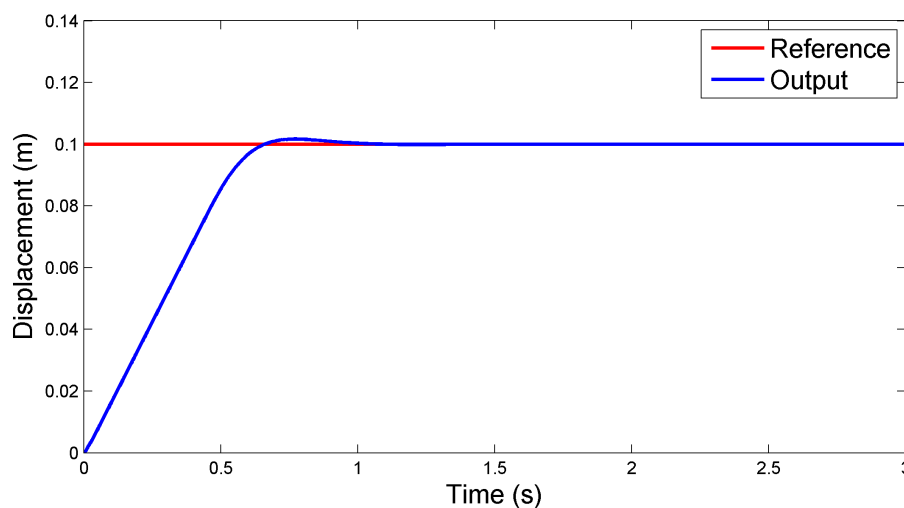


Figure 5.11.: System Output with State Feedback Controller Based on Exact Linearization Method When Multi Parameters Change

5.7. Disturbance Decoupling and Attenuation

In practical electro-hydraulic servo system engineers have to face the effects of external disturbance. In §4.5 the problems when and how one can eliminate or weaken the influence of external disturbance have been discussed. In this section the nonlinear model of electro-hydraulic servo system derived in §5.3 with disturbance model will be studied by simulation so as to check whether the influence of external disturbance can be eliminated or weakened.

5.7.1. Disturbance Decoupling

The nonlinear model of electro-hydraulic servo system is given by Eq. (5.7) and it is assumed that the external disturbance model is $\underline{p}(\underline{x})w$ hence the

5.7. Disturbance Decoupling and Attenuation

nonlinear model of the system with disturbance can be written as:

$$\begin{cases} \dot{\underline{x}} = \underline{f}(\underline{x}) + \underline{g}(\underline{x})u + \underline{p}(\underline{x})w \\ y = h(\underline{x}) \end{cases} \quad (5.15)$$

$$\text{where } \underline{f}(\underline{x}) = \begin{bmatrix} x_2 \\ \frac{A}{m_t}x_3 - \frac{F_l}{m_t} \\ -\frac{4AK_0}{V_t}x_2 - \frac{4K_0C_{tp}}{V_t}x_3 \end{bmatrix}, \underline{g}(\underline{x}) = \begin{bmatrix} 0 \\ 0 \\ \frac{4K_0\hat{K}}{V_t}\sqrt{p_s - \text{sign}(i)x_3} \end{bmatrix},$$

$$\underline{p}(\underline{x}) = \begin{bmatrix} a \\ b \\ c \end{bmatrix} \quad (a, b \text{ and } c \text{ are unknown parameters}), h(\underline{x}) = x_1, u \in R \text{ and}$$

$w \in R$ are system input and disturbance input respectively.

Now whether the system output y can be decoupled from the disturbance input w completely should be verified. According to Proposition 4.1 the system relative degree r should be less than the disturbance relative degree ρ if the complete decoupling can be realized. In §5.4 it is obtained that $r = 3$ consequently it is expected that $\rho \geq 4$. According to the definition of disturbance relative degree ρ in §4.5.1.1 one can have:

$$L_{\underline{p}}L_{\underline{f}}^k h(\underline{x}) = 0, \quad (0 \leq k \leq 2).$$

Therefore one can have:

$$\begin{aligned} L_{\underline{p}}L_{\underline{f}}^0 h(\underline{x}) &= \frac{\partial h(\underline{x})}{\partial \underline{x}} \underline{p}(\underline{x}) = [1 \quad 0 \quad 0] \begin{bmatrix} a \\ b \\ c \end{bmatrix} \\ &= a = 0 \\ L_{\underline{f}}h(\underline{x}) &= \frac{\partial h(\underline{x})}{\partial \underline{x}} \underline{f}(\underline{x}) = [1 \quad 0 \quad 0] \begin{bmatrix} x_2 \\ \frac{A}{m_t}x_3 - \frac{F_l}{m_t} \\ -\frac{4AK_0}{V_t}x_2 - \frac{4K_0C_{tp}}{V_t}x_3 \end{bmatrix} \end{aligned}$$

5. Design and Simulation of Control System Based on Exact Linearization

$$\begin{aligned}
 &= x_2 \\
 L_{\underline{p}}L_{\underline{f}}h(\underline{x}) &= \frac{\partial[L_{\underline{f}}h(\underline{x})]}{\partial \underline{x}}\underline{p}(\underline{x}) = [0 \quad 1 \quad 0] \begin{bmatrix} a \\ b \\ c \end{bmatrix} \\
 &= b = 0 \\
 L_{\underline{f}}^2h(\underline{x}) &= \frac{\partial[L_{\underline{f}}h(\underline{x})]}{\partial \underline{x}}\underline{f}(\underline{x}) = [0 \quad 1 \quad 0] \begin{bmatrix} x_2 \\ \frac{A}{m_t}x_3 - \frac{F_l}{m_t} \\ -\frac{4AK_o}{V_t}x_2 - \frac{4K_oC_{tp}}{V_t}x_3 \end{bmatrix} \\
 &= \frac{A}{m_t}x_3 - \frac{F_l}{m_t} \\
 L_{\underline{p}}L_{\underline{f}}^2h(\underline{x}) &= \frac{\partial[L_{\underline{f}}^2h(\underline{x})]}{\partial \underline{x}}\underline{p}(\underline{x}) = [0 \quad 0 \quad \frac{A}{m_t}] \begin{bmatrix} a \\ b \\ c \end{bmatrix} \\
 &= \frac{A}{m_t}c = 0.
 \end{aligned}$$

Hence one can get the conclusion that if the output y of electro-hydraulic servo system can be decoupled from the disturbance input w completely, $\underline{p}(\underline{x})$ should be a zero vector however it is not possible when the system has external disturbance. So in electro-hydraulic servo system the complete disturbance decoupling can not be realized.

5.7.2. Disturbance Attenuation

Since the disturbance decoupling method is not effective, one can only choose to weaken the influence of external disturbance with the method introduced in §4.5.2. The nonlinear model of electro-hydraulic servo system

5.7. Disturbance Decoupling and Attenuation

with external disturbance can be expressed by

$$\begin{cases} \dot{\underline{x}} = \underline{f}(\underline{x}) + \underline{g}(\underline{x})u + \underline{p}(\underline{x})w \\ y = h(\underline{x}) \end{cases} \quad (5.16)$$

$$\text{where } \underline{f}(\underline{x}) = \begin{bmatrix} x_2 \\ \frac{A}{m_t}x_3 - \frac{F_l}{m_t} \\ -\frac{4AK_0}{V_t}x_2 - \frac{4K_0C_{tp}}{V_t}x_3 \end{bmatrix}, \underline{g}(\underline{x}) = \begin{bmatrix} 0 \\ 0 \\ \frac{4K_0\hat{K}}{V_t}\sqrt{p_s - \text{sign}(i)x_3} \end{bmatrix},$$

$$\underline{p}(\underline{x}) = \begin{bmatrix} 0 \\ 0 \\ 1 \end{bmatrix}, h(\underline{x}) = x_1, u \in \mathbb{R} \text{ and } w \in \mathbb{R} \text{ are system input and distur-$$

bance input respectively. Furthermore one can have:

$$\text{rank}[\underline{g}, \underline{p}] = \text{rank}[\underline{g}] = 1 \quad (5.17)$$

hence the system satisfies the matching condition.

Since the relative degree of the system r is equal to the system order n according to §5.4 one can select the coordinate transformation (5.8) and the original nonlinear system can be transformed to:

$$\dot{\underline{z}} = \underline{A}\underline{z} + \underline{b}v + \underline{e}w \quad (5.18)$$

$$\text{where } \underline{A} = \begin{pmatrix} 0 & 1 & 0 \\ 0 & 0 & 1 \\ 0 & 0 & 0 \end{pmatrix}, \underline{b} = \begin{bmatrix} 0 \\ 0 \\ 1 \end{bmatrix}, \underline{e} = \begin{bmatrix} 0 \\ 0 \\ L_{\underline{p}}L_{\underline{f}}^2h(\underline{x}) \end{bmatrix},$$

$$v = L_{\underline{f}}^3h(\underline{x}) + L_{\underline{g}}L_{\underline{f}}^2h(\underline{x})u \text{ and } \underline{z} = [z_1 \ z_2 \ z_3]^T.$$

Furthermore according to §4.3.5 and §5.4 one can have

$$L_{\underline{p}}L_{\underline{f}}^2h(\underline{x}) = \frac{\partial[L_{\underline{f}}^2h(\underline{x})]}{\partial \underline{x}} \underline{p}(\underline{x}) = \begin{bmatrix} 0 & 0 & \frac{A}{m_t} \end{bmatrix} \begin{bmatrix} 0 \\ 0 \\ 1 \end{bmatrix}$$

5. Design and Simulation of Control System Based on Exact Linearization

$$\begin{aligned}
 &= \frac{A}{m_t} \\
 L_{\underline{g}}L_{\underline{f}}^2h(\underline{x}) &= \frac{\partial[L_{\underline{f}}^2h(\underline{x})]}{\partial\underline{x}}\underline{g}(\underline{x}) = \begin{bmatrix} 0 & 0 & \frac{A}{m_t} \end{bmatrix} \begin{bmatrix} 0 \\ 0 \\ \frac{4K_o\hat{K}}{V_t}\sqrt{p_s - \text{sign}(i)x_3} \end{bmatrix} \\
 &= \frac{4AK_o\hat{K}}{m_tV_t}\sqrt{p_s - \text{sign}(i)x_3} \\
 L_{\underline{f}}^3h(\underline{x}) &= \frac{\partial[L_{\underline{f}}^2h(\underline{x})]}{\partial\underline{x}}\underline{f}(\underline{x}) = \begin{bmatrix} 0 & 0 & \frac{A}{m_t} \end{bmatrix} \begin{bmatrix} x_2 \\ \frac{A}{m_t}x_3 - \frac{F_t}{m_t} \\ -\frac{4AK_o}{V_t}x_2 - \frac{4K_oC_{tp}}{V_t}x_3 \end{bmatrix} \\
 &= -\frac{4A^2K_o}{m_tV_t}x_2 - \frac{4AK_oC_{tp}}{m_tV_t}x_3.
 \end{aligned}$$

Then the switching function can be selected as:

$$s(\underline{z}) = \underline{c}^T \underline{z} = c_1z_1 + c_2z_2 + z_3 \quad (5.19)$$

where $\underline{c} = [c_1 \ c_2 \ 1]^T$. Thus when the system makes sliding mode motion, one can have:

$$z_3 = -c_1z_1 - c_2z_2 \quad (5.20)$$

and the sliding mode equation is given by

$$\begin{bmatrix} \dot{z}_1 \\ \dot{z}_2 \end{bmatrix} = \begin{bmatrix} 0 & 1 \\ 0 & 0 \end{bmatrix} \begin{bmatrix} z_1 \\ z_2 \end{bmatrix} + \begin{bmatrix} 0 \\ 1 \end{bmatrix} z_3. \quad (5.21)$$

Thus a linear subsystem described by Eq. (5.21) with the feedback (5.20) is derived. Now one can calculate the values of c_1 and c_2 with the pole assignment method based on linear control theory. Supposing the two poles required are

$$s_1 = -7.07 + 7.07i$$

$$s_2 = -7.07 - 7.07i$$

5.7. Disturbance Decoupling and Attenuation

one can derive that $c_1 = 99.9698$ and $c_2 = 14.14$ so as to achieve

$$\underline{c} = [c_1 \ c_2 \ 1]^T = [99.9698 \ 14.14 \ 1]^T. \quad (5.22)$$

Then the exponential reaching law is selected thus according to Eq. (4.64) the equivalent control input v is given by:

$$v = (\underline{c}^T \underline{b})^{-1} (-\underline{c}^T \underline{A}z - \varepsilon \cdot \text{sgn}(s) - k \cdot s) = -c_1 z_2 - c_2 z_3 - \varepsilon \cdot \text{sgn}(s) - k \cdot s. \quad (5.23)$$

Here it is set that $\varepsilon = 1$ and $k = 10000$. Thus one can calculate the control input u of the original nonlinear system with Eq. (5.10). Now the state feedback controller with exact linearization method derived in §5.5.2.2 and the sliding mode variable structure controller with exact linearization method is achieved therefore one can compare the disturbance resistance of them with simulation. It is assumed that the external disturbance is a sinusoidal signal: $w = 10^6 \cdot \sin(2\pi \cdot t)$ where t is time. The simulation results are shown in Figure 5.12 and Figure 5.13.

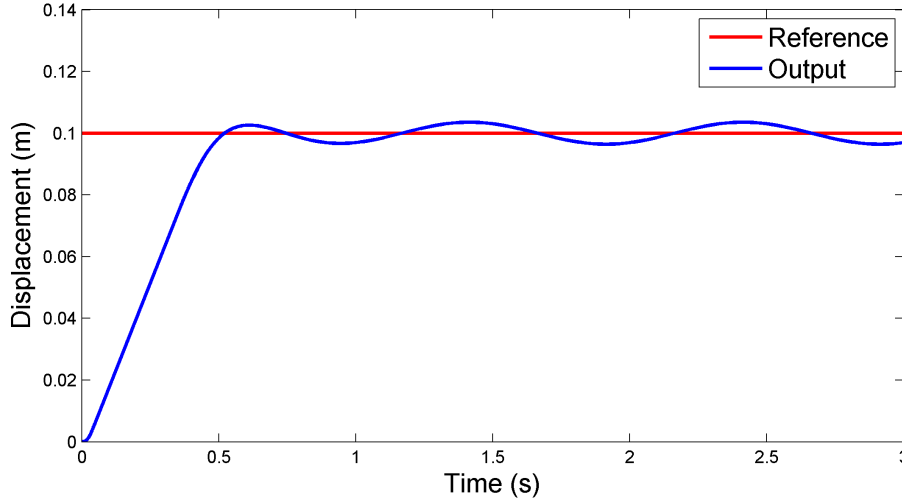


Figure 5.12.: System Output with State Feedback Controller Based on Exact Linearization Method with External Disturbance

5. Design and Simulation of Control System Based on Exact Linearization

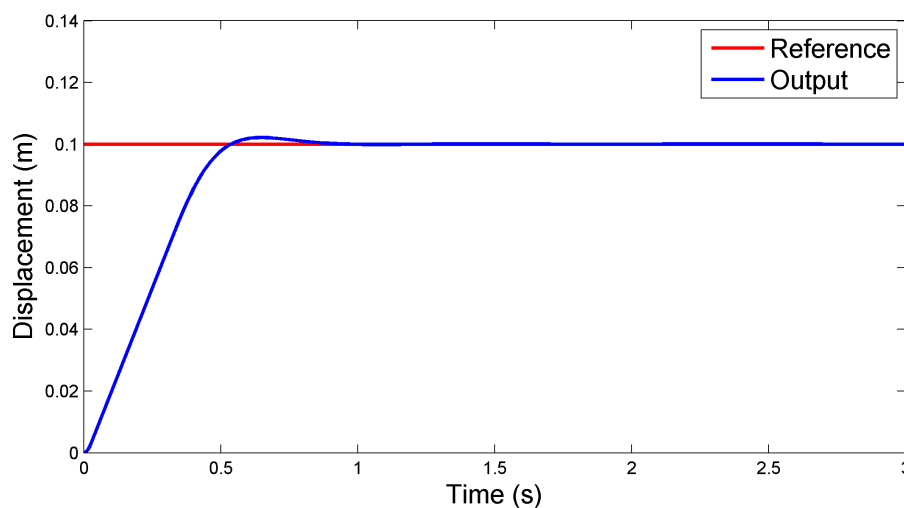


Figure 5.13.: System Output with Sliding Mode Variable Structure Controller Based on Exact Linearization Method with External Disturbance

From Figure 5.12 one can find that the system output y is influenced by the external disturbance w i.e. the general state feedback controller with exact linearization method does not have enough anti disturbance ability while from Figure 5.13 one can observe that the system output still has good dynamic and static performance and furthermore the effects of external disturbance are negligible. This verifies that the sliding mode variable structure controller with exact linearization method has satisfying anti disturbance performance.

5.8. Summary

In this chapter the nonlinear model of electro-hydraulic servo position control system built in Chapter 3 is linearized with the exact linearization method via state feedback. Then the state feedback controllers is designed based on exact linearization method and approximate linearization method respectively and simulation is run in Simulink. The results show that the

5.8. Summary

control effect of the exact linearization controller is better than that of approximate linearization controller when the system works far away from the equilibrium point. This is due to the factor that the exact linearization method via state feedback is essentially different from the approximate linearization method based on Taylor expansion. The latter method is effective only near the working point (equilibrium point) because it loses parts of system information while the former method is a kind of coordinate transformation. As long as the physical equations of the original nonlinear system are accurate, the linearized system based on exact linearization method is accurate. Consequently the original nonlinear system can be linearized completely with the exact linearization method via state feedback.

Furthermore the robustness of the electro-hydraulic servo system with state feedback controller based on exact linearization method is researched. This is significant because modeling errors always exist and real system is time variant. The simulation results show that the system still has satisfying dynamic and static performance even if some of the parameters deviate from the nominal values greatly. It verifies the strong robustness of the control system.

Finally the external disturbance problem is discussed since in practical system external disturbance always exists. Firstly it is proved that the system output of electro-hydraulic servo position control system can not be decoupled from the disturbance input completely. Then the sliding mode variable structure controller based on exact linearization method via state feedback is applied. The effectiveness of this controller is confirmed by the simulation results.

5. Design and Simulation of Control System Based on Exact Linearization

6. Iterative Learning Control Theory

6.1. Introduction

6.1.1. Background and Motivation

Generally speaking the task of control system is to seek for the control signal $u(t)$ so that the output signal $y(t)$ can meet the requirements. For instance one of the control tasks is to make the output signal $y(t)$ as small as possible (or as close as possible to some equilibrium point) while another one is to make the error signal $e(t) = r(t) - y(t)$ as small as possible where $r(t)$ is the reference signal. The former is called regulating problem and the latter is called tracking problem. Obviously regulating problem is the special case of the tracking problem. Currently most of the control algorithms realize control tasks asymptotically that is to find the control signal $u(t)$ so as to achieve $\lim_{t \rightarrow \infty} y(t) = 0$ (asymptotically regulating) or $\lim_{t \rightarrow \infty} e(t) = 0$ (asymptotically tracking). In engineering researchers often use the transient performance index and the steady-state performance index to evaluate the control effects of asymptotically regulating or asymptotically tracking.

There also exists another kind of tracking problem in engineering of which the task is to seek for the control signal $u(t)$ so that the output signal $y(t)$ can realize zero-error tracking along the whole desired trajectory in the finite time interval $[0, T]$ that is $e(t) = 0, t \in [0, T]$. This is called perfect tracking problem in finite time interval. This kind of tracking problem has practical background such as industrial robots with repetitive tasks of handling, welding and assembly; numerical control machines; servo systems

6. Iterative Learning Control Theory

with periodic reference signal and so on. Nevertheless it is difficult for researchers to apply the conventional control methods to realize perfect tracking consequently researchers try to find a new control algorithm to complete this control task.

One of the essential characteristics of creatures is "learning". Learning is also one of the basic intelligent behaviors of human beings and plays a very important role in human's evolutionary process. Learning control is one of the attempts to imitate various excellent control and regulation mechanisms of human being itself. To give control system the learning ability so that the system can improve control performance continuously by itself in the operation process is one of the aims pursued by researchers and engineers.

Learning control system is such an automatic control system that it can achieve the information of controlled process and environment, accumulate control experiences and improve control performance progressively in the operation process. The theory and technology of learning control has become one of the important branches of intelligent control. Obviously to realize intelligent control researchers should introduce "learning" into control system.

Iterative learning control (ILC) is one of the new fields of research on control theory and application and is one of the branches which have strict mathematical description in intelligent control. The classical iterative learning control theory is based on contraction mapping theory and it requires that the system should be Lipschitz continuous. Furthermore the system should satisfy the assumed conditions as follows [161]:

- Every trial (iteration, repetition and so on) should be in a fixed finite time interval that is $t \in [0, T]$;
- The desired output signal $y_d(t), t \in [0, T]$ is given a priori;
- The initial state of the system should be the same at the beginning of each iteration that is $\underline{x}_k(0) = \underline{x}(0)$ for $k = 1, 2, \dots$;
- The dynamic performance of the system keeps invariant in each iteration, that is to say, the system is repeatable;
- The output signal $y_k(t)$ of the system in each iteration can be measured;

- The dynamics of the system is invertible, that is, for a given desired output signal $y_d(t), t \in [0, T]$ there exists a unique control signal $u_d(t)$ that drives the system to produce the output signal $y_d(t)$.

Hence the control task of ILC is to realize perfect tracking in a finite time interval in an environment of repetitive operation. This control task can not be completed by the conventional control methods independently and directly because with these methods the control system can not "learn" anything from the previous operations. Without learning even if the control system executes the same task repeatedly, the system can only achieve the same performance without improvement.

The basic idea of ILC is to use information from previous control processes to improve the control effects of current operation so that the control system can track the desired trajectory as accurately as possible in a given time interval after several iterations. The algorithm of ILC is based on learning with memory.

ILC has a lot of advantages. For example ILC can deal with the uncertain dynamic system with simple algorithm and little prior knowledge. Moreover it is not necessary for controller to identify system parameters in the process of operation. Furthermore since ILC is a kind of algorithms with memory it can adjust the control signal according to the information from memory quickly.

6.1.2. Mathematical Description of ILC

Considering the dynamic system with repetitive operation as follows:

$$\begin{cases} \dot{\underline{x}}_k(t) = \underline{f}[\underline{x}_k(t), \underline{u}_k(t), t] \\ \underline{y}_k(t) = \underline{h}[\underline{x}_k(t), \underline{u}_k(t), t] \end{cases} \quad (6.1)$$

where $\underline{x}_k(t) \in R^n$, $\underline{u}_k(t) \in R^r$ and $\underline{y}_k(t) \in R^m$ are system states, control signals and output signals on trial k respectively. Given the desired output signals $\underline{y}_d(t) \in R^m$ in the given time interval $[0, T]$, one can have the error signals $\underline{e}_k(t) = \underline{y}_d(t) - \underline{y}_k(t)$ of the system on trial k thus the general

6. Iterative Learning Control Theory

learning law of ILC is given by

$$\underline{u}_{k+1}(t) = L[\underline{u}_k(t), \underline{e}_k(t)] \quad (6.2)$$

which is called open-loop ILC and

$$\underline{u}_{k+1}(t) = L[\underline{u}_k(t), \underline{e}_{k+1}(t)] \quad (6.3)$$

which is called closed-loop ILC. Note that L is the general learning operator and has a lot of different forms.

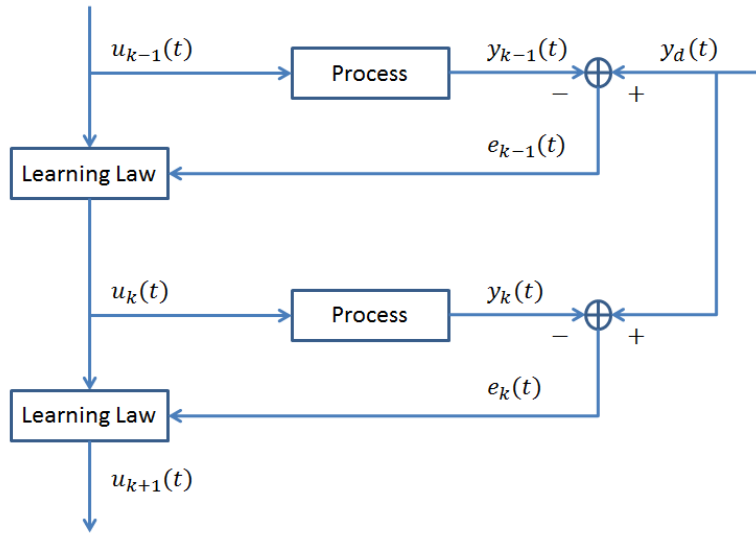


Figure 6.1.: Typical Control Structure of Open-Loop ILC

If the error signals $\underline{e}_k(t)$ tend to zero or some constants uniformly as $k \rightarrow \infty$ then the learning law of ILC above is convergent. Convergence is one of the most important problems of ILC. The ILC algorithm has practical significance only when the process of iterative learning is convergent.

An effective ILC algorithm not only makes the output errors of the system smaller after each iteration but also has fast convergence rate so that the algorithm is applicable in engineering. Furthermore the convergence of ILC

6.2. Literature Review of Iterative Learning Control Theory

algorithm should be independent of desired trajectory, that is, given a new desired trajectory the ILC algorithm should be still effective without any modification.

In practical applications the control signals of each iteration can be calculated after last iteration and moreover they can also be calculated and saved online in last iteration. Therefore compared with the conventional control algorithms, ILC can utilize more system information from each iteration.

A typical control structure of open-loop ILC is given in Figure 6.1. Please note that in some cases the “process” in Figure 6.1 can be regarded as a sub control system. For example in the next chapter the “process” is a feedback control system composed of a PI controller and valve-controlled cylinder system thus the control signal $u_k(t)$ on trial k is the reference signal of the feedback control system.

6.2. Literature Review of Iterative Learning Control Theory

In 1978 Uchiyama introduced the conception of learning based on repetitive training in his Japanese paper which is regarded as the earliest research results of ILC. In 1984 Arimoto and his colleagues expanded this conception [162]. They proposed the first ILC algorithm for linear time-invariant system and then proved the convergence of the algorithm with the norm of time weighted function (λ norm). From then on ILC has attracted wide attention of researchers.

Through approximately 30 years development, a lot of research results on the theory and application of ILC are achieved by researchers and engineers. For example ILC algorithms have developed from open-loop learning to closed-loop learning. The application fields of ILC have expanded from SISO systems to MIMO systems and from linear systems to nonlinear systems. More and more mathematical theories are introduced to analyze ILC such as contractive mapping theory, geometry theory and so on. The control structures of ILC have developed from single structures to complex

6. Iterative Learning Control Theory

structures such as robust ILC, adaptive ILC and so on. The development of ILC is introduced briefly as follows.

6.2.1. Algorithms

6.2.1.1. PID-Type ILC

ILC algorithm has a lot of forms while the basic and simple one is the PID-type ILC which uses the proportional, integral and derivative values of the system output errors to update reference signal and also has several different types. Arimoto and his colleagues have made enormous contribution to this field of research. They firstly propose the D-type [162], PD-type and PID-type [163] ILC algorithm. Especially they introduce the λ norm which is an important mathematical tool and then with this tool they obtain the sufficient condition of convergence of the ILC algorithms above. The λ norm has become the basic method to analyze the convergence of various ILC algorithms. Moreover, aiming at the robot system, they propose the P-type and PI-type ILC algorithm and then analyze the robustness and the uniform convergence of these ILC algorithms with passivity condition and λ norm [164].

Aiming at more general systems such as nonlinear systems, time-variant systems and so on, researchers have done lots of work and achieved many results. In [165] a P-type ILC algorithm is proposed for a class of uncertain nonlinear time-variable systems and the robustness, convergence and performance of this algorithm is studied. In [166] an open-closed-loop D-type ILC algorithm is investigated for a class of nonlinear time-variable systems and the sufficient convergence condition is given and proved. In [167] they show that the integral value of the system tracking error in ILC algorithm is helpful for system convergence and then they realize the optimal design of PI-type ILC scheme. In [168] they propose a PD-type ILC algorithm for a class of nonlinear systems and then they give and prove the sufficient condition for guaranteeing the convergence of the system. In [169] an open-closed-loop PID-type ILC algorithm is studied for uncertain time-delay systems and then the robustness and convergence of the system is discussed.

6.2. Literature Review of Iterative Learning Control Theory

Furthermore some scientists research on the improved PID-type ILC and obtain some results. In [170] Hu and Xiao propose three kinds of higher-order ILC algorithms:

P-type:

$$u_{k+1}(t) = \sum_{j=1}^r \Lambda_j u_{k-j+1} + \sum_{j=1}^r P_j e_{k-j+1} \quad (6.4)$$

D-type:

$$u_{k+1}(t) = \sum_{j=1}^r \Lambda_j u_{k-j+1} + \sum_{j=1}^r D_j \dot{e}_{k-j+1} \quad (6.5)$$

and PD-type:

$$u_{k+1}(t) = \sum_{j=1}^r \Lambda_j u_{k-j+1} + \sum_{j=1}^r (P_j + D_j \frac{d}{dt}) e_{k-j+1}. \quad (6.6)$$

Compared with conventional PID-type ILC algorithms, higher-order ones utilize not only the input-output information of last iteration but also the information of previous several iterations so as to provide the control signal more accurately and effectively.

PID-type ILC algorithms are sensitive to perturbation of initial error or output error. To overcome this shortcoming Heinzinger and his colleagues propose the D-type learning law with forgetting factor [171]. And then Arimoto and his colleagues propose the P-type learning law with forgetting factor [172]. The general form of PID-type ILC algorithms with forgetting factor is given by:

$$u_{k+1}(t) = \alpha u_0(t) + (1 - \alpha) u_k(t) + (K_P + K_I \int dt + K_D \frac{d}{dt}) e_k(t) \quad (6.7)$$

where $\alpha \in [0, 1)$ is the forgetting factor. Introducing the forgetting factor, the influence of early information will decrease with the increase of iteration times so that the variation of control signal can be more smooth.

PID-type ILC algorithm has a lot of advantages. For example the convergence condition is simple and relevant to only a few parameters; the PID-type ILC algorithm has good robustness to the uncertain systems; the algorithm is simple and useful with low computational complexity; it requires

6. Iterative Learning Control Theory

little prior knowledge. Consequently PID-type ILC algorithm is one of the most mature ILC strategies. Nevertheless it has some disadvantages. For instance with the derivative part the ILC algorithm is easily influenced by noise while without it the convergence condition of the ILC algorithm is not so easy to satisfy. Furthermore the desired control input signal maybe does not exist thus the learning parameters from convergence condition is not proper so as to cause significant error between the desired output signal and the real one. Finally it is difficult to find the proper values for the learning parameters which can satisfy the requirements of both convergence rate and system stability.

6.2.1.2. Robust ILC

In practical engineering, control system should be stable and have good dynamic and static performance. Furthermore it should be robust to uncertainties and disturbances of the system. The research on the robustness of ILC system mainly focuses on whether the system can keep convergent and stable when there exist external disturbances, system uncertainties and desired trajectory varying with iterations.

(1) Robustness to External Disturbances

In [173] Pi and Panaliappan discuss the robustness of discrete nonlinear system with open-closed-loop ILC algorithm to the bounded uncertainty of system state, output disturbance and initial error. In [174] Kim et al. propose a higher-order ILC algorithm for the discrete system and then discuss the robustness of the system to external disturbance. In [175] Shao et al. propose a design method of robust ILC and then give the sufficient and necessary condition to ensure robust bounded-input bounded-output stability when the system tracks arbitrary bounded output. The control system is robust to uncertain initial condition and external disturbance and furthermore can improve control performance gradually. In [176] aiming at uncertain linear controlled object with initial error and input-output disturbance, Liu and Lin propose an ILC framework and then give the sufficient condition of robust convergence in frequency domain.

(2) Robustness to System Uncertainties

6.2. Literature Review of Iterative Learning Control Theory

Aiming at a class of uncertain systems, of which the uncertain part can be treated as the product of unknown state-independent functions and known state-dependent functions, Xu and Viswanathan propose an adaptive robust iterative learning controller with dead zone scheme [177]. The iterative learning controller deals with the structured system uncertainties and the dead zone scheme ensures that the tracking error of the system is bounded. In [178] aiming at uncertain robotic systems Yang et al. design an adaptive robust iterative learning controller which is robust to both of the structured and unstructured uncertainty. In [179] aiming at uncertain linear time-invariant system Tayebi and Zaremba propose an ILC algorithm based on internal model control. They discuss the convergence of ILC and then transform it into robust control problem. Finally they design the robust controller with the μ synthesis method. In [180] Yang and Li propose an adaptive robust ILC algorithm for a class of uncertain nonlinear systems. The learning control deals with the periodic system uncertainty and the adaptive sliding mode control deals with the nonperiodic one. Moreover they use the radial basis function (RBF) neural network to learn the uncertain upper bound of the system adaptively.

(3) Robustness to Desired Trajectory Varying with Iterations

Most of the conventional ILC algorithms work according to the desired trajectory of the system directly hence generally speaking the prerequisite for the convergence of ILC algorithms is that the desired trajectory should keep the same with iterations, that is, the desired trajectory should have strict repeatability. Nevertheless the application range of ILC algorithms is limited according to this prerequisite. Aiming at the desired trajectory which varies with iterations, researchers have done a lot of work and achieved some important results. Saab et al. apply a PID-type ILC law with forgetting factor to solve the problem of tracking slowly varying trajectories [181]. Choi and Park introduce the neural network into ILC system to learn the new trajectory so as to solve the problem of tracking the desired trajectory varying with iterations. However it is still difficult to track the trajectory precisely [182]. In [183] based on the conventional open-closed-loop ILC, Liu discusses in frequency domain the sufficient condition of robust convergence of ILC algorithm which is robust to external disturbance and initial error when the desired trajectory varies slowly. Furthermore aiming at linear

6. Iterative Learning Control Theory

system with multiplicative uncertainty, he designs the robust ILC law with the μ synthesis method.

6.2.1.3. Adaptive ILC

Adaptive control and ILC have the same characteristic of learning, that is, adaptive control is a kind of learning process aiming at parameter while ILC is the one aiming at control input. Consequently researchers try to combine adaptive control theory and ILC theory thus the adaptive ILC algorithms are proposed.

The basic idea of adaptive ILC is to make full use of the prior knowledge of the system and then apply adaptive iterative learning aiming at the uncertain parameters of the system and the unknown control gain of the controller. French and Rogers propose an adaptive ILC algorithm aiming at the nonlinear system with uncertain parameters using the Lyapunov method [184]. The adaptive learning for parameters is along the direction of time axis however this algorithm is suitable only for the systems with time invariant or slow time-varying parameters. Xu and Tan propose an ILC method for the nonlinear systems with time-varying parametric uncertainties based on the composite energy function and obtain the learning law for the time-varying parameters through learning along the direction of iterative axis [185]. Aiming at uncertain robotic systems Park and his colleagues propose an adaptive iterative learning controller and both of the parameter estimation and learning control are along the direction of iterative axis [186]. Choi and Lee propose an adaptive ILC algorithm for the uncertain robotic systems with external disturbance [187]. This algorithm estimates the uncertain parameters in the time domain and identifies and compensates the repetitive disturbances in the iteration domain so that the tracking error converges uniformly in the iteration domain. In [188] Liu discusses the adaptive ILC problems of time-delay systems with time-varying parameters. Aiming at two kinds of nonlinear systems with unknown control gains, he applies the Nussbaum function and Lyapunov-Krasovskii function respectively to design the adaptive ILC law with backstepping technology. All of the research results above expand the application range of adaptive control and ILC.

6.2.1.4. Optimal ILC

The control objective of ILC is to reduce tracking error gradually through iterative learning hence the problem of minimizing the error can be transformed into the optimization problem.

Furuta and his colleagues firstly introduce the conception of optimization into ILC [189]. They use the steepest descent method to calculate optimal control signal. This algorithm achieves good results in the controllable system with delays. In [190] Buchheit et al. propose another ILC algorithm based on optimization, which uses Newton-Raphson method to calculate ideal input signal. Moreover to reduce the sensitivity of the system to noise, researchers propose several other ILC algorithms based on optimization. Tao et al. propose a discrete ILC algorithm based on optimization by using the quadratic function with penalty term as the objective function of optimization [191]. This algorithm can reduce the sensitivity of the system to noise effectively nevertheless the convergence speed is decreased.

Furthermore genetic algorithm is a kind of highly-parallel random adaptive search algorithm based on natural selection theory and evolutionism of biology. It works without constraint conditions such as differentiability, continuity and so on and moreover it does not require other auxiliary information. Furthermore it has a lot of advantages such as simplicity, universality, robustness and so on. Consequently it becomes one of the important tools to solve optimization problem. For instance aiming at the nonlinear ILC problem based on norm optimization, Hatzikos et al. propose the genetic algorithm to solve the norm optimization problem of ILC and then they achieve good result, that is, the norm of the error decreases monotonically [192]. However the algorithm supposes that the controlled object does not have uncertainties which is not reasonable in practical ILC systems. How to solve this problem is the key to apply genetic algorithm in practical engineering.

6.2.1.5. Model Reference ILC

Model reference ILC algorithms have several different forms. One of them is to update parameters of the system model with system identification

6. Iterative Learning Control Theory

methods according to operation information of the system in each iteration and then construct the ILC algorithm with model parameters. This model reference ILC algorithm is a kind of PID-type ILC algorithm with systematic design method for learning parameters essentially. However the relationship between the designed learning parameters, the convergence rate and the tracking performance is not clear. For instance Oh and his colleagues construct the ILC algorithm with the inverse model of the system [193]. The convergence condition of the algorithm is very simple and is relevant to only a few parameters of the system model hence it allows large model errors.

Another commonly used model reference ILC algorithm is the one combined with predictive control. This algorithm utilizes the design idea of model prediction, rolling optimization and feedback correction of predictive control, that is, based on conventional control it applies model prediction after each iteration, replaces rolling optimization with global optimization and finally obtains ILC algorithm according to the optimum index. For example Bone proposes a novel ILC law combined with generalized predictive control (GPC) and the simulation results show that compared with ordinary GPC this novel control law can improve the tracking precision of the system while compared with general ILC it can improve the robustness of the algorithm [194]. In [195] they propose the predictive optimal ILC algorithm based on predictive control technology. Based on the same quadratic criterion Lee and his colleagues propose a model-based ILC algorithm and then they analyze the robustness of the system with disturbance [196]. Furthermore Kim and his colleagues obtain the reduced-order design method of the model reference ILC algorithm based on quadratic criterion with the singular value decomposition technology [197].

6.2.1.6. Feedback-Feedforward ILC

As two main means for control, feedback and feedforward are widely used in control systems. ILC is a kind of feedforward control technology essentially. However in practical engineering if the controlled system is not stable, it is not allowed to apply open-loop ILC algorithm individually. Even

6.2. Literature Review of Iterative Learning Control Theory

if the controlled system is stable, before the iterative learning process converges, open-loop ILC algorithms might cause large control error which is not acceptable in many practical applications. Applying feedback control technology can stabilize the system and decrease the error. Kuc and his colleagues propose a feedback-feedforward ILC algorithm [198]:

$$\begin{cases} u_k(t) = u_k^f(t) + u_k^b(t) \\ u_k^b(t) = F(e_k(t)) \\ u_{k+1}^f(t) = u_k^f(t) + L(e_k(t)) \end{cases} \quad (6.8)$$

where $u_k^f(t)$ is the feedforward learning input and $u_k^b(t)$ is the feedback error input.

Aiming at the linear plant G , Amann and his colleagues propose the general form of ILC algorithms with feedback-feedforward effects [199]:

$$u_{k+1} = u_k + K_0[e_k] + K_1[e_{k+1}] \quad (6.9)$$

where $K_0[e_k]$ is a trial-to-trial feedforward control and $K_1[e_{k+1}]$ is termed a current trial feedback control. Then they obtain the sufficient condition of convergence of the algorithm above with the contractive mapping theory:

$$\left\| (I + GK_1)^{-1} (I + GK_0) \right\|_{\infty} < 1 \quad (6.10)$$

and furthermore according to the sufficient condition of convergence they propose the design procedure for the feedback-feedforward ILC algorithm with H_{∞} optimization technique.

The early ILC algorithms mainly use open-loop structure. In recent years most of the ILC algorithms adopt composite structure which combines the open-loop control and closed-loop control. Generally speaking these algorithms are feedback-feedforward ILC algorithms [200].

6.2.2. Convergence Speed

Stability of ILC algorithm is the prerequisite of system operation, which ensures that the control system will not diverge with the increment of iteration number. However it is meaningless to consider only the stability

6. Iterative Learning Control Theory

of ILC. The control signal obtained is the optimal one only when the iterative learning process can converge to the desired value. Stability and convergence of the ILC algorithm is given by the convergence condition nevertheless the convergence speed is not embodied because all the convergence conditions are given when iteration number $k \rightarrow \infty$. Aiming at this problem researchers have made a lot of work and achieved some results.

In [201] Togai and Yamano propose several optimal algorithms such as steepest descent method, Newton-Raphson method and Gauss-Newton method however the prerequisite is that the structure and parameters of the dynamic process should be known accurately which means that ILC gives up its advantages. More researchers focus on the research on learning laws in the hope of achieving the fastest learning convergence speed. When Bien and Hub propose the higher order ILC algorithm they point out that utilizing the information from previous multiple learning simultaneously can increase the learning speed significantly [202].

ILC is a kind of feedforward control technology essentially. Although the sufficient conditions for convergence of most learning laws are proved, the convergence speed is not satisfying. Nevertheless utilizing the real time system information or the feedback control part to update the control variable can accelerate the convergence speed greatly. In [203] they use current error information to update control variable which is a kind of closed-loop learning law. The proof and simulation results show that this learning law has fast convergence. In [204] aiming at linear system Xu and Yang apply the H_∞ control theory to optimize the ILC algorithm so as to increase learning convergence speed. In [205] Wang analyzes various factors which influence the convergence rate of ILC theoretically and makes detailed derivation aiming at the P-type open-loop learning law. Finally the theoretical results are given.

6.2.3. Initial State

When researchers use ILC technology to design controller they only need error signals and/or error derivative signals of the controlled objects from

6.2. Literature Review of Iterative Learning Control Theory

each iteration. Using this technology, iterative learning always starts from some initial point which is the initial state or initial output of the system. Nearly all the sufficient conditions for convergence require that the initial point of each iteration should keep the same. Solving the initial condition problem of ILC theory effectively is one of the goals pursued by researchers. Currently most of the ILC algorithms proposed require that the initial state of the controlled system in each iteration is the same as that of desired trajectory, that is, the initial condition should be satisfied:

$$\underline{x}_k(0) = \underline{x}_d(0) \quad k = 0, 1, 2, \dots \quad (6.11)$$

where \underline{x}_k is the system state on trial k and \underline{x}_d is the desired one.

However in practical engineering applications it is difficult for ILC system to obtain the initial state of the desired tracking trajectory. Moreover there exists initial state deviation and measurement noise in each iteration. Aiming at this problem researchers make a lot of work and obtain some achievements. Heinzinger and Fenwick point out that the stability and convergence of the system will not be influenced by initial state when it is repeatable [206]. In [207] they utilize the forgetting factor to control the influence of initial state error. On the premise that the system is convergent, they propose an initial state learning scheme so that the initial state can tend to the desired one thus the controlled system can track the desired trajectory accurately. In [208] they research on the influence of non-zero initial error on the convergence of learning law and discuss the function of the parameters of the learning law in control system in detail. Finally they analyze the robustness of the learning law and propose a method called "ILC with multi-modal input". In [209] aiming at linear time-invariant systems Ren and Gao propose a new ILC scheme with input and initial state learning, which can neglect the limitation on the initial state of the control system.

6.2.4. Analysis Methods

The commonly used methods for system analysis and convergence proof are norm theory, Lyapunov stability theory, operator theory, frequency do-

6. Iterative Learning Control Theory

main analysis theory, 2-D stability theory, H_∞ method, geometric method and so on.

Most of the published papers on convergence analysis of ILC system are in the sense of norm however norm is only a mathematical concept designed for convergence analysis of ILC and it ignores the dynamic characteristics of the system along the time axis. Although λ -norm is equal to *sup*-norm, in the tracking tasks *sup*-norm can achieve more accurate measurement results than λ -norm. In [210] they find that huge overshoot in the output error may happen although the ILC algorithm is proved to be convergent with respect to λ -norm. In [211] Sun and Wang prove the convergence of sampled-data ILC with *sup*-norm.

French and Rogers design the ILC algorithm for a class of nonlinear systems based on adaptive Lyapunov stability theory so that the tracking error decreases monotonically [184]. In [193] they firstly use operator theory to prove the convergence of ILC algorithm for a class of linear periodic systems. In [212] they propose a design method in frequency domain for iterative learning controller and then they give the sufficient condition for convergence of ILC algorithm in arbitrary initial states. In [213] they build the Roesser discrete model of MIMO discrete linear system with 2-D system theory and prove the learning convergence condition of ILC system with asymptotic stability theory of 2-D model by analyzing the 2-D error equations. Padiou and Su analyze the convergence of ILC of linear time-invariant system with H_∞ method and then give the sufficient condition for convergence [214]. In [215] they analyze the vector diagram from Arimoto's algorithm with geometric method and then achieve a new ILC algorithm.

6.2.5. Applications

ILC theory is firstly proposed to solve the tracking control problems of robot systems. After several decades of development ILC has achieved a lot of results in the field of robotics in the world. In [216] they propose a new linear ILC algorithm aiming at the trajectory tracking problems of robotic manipulators. They combine the traditional PI control algorithm and the ILC algorithm so that the tracking errors of position, velocity and

6.2. Literature Review of Iterative Learning Control Theory

acceleration can be asymptotically stable in the case of high nonlinearity. In [217] Luca and Ulivi propose an ILC algorithm based on frequency domain analysis aiming at robotic manipulators with elastic joints and solve the output tracking problems of robotic manipulators. In [218] aiming at high-g geared industrial manipulators they propose an ILC algorithm in the frequency domain. This algorithm includes a PD controller with fixed gain and ILC algorithm so as to improve the tracking performance.

The analysis above shows that ILC is widely applied in the field of robot systems because of the characteristics of ILC and robots. Moreover researchers also try to expand the application areas of ILC so that this method can be applied in other industrial processes which have the characteristics of repetitive motion obviously so as to improve the dynamic performance of control systems. In [175] they propose a robust ILC algorithm and apply it in injection molding machine system successfully. Pandit and Buchheit apply ILC algorithm in the cyclic process of aluminum extruder and achieve good control effects [219]. In [196] they present new model-based ILC algorithms with quadratic performance criteria for chemical process control. In [220] the applications of ILC in autonomous underwater vehicles are discussed. Aiming at repeatability of operation of high speed hydraulic press, Pang and Li apply the PID-type iterative learning controller in control system of high speed hydraulic press so that the error from each forging process will be used in the next control process [221]. In [222] they apply ILC in excitation control of synchronous generator so as to modify control input by iterative learning. The simulation results show that the quality of the terminal voltage and the stability of the power systems is improved. In [223] they apply ILC algorithm in temperature control of batch reactor and achieve satisfying results. In [224] they combine the ILC and biomedicine and get achievements in functional neuromuscular stimulation system. It is difficult to build the dynamic models for tobacco fermentation process because of its complexity nevertheless the process is repeatable. Aiming at this characteristic Yao and Yang make the preliminary research on application of ILC in ferment system of tobacco leaf [225].

Especially in most cases the desired output signal of electro-hydraulic servo system is periodic signal in fatigue testing. In the circumstances it is worthwhile to research how to apply ILC algorithm in electro-hydraulic servo system. In [226] they develop a discrete closed-loop D-type ILC scheme

6. Iterative Learning Control Theory

for electro-hydraulic position servo system with parameter uncertainties. In [227] a feedback-feedforward ILC algorithm is proposed to control hydraulic motion platform. The feedforward part can improve the control precision and the feedback part can improve the robustness of the system. In [228] the control algorithms of open loop and closed loop ILC are designed to raise the control accuracy of the system and eliminate the influences of dead zone and time lag nonlinearities.

Furthermore ILC also can be applied in other industrial processes such as industrial packaging machine [229], linear motor [230], numerical control machine tool [231], batch processes [232], video cassette recording servo system [233], semiconductor manufacturing [234] and so on.

6.3. PID-Type ILC Based on Frequency Domain Filtering

6.3.1. PID-Type ILC

As the earliest and simplest form of ILC, PID-type ILC has been widely studied. In [162] Arimoto and his colleagues firstly propose the D-type ILC:

$$u_{k+1}(t) = u_k(t) + K_D \dot{e}_k(t) \quad (6.12)$$

where K_D is the constant gain. Once K_D is given, the tracking performance and convergence rate of the learning system is then determined. To improve the control effects of the system, researchers try to add some adjustable parameters into the learning law. Thus many different learning forms such as P-type, PI-type and PD-type learning laws are proposed and applied in practical engineering. Generally speaking all of them can be regarded as the special forms of PID-type ILC:

$$u_{k+1}(t) = u_k(t) + (K_P + K_I \int dt + K_D \frac{d}{dt})e_k(t) \quad (6.13)$$

where K_P , K_I and K_D are the proportional, integral and derivative gains respectively. Here $e_k(t)$ is used as the error information hence it is called

6.3. PID-Type ILC Based on Frequency Domain Filtering

open-loop PID-type ILC. Similarly, if $e_{k+1}(t)$ is used as the error information, the algorithm is called closed-loop PID-type ILC.

6.3.2. Convergence Analysis

Many researchers use norm theory to prove the convergence of ILC algorithms however this causes some problems. For instance norm is only a mathematical concept designed for convergence analysis of ILC algorithms and it ignores the dynamic characteristics of the system along the time axis. Consequently by using norm theory for reference, Zhang and Lin prove the convergence of the D-type ILC algorithm with operator theory [235]. This proof method is better than the one only based on norm theory because it considers the dynamic characteristics of the system along the time axis. Based on their results the convergence of the PID-type ILC algorithm can be proved as follows.

6.3.2.1. Mathematical Foundation

(1) Definition of Norm

Definition 6.1. Let X be a linear space and $\|x\|$ be a mapping from X to $[0, +\infty)$. If they satisfy:

- \forall constant a , $\|a \cdot x\| = |a| \cdot \|x\|$;
- $\forall x, y \in X$, $\|x + y\| \leq \|x\| + \|y\|$;
- $\|x\| = 0$ if and only if x is a zero element;

then the mapping $\|\cdot\|$ is called the norm of x and the space X on which the norm $\|\cdot\|$ is defined is then called a normed space.

Definition 6.2. Let $C[a, b]$ be the set of all the continuous functions on $[a, b]$ interval thus $\forall f \in C[a, b]$ the norm of f can be defined as:

$$\|f\| = |f(t)|_{max}, \quad (a \leq t \leq b).$$

6. Iterative Learning Control Theory

Definition 6.3. Let $C_r[a, b]$ be the set of all the continuous r -dimensional vector valued functions on $[a, b]$ interval thus $\forall \underline{f} = [f_1(t), f_2(t), \dots, f_r(t)] \in C_r[a, b]$ the norm of f can be defined as:

$$\|\underline{f}\| = |f_i(t)|_{\max}, \quad (1 \leq i \leq r, a \leq t \leq b).$$

(2) Spectrum and Spectral Radius of Operator

Definition 6.4. Let X and Y be normed spaces and S be a mapping from X to Y , then S is called an operator from X to Y and can be denoted as $S : X \rightarrow Y$.

Definition 6.5. Let X and Y be normed spaces and $S : X \rightarrow Y$ be an operator. If $\forall x, y \in X$ and \forall constants a, b the operator S satisfies:

$$S(ax + by) = aS(x) + bS(y)$$

then S is called linear operator.

Definition 6.6. Let X and Y be normed spaces and $S : X \rightarrow Y$ be a linear operator. If

$$\sup \|S(x)\| < +\infty, \quad (\|x\| \leq 1)$$

then S is called bounded linear operator. Furthermore $\sup \|S(x)\|$ is called the operator norm of S which can be denoted as $\|S\|$.

Moreover if $S : X \rightarrow Y$ is a bounded linear operator, then $\forall x \in X$, one can have:

$$\|S(x)\| \leq \|S\| \cdot \|x\|.$$

Definition 6.7. Let X be a normed space and $S : X \rightarrow X$ be a bounded linear operator. Then the spectrum of S is a set of all the constants λ which satisfy that the mapping $\lambda I - S$ is neither injection nor surjection. The spectrum of S is denoted as $\sigma(S)$, that is

$$\sigma(S) = \{\lambda | \lambda I - S \text{ is neither injection nor surjection}\}$$

where $I : X \rightarrow X$ is the identity mapping i.e. $\forall x \in X, Ix = x$.

6.3. PID-Type ILC Based on Frequency Domain Filtering

Furthermore the conception that $\lambda I - S$ is not injection means that $\exists x_1, x_2 \in X, (x_1 \neq x_2), (\lambda I - S)x_1 = (\lambda I - S)x_2$. And the conception that $\lambda I - S$ is not surjection means that the image set of $\lambda I - S$ is not equal to X .

Definition 6.8. Let $S : X \rightarrow X$ be a bounded linear operator then the spectral radius $\rho(S)$ of S is:

$$\rho(S) = \sup\{|\lambda| \mid \lambda \in \sigma(S)\}.$$

Especially if the operator S can be regarded as a matrix: $S(\underline{x}) = \underline{S} \cdot \underline{x}$, then the spectral radius of S is:

$$\rho(S) = \max\{|\lambda_k|, k = 1, 2, \dots, n\}$$

where λ_k are the eigenvalues of the matrix \underline{S} . If λ_k is a complex number ($\lambda_k = a + bi$) then:

$$|\lambda_k| = \sqrt{a^2 + b^2}.$$

(3) Lemmas

Lemma 6.1 [236]. (Bellman-Gronwall Lemma) Let $u(t)$, $\alpha(t)$ and $\beta(t)$ be real-valued continuous functions defined on $[0, T]$. In addition $\beta(t)$ is non-negative on $[0, T]$. If $u(t)$ satisfies

$$u(t) \leq \alpha(t) + \int_0^t \beta(s)u(s) ds, \quad \forall t \in [0, T]$$

then

$$u(t) \leq \alpha(t) + \int_0^t \alpha(s)\beta(s)e^{\int_s^t \beta(r) dr} ds, \quad \forall t \in [0, T].$$

Especially if $\alpha(t)$ is non-decreasing on $[0, T]$ then

$$u(t) \leq \alpha(t)e^{\int_0^t \beta(s) ds}, \quad \forall t \in [0, T].$$

Lemma 6.2 [236]. Let $\{b_k\}_{k \geq 0}$ ($b_k \geq 0$) be a convergent sequence of constants. The operator $Q_k : C_r[0, T] \rightarrow C_r[0, T]$ satisfies

$$\|Q_k[\underline{u}(t)]\| \leq M(b_k + \int_0^t \|\underline{u}(s)\| ds) \quad (\forall \underline{u}(t) \in C_r[0, T])$$

6. Iterative Learning Control Theory

where $M \geq 1$ is a constant. Let $\underline{P}(t)$ be a $r \times r$ continuous function matrix. Then $\underline{P}(t)$ can be regarded as an operator $P : C_r[0, T] \rightarrow C_r[0, T]$:

$$P[\underline{u}(t)] = \underline{P}(t)\underline{u}(t).$$

If the spectral radius $\rho(P) < 1$ then

$$\lim_{n \rightarrow \infty} \|(P + Q_n)(P + Q_{n-1}) \cdots (P + Q_0)[u(t)]\| \leq M_0 \lim_{k \rightarrow \infty} b_k$$

where M_0 is a constant and only related with $\rho(P)$ and M .

6.3.2.2. Problem Description

The following SISO linear time-varying system is considered:

$$\begin{cases} \dot{\underline{x}}(t) = \underline{A}(t)\underline{x}(t) + \underline{b}(t)u(t) \\ y(t) = \underline{c}^T(t)\underline{x}(t) \end{cases} \quad (6.14)$$

where $\underline{x}(t) \in R^n$ is system state, $y(t) \in R$ is system output signal, $u(t) \in R$ is control signal, $\underline{A}(t)$ is state matrix with proper dimension, $\underline{b}(t)$ and $\underline{c}(t)$ are input and output parametric vectors respectively with proper dimension. The control requirement is that the system output $y(t)$ should track the desired output $y_d(t)$ precisely in the time interval $[0, T]$.

6.3.2.3. Convergence Proof

If the ILC algorithm is applied to realize the control target above, the dynamic equation of the ILC system on trial k can be described as:

$$\begin{cases} \dot{\underline{x}}_k(t) = \underline{A}(t)\underline{x}_k(t) + \underline{b}(t)u_k(t) \\ y_k(t) = \underline{c}^T(t)\underline{x}_k(t) \end{cases} \quad (6.15)$$

and the output error on trial k is defined as

$$e_k(t) = y_d(t) - y_k(t). \quad (6.16)$$

6.3. PID-Type ILC Based on Frequency Domain Filtering

Furthermore it can be defined that $\delta \underline{x}_k(t) = \underline{x}_d(t) - \underline{x}_k(t)$, $\delta y_k(t) = y_d(t) - y_k(t)$ and $\delta u_k(t) = u_d(t) - u_k(t)$ where $\underline{x}_d(t)$, $y_d(t)$ and $u_d(t)$ are the desired system state, output and input respectively. Now one can apply the PID-type ILC algorithm given as

$$u_{k+1}(t) = u_k(t) + [K_P(t) + K_I(t) \int dt + K_D(t) \frac{d}{dt}] e_k(t) \quad (6.17)$$

so that the convergence theorem is given as follows.

Theorem 6.1. It is supposed that the controlled system is described by Eq. (6.14) and the ILC algorithm is given by Eq. (6.17). If in the time interval $[0, T]$ the whole system satisfies the following conditions:

(A1) $\underline{A}(t)\underline{x}(t)$ satisfies the Lipschitz condition for \underline{x} i.e. $\exists M > 0$ so that

$$\|\underline{A}(t)\underline{x}_1(t) - \underline{A}(t)\underline{x}_2(t)\| \leq M\|\underline{x}_1(t) - \underline{x}_2(t)\| \quad (\forall t \in [0, T], \forall \underline{x}_1, \underline{x}_2 \in R^n);$$

(A2) the ordered list of initial state error of each iteration $\{\delta \underline{x}_k(0)\}_{k \geq 0}$ is a sequence converging to zero;

(A3) there exists the unique desired input $u_d(t)$ so that the system has the desired state and output;

(A4) $\underline{c}(t)$ exists in the time interval $[0, T]$ and moreover $\underline{b}(t)$, $\underline{c}(t)$ and $\underline{\dot{c}}(t)$ are bounded;

(A5) $K_P(t)$, $K_I(t)$ and $K_D(t)$ are bounded;

then the sufficient condition that for arbitrary initial input $u_0(t)$ and initial state $\underline{x}_k(0)$ of each iteration, the sequences $\{\underline{x}_k(t)\}_{k \geq 0}$, $\{y_k(t)\}_{k \geq 0}$ and $\{u_k(t)\}_{k \geq 0}$ uniformly converge to $\underline{x}_d(t)$, $y_d(t)$ and $u_d(t)$ respectively for $t \in [0, T]$ is that the spectral radius satisfies:

$$\rho[1 - K_D(t)\underline{c}^T(t)\underline{b}(t)] < 1 \quad \forall t \in [0, T]. \quad (6.18)$$

Proof. According to Eq. (6.14) one can have

$$\begin{aligned} \delta \underline{\dot{x}}_k(t) &= \underline{\dot{x}}_d(t) - \underline{\dot{x}}_k(t) \\ &= \underline{A}(t)\underline{x}_d(t) + \underline{b}(t)u_d(t) - \underline{A}(t)\underline{x}_k(t) - \underline{b}(t)u_k(t) \end{aligned}$$

6. Iterative Learning Control Theory

$$= \underline{A}(t)\delta\underline{x}_k(t) + \underline{b}(t)\delta u_k(t) \quad (6.19)$$

$$\delta y_k(t) = \underline{c}^T(t)\underline{x}_d(t) - \underline{c}^T(t)\underline{x}_k(t) = \underline{c}^T(t)\delta\underline{x}_k(t) \quad (6.20)$$

$$\begin{aligned} \delta u_{k+1}(t) &= u_d(t) - u_{k+1}(t) \\ &= \delta u_k(t) + u_k(t) - u_{k+1}(t) \\ &= \delta u_k(t) - K_P(t)\delta y_k(t) - K_I(t) \int_0^t \delta y_k(s) ds - K_D(t)\delta \dot{y}_k(t) \\ &= \delta u_k(t) - K_P(t)\underline{c}^T(t)\delta\underline{x}_k(t) - K_I(t) \int_0^t \underline{c}^T(s)\delta\underline{x}_k(s) ds \\ &\quad - K_D(t)\{\dot{\underline{c}}^T(t)\delta\underline{x}_k(t) + \underline{c}^T(t)[\underline{A}(t)\delta\underline{x}_k(t) + \underline{b}(t)\delta u_k(t)]\} \\ &= \delta u_k(t) - K_P(t)\underline{c}^T(t)\delta\underline{x}_k(t) \\ &\quad - K_I(t) \int_0^t \underline{c}^T(s)\delta\underline{x}_k(s) ds - K_D(t)\dot{\underline{c}}^T(t)\delta\underline{x}_k(t) \\ &\quad - K_D(t)\underline{c}^T(t)[\underline{A}(t)\delta\underline{x}_k(t) + \underline{b}(t)\delta u_k(t)]. \end{aligned} \quad (6.21)$$

Then the operator $P : C[0, T] \rightarrow C[0, T]$ can be defined as

$$P[u(t)] = [1 - K_D(t)\underline{c}^T(t)\underline{b}(t)]u(t) \quad (6.22)$$

and the operator $Q_k : C[0, T] \rightarrow C[0, T]$ as

$$\begin{aligned} Q_k[u(t)] &= -K_P(t)\underline{c}^T(t)\underline{x}(t) - K_I(t) \int_0^t \underline{c}^T(s)\underline{x}(s) ds \\ &\quad - K_D(t)\dot{\underline{c}}^T(t)\underline{x}(t) - K_D(t)\underline{c}^T(t)\underline{A}(t)\underline{x}(t) \end{aligned} \quad (6.23)$$

where $\underline{x}(t) \in C_n[0, T]$ is the solution of the system (6.14) with the initial state $\underline{x}(0)$. Thus one can have

$$\begin{aligned} \delta u_{k+1}(t) &= P[\delta u_k(t)] + Q_k[\delta u_k(t)] \\ &= (P + Q_k)[\delta u_k(t)] \\ &= (P + Q_k)(P + Q_{k-1}) \cdots (P + Q_0)[\delta u_0(t)]. \end{aligned} \quad (6.24)$$

6.3. PID-Type ILC Based on Frequency Domain Filtering

Now Q_k should be estimated. If $\underline{x}(t)$ is the solution of the dynamic equation (6.14) then according to conditions (A1) and (A4) $\exists M > 0$ and $N > 0$ so that

$$\begin{aligned}\|\underline{x}(t)\| &= \|\underline{x}(0) + \int_0^t \underline{A}(s)\underline{x}(s) \, ds + \int_0^t \underline{b}(s)u(s) \, ds\| \\ &\leq \|\underline{x}(0)\| + M \int_0^t \|\underline{x}(s)\| \, ds + N \int_0^t \|u(s)\| \, ds.\end{aligned}\quad (6.25)$$

Thus based on Lemma 6.1 one can have

$$\begin{aligned}\|\underline{x}(t)\| &\leq \|\underline{x}(0)\| + N \int_0^t \|u(s)\| \, ds \\ &\quad + \int_0^t M \left[\|\underline{x}(0)\| + N \int_0^s \|u(\sigma)\| \, d\sigma \right] e^{\int_s^t M \, dr} \, ds \\ &= \|\underline{x}(0)\| + N \int_0^t \|u(s)\| \, ds \\ &\quad + \int_0^t M \left[\|\underline{x}(0)\| + N \int_0^s \|u(\sigma)\| \, d\sigma \right] e^{M(t-s)} \, ds \\ &\leq \|\underline{x}(0)\| + N \int_0^t \|u(s)\| \, ds + Me^{MT} \int_0^t \|\underline{x}(0)\| \, ds \\ &\quad + MNe^{MT} \int_0^t \int_0^s \|u(\sigma)\| \, d\sigma \, ds \\ &= \|\underline{x}(0)\| + N \int_0^t \|u(s)\| \, ds + Me^{MT} t \|\underline{x}(0)\| \\ &\quad + MNe^{MT} \int_0^t \int_\sigma^t \|u(\sigma)\| \, ds \, d\sigma \\ &= \|\underline{x}(0)\| + N \int_0^t \|u(s)\| \, ds + Me^{MT} t \|\underline{x}(0)\| \\ &\quad + MNe^{MT} \int_0^t (t - \sigma) \|u(\sigma)\| \, d\sigma\end{aligned}$$

6. Iterative Learning Control Theory

$$\begin{aligned}
&\leq \|\underline{x}(0)\| + N \int_0^t \|u(s)\| \, ds + MTe^{MT} \|\underline{x}(0)\| \\
&\quad + MTNe^{MT} \int_0^t \|u(\sigma)\| \, d\sigma \\
&= (1 + MTe^{MT}) \|\underline{x}(0)\| + N(1 + MTe^{MT}) \int_0^t \|u(s)\| \, ds \\
&\leq M_1 \left[\|\underline{x}(0)\| + \int_0^t \|u(s)\| \, ds \right] \tag{6.26}
\end{aligned}$$

where $M_1 = \max\{(1 + MTe^{MT}), N(1 + MTe^{MT})\}$.

Then according to conditions (A4) and (A5) $\exists M_2 > 0, M_3 > 0$ and $M_4 > 0$ so that

$$\begin{aligned}
&\| -K_P(t)\underline{c}^T(t)\underline{x}(t) - K_I(t) \int_0^t \underline{c}^T(s)\underline{x}(s) \, ds \| \\
&\leq \|K_P(t)\underline{c}^T(t)\underline{x}(t)\| + \|K_I(t) \int_0^t \underline{c}^T(s)\underline{x}(s) \, ds \| \\
&\leq M_2 \|\underline{x}(t)\| + M_3 \int_0^t \|\underline{x}(s)\| \, ds \\
&\leq M_2 \|\underline{x}(t)\| + M_3 \int_0^t M_1 \left[\|\underline{x}(0)\| + \int_0^\tau \|u(s)\| \, ds \right] \, d\tau \\
&= M_2 \|\underline{x}(t)\| + M_3 M_1 \int_0^t \|\underline{x}(0)\| \, d\tau + M_3 M_1 \int_0^t \int_0^\tau \|u(s)\| \, ds \, d\tau \\
&= M_2 \|\underline{x}(t)\| + M_3 M_1 \int_0^t \|\underline{x}(0)\| \, d\tau + M_3 M_1 \int_0^t \int_s^t \|u(s)\| \, d\tau \, ds \\
&= M_2 \|\underline{x}(t)\| + M_3 M_1 \int_0^t \|\underline{x}(0)\| \, d\tau + M_3 M_1 \int_0^t (t-s) \|u(s)\| \, ds \\
&\leq M_2 \|\underline{x}(t)\| + M_3 M_1 T \|\underline{x}(0)\| + M_3 M_1 T \int_0^t \|u(s)\| \, ds
\end{aligned}$$

6.3. PID-Type ILC Based on Frequency Domain Filtering

$$\begin{aligned}
&\leq M_2M_1 \left[\|\underline{x}(0)\| + \int_0^t \|u(s)\| \, ds \right] + M_3M_1T\|\underline{x}(0)\| \\
&\quad + M_3M_1T \int_0^t \|u(s)\| \, ds \\
&= (M_2M_1 + M_3M_1T)\|\underline{x}(0)\| + (M_2M_1 + M_3M_1T) \int_0^t \|u(s)\| \, ds \\
&= M_4 \left[\|\underline{x}(0)\| + \int_0^t \|u(s)\| \, ds \right] \tag{6.27}
\end{aligned}$$

where $M_4 = M_2M_1 + M_3M_1T$.

Similarly according to conditions (A4) and (A5) $\exists M_5 > 0$ and $M_6 > 0$ so that

$$\begin{aligned}
&\| -K_D(t)\dot{\underline{c}}^T(t)\underline{x}(t) - K_D(t)\underline{c}^T(t)\underline{A}(t)\underline{x}(t) \| \\
&\leq \|K_D(t)\dot{\underline{c}}^T(t)\underline{x}(t)\| + \|K_D(t)\underline{c}^T(t)\underline{A}(t)\underline{x}(t)\| \\
&\leq M_5\|\underline{x}(t)\| \\
&\leq M_5M_1 \left[\|\underline{x}(0)\| + \int_0^t \|u(s)\| \, ds \right] \\
&= M_6 \left[\|\underline{x}(0)\| + \int_0^t \|u(s)\| \, ds \right]. \tag{6.28}
\end{aligned}$$

Consequently $\exists M_7 > 0$ so that

$$\begin{aligned}
\|Q_k[u(t)]\| &\leq \| -K_P(t)\underline{c}^T(t)\underline{x}(t) - K_I(t) \int_0^t \underline{c}^T(s)\underline{x}(s) \, ds \| \\
&\quad + \| -K_D(t)\dot{\underline{c}}^T(t)\underline{x}(t) - K_D(t)\underline{c}^T(t)\underline{A}(t)\underline{x}(t) \| \\
&\leq M_4 \left[\|\underline{x}(0)\| + \int_0^t \|u(s)\| \, ds \right] + M_6 \left[\|\underline{x}(0)\| + \int_0^t \|u(s)\| \, ds \right] \\
&= M_7 \left[\|\underline{x}(0)\| + \int_0^t \|u(s)\| \, ds \right] \tag{6.29}
\end{aligned}$$

6. Iterative Learning Control Theory

where $M_7 = M_4 + M_6$.

Therefore one can have

$$\|Q_k[\delta u_0(t)]\| \leq M_7 \left[\|\delta \underline{x}_0(0)\| + \int_0^t \|\delta u_0(s)\| ds \right]. \quad (6.30)$$

Thus according to Lemma 6.2, Eq. (6.24) and Eq. (6.30) one can achieve the following result.

If $\rho(P) < 1$ then

$$\begin{aligned} \lim_{n \rightarrow \infty} \|\delta u_{n+1}(t)\| &= \lim_{n \rightarrow \infty} \|(P + Q_n)(P + Q_{n-1}) \cdots (P + Q_0)[\delta u_0(t)]\| \\ &\leq M_0 \lim_{k \rightarrow \infty} b_k \\ &= M_0 \|\delta \underline{x}_0(0)\| \end{aligned} \quad (6.31)$$

where $b_k = \|\delta \underline{x}_0(0)\|$, $k = 0, 1, 2, \dots$.

Similarly replacing $\delta u_0(t)$ with $\delta u_1(t)$ one can obtain the following result.

If $\rho(P) < 1$ then

$$\begin{aligned} \lim_{n \rightarrow \infty} \|\delta u_{n+1}(t)\| &= \lim_{n \rightarrow \infty} \|(P + Q_n)(P + Q_{n-1}) \cdots (P + Q_1)[\delta u_1(t)]\| \\ &\leq M_0 \lim_{k \rightarrow \infty} b_k \\ &= M_0 \|\delta \underline{x}_1(0)\| \end{aligned} \quad (6.32)$$

where $b_k = \|\delta \underline{x}_1(0)\|$, $k = 0, 1, 2, \dots$.

In the same way one can achieve

$$\lim_{n \rightarrow \infty} \|\delta u_{n+1}(t)\| \leq M_0 \|\delta \underline{x}_k(0)\| \quad (\forall k \geq 0). \quad (6.33)$$

According to condition (A2) the following equation holds:

$$\lim_{k \rightarrow \infty} \|\delta \underline{x}_k(0)\| = 0. \quad (6.34)$$

Hence one can obtain

$$\lim_{n \rightarrow \infty} \|\delta u_{n+1}(t)\| \leq 0. \quad (6.35)$$

6.3. PID-Type ILC Based on Frequency Domain Filtering

Then since norm is nonnegative one can get

$$\lim_{n \rightarrow \infty} \|\delta u_{n+1}(t)\| = 0 \quad (6.36)$$

that is

$$\lim_{n \rightarrow \infty} \delta u_n(t) = 0 \quad (6.37)$$

holds uniformly with respect to t .

□

6.3.3. Frequency Domain Filtering

As discussed in §6.2.1.1 PID-type ILC algorithm has a lot of advantages however it also has several disadvantages. For example it is difficult to select the proper values of learning parameters because of the contradiction between convergence speed and system stability. On the one hand with the large learning parameters the control system converges fast nevertheless the algorithm is not stable. On the other hand with the small learning parameters the algorithm is stable however it converges slowly. Considering the process dynamics, excessive learning parameters will cause mutation and oscillation of control signal outputted by iterative learning controller and finally cause system instability with the iterations.

Consequently researchers try to apply time-domain filters so as to make the control signal smooth thus the contradiction between convergence speed and system stability can be solved. However applying time-domain filters will cause new problems. For instance time domain filtering (TDF) causes phase lag. Especially different frequency components have different phase lag thus the filtered signal is distorted.

Hence in this dissertation frequency domain filtering (FDF) will be applied so as to make control signal smooth. The principle of digital frequency domain filtering is to apply discrete Fourier transform to the sampled data of input signal with fast Fourier transform (FFT) method. Then according to the requirement of filtering one can set the frequency components, which need to be removed, to zero directly. However sometimes the abrupt truncation of frequency-domain data will cause leakage of power spectrum

6. Iterative Learning Control Theory

which causes the distortion of filtered signal. In this case one has to set them to zero by adding a gradually changed transitional frequency band. For example one can add a transitional frequency band composed of cosine window function between the passband and stopband. Finally discrete inverse Fourier transform is applied to the data filtered with the inverse fast Fourier transform (IFFT) method so as to obtain the time domain signal.

The digital frequency domain filtering can be denoted as

$$y(r) = \frac{1}{N} \sum_{k=0}^{N-1} H(k)X(k)e^{j2\pi kr/N} \quad (r = 0, 1, \dots, N-1) \quad (6.38)$$

where $X(k)$ is the discrete Fourier transform of input signal, $y(r)$ is the filtered discrete time domain signal, $H(k)$ is the frequency response function of filter which determines the filtering mode and characteristics, r is the order number of sampling points in time domain, k is the order number of sampling points in frequency domain and N is the number of sampling.

FDF method has good frequency selectivity and flexibility. Furthermore the filtering process is multiplication of the Fourier spectrum of the signal and the frequency characteristics of the filter therefore the calculation speed of FDF is faster than that of TDF which is a process of convolution. Moreover FDF will not cause problems of time shift and distortion.

Consequently a frequency domain filter will be added in this open-loop PID-type ILC algorithm. To be specific, firstly the system error signal $e_k(t)$ will be filtered by the frequency domain filter. Then the iterative learning controller will calculate the new system input signal $u_{k+1}(t)$ with the filtered system error signal $ef_k(t)$. Thus the algorithm is given by

$$u_{k+1}(t) = u_k(t) + [K_P(t) + K_I(t) \int dt + K_D(t) \frac{d}{dt}]ef_k(t). \quad (6.39)$$

And the control structure of open-loop PID-type ILC algorithm based on digital frequency domain filtering technology is given in Figure 6.2.

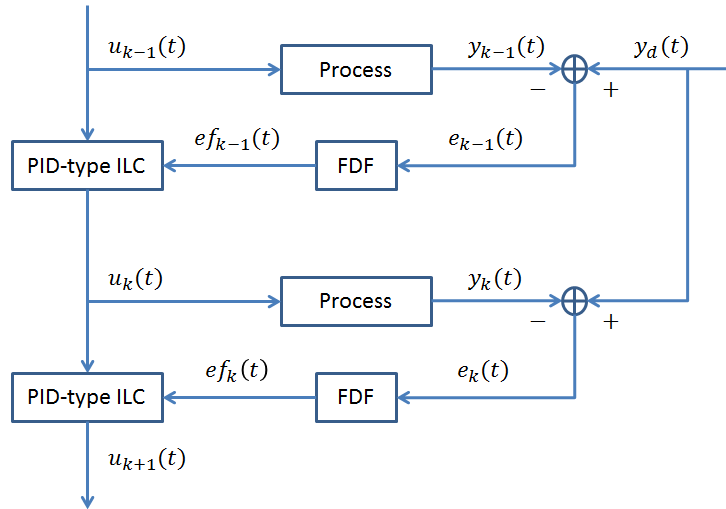


Figure 6.2.: Control Structure of Open-Loop PID-Type ILC with Frequency Domain Filter

6.4. Adaptive ILC

6.4.1. Algorithm Description

PID-type ILC algorithm based on FDF allows engineers to select large learning parameters while both the convergence rate and algorithm stability is still satisfying. However it is not so convenient for researchers to find the proper values of the learning parameters. As discussed in §6.2.1.3, adaptive control is a learning process aiming at parameter while ILC is the one aiming at control input hence researchers combine adaptive control and ILC thus they propose the conception of adaptive ILC algorithm. In the adaptive ILC algorithm the values of the learning parameters of the iterative learning controller are updated by the adaptive algorithm while the control input of controlled system is updated by the ILC algorithm. The advantage is that it is convenient to apply this algorithm in practical system since engineers do not have to estimate the values of the learning

6. Iterative Learning Control Theory

parameters.

There are many adaptive algorithms which can estimate the values of the learning parameters of iterative learning controller. The adaptive algorithm with Nussbaum function is one of them. It has a lot of advantages. For instance the algorithm is simple and easy to be implemented. Moreover it does not need the prior information of controlled system. Consequently it is studied by many researchers [237], [238], [239], [240]. Based on their research results, the adaptive ILC algorithm with Nussbaum-type gain is proposed as follows.

6.4.1.1. Problem Description

The following SISO linear time-invariant system is considered:

$$\begin{cases} \dot{\underline{x}}(t) = \underline{A}\underline{x}(t) + \underline{b}u(t) \\ y(t) = \underline{c}^T \underline{x}(t) \end{cases} \quad (6.40)$$

where $\underline{x}(t) \in R^n$ is system state, $y(t) \in R$ is system output signal, $u(t) \in R$ is control signal, \underline{A} is state matrix with proper dimension, \underline{b} and \underline{c} are input and output parametric vectors respectively with proper dimension. The control requirement is that the system output $y(t)$ should track the desired output $y_d(t)$ precisely in the time interval $[0, T]$.

If the ILC algorithm is applied to realize the control target above, the dynamic equation of the ILC system on trial k can be described as:

$$\begin{cases} \dot{\underline{x}}_k(t) = \underline{A}\underline{x}_k(t) + \underline{b}u_k(t) \\ y_k(t) = \underline{c}^T \underline{x}_k(t) \end{cases} \quad (6.41)$$

and the output error on trial k is defined as

$$e_k(t) = y_d(t) - y_k(t). \quad (6.42)$$

Furthermore the desired system state $\underline{x}_d(t)$, output $y_d(t)$ and input $u_d(t)$ satisfy

$$\begin{cases} \dot{\underline{x}}_d(t) = \underline{A}\underline{x}_d(t) + \underline{b}u_d(t) \\ y_d(t) = \underline{c}^T \underline{x}_d(t) \end{cases} . \quad (6.43)$$

Moreover three assumptions are made as follows:

- $\underline{x}_k(0) = \underline{x}_d(0) = \underline{x}_0$ ($k = 1, 2, 3, \dots$);
- $0 < \theta_{min} \leq |\underline{c}^T \underline{b}| \leq \theta_{max}$ where $|\bullet|$ means absolute value, θ_{min} and θ_{max} are positive constants;
- $\underline{c}^T \underline{A}\underline{x}_k(t)$, $\underline{c}^T \underline{A}\underline{x}_d(t)$, $\underline{c}^T \underline{b}$, $u_d(t)$ and $u_k(t)$ are bounded.

6.4.1.2. Nussbaum Function

The Nussbaum function is selected as follows [237]

$$v(\xi) = \cos\left(\frac{\pi}{2}\xi\right) \exp(\xi^2) \quad (6.44)$$

where $\xi \in R$ is the parameter of the Nussbaum function. In addition one can define

$$\gamma = \begin{cases} \gamma_a, & v(\xi) \geq 0 \\ \gamma_b, & v(\xi) < 0 \end{cases} \quad (6.45)$$

where $\gamma_a \in R$, $\gamma_b \in R$, $\gamma_a > 0$ and $\gamma_b > 0$.

Lemma 6.3 [237]. $\forall s_0 \in R$ the Nussbaum function $v(\bullet)$ satisfies

$$\begin{cases} \lim_{s \rightarrow \infty} \sup \frac{1}{s} \int_{s_0}^s \gamma v(\xi) d\xi = +\infty \\ \lim_{s \rightarrow \infty} \inf \frac{1}{s} \int_{s_0}^s \gamma v(\xi) d\xi = -\infty \end{cases} \quad (6.46)$$

where *sup* means supremum which is referred to the least upper bound of the function and *inf* means infimum which is referred to the greatest lower bound of the function.

6. Iterative Learning Control Theory

6.4.1.3. Adaptive ILC Algorithm

The adaptive ILC algorithm with the Nussbaum type gain is given by [237]:

$$u_k(t) = v[p_k(t)]e_k(t) + u_{k-1}(t) \quad (6.47)$$

$$\dot{p}_k(t) = e_k^2(t) \quad (6.48)$$

$$p_k(0) = p_{k-1}(T) \quad (6.49)$$

and the corresponding control structure of the adaptive ILC algorithm is given in Figure 6.3.

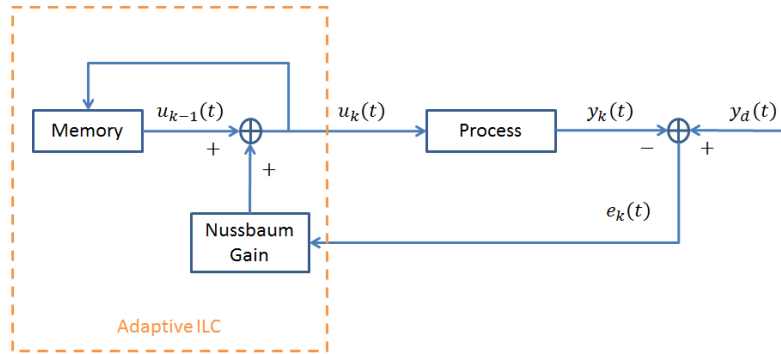


Figure 6.3.: Control Structure of Adaptive ILC

6.4.2. Convergence Analysis

In [237] Jiang and Chen propose the adaptive ILC algorithm with the Nussbaum type gain for SISO system and then discuss the convergence of the algorithm in detail. Consequently here their results will be introduced briefly.

Theorem 6.2. It is supposed that the controlled system is described by Eq. (6.40) and the ILC algorithm is given by Eq. (6.47), Eq. (6.48) and Eq. (6.49).

If in the time interval $[0, T]$ the whole system satisfies the three assumptions in §6.4.1.1 then $e_k(t)$ can converge to 0 uniformly when $k \rightarrow \infty$.

Proof. An auxiliary function is defined as follows

$$V(\xi) = \frac{1}{2}\xi^2. \quad (6.50)$$

Thus one can get

$$V[e_k(t)] = \frac{1}{2}e_k^2(t) \quad (6.51)$$

hence

$$\begin{aligned} \frac{dV[e_k(t)]}{dt} &= e_k(t)\dot{e}_k(t) \\ &= e_k(t)\{\dot{y}_d(t) - \dot{y}_k(t)\} \\ &= e_k(t)\{\underline{c}^T \dot{x}_d(t) - \underline{c}^T \dot{x}_k(t)\} \\ &= e_k(t)\{\underline{c}^T \underline{A}x_d(t) + \underline{c}^T \underline{b}u_d(t) \\ &\quad - \underline{c}^T \underline{A}x_k(t) - \underline{c}^T \underline{b}u_k(t)\} \\ &= e_k(t)\{\underline{c}^T \underline{A}[x_d(t) - x_k(t)] + \underline{c}^T \underline{b}u_d(t) \\ &\quad - \underline{c}^T \underline{b}u_{k-1}(t) - \underline{c}^T \underline{b}v[p_k(t)]e_k(t)\}. \end{aligned} \quad (6.52)$$

According to the assumptions one can obtain

$$\underline{c}^T \underline{A}[x_d(t) - x_k(t)] + \underline{c}^T \underline{b}u_d(t) - \underline{c}^T \underline{b}u_{k-1}(t) \leq w|e_k(t)| \quad (6.53)$$

where $w \in R$ is positive and bounded.

When $\underline{c}^T \underline{b} > 0$ (if $\underline{c}^T \underline{b} < 0$ the proof procedure is similar) i.e. $0 < \theta_{min} \leq \underline{c}^T \underline{b} \leq \theta_{max}$, one can define

$$\theta = \begin{cases} \theta_{min}, & v[p_k(t)] \geq 0 \\ \theta_{max}, & v[p_k(t)] < 0 \end{cases} \quad (6.54)$$

6. Iterative Learning Control Theory

thus one can have

$$-\underline{c}^T \underline{b} v[p_k(t)] \leq -\theta v[p_k(t)]. \quad (6.55)$$

Consequently one can derive

$$\begin{aligned} \frac{dV[e_k(t)]}{dt} &\leq e_k(t)w|e_k(t)| - e_k(t)\theta v[p_k(t)]e_k(t) \\ &\leq w|e_k(t)|^2 - \theta v[p_k(t)]e_k^2(t) \\ &= \{w - \theta v[p_k(t)]\}e_k^2(t) \\ &= \{w - \theta v[p_k(t)]\}\dot{p}_k(t). \end{aligned} \quad (6.56)$$

Thus with integration one can achieve

$$\begin{aligned} 0 &\leq V[e_k(t)] \\ &\leq \int_0^t \{w - \theta v[p_k(t)]\}\dot{p}_k(t) dt \\ &= \int_{p_k(0)}^{p_k(t)} \{w - \theta v[p_k(t)]\} dp_k(t), \quad t \in [0, T]. \end{aligned} \quad (6.57)$$

Then according to Eq. (6.49) one can obtain

$$\begin{aligned} 0 &\leq \sum_{j=1}^{k-1} V[p_j(T)] + V[p_k(t)] \\ &= w[p_k(t) - p_1(0)] - \int_{p_1(0)}^{p_k(t)} \theta v(p) dp. \end{aligned} \quad (6.58)$$

It is assumed that when $k \rightarrow \infty$, $p_k(t)$ is unbounded then according to Eq. (6.48) and Eq. (6.49) one can get $p_k(t) \rightarrow +\infty$ when $k \rightarrow \infty$.

Thus one can achieve

$$\begin{aligned} 0 &\leq \frac{1}{p_k(t)} w[p_k(t) - p_1(0)] - \frac{1}{p_k(t)} \int_{p_1(0)}^{p_k(t)} \theta v(p) dp \\ &= w[1 - \frac{p_1(0)}{p_k(t)}] - \frac{1}{p_k(t)} \int_{p_1(0)}^{p_k(t)} \theta v(p) dp. \end{aligned} \quad (6.59)$$

However when $p_k(t) \rightarrow +\infty$, Eq. (6.59) is in contradiction with Eq. (6.46). Hence $p_k(t)$ should be bounded when $k \rightarrow \infty$. Thus according to Eq. (6.48) and Eq. (6.49) when $k \rightarrow \infty$, $e_k(t)$ will converge to 0 uniformly.

□

6.5. Inverse Model ILC

6.5.1. Algorithm Description

One of the advantages of PID-type ILC and adaptive ILC is that researchers do not need the information of controlled system when they apply the ILC algorithms in the practical system. However some researchers think that if they can achieve the information of controlled system, such as system model, so as to combine the ILC algorithms and system information, the control effects will be improved [241]. Hence they propose some ILC algorithms based on system information. One of them is the inverse model ILC algorithm which is effective and realizable in practical engineering. In [242] the researchers propose the inverse model ILC algorithm and then give the convergence condition of the algorithm. Therefore here their results is introduced briefly.

6.5.1.1. Problem Description

SISO linear system is considered here. Supposing that G_p is the transfer function of the process then one can obtain

$$Y = G_p U \quad (6.60)$$

where Y is the system output signal and U is the control signal. The control requirement is to obtain the desired control signal U_d so that the process can track the desired output signal Y_d precisely.

6. Iterative Learning Control Theory

If the ILC algorithm is applied to realize the control target above, the system on trial k should satisfy:

$$Y_k = G_p U_k \quad (6.61)$$

and the output error on trial k is defined as

$$E_k = Y_d - Y_k. \quad (6.62)$$

Furthermore the desired output signal Y_d and control signal U_d satisfy

$$Y_d = G_p U_d. \quad (6.63)$$

6.5.1.2. Inverse Model ILC Algorithm

If on the next trial $k + 1$ the perfect convergence of the system signals to the desired ones is achieved i.e. $U_{k+1} = U_d$ and $Y_{k+1} = Y_d$, then according to Eq. (6.61), Eq. (6.62) and Eq. (6.63) one has

$$U_{k+1} = U_d = U_k + \frac{1}{G_p} E_k. \quad (6.64)$$

If both the process G_p and the data of the previous trials can be known perfectly, the desired control signal U_d can be calculated directly with Eq. (6.64). This implies that Eq. (6.64) is a good ILC algorithm which can obtain perfect control effects. However it is impossible to know the process G_p perfectly. Fortunately in most cases with system modeling and identification one can achieve the estimation G_p^* of the process which can replace G_p . Thus the inverse model ILC algorithm is given by

$$U_{k+1} = U_k + \frac{1}{G_p^*} E_k \quad (6.65)$$

and the corresponding control structure of the inverse model ILC algorithm is given in Figure 6.4.

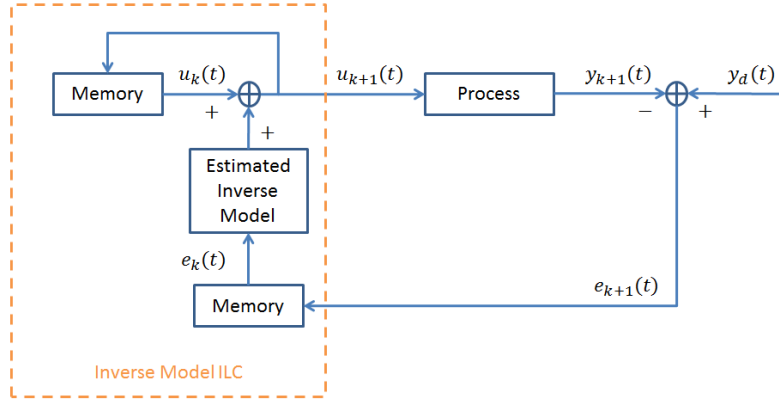


Figure 6.4.: Control Structure of Inverse Model ILC

6.5.2. Convergence Analysis

Theorem 6.3. It is supposed that the controlled system is described by Eq. (6.60) and the ILC algorithm is given by Eq. (6.65). It is assumed that the initial conditions of the system are nearly the same on each trial. If the estimated transfer function G_p^* of the process satisfies that

$$\sup_{\omega} \left| 1 - \frac{G_p(j\omega)}{G_p^*(j\omega)} \right| < 1 \quad (6.66)$$

then the output error can converge to 0 uniformly when $k \rightarrow \infty$.

Proof. According to Eq. (6.61) the following expression is achieved

$$Y_{k+1} - Y_k = G_p(U_{k+1} - U_k). \quad (6.67)$$

And then according to Eq. (6.62) and Eq. (6.65) one can obtain

$$U_{k+1} = U_k + \frac{1}{G_p^*}(Y_d - Y_k). \quad (6.68)$$

6. Iterative Learning Control Theory

Multiplying both sides of Eq. (6.68) by G_p one can achieve

$$G_p U_{k+1} = G_p U_k + \frac{G_p}{G_p^*} (Y_d - Y_k) \quad (6.69)$$

and thus one can have

$$G_p (U_{k+1} - U_k) = \frac{G_p}{G_p^*} (Y_d - Y_k). \quad (6.70)$$

Substituting Eq. (6.70) into Eq. (6.67) the following relationship can be achieved

$$Y_{k+1} = \left(1 - \frac{G_p}{G_p^*}\right) Y_k + \frac{G_p}{G_p^*} Y_d \quad (6.71)$$

and by multiplying both sides of Eq. (6.71) with -1 one can obtain

$$-Y_{k+1} = -\left(1 - \frac{G_p}{G_p^*}\right) Y_k - \frac{G_p}{G_p^*} Y_d. \quad (6.72)$$

Adding Y_d to the both sides of Eq. (6.72), it is then arranged as follows

$$E_{k+1} = \left(1 - \frac{G_p}{G_p^*}\right) E_k. \quad (6.73)$$

Now the Euclidean norm $\|\bullet\|_2$ is introduced as follows

$$\|E\|_2^2 = \frac{1}{2\pi} \int_{-\infty}^{+\infty} |E(j\omega)|^2 d\omega = \int_0^{\infty} |e(t)|^2 dt. \quad (6.74)$$

Thus taking the Euclidean norm to the both sides of Eq. (6.73) one can derive

$$\begin{aligned} \|E_{k+1}\|_2 &= \left\| \left(1 - \frac{G_p}{G_p^*}\right) E_k \right\|_2 \\ &\leq \left\| 1 - \frac{G_p}{G_p^*} \right\|_2 \cdot \|E_k\|_2 \end{aligned} \quad (6.75)$$

where $\|1 - G_p/G_p^*\|_2$ is the induced operator norm which is defined by

$$\left\|1 - \frac{G_p}{G_p^*}\right\|_2 = \sup_{\omega} \left|1 - \frac{G_p(j\omega)}{G_p^*(j\omega)}\right|. \quad (6.76)$$

Consequently if the estimated model G_p^* of the process satisfies that

$$\sup_{\omega} \left|1 - \frac{G_p(j\omega)}{G_p^*(j\omega)}\right| < 1$$

then the output error can converge to 0 uniformly when $k \rightarrow \infty$.

□

6.6. Summary

In this chapter the basic concepts of ILC are introduced. Moreover the development of ILC theory is presented. Furthermore three typical ILC algorithms are discussed. Firstly a PID-type ILC algorithm based on frequency domain filtering technology is introduced. One of the advantages of this algorithm is that it is simple. Additionally with filtering technology both of the convergence rate and algorithm stability is satisfying. However one problem of the algorithm is that it is not so easy to determine the values of the learning parameters. Aiming at this problem an adaptive ILC algorithm with Nussbaum type gain is proposed. With this algorithm the values of the learning parameters can be calculated adaptively thus researchers do not have to estimate the proper values for the learning parameters. Finally since sometimes system information can be obtained (for example with system modeling and identification one can estimate the model of controlled system), an inverse model ILC algorithm is introduced. In a word all the three ILC algorithms are simple and thus they are realizable in practical engineering. At the same time the convergence conditions of the three ILC algorithms are given and proved. In the next chapter the three ILC algorithms will be applied in electro-hydraulic servo system respectively to verify and compare their control performances.

6. Iterative Learning Control Theory

7. Simulation and Experimental Research on Iterative Learning Control

In Chapter 6 three ILC algorithms are proposed: PID-type ILC algorithm based on frequency domain filtering technology, adaptive ILC algorithm with Nussbaum type gain and inverse model ILC algorithm. Now whether these ILC algorithms derived are applicable should be verified. There are two methods to verify the control algorithms: simulation verification and experiment verification. The direct way is experiment verification since the final purpose of the research on ILC algorithms is to apply them in practical engineering. However simulation verification has a lot of advantages such as rapidity, convenience, economy and so on. Consequently in this chapter simulation and experiment will be made respectively so as to verify and compare the control effects of the ILC algorithms developed in Chapter 6 comprehensively and completely. Especially the contributions of this chapter are as follows:

- designing iterative learning controllers with PID-type ILC algorithm, adaptive ILC algorithm and inverse model ILC algorithm respectively;
- applying the iterative learning controllers designed with the three ILC algorithms respectively in valve-controlled cylinder system in simulation and experiment;
- comparing and analyzing the control performances of the three ILC algorithms.

7.1. Simulation of SISO Electro-Hydraulic Servo Position Control System

In this section the ILC algorithms will be applied in the electro-hydraulic servo position control system respectively in simulation. Since ILC is a kind of feedforward control which can not improve the stability of the control system, a PI controller is introduced for the valve-controlled cylinder system to realize feedback control [243]. Given proper values of the control parameters of the PI controller the feedback control system can stabilize the plant. Fig. 7.1 shows the structure of the feedback control system which is the “process” in Figure 6.2, Figure 6.3 and Figure 6.4. Thus one only has to consider the convergence and stability of the ILC algorithm itself [243].

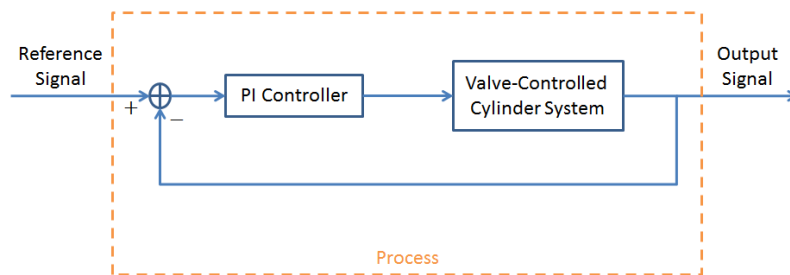


Figure 7.1.: Structure of the Feedback Control System Composed of a PI Controller and the Valve-Controlled Cylinder System

Furthermore in position control the valve-controlled cylinder system contains a 40kN cylinder which works under friction, a MOOG G761-3003 servo valve of which the rated flow is 19l/min and a position sensor. The model of the valve-controlled cylinder system is given by Eq. (3.32) and the values of the model parameters are given by Table 3.2.

Most of the signals can be regarded as the sum of a series of sinusoidal signals according to the result of fourier transform, consequently sinusoidal signal plays an important role in signal analysis and processing. Thus in

7.1. Simulation of SISO Electro-Hydraulic Servo Position Control System

simulation a sinusoidal signal is used, of which the amplitude is 10 mm and the frequency is 5 Hz, as the desired output signal y_d of the system.

Moreover the sample rate of the digital control system is $f_s = 5$ kHz. Additionally the simulation environment is Simulink/Matlab. Especially please note that the phase lag of the system output is compensated manually not only in simulation results but also in experimental results.

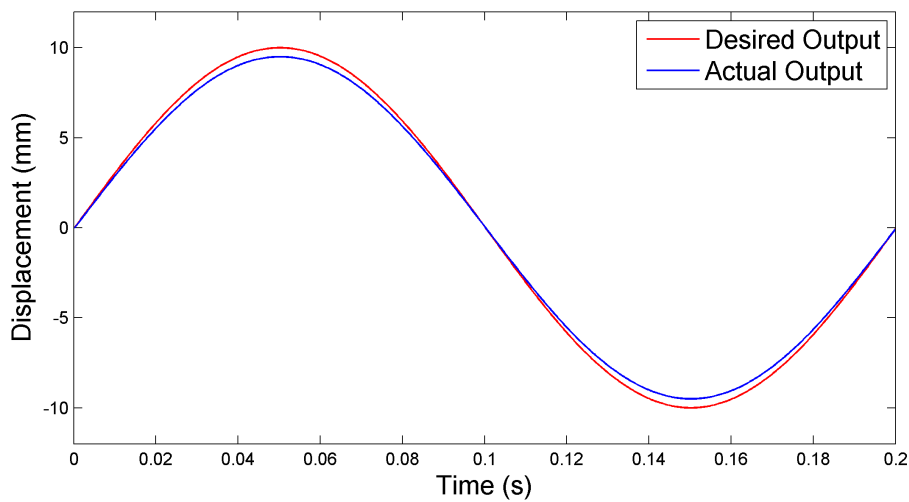


Figure 7.2.: Comparison of the Desired Output and the Actual Output of the System without ILC Algorithm

Firstly y_d is used as the setpoint signal directly so as to achieve the control results without ILC algorithm i.e. only an ordinary PI controller is used. Figure 7.2 shows the simulation result which is the comparison between the desired output signal and the simulated system output signal. From Figure 7.2 one can find that the output error between the desired output signal and the actual output signal is too big which is not acceptable in engineering. Therefore simulation will be made with the three ILC algorithms respectively to verify whether they can improve the control effects. Moreover with simulation one can know which algorithm can achieve the best control effects. The simulation results are given as follows.

7. Simulation and Experimental Research on Iterative Learning Control

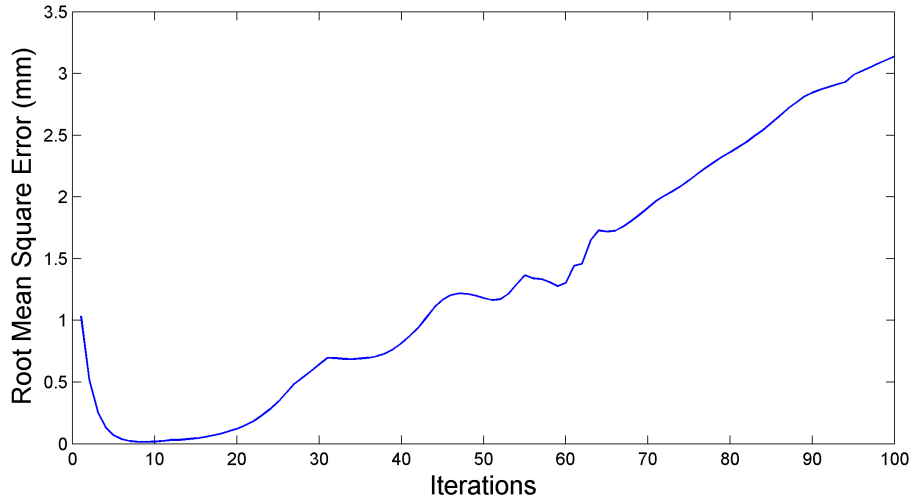


Figure 7.3.: RMS Errors of Open-Loop P-Type ILC System without Filtering Technology

7.1.1. Simulation of P-Type ILC Algorithm

There are many different forms of PID-type ILC algorithm. The simplest one is the P-type ILC algorithm. Hence here open-loop P-type ILC algorithm is applied in the electro-hydraulic servo position control system. In Eq. (6.17) the learning parameters are given by

$$\begin{cases} K_P = 0.5 \\ K_I = 0 \\ K_D = 0 \end{cases} \quad (7.1)$$

thus one can get the traditional open-loop P-type ILC algorithm without filtering technology. After simulation the calculated root mean square (RMS) errors of the system between the desired output signal and the actual output signal for each iteration are given by Figure 7.3.

Figure 7.3 shows that with a large learning parameter $K_P = 0.5$ the control system converges fast i.e. after 8 iterations the RMS error of the system is

7.1. Simulation of SISO Electro-Hydraulic Servo Position Control System

very small. Nevertheless from the 12th iteration the algorithm is not stable any more since the RMS error increases dramatically.

Now the FDF-extended open-loop P-type ILC algorithm described by Eq. (6.39) is applied with the same learning parameters given by Eq. (7.1). The overall control structure is given by Figure 6.2. Moreover the cutoff frequency of the lowpass frequency domain filter is $f_c = 20$ Hz. Figure 7.4 to Figure 7.6 are the simulation results for it.

Figure 7.4 shows the comparison of the desired output and actual output of the system after 20 iterations and Figure 7.5 describes the relative error of the system output after 20 iterations where the relative error $e_k^r(t)$ on trial k is defined by

$$e_k^r(t) = \frac{e_k(t)}{|y_d(t)|_{max}}.$$

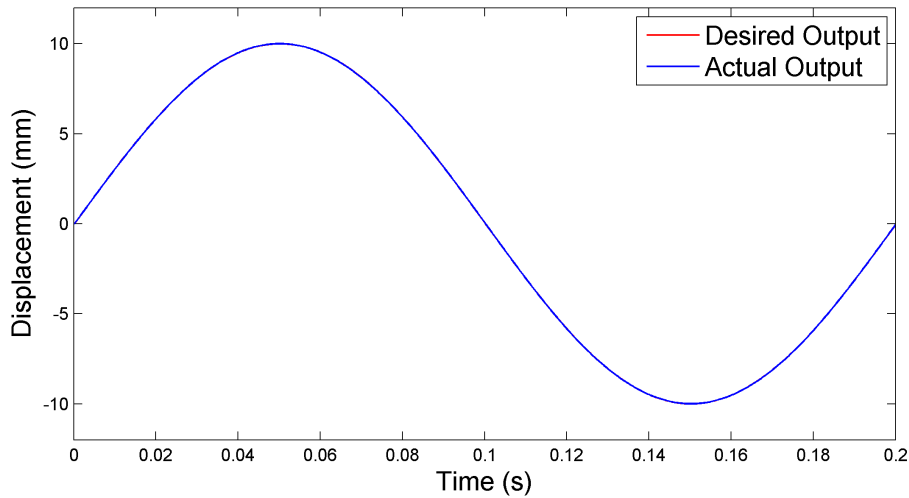


Figure 7.4.: Comparison of the Desired Output and the Actual Output of the System with Open-Loop P-Type ILC Algorithm Based on FDF after 20 Iterations

Observing Figure 7.4 and Figure 7.5 one can find that after 20 iterations the actual output curve of the system is almost coincident with the desired

7. Simulation and Experimental Research on Iterative Learning Control

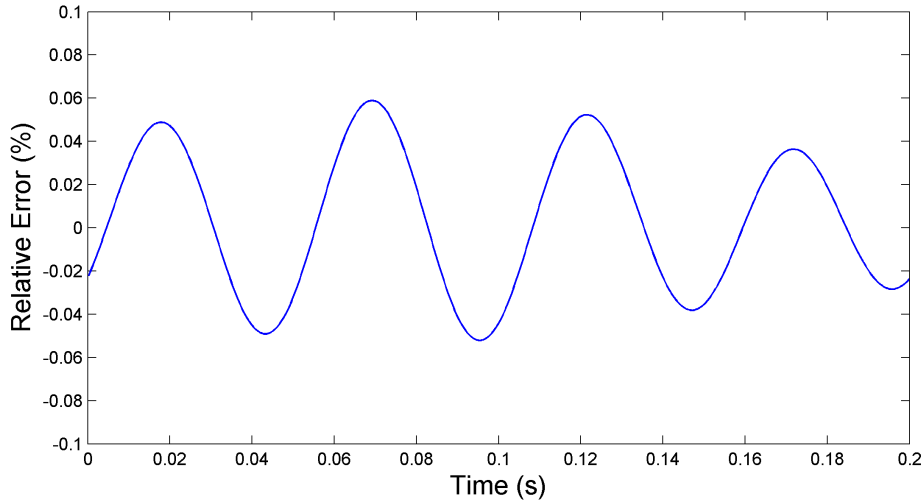


Figure 7.5.: Relative Error of the System Output with Open-Loop P-Type ILC Algorithm Based on FDF after 20 Iterations

output one and the relative error of the system output is very small. Therefore with the FDF technology the convergence speed of the ILC algorithm is still satisfying.

Furthermore Figure 7.6 shows the RMS errors of the system output with iterations. It is clear that on the one hand the RMS error of the system is already very small after approximately 8 iterations i.e. the ILC system based on FDF technology has fast convergence rate and on the other hand the ILC algorithm remains stable after 100 iterations. In a word the open-loop P-type ILC algorithm based on FDF technology obtains good control effects i.e. both the convergence speed and algorithm stability is satisfying.

7.1.2. Simulation of Adaptive ILC Algorithm

In this part the adaptive ILC algorithm with the Nussbaum type gain given by Eq. (6.47) to Eq. (6.49) is applied in the electro-hydraulic servo position

7.1. Simulation of SISO Electro-Hydraulic Servo Position Control System

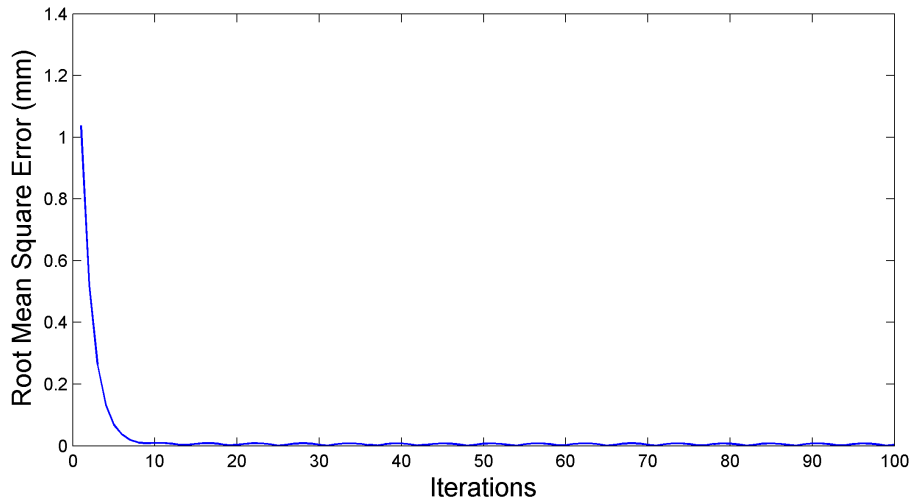


Figure 7.6.: RMS Errors of the Control System Using Open-Loop P-Type ILC Algorithm Based on FDF

control system. Furthermore Figure 6.3 describes the overall control structure of the algorithm. Figure 7.7 to Figure 7.9 are the simulation results for it.

Figure 7.7 represents the comparison of the desired output and actual output of the system after 20 iterations and Figure 7.8 represents the relative error of the system output after 20 iterations.

Note from Figure 7.7 and Figure 7.8 that after 20 iterations the actual output curve of the system is almost coincident with the desired output one and the relative error of the system output is very small. Thus the convergence speed of the adaptive ILC algorithm remains satisfying.

Especially Figure 7.9 shows the RMS errors of the system output with iterations. It is obvious that on the one hand the RMS error of the system output is already very small after approximately 5 iterations i.e. the adaptive ILC algorithm has fast convergence rate and on the other hand the ILC algorithm still keeps stable after 100 iterations. In short the adaptive ILC algorithm with the Nussbaum type gain achieves good control effects i.e.

7. Simulation and Experimental Research on Iterative Learning Control

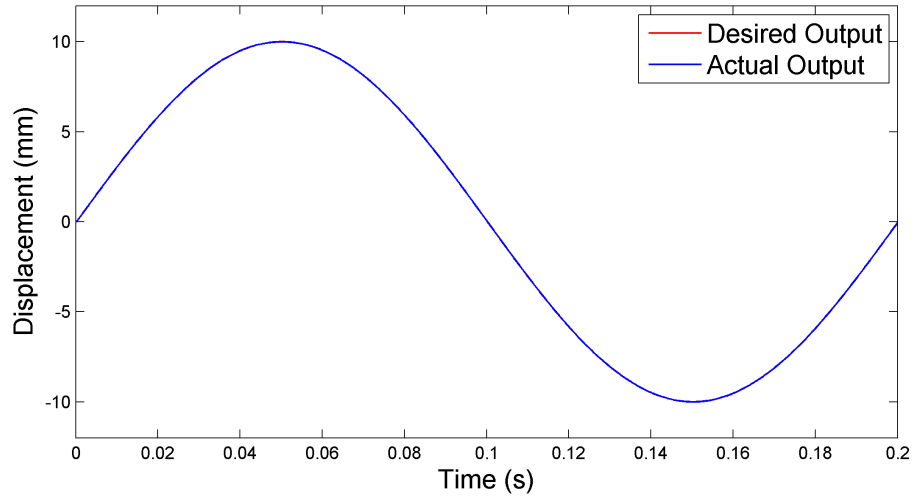


Figure 7.7.: Comparison of the Desired Output and the Actual Output of the System with Adaptive ILC Algorithm after 20 Iterations

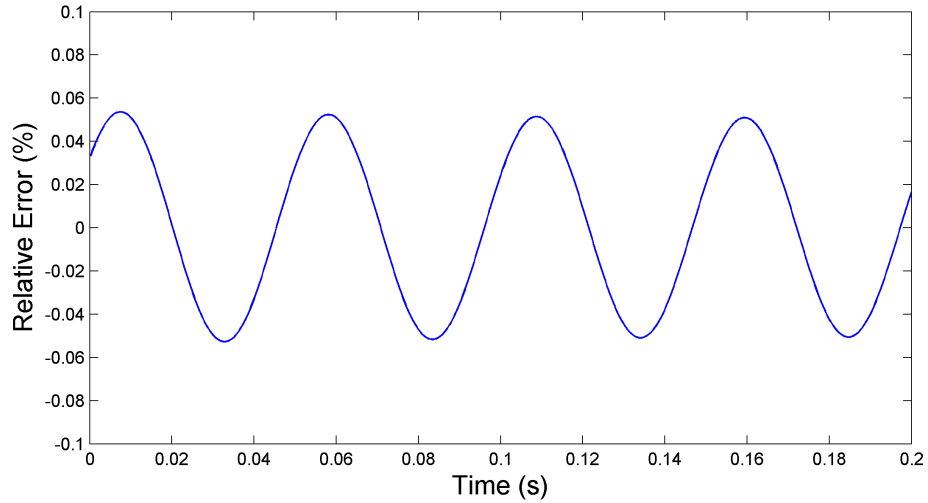


Figure 7.8.: Relative Error of the System Output with Adaptive ILC Algorithm after 20 Iterations

7.1. Simulation of SISO Electro-Hydraulic Servo Position Control System

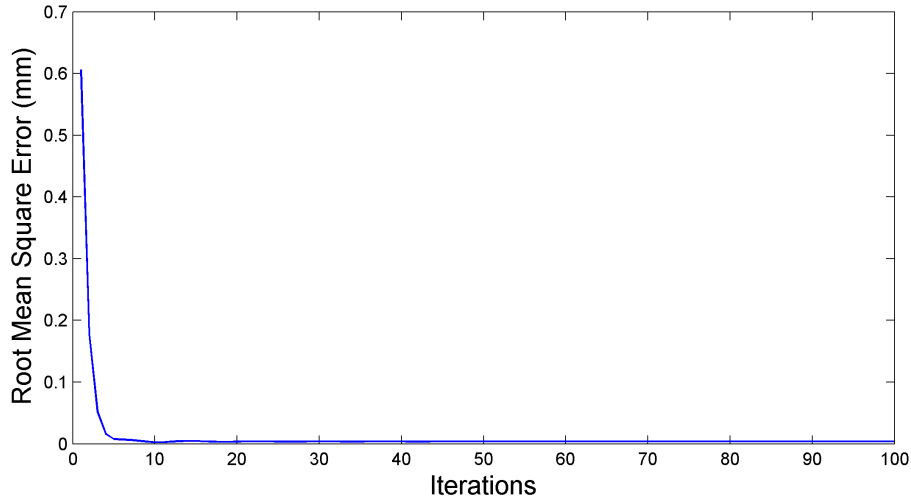


Figure 7.9.: RMS Errors of the Control System Using Adaptive ILC Algorithm

both the convergence speed and algorithm stability is satisfying.

7.1.3. Simulation of Inverse Model ILC Algorithm

Now the inverse model ILC algorithm described by Eq. (6.65) is applied in the electro-hydraulic servo position control system. The original model of valve-controlled cylinder system is given by Eq. (3.32) and the values of the model parameters are given by Table 3.2. Thus according to Fig. 7.1, given proper parameters of the PI controller, the model of closed-loop control system composed of the PI controller and valve-controlled cylinder system can be calculated. Especially this model calculated is the process model G_p in the inverse model ILC algorithm. Then with the inverse of G_p , the inverse model ILC algorithm for electro-hydraulic servo position control system can be established.

However the model described by Eq. (3.32) is a fourth order system thus the process model G_p will be a high order system. Hence the inverse model ILC algorithm established based on the inverse of G_p will be complex. In

7. Simulation and Experimental Research on Iterative Learning Control

SISO system control the algorithm is still realizable nevertheless in MIMO system control the algorithm will bring great computation load to the controller. Consequently one has to simplify the model of valve-controlled cylinder system. Fortunately in [160] it is introduced that the model of valve-controlled cylinder system can be reduced to a low order system if the frequency of setpoint signal of the system is low enough (< 20 Hz). Therefore here a second order system is used to replace the fourth order model of valve-controlled cylinder system as follows

$$G_{vc} = \frac{\frac{K_{sv}}{A}}{\omega_h^2 s^2 + \frac{2\zeta_h}{\omega_h} s + 1} \quad (7.2)$$

where G_{vc} is the reduced order model of valve-controlled cylinder system. Moreover the values of the model parameters are still given by Table 3.2.

Consequently according to Fig. 7.1, given proper parameters of the PI controller, the model of closed-loop control system composed of the PI controller and valve-controlled cylinder system can be calculated with the reduced order model G_{vc} i.e. the simplified process model G_{sim} is obtained. In most cases the order of the numerator of the inverse of G_{sim} is higher than that of the denominator of the inverse of G_{sim} which is not realizable in practical system. One method to solve this problem is adding a low pass filter in series to the inverse of G_{sim} . The cutoff frequency of the low pass filter should be much higher than that of setpoint signal. Additionally the order of the low pass filter depends on the order difference between the numerator and denominator of the inverse of G_{sim} . Here a first order inertial element will be used, of which the cutoff frequency is 200 Hz and the gain is adjustable. Thus the inverse model $1/G_p^*$ used in the ILC algorithm is given by

$$\frac{1}{G_p^*} = \frac{G_{ine}}{G_{sim}} \quad (7.3)$$

where G_{ine} is the transfer function of the first order inertial element.

Thus one can apply the inverse model ILC algorithm described by Eq. (6.65) in simulation. Moreover Figure 6.4 shows the overall control structure of the algorithm. Figure 7.10 to Figure 7.12 are the simulation results for it.

7.1. Simulation of SISO Electro-Hydraulic Servo Position Control System

Figure 7.10 shows the comparison of the desired output and actual output of the system after 20 iterations and Figure 7.11 shows the relative error of the system output after 20 iterations.

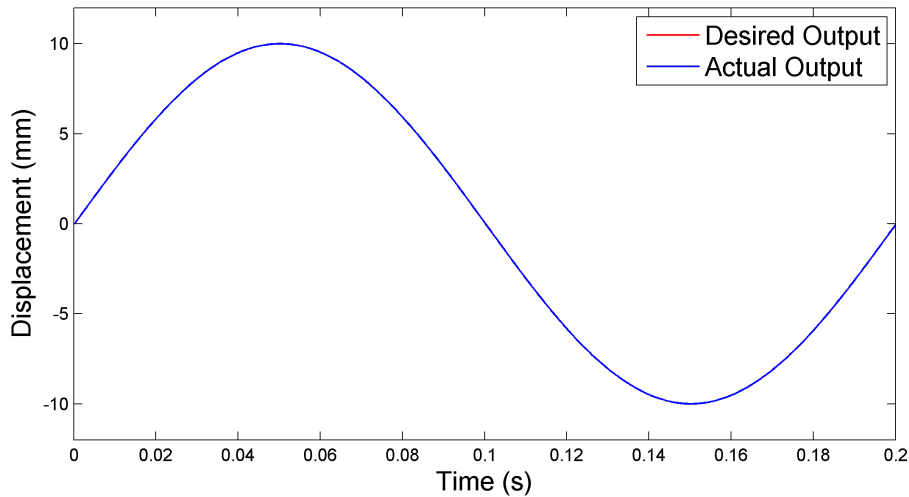


Figure 7.10.: Comparison of the Desired Output and the Actual Output of the System with Inverse Model ILC Algorithm after 20 Iterations

Observing Figure 7.10 and Figure 7.11 one can find that after 20 iterations the actual output curve of the system is almost coincident with the desired output one and the relative error of the system output becomes very small. Hence the convergence rate of the inverse model ILC algorithm is satisfying.

Particularly Figure 7.12 describes the RMS errors of the system output with iterations. It is clear that on the one hand the RMS error of the system output is already very small after approximately 8 iterations i.e. the inverse model ILC algorithm has fast convergence rate and on the other hand the ILC algorithm remains stable after 100 iterations. In a word the inverse model ILC algorithm obtains good control effects i.e. both the convergence rate and algorithm stability is satisfying.

Finally the control performances of the three ILC algorithms should be compared. Observing Figure 7.5 one can find that by using the open-loop

7. Simulation and Experimental Research on Iterative Learning Control

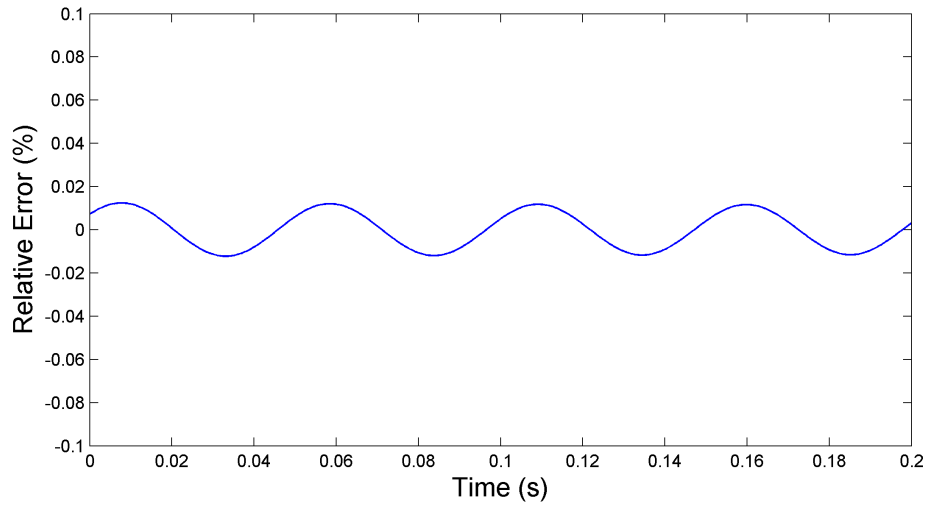


Figure 7.11.: Relative Error of the System Output with Inverse Model ILC Algorithm after 20 Iterations

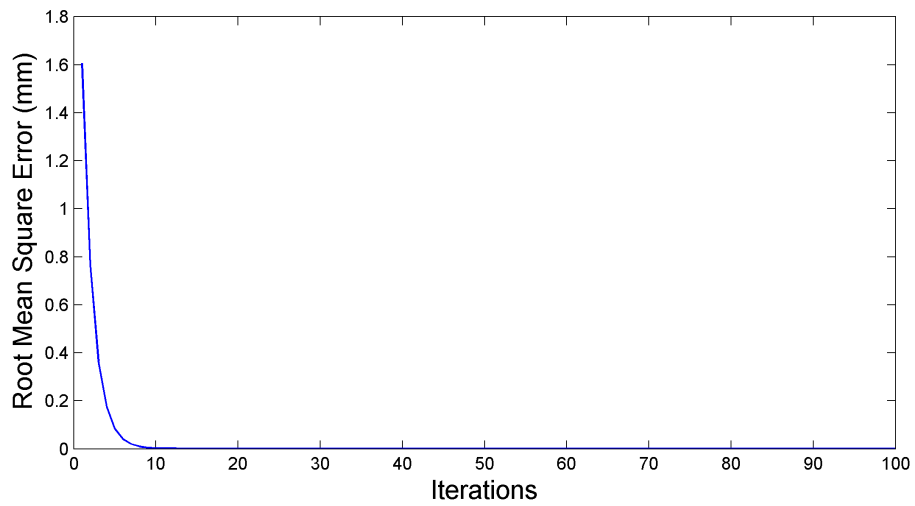


Figure 7.12.: RMS Errors of the Control System Using Inverse Model ILC Algorithm

7.2. Experiment of SISO Electro-Hydraulic Servo Position Control System

P-type ILC algorithm based on FDF technology the relative error of the system output is within a range of $\pm 0.06\%$ after 20 iterations. Moreover from Figure 7.8 one can find that by using the adaptive ILC algorithm with the Nussbaum type gain the relative error of the system output is within a range of $\pm 0.05\%$ after 20 iterations. The control effects of the adaptive ILC algorithm are similar as that of the P-type ILC one. Furthermore from Figure 7.11 one can observe that by using the inverse model ILC algorithm the relative error of the system output is within a range of $\pm 0.02\%$ after 20 iterations i.e. the inverse model ILC algorithm can achieve the best control effects of the three ILC algorithms. The reason is that given the information of controlled system, the ILC algorithm is more pertinent. Especially observing Figure 7.6, Figure 7.9 and Figure 7.12 one can find that the convergence speed of the three ILC algorithms is nearly the same.

In summary the open-loop P-type ILC algorithm based on FDF technology has the simplest form of the three ILC algorithms and the control effects are satisfying however researchers have to estimate the proper value for the learning parameter of the algorithm. The adaptive ILC algorithm with the Nussbaum type gain can solve this problem. The value of the learning parameter of the adaptive ILC algorithm can be updated adaptively thus researchers do not have to estimate the proper value for the learning parameter. Furthermore the control effects of the adaptive ILC algorithm are similar as that of the P-type ILC algorithm nevertheless the adaptive ILC algorithm is more complex than the P-type ILC algorithm. The inverse model ILC algorithm can achieve the best control effects of the three ILC algorithms but to use this algorithm researchers have to build proper model for controlled system.

7.2. Experiment of SISO Electro-Hydraulic Servo Position Control System

In this section the three ILC algorithms obtained in Chapter 6 will be applied in the real world electro-hydraulic servo position control system respectively to verify and compare the control effects of the three ILC algorithms. In simulation many non-ideal factors such as nonlinearity, distur-

7. Simulation and Experimental Research on Iterative Learning Control

bance, time-variant factor and so on are ignored. However these non-ideal factors exist in practical electro-hydraulic servo system and lead to deterioration of control effects of the system. Hence the reference values of the simulation results are limited. Furthermore the final purpose of the research on ILC algorithms is to apply them in practical engineering. Consequently it is necessary to experimentally study the ILC algorithms.

As introduced in §7.1 ILC can not improve the stability of control system therefore the PI controller will still be used for the valve-controlled cylinder system to realize feedback control so that the electro-hydraulic servo control system can be stabilized with proper control parameters of the PI controller. Thus one only has to consider the convergence and stability of the ILC algorithm itself [243]. Hence the structure of the feedback control system is still described by Fig. 7.1.

Furthermore the valve-controlled cylinder system contains a 40kN cylinder which works under friction, a MOOG G761-3003 servo valve of which the rated flow is 19l/min and a position sensor. The model of this valve-controlled cylinder system is already used in the simulation of SISO electro-hydraulic servo position control system in §7.1. Additionally the control parameters of the PI controller are the same as that used in simulation, to realize feedback control. Thus in simulation and experiment the same electro-hydraulic servo position control system are used which is the basis of comparison between the simulation results and experimental results. Moreover Figure 7.13 shows the photograph of the real world electro-hydraulic servo position control system for the experiment.

It is introduced in §7.1 that sinusoidal signal is an important tool in signal analysis and processing. Hence here the same sinusoidal signal as that used in simulation will be used i.e. the sinusoidal signal, of which the amplitude is 10 mm and the frequency is 5 Hz, is used as the desired output signal y_d of the system. Additionally to further verify the effectiveness of the three ILC algorithms, random signal is also used as the desired output signal y_d of the system. Figure 7.14 shows the frequency spectrum of the random signal used in the experiment.

Additionally the sample rate of the digital control system is $f_s = 5$ kHz and the filter-limited signal bandwidth is reduced to the range of 0...300 Hz

7.2. Experiment of SISO Electro-Hydraulic Servo Position Control System

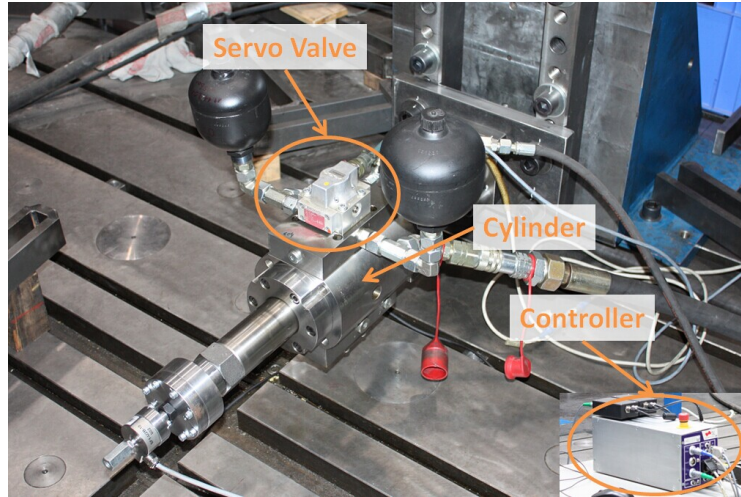


Figure 7.13.: Real World Electro-Hydraulic Servo Position Control System

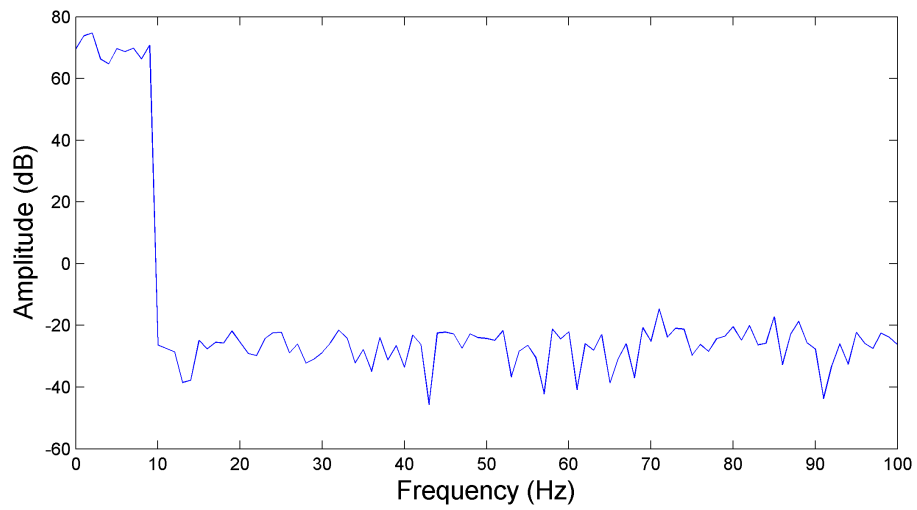


Figure 7.14.: Frequency Spectrum of the Random Signal Used in the Experiment

7. Simulation and Experimental Research on Iterative Learning Control

[243]. Particularly the time delay of the whole system, which seriously affects the control effects, can not be compensated by the ILC algorithms themselves. Consequently the appearing time delay is estimated based on measurement results and then is compensated prior to any signal comparison inside the ILC system [243].

In the experiment firstly the sinusoidal signal is used as the setpoint signal directly so as to achieve the control results without ILC algorithm i.e. only an ordinary PI controller is used. Figure 7.15 shows the experimental results which are the comparison between the desired output signal and the actual system output signal. Observing Figure 7.15 one can find that the valve-controlled cylinder system with an ordinary PI controller reveals a significant difference between the desired output signal and the actual output signal which is not allowed in engineering. Consequently the three ILC algorithms will be applied respectively in the experiment to verify whether they can improve the control effects. Furthermore based on the experimental results one will know which algorithm can achieve the best control effects. The experimental results are given as follows.

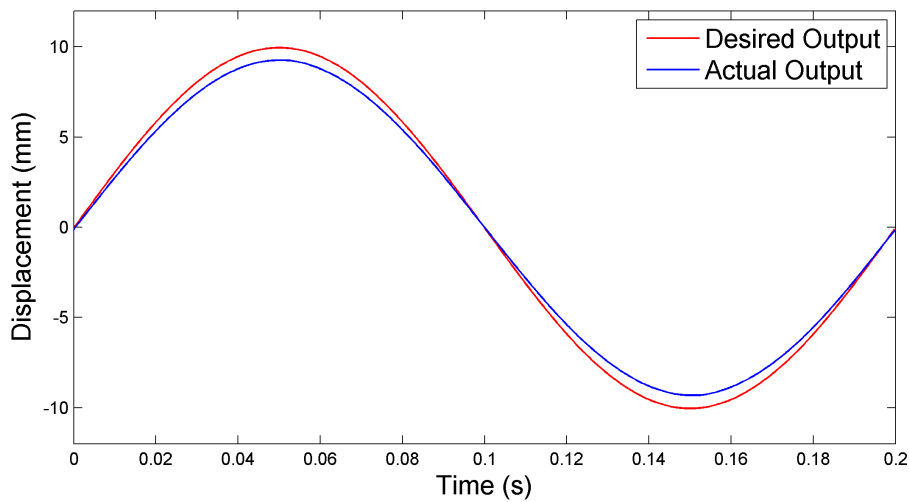


Figure 7.15.: Comparison of the Desired Output and the Actual Output of the System without ILC Algorithm

7.2. Experiment of SISO Electro-Hydraulic Servo Position Control System

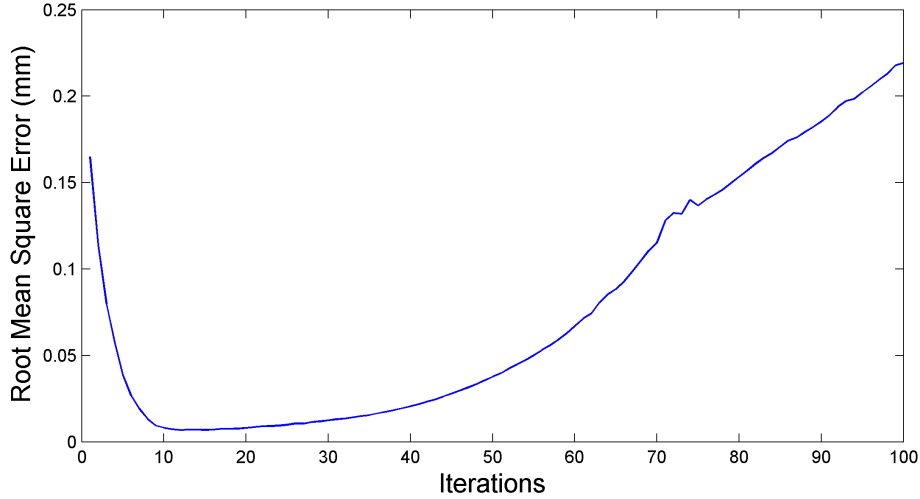


Figure 7.16.: RMS Errors of Open-Loop P-Type ILC System without Filtering Technology

7.2.1. Experiment of P-Type ILC Algorithm

In this part firstly the traditional open-loop P-type ILC algorithm without filtering technology is applied in the real world electro-hydraulic servo position control system. The algorithm is described by Eq. (6.17) and the learning parameters are given by Eq. (7.1) i.e. the same algorithm and learning parameters as that used in simulation are used. After experiment the calculated RMS errors of the system between the desired output signal and the actual output signal for each iteration are given by Figure 7.16.

Figure 7.16 indicates that given a large learning parameter $K_p = 0.5$ the control system converges fast i.e. after 10 iterations the RMS error of the system is small enough. However from the 20th iteration the algorithm is not stable any more since the RMS error increases greatly.

Hence the FDF-extended open-loop P-type ILC algorithm described by Eq. (6.39) is applied with the same learning parameters given by Eq. (7.1). The overall control structure is given by Figure 6.2. Moreover the cutoff frequency of the lowpass frequency domain filter is $f_c = 20$ Hz. Figure 7.17 to Figure 7.19 are the experimental results for it.

7. Simulation and Experimental Research on Iterative Learning Control

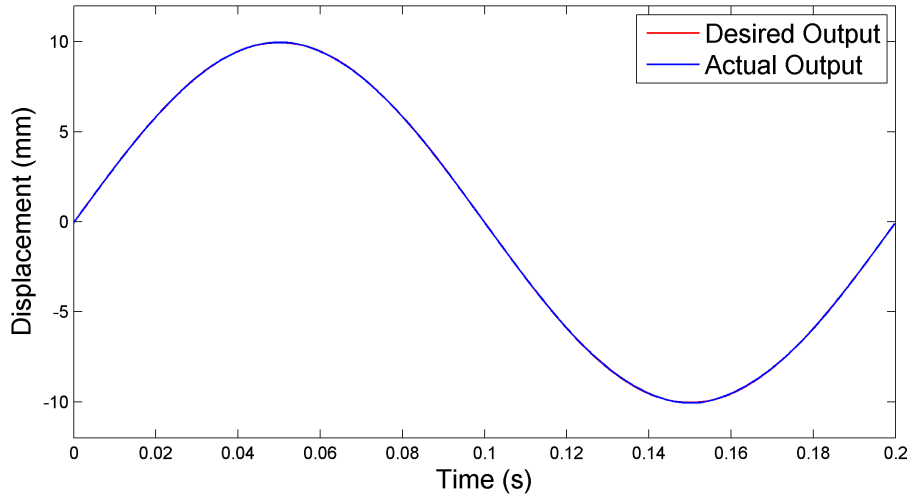


Figure 7.17.: Comparison of the Desired Output and the Actual Output of the System with Open-Loop P-Type ILC Algorithm Based on FDF after 20 Iterations

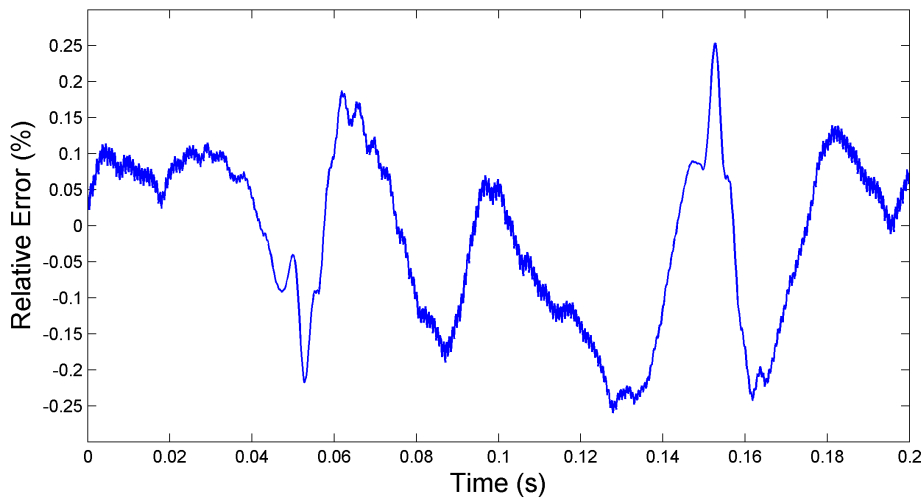


Figure 7.18.: Relative Error of the System Output with Open-Loop P-Type ILC Algorithm Based on FDF after 20 Iterations

7.2. Experiment of SISO Electro-Hydraulic Servo Position Control System

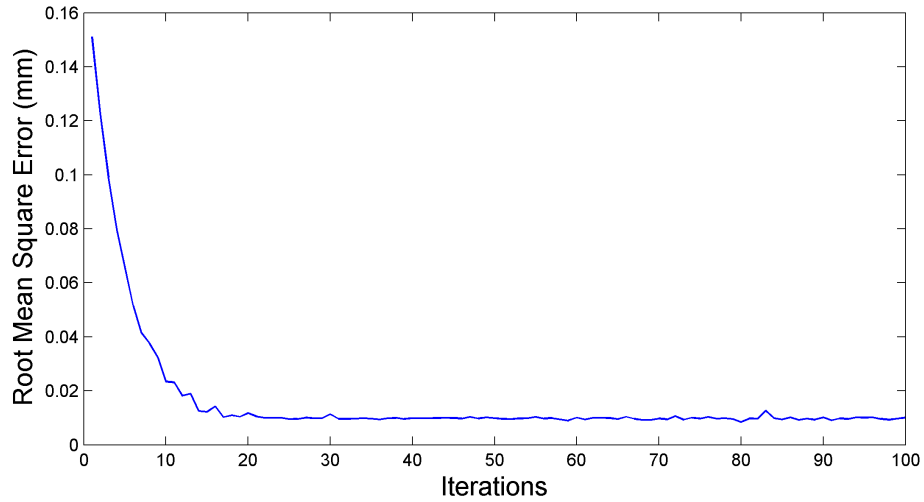


Figure 7.19.: RMS Errors of the Control System Using Open-Loop P-Type ILC Algorithm Based on FDF

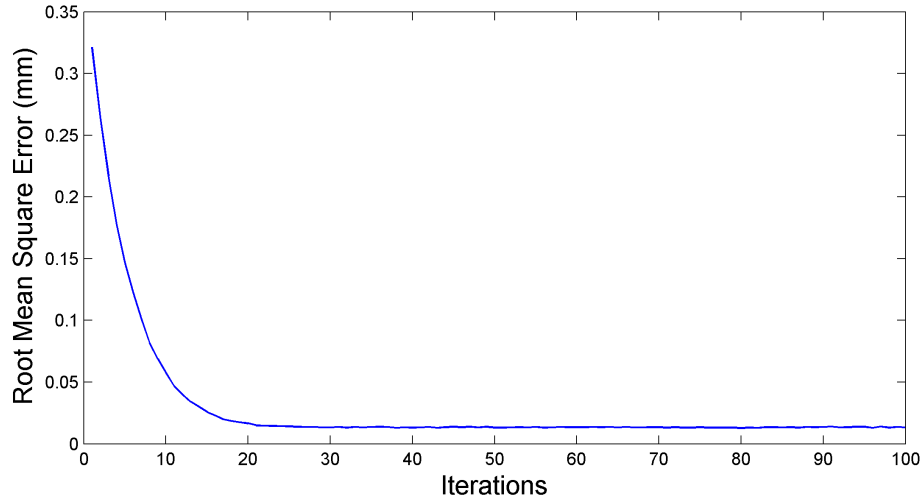


Figure 7.20.: RMS Errors of the Control System Using Open-Loop P-Type ILC Algorithm Based on FDF with Random Signal

7. Simulation and Experimental Research on Iterative Learning Control

Figure 7.17 shows the comparison of the desired output and actual output of the system after 20 iterations and Figure 7.18 describes the relative error of the system output after 20 iterations.

Observing Figure 7.17 and Figure 7.18 one can find that after 20 iterations the actual output curve of the system is almost coincident with the desired output one and the relative error of the system output is very small. Therefore with the FDF technology the convergence speed of the ILC algorithm remains satisfying.

Moreover Figure 7.19 indicates the RMS errors of the system output with iterations. It is clear that on the one hand the RMS error of the system is already very small after approximately 20 iterations i.e. the ILC system based on FDF technology has fast convergence rate and on the other hand the ILC algorithm remains stable after 100 iterations.

To further verify the effectiveness of the open-loop P-type ILC algorithm based on FDF technology, a type of random signal is used as the desired output signal y_d of the system. Figure 7.14 shows the frequency spectrum of the random signal. Figure 7.20 indicates the RMS errors of the system output with iterations. Confined to the length of the dissertation, other experimental results of the open-loop P-type ILC algorithm based on FDF technology with random signal are given in appendix. Comparing Figure 7.19 and Figure 7.20 it can be found that the ILC system still achieves satisfying control performance with random signal. In a word the open-loop P-type ILC algorithm based on FDF technology obtains good control effects i.e. both the convergence speed and algorithm stability is good.

7.2.2. Experiment of Adaptive ILC Algorithm

In this part the adaptive ILC algorithm with the Nussbaum type gain given by Eq. (6.47) to Eq. (6.49) is applied in the real world electro-hydraulic servo position control system. Moreover Figure 6.3 shows the overall control structure of the algorithm. Figure 7.21 to Figure 7.23 are the experimental results for it.

7.2. Experiment of SISO Electro-Hydraulic Servo Position Control System

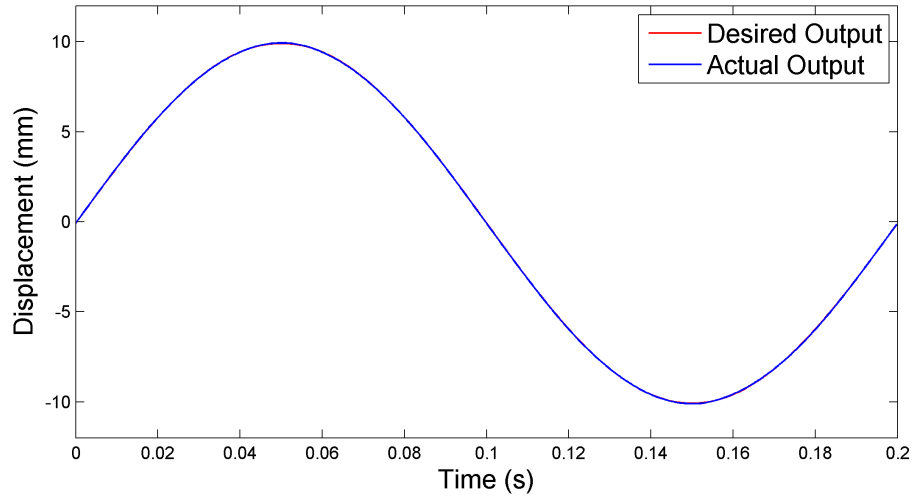


Figure 7.21.: Comparison of the Desired Output and the Actual Output of the System with Adaptive ILC Algorithm after 20 Iterations

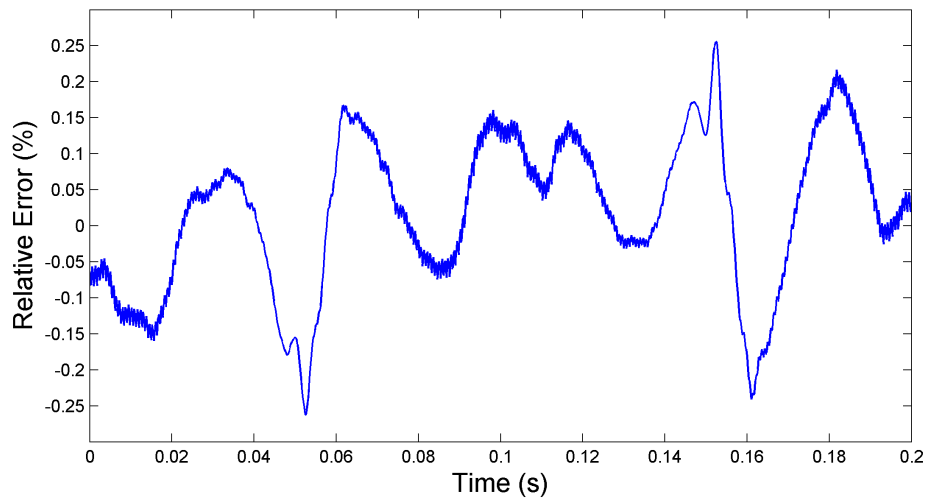


Figure 7.22.: Relative Error of the System Output with Adaptive ILC Algorithm after 20 Iterations

7. Simulation and Experimental Research on Iterative Learning Control

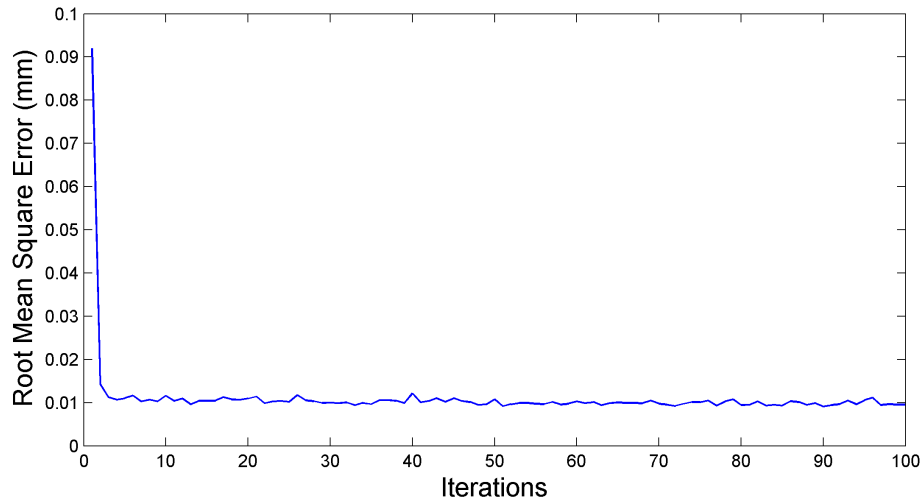


Figure 7.23.: RMS Errors of the Control System Using Adaptive ILC Algorithm

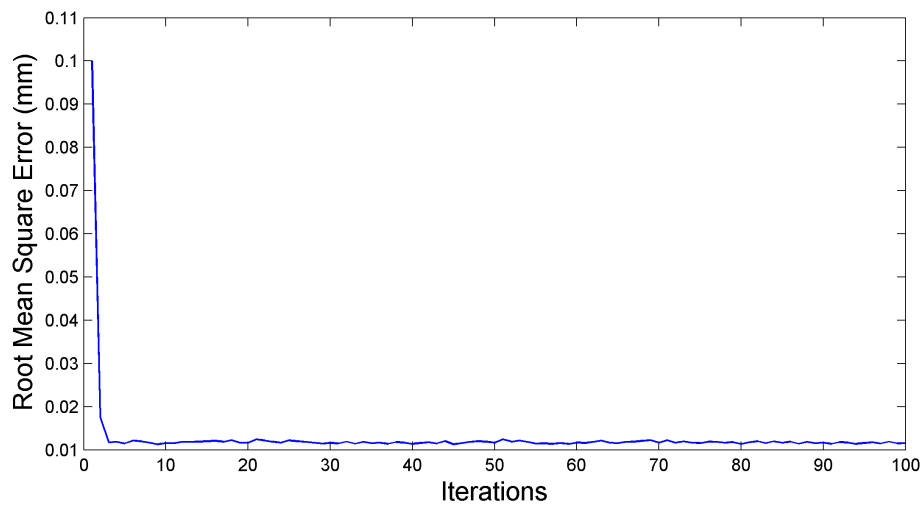


Figure 7.24.: RMS Errors of the Control System Using Adaptive ILC Algorithm with Random Signal

7.2. Experiment of SISO Electro-Hydraulic Servo Position Control System

Figure 7.21 represents the comparison of the desired output and actual output of the system after 20 iterations and Figure 7.22 represents the relative error of the system output after 20 iterations.

Note from Figure 7.21 and Figure 7.22 that after 20 iterations the actual output curve of the system is almost coincident with the desired output one and the relative error of the system output is very small. Hence the convergence speed of the adaptive ILC algorithm is satisfying.

Particularly Figure 7.23 describes the RMS errors of the system output with iterations. It is obvious that on the one hand the RMS error of the system output is already very small after approximately 3 iterations i.e. the adaptive ILC algorithm has fast convergence rate and on the other hand the ILC algorithm still keeps stable after 100 iterations.

To further verify the effectiveness of the adaptive ILC algorithm with the Nussbaum type gain, a type of random signal is used as the desired output signal y_d of the system. Figure 7.14 shows the frequency spectrum of the random signal. Figure 7.24 indicates the RMS errors of the system output with iterations. Confined to the length of the dissertation, other experimental results of the adaptive ILC algorithm with the Nussbaum type gain with random signal are given in appendix. Comparing Figure 7.23 and Figure 7.24 it can be observed that the ILC system still obtains satisfying control performance with random signal. In short the adaptive ILC algorithm with the Nussbaum type gain achieves good control effects i.e. both the convergence speed and algorithm stability is good.

7.2.3. Experiment of Inverse Model ILC Algorithm

In this part the inverse model ILC algorithm described by Eq. (6.65) is applied in the real world electro-hydraulic servo position control system. The same inverse model $1/G_p^*$ as that used in simulation in §7.1.3 is used and moreover Figure 6.4 shows the overall control structure of the algorithm. Figure 7.25 to Figure 7.27 are the experimental results for it.

7. Simulation and Experimental Research on Iterative Learning Control

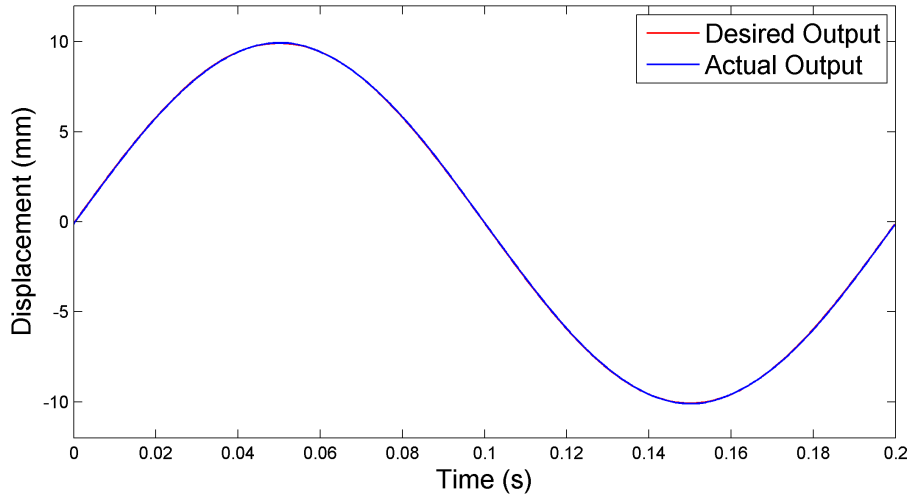


Figure 7.25.: Comparison of the Desired Output and the Actual Output of the System with Inverse Model ILC Algorithm after 20 Iterations

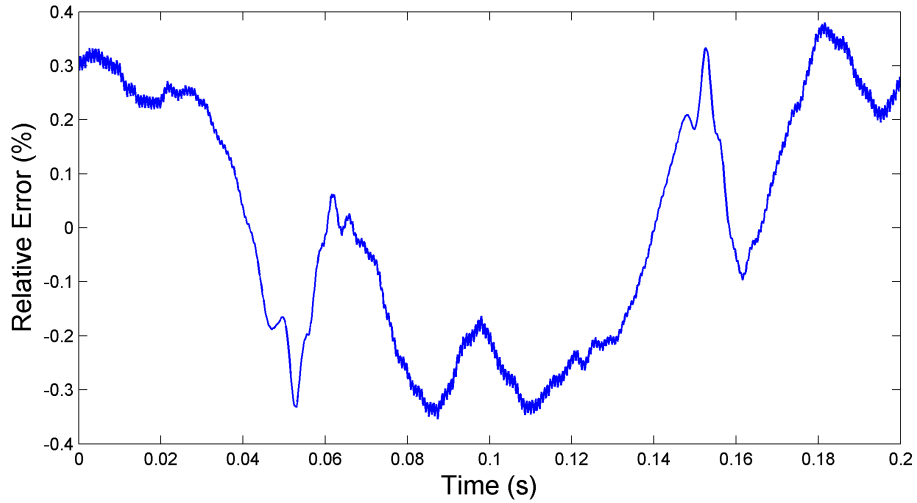


Figure 7.26.: Relative Error of the System Output with Inverse Model ILC Algorithm after 20 Iterations

7.2. Experiment of SISO Electro-Hydraulic Servo Position Control System

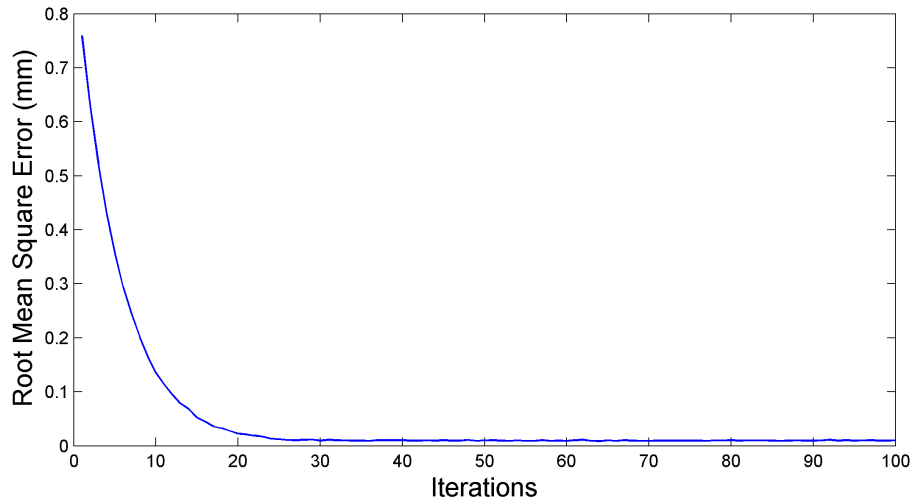


Figure 7.27.: RMS Errors of the Control System Using Inverse Model ILC Algorithm

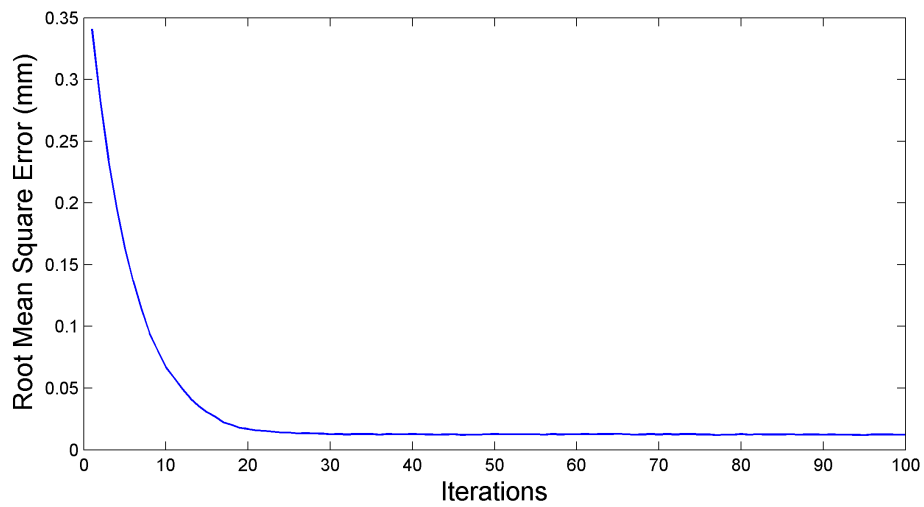


Figure 7.28.: RMS Errors of the Control System Using Inverse Model ILC Algorithm with Random Signal

7. Simulation and Experimental Research on Iterative Learning Control

Figure 7.25 shows the comparison of the desired output and actual output of the system after 20 iterations and Figure 7.26 shows the relative error of the system output after 20 iterations.

Observing Figure 7.25 and Figure 7.26 one can find that after 20 iterations the actual output curve of the system is almost coincident with the desired output one and the relative error of the system output becomes very small. Consequently the convergence rate of the inverse model ILC algorithm is good.

Especially Figure 7.27 describes the RMS errors of the system output with iterations. It is clear that on the one hand the RMS error of the system output is already small enough after approximately 20 iterations i.e. the inverse model ILC algorithm has fast convergence rate and on the other hand the ILC algorithm remains stable after 100 iterations.

To further verify the effectiveness of the inverse model ILC algorithm, a type of random signal is used as the desired output signal y_d of the system. Figure 7.14 shows the frequency spectrum of the random signal. Figure 7.28 indicates the RMS errors of the system output with iterations. Confined to the length of the dissertation, other experimental results of the inverse model ILC algorithm with random signal are given in appendix. Comparing Figure 7.27 and Figure 7.28 it can be found that the ILC system still achieves satisfying control performance with random signal. In a word the inverse model ILC algorithm obtains good control effects i.e. both the convergence rate and algorithm stability is satisfying.

Now the control effects of the three ILC algorithms should be compared. Observing Figure 7.18 one can find that by using the open-loop P-type ILC algorithm based on FDF technology the relative error of the system output is within a range of $\pm 0.25\%$ after 20 iterations. Furthermore from Figure 7.22 one can find that by using the adaptive ILC algorithm with the Nussbaum type gain the relative error of the system output is within a range of $\pm 0.25\%$ after 20 iterations. The control effects of the adaptive ILC algorithm are similar as that of the P-type ILC one. Moreover from Figure 7.26 one can observe that by using the inverse model ILC algorithm the relative error of the system output is within a range of $\pm 0.4\%$ after 20 iterations i.e. the control effects of the inverse model ILC algorithm are worse than that of the P-type ILC and adaptive ILC algorithms.

7.2. Experiment of SISO Electro-Hydraulic Servo Position Control System

Particularly from Figure 7.19, Figure 7.23 and Figure 7.27 one can observe that the convergence speed of the P-type ILC and the inverse model ILC algorithms is nearly the same while the adaptive ILC algorithm obtains the fastest convergence speed of the three ILC algorithms. The reason is that the value of the learning parameter of the adaptive ILC algorithm can be continuously adjusted according to the practical error. Nevertheless the convergence speed of all the three ILC algorithms is acceptable.

Furthermore comparing the simulation results with the experimental results it is found that the control precision of the three ILC algorithms in experiment is not as high as that in simulation. It is because in simulation the electro-hydraulic servo system is ideal i.e. all the non-ideal factors such as external disturbance, nonlinearities, time variation and so on are ignored while in experiment all these non-ideal factors influence the control precision largely. Especially it can be found that in simulation the inverse model ILC algorithm achieves the best control effects while in experiment it obtains the worst control effects of the three ILC algorithms. The reason is that the model which is applied in the inverse model ILC algorithm is a simplified linear model but the real world electro-hydraulic servo system is a complex nonlinear system, which leads to the error between the model and the practical system. Moreover the P-type ILC and adaptive ILC algorithms do not need the information of controlled system while the inverse model ILC algorithm relies on system model hence in experiment the control accuracy of the inverse model ILC algorithm is more easily to be affected by the error between simulation model and practical system. Anyway, the control performances of all the three ILC algorithms in experiment are satisfying in engineering.

In summary the control performance the open-loop P-type ILC algorithm based on FDF technology in real world electro-hydraulic servo position control system is satisfying. The advantage of the P-type ILC algorithm is that it has a very simple form while the disadvantage is that researchers have to estimate a proper learning parameter for it. Furthermore the adaptive ILC algorithm with the Nussbaum type gain can achieve the same control performance as that of P-type ILC algorithm. The advantage of the adaptive ILC algorithm is that the value of the learning parameter can be updated adaptively while the disadvantage is that the algorithm is complex. Moreover although the control performance of the inverse model ILC

7. Simulation and Experimental Research on Iterative Learning Control

algorithm is not as good as that of the P-type ILC and adaptive ILC algorithms, it is still satisfying in engineering. However the prerequisite for applying inverse model ILC algorithm is to build an accurate model for controlled system which is time consuming thus this algorithm is not applicable in practical engineering. Therefore the P-type ILC and adaptive ILC algorithms are recommended for real world electro-hydraulic servo position control systems.

7.3. Experiment of SISO Electro-Hydraulic Servo Force Control System

In the last section the conclusion is obtained that the inverse model ILC algorithm is not applicable in practical engineering. Consequently in this section the P-type ILC and adaptive ILC algorithms will be applied in the real world electro-hydraulic servo force control system respectively to further verify and compare the control performances of the two ILC algorithms. The valve-controlled cylinder system contains a 40kN cylinder which works under friction, a MOOG G761-3003 servo valve of which the rated flow is 191/min, an aluminium bar as the unit under test (UUT) and a force sensor. Likewise, a PI controller is used to realize feedback control and Fig. 7.1 shows the structure of the feedback control system. Moreover Figure 7.29 shows the photograph of the real world electro-hydraulic servo force control system for the experiment.

As introduced in §7.1 sinusoidal signal is important in signal analysis and processing. Thus in this experiment a sinusoidal signal, of which the amplitude is 1 kN and the frequency is 5 Hz, is used as the desired output signal y_d of the system. Furthermore the sample rate of the digital control system is $f_s = 5$ kHz and the filter-limited signal bandwidth is reduced to the range of 0 . . . 300 Hz [243]. Especially since the time delay of the whole system can not be compensated by the ILC algorithms themselves, it is estimated based on measurement results and then compensated prior to any signal comparison inside the ILC system [243].

7.3. Experiment of SISO Electro-Hydraulic Servo Force Control System

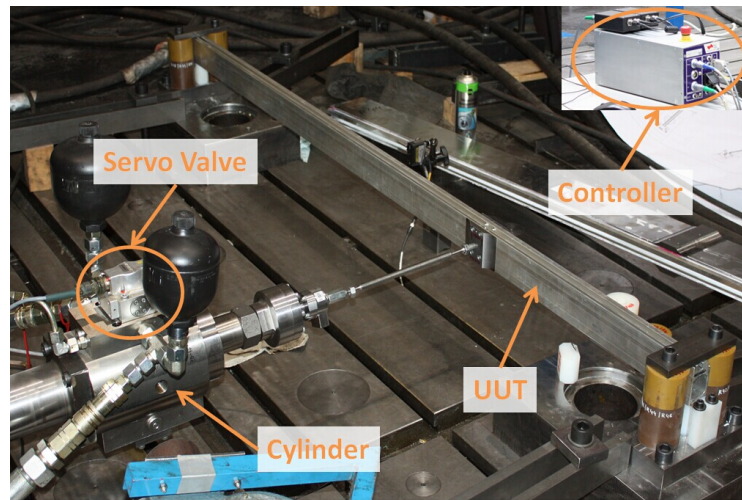


Figure 7.29.: Real World Electro-Hydraulic Servo Force Control System

In the experiment firstly the sinusoidal signal is used as the setpoint signal directly so as to achieve the control results without ILC algorithm i.e. only an ordinary PI controller is used. Figure 7.30 describes the experimental results which are the comparison between the desired output signal and the actual system output signal. From Figure 7.30 one can observe that the valve-controlled cylinder system with an ordinary PI controller nearly can not work. It leads to a large difference between the desired output signal and the actual output signal which is not acceptable in engineering. Especially it is found that there is a contradiction between stability and accuracy i.e. with large parameters of PI controller the output error will be decreased however the system is not stable while with small parameters the system is stable nevertheless the output error is big. The reason is that the force control system works under many non-ideal factors such as low stiffness, nonlinear factors and so on. Therefore the two ILC algorithms will be applied respectively in the experiment to verify whether they can improve the control effects. Furthermore based on the experimental results one can compare the control performances of the two ILC algorithms so as to know which algorithm is better. The experimental results are given as follows.

7. Simulation and Experimental Research on Iterative Learning Control

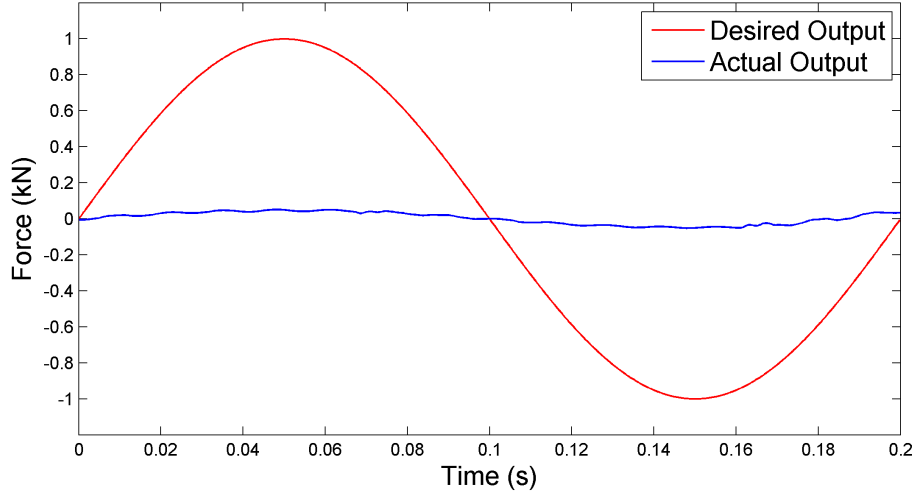


Figure 7.30.: Comparison of the Desired Output and the Actual Output of the System without ILC Algorithm

7.3.1. Experiment of P-Type ILC Algorithm

It is already revealed in §7.2.1 that given a large learning parameter the P-type ILC algorithm converges fast however the algorithm is not stable without FDF technology. Consequently here the FDF-extended open-loop P-type ILC algorithm described by Eq. (6.39) is directly applied in the real world electro-hydraulic servo force control system and the learning parameters are given by

$$\begin{cases} K_P = 0.8 \\ K_I = 0 \\ K_D = 0 \end{cases} \quad (7.4)$$

The overall control structure is given by Figure 6.2. Furthermore the cutoff frequency of the lowpass frequency domain filter is $f_c = 20$ Hz. Figure 7.31 to Figure 7.33 are the experimental results for it.

Figure 7.31 represents the comparison of the desired output and actual out-

7.3. Experiment of SISO Electro-Hydraulic Servo Force Control System

put of the system after 40 iterations and Figure 7.32 represents the output error of the system after 40 iterations.

Note from Figure 7.31 that after 40 iterations the waveforms of the actual output signal and the desired output one fit well however there exists fluctuation in the actual output signal which leads to output error. The reason of system fluctuation is that in this experiment the electro-hydraulic servo force control system works under severe conditions. For example compared with other units under test, the stiffness of the aluminium bar is deficient. Moreover the clearance between the aluminium bar and the fixtures is too large. The output error caused by system fluctuation can not be compensated by P-type ILC algorithm. Furthermore observing Figure 7.32 one can find that after 40 iterations the output error of the system is within a range of ± 0.05 kN which is similar as the amplitude of system fluctuation. Anyway, the control accuracy and the convergence speed of the P-type ILC algorithm in this experiment is satisfying.

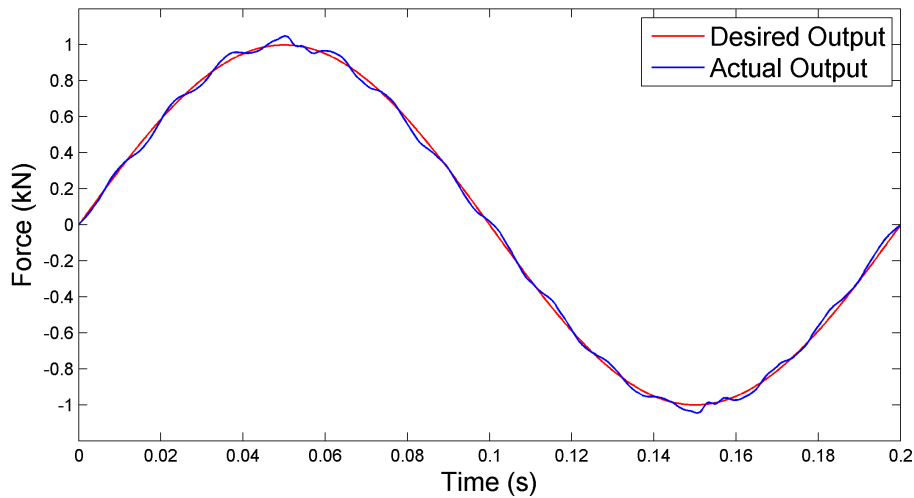


Figure 7.31.: Comparison of the Desired Output and the Actual Output of the System with Open-Loop P-Type ILC Algorithm Based on FDF after 40 Iterations

Particularly Figure 7.33 describes the RMS errors of the system output with iterations. It is obvious that on the one hand the RMS error of the system

7. Simulation and Experimental Research on Iterative Learning Control

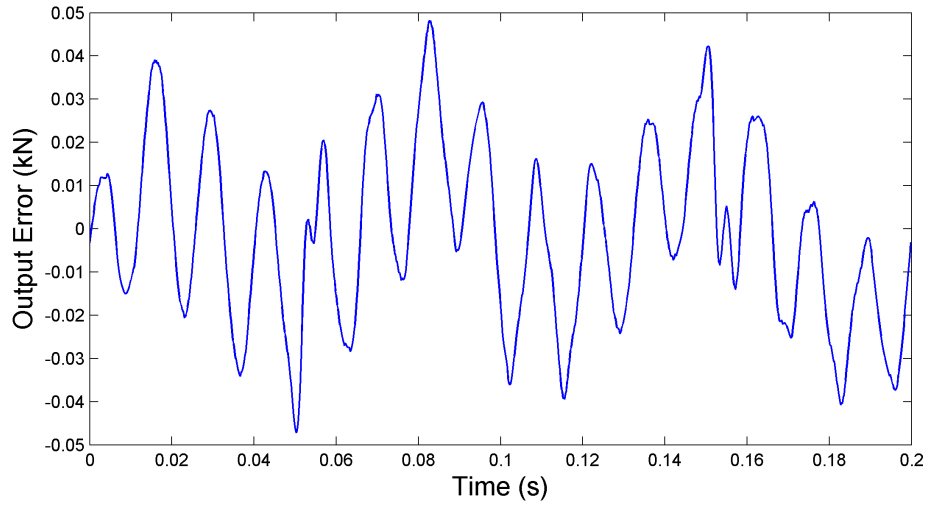


Figure 7.32.: Output Error of the System with Open-Loop P-Type ILC Algorithm Based on FDF after 40 Iterations

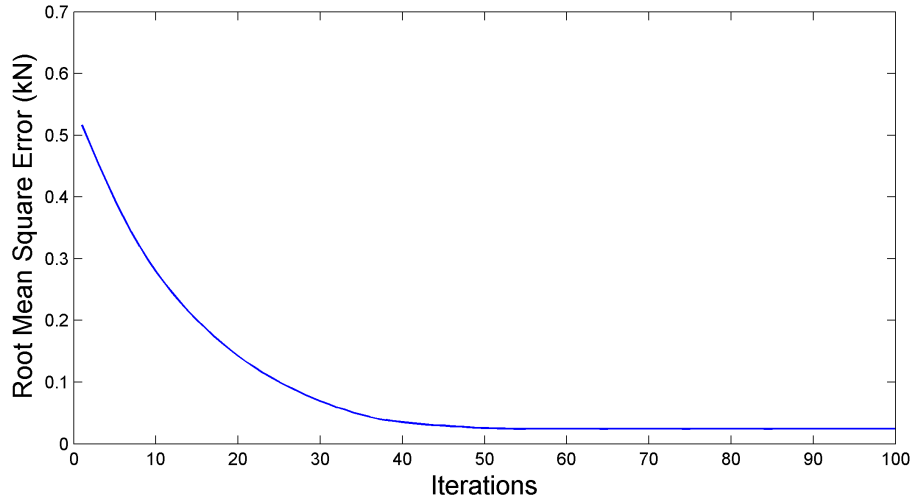


Figure 7.33.: RMS Errors of the Control System Using Open-Loop P-Type ILC Algorithm Based on FDF

7.3. Experiment of SISO Electro-Hydraulic Servo Force Control System

output is small after approximately 40 iterations i.e. the P-type ILC algorithm has fast convergence rate and on the other hand the ILC algorithm still keeps stable after 100 iterations. In short the open-loop P-type ILC algorithm based on FDF technology achieves good control effects i.e. both the convergence speed and algorithm stability is satisfying.

7.3.2. Experiment of Adaptive ILC Algorithm

In this part the adaptive ILC algorithm with the Nussbaum type gain given by Eq. (6.47) to Eq. (6.49) is applied in the real world electro-hydraulic servo force control system. Figure 6.3 shows the overall control structure of the algorithm. Figure 7.34 to Figure 7.36 are the experimental results for it.

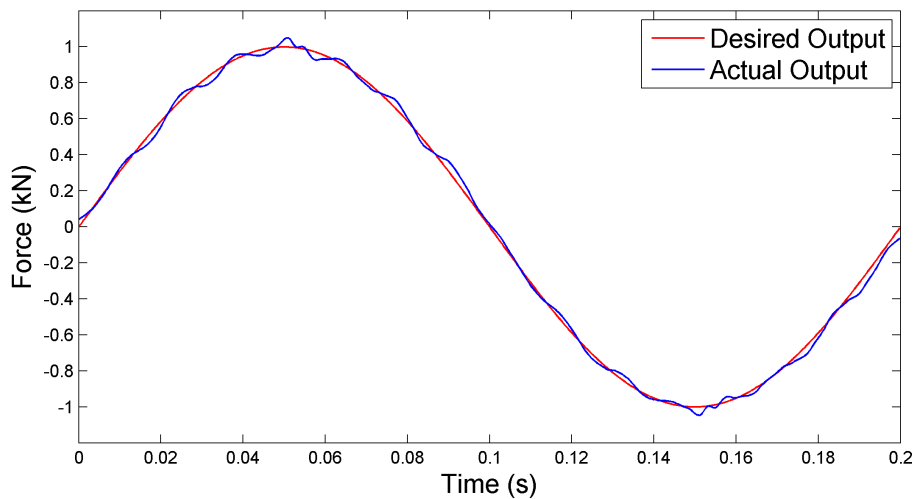


Figure 7.34.: Comparison of the Desired Output and the Actual Output of the System with Adaptive ILC Algorithm after 40 Iterations

Figure 7.34 shows the comparison of the desired output and actual output of the system after 40 iterations and Figure 7.35 represents the output error of the system after 40 iterations.

7. Simulation and Experimental Research on Iterative Learning Control

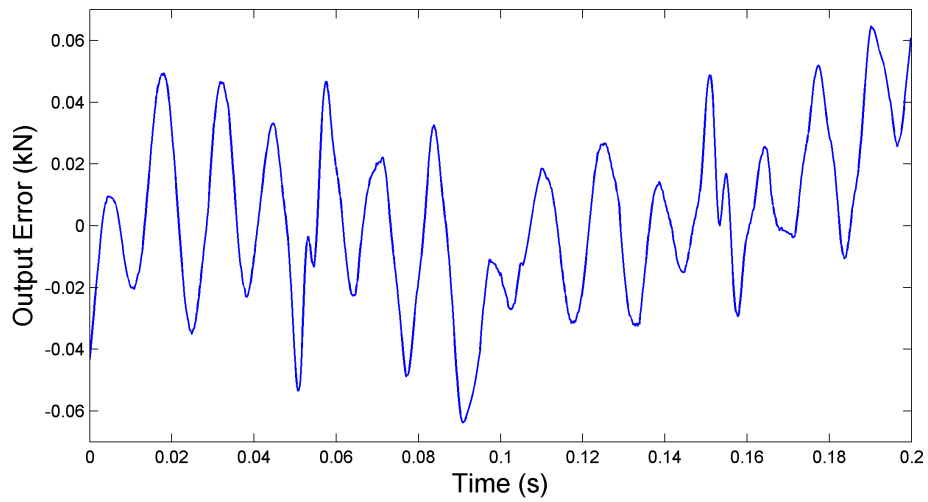


Figure 7.35.: Output Error of the System with Adaptive ILC Algorithm after 40 Iterations

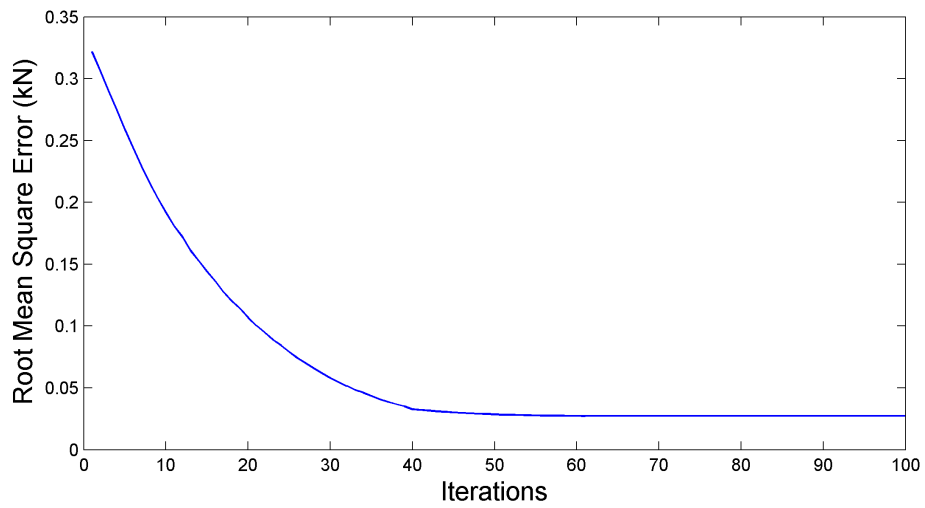


Figure 7.36.: RMS Errors of the Control System Using Adaptive ILC Algorithm

7.4. Summary

Observing Figure 7.34 one can find that after 40 iterations the waveforms of the actual output signal and the desired output one fit well nevertheless there still exists fluctuation in the actual output signal which leads to output error. The reason of system fluctuation is already explained in §7.3.1. Moreover the output error caused by system fluctuation can not be compensated by adaptive ILC algorithm neither. Furthermore from Figure 7.35 one can observe that after 40 iterations the output error of the system is within a range of ± 0.065 kN which is a little larger than that of the system using P-type ILC algorithm. Anyway, the control accuracy and convergence speed of the adaptive ILC algorithm in this experiment is still acceptable.

Especially Figure 7.36 shows the RMS errors of the system output with iterations. It is clear that on the one hand the RMS error of the system output becomes acceptable after approximately 40 iterations i.e. the adaptive ILC algorithm has fast convergence rate and on the other hand the ILC algorithm remains stable after 100 iterations. In a word the adaptive ILC algorithm with the Nussbaum type gain obtains good control effects i.e. both the convergence speed and algorithm stability is acceptable.

In summary the real world electro-hydraulic servo system works under severe conditions in this force control experiment. The valve-controlled cylinder system with an ordinary PI controller nearly can not work. Therefore the P-type ILC and adaptive ILC algorithms are applied respectively in the control system to improve control performance. Experimental results show that both of the two ILC algorithms are effective. Although the output error caused by system fluctuation can not be compensated by the two ILC algorithms, their control performances are acceptable. Particularly their convergence speed and algorithm stability is satisfying.

7.4. Summary

In this chapter the three ILC algorithms developed in Chapter 6 are applied in electro-hydraulic servo system respectively so that their control performances can be verified and compared.

7. Simulation and Experimental Research on Iterative Learning Control

Firstly they are applied in electro-hydraulic servo position control system respectively in simulation. The results show that all the three ILC algorithms can obtain good control performances. Particularly the control effect of the inverse model ILC algorithm is the best of the three ILC algorithms.

Secondly they are applied in real world electro-hydraulic servo position control system respectively. The experimental results show that the control performances of all the three ILC algorithms are satisfying. However the control effect of the inverse model ILC algorithm is not as good as that of the P-type ILC and adaptive ILC algorithms. The reason is that the P-type ILC and adaptive ILC algorithms do not need the information of controlled system while the inverse model ILC algorithm relies on system model hence in experiment the control accuracy of the inverse model ILC algorithm is more easily to be affected by the error between simulation model and practical system. Moreover considering that the prerequisite for applying inverse model ILC algorithm is to build an accurate model for controlled system which is time consuming thus this algorithm is not applicable in practical engineering. Consequently the P-type ILC and adaptive ILC algorithms are recommended for real world electro-hydraulic servo position control systems.

Finally the P-type ILC and adaptive ILC algorithms are applied in real world electro-hydraulic servo force control system respectively so as to further validate and compare their control performances. Especially in this experiment the electro-hydraulic servo force control system works under severe conditions. The experimental results indicate that the valve-controlled cylinder system with an ordinary PI controller nearly can not work. And then when the two ILC algorithms are added respectively in control system, the control performances of the force control system are improved greatly although the output error caused by system fluctuation can not be compensated by the two ILC algorithms. Anyway, the control performances of the two ILC algorithms are acceptable. Therefore it can be concluded that the P-type ILC and adaptive ILC algorithms are effective and applicable not only in real world electro-hydraulic servo position control system but also in force control system.

8. Conclusion and Prospect

8.1. Conclusion

This dissertation focuses on solutions for several practical problems related to high precision control of electro-hydraulic servo system. Firstly by analyzing the structure and working principle of electro-hydraulic servo system, the position control model of electro-hydraulic servo system is built. Particularly the friction of the cylinders with bearing strip is not negligible i.e. an extra model for the friction is necessary. In this dissertation a simple linear friction model is used. The friction is proportional to the velocity of the piston rod so that the friction can be treated as part of system damping. Since some parameters of the system model are unknown, then system identification is used to estimate the values of these unknown parameters so that the deterministic position control model of electro-hydraulic servo system can be obtained. Especially a novel system identification method called black-grey box model identification method is developed to improve the identification accuracy. The experimental results of system identification show that the modeling method is correct and the precision of the identified model is satisfying.

Secondly in practical electro-hydraulic servo system there are two types of nonlinear factors: the first type comes from the flow-pressure characteristics of electro-hydraulic servo valve and the second type contains several other typical nonlinearities while this dissertation focuses on the first type of nonlinear factors. First the exact linearization theory based on differential geometry is introduced. Then the nonlinear model of electro-hydraulic servo position control system is built and simplified. Furthermore the nonlinear model is exactly linearized via state feedback.

8. Conclusion and Prospect

Especially the performance of two linearization methods is compared: approximate linearization method based on Taylor expansion and exact linearization method based on differential geometry. Simulation results indicate that the approximate linearization method is locally effective i.e. when the controlled system operates within a small range of the equilibrium point the control effect is good nevertheless when it deviates from the equilibrium point seriously the control effect is not acceptable; while the exact linearization method is globally effective i.e. within the whole working range of the controlled system the control effect is satisfying. Furthermore the robustness of electro-hydraulic servo position control system based on exact linearization is discussed. Simulation results show that even if some of the system parameters deviate from the nominal values greatly, the performance of the control system is still satisfying i.e. the control system has strong robustness. At last the external disturbance problem of electro-hydraulic servo position control system is presented. Theoretical analysis indicates that the system output of electro-hydraulic servo position control system can not be decoupled from the disturbance input completely and simulation results show that by using the sliding mode variable structure controller based on exact linearization method via state feedback, the control system has good anti disturbance performance when the disturbance satisfies certain conditions.

Finally in this dissertation three ILC algorithms are presented: PID-type ILC algorithm, adaptive ILC algorithm and inverse model ILC algorithm. Firstly basic principles and convergence conditions of the three ILC algorithms are introduced. Then control effects of the three ILC algorithms in electro-hydraulic servo system are compared and discussed with simulation and experiment.

First the three developed ILC algorithms are applied in electro-hydraulic servo position control system respectively in simulation. The simulation results show that the control performances of all the three ILC algorithms are satisfying. Then the three ILC algorithms are applied in real world electro-hydraulic servo position control system respectively. The experimental results indicate that the control performances of all the three ILC algorithms are satisfying. Nevertheless considering the prerequisite for applying inverse model ILC algorithm and comparing the control performances of the three ILC algorithms in real world electro-hydraulic servo system, the in-

verse model ILC algorithm is not applicable in practical applications i.e. the P-type ILC and adaptive ILC algorithms are recommended for real world electro-hydraulic servo systems. At last, the two recommended ILC algorithms are applied in real world electro-hydraulic servo force control system respectively to further verify their effectiveness. The experimental results show that although the real world force control system works under severe conditions, the control performances of the two ILC algorithms are still acceptable. Consequently it is concluded that the P-type ILC and adaptive ILC algorithms are effective and applicable not only in real world electro-hydraulic servo position control system but also in force control system.

8.2. Prospect

In this dissertation several control problems related to electro-hydraulic servo system are studied and some positive results are achieved. However there are still a lot of interesting topics which deserve further study.

Firstly in this dissertation the accurate position control model of SISO electro-hydraulic servo system are built and identified. Nevertheless force control system is also very important in fatigue tests consequently future work in this area could be expanded to modeling and identification of SISO electro-hydraulic servo force control system. Furthermore many fatigue tests need MIMO electro-hydraulic servo system hence the focus of the future study in this area could be placed on modeling and identification of MIMO electro-hydraulic servo system.

Secondly in this dissertation the nonlinear model of SISO electro-hydraulic servo position control system is linearized with the exact linearization method based on differential geometry therefore future work in this area might aim at how to exactly linearize the nonlinear model of SISO electro-hydraulic servo force control system and MIMO electro-hydraulic servo system. In addition this dissertation only considers the nonlinear factor from the flow-pressure characteristics of electro-hydraulic servo valve consequently future work in this area could be extended to the exact linearization problems of other types of nonlinear factors such as saturation nonlin-

8. Conclusion and Prospect

earity, dead zone nonlinearity, backlash nonlinearity, hysteretic nonlinearity and so on.

Finally in this dissertation three types of commonly used ILC algorithms are applied in SISO electro-hydraulic servo system hence the focus of the future study in this area could be placed on application of the three ILC algorithms in MIMO electro-hydraulic servo system. Furthermore there are other types of ILC algorithms such as neural network ILC algorithm, fuzzy ILC algorithm, optimal ILC algorithm and so on however these algorithms have some problems which lead to difficulties of applying them in practical engineering. Therefore future work in this area could be expanded to the research on application of these ILC algorithms in electro-hydraulic servo system.

Bibliography

- [1] Sun Z. L. *Mechanical Design*. Northeastern University Press, 2000.
- [2] Wang Z. L. *Modern Hydraulic Control*. China Machine Press, 1997.
- [3] Murrenhoff H. "Systematic approach to the control of hydrostatic drives." In: *Journal of Systems and Control Engineering* 13 (1999), pp. 333–347.
- [4] Mare J.-C. and Moulaire P. "Expert rules for the design of position control of electrohydraulic actuators." In: *Proc of the 6th Scandinavian International Conference on Fluid Power*. Vol. 2. May 1999, pp. 1267–1280.
- [5] Guglielmino E. and Edge K. A. "Modelling of an electrohydraulically-activated friction damper in a vehicle application." In: *ASME International Mechanical Engineering Congress and Exposition*. 2001.
- [6] Manhartsgruber B. and Scheidl R. "Non-linear control of hydraulic servodrives based on a singular perturbation approach." In: *Proceedings of Power Transmission and Motion Control*. Sept. 1998, pp. 301–313.
- [7] Hametner G. et al. "Positioning control of a hydraulic press by a variable speed motor." In: *Proceedings of Power Transmission and Motion Control*. Sept. 2002, pp. 203–214.
- [8] Maekinen E. and Virvalo T. "On the motion control of a water hydraulic servo cylinder drive." In: *Proc of the 7th Scandinavian International Conference on Fluid Power*. Vol. 1. May 2001, pp. 109–123.
- [9] Virvalo T. "Hydraulic motion control - robustness against inertia load changes." In: *Proc of the 5th JFPS International Symposium on Fluid Power*. Vol. 2. Nov. 2002, pp. 561–566.

Bibliography

- [10] Maekinen E. and Virvalo T. "Improving the accuracy of the water hydraulic position servo by compensating servo-valve nonlinearities." In: *Proceeding of Power Transmission and Motion Control*. 2002, pp. 283–295.
- [11] Whiting I. "Control developments in servo hydraulic actuation products." In: *Seminar on Recent Developments in Control Techniques for Actuators*. Dec. 2002.
- [12] Suzuki K., Sugi S., and Ueda H. "Improving the characteristics of an electrohydraulic servo system with a nonsymmetrical cylinder by ZPETC and linearization." In: *Proc of the 4th JHPS International Symposium on Fluid Power*. 1999, pp. 93–98.
- [13] Garstenauer M. and Kurz M. "The 'Smalve' - integrated digital control of a hydraulic servo drive." In: *Proceedings of Power Transmission and Motion Control*. Sept. 2002, pp. 45–57.
- [14] Alleyne A. "On the limitations of force tracking control for hydraulic servo systems." In: *Transactions of ASME* 121 (June 1999), pp. 184–190.
- [15] Edge K. A. "The control of fluid power system - responding to the challenges." In: *Journal of Systems and Control Engineering* 211 (1997), pp. 91–110.
- [16] Wu Z. S., Ji Y. T., and Xu W. B. "Digital adaptive regulator based on pole-zero placement with δ transform method and its application." In: *Chinese Journal of Mechanical Engineering* 38.3 (2002), pp. 127–130.
- [17] Zhang Y. and Alleyne A. "A novel approach to active vibration isolation with electrohydraulic actuators." In: *Proc ASME IMECE*. Nov. 2001.
- [18] Chang, M-H., and Murrenhoff H. "Adaptive servo-control for hydraulic excavators." In: *Proceedings of Power Transmission and Motion Control*. Sept. 1998, pp. 81–95.
- [19] Utkin V. I. "Variable structure systems with sliding modes." In: *IEEE Trans Auto Control*. Vol. 22. 2. 1977, pp. 212–222.
- [20] Gao W. B. *Theory and Design Method of Variable Structure Control*. Science Press, 1998.

- [21] Handroos H. and Liu Y. "Sliding mode control of a hydraulic position servo with different kinds of loads." In: *Proceeding of Power Transmission and Motion Control*. Sept. 1998, pp. 379–392.
- [22] Liu Y. and Handroos H. "Control of a hydraulically driven flexible manipulator using sliding mode." In: *ASME International Mechanical Engineering Congress and Exposition*. Vol. 7. Nov. 2000, pp. 9–21.
- [23] Yanada H. and Shimahara M. "Sliding mode control of an electrohydraulic servo motor using a gain scheduling type observer and controller." In: *Journal of Systems and Control Engineering* 211.16 (1997), pp. 407–416.
- [24] Yanada H. and Ohnishi H. "Frequency-shaped sliding mode control of an electrohydraulic servo-motor." In: *Journal of Systems and Control Engineering* 213.16 (1999), pp. 441–448.
- [25] Fung R. F., Wang Y. C., and Yang R. T. Huang H. H. "A variable structure control with proportional and integral compensation for electrohydraulic position servo control system." In: *Mechatronics* 7.1 (1997), pp. 67–81.
- [26] Cho S. H. and Edge K. A. "Adaptive sliding mode tracking control of hydraulic servosystems with unknown non-linear friction and modelling error." In: *Journal of Systems and Control Engineering* 214.14 (2000), pp. 247–257.
- [27] Cho S. H. et al. "Sliding mode tracking control of a low-pressure water hydraulic cylinder under nonlinear friction." In: *Journal of Systems and Control Engineering* 216.15 (2002), pp. 383–392.
- [28] Li Y. H. and Wang Z. L. "New type of variable structure control law with application to electro-hydraulic servo systems." In: *Journal of Beijing University of Aeronautics and Astronautics* 23.6 (1997), pp. 692–697.
- [29] Slotine J. J. E. "Tracking control of non-linear systems using sliding surfaces with application to robot manipulators." In: *Int J Control* 38.2 (1983), pp. 465–492.
- [30] Gao W. B. "Variable structure control of discrete-time systems." In: *Acta Automatica Sinica* 21.2 (1995), pp. 154–160.

Bibliography

- [31] Feng C. B. *Analysis and Design of Nonlinear Control Systems*. Publishing House of Southeast University, 1990.
- [32] Li Y. H., Yang M. L., and Zhang Z. H. "Study on second-order sliding mode control law for electro-hydraulic servo system." In: *Chinese Journal of Mechanical Engineering* 41.3 (2005), pp. 72–75.
- [33] Chern T. L. and Wu Y. C. "An optimal variable structure control with integral compensation for electrohydraulic position servo control systems." In: *IEEE Trans on Industrial Electronics*. Vol. 39. 5. 1992, pp. 460–463.
- [34] Sanada K. "A method of designing a robust force controller of a waterhydraulic servo system." In: *Journal of Systems and Control Engineering* 216.12 (2002), pp. 135–141.
- [35] Pommier V. et al. "Robust control of hydraulic actuators by linearization and crone techniques." In: *International Conference on Recent Advances in Aerospace Actuation Systems and Components*. June 2001, pp. 85–89.
- [36] Plummer A. R. "Servosystem design with control signal saturation." In: *Proceedings of Power Transmission and Motion Control*. Sept. 1999, pp. 31–44.
- [37] Katoh H., Nishiumi T., and Konami S. "Precise positioning control for a hydraulic motor system with dead zone using a state feedback neural network." In: *Proc of the 5th JFPS International Symposium on Fluid Power*. Vol. 1. Nov. 2002, pp. 199–204.
- [38] Hwang U. K. and Cho S. H. "Application of a neural network for identification and control of a servovalve controlled hydraulic cylinder system." In: *Proc of the 5th JFPS International Symposium on Fluid Power*. Vol. 1. Nov. 2002, pp. 205–210.
- [39] Burton R. T. et al. "Neural networks and hydraulic control - from simple to complex applications." In: *Journal of Systems and Control Engineering* 213.15 (1999), pp. 349–358.
- [40] Becker U. "The behaviour of position controller actuator with switching valves and a fuzzy controller." In: *Proc of the 7th Scandinavian International Conference on Fluid Power*. Vol. 2. May 2001, pp. 149–157.

- [41] Jones E., Dobson A., and Roskilly A. P. "Design of a reduced-rule selforganising fuzzy logic controller for water hydraulic applications." In: *Journal of Systems and Control Engineering* 214.15 (2000), pp. 371–381.
- [42] Pai K. R. and Shih M. C. "Multi-speed control of a hydraulic cylinder using self-tuning fuzzy control method." In: *Proc of the 4th JHPS International Symposium on Fluid Power*. 1999, pp. 99–104.
- [43] Chen C. K. and Zeng W. C. "The iterative learning control for the position tracking of the hydraulic cylinder." In: *Proc of the 5th JFPS International Symposium on Fluid Power*. Vol. 2. Nov. 2002, pp. 591–596.
- [44] Zhao J., Sokola M. A., and Edge K. A. "Self-learning control algorithm for an injection moulding machine." In: *Proc of the 17th International Conference on Hydraulics and Pneumatics*. June 2001.
- [45] Shinada M. and Kojima E. "Improvement of acceleration tracking accuracy of electrohydraulic vibration testing machine." In: *Proc of the 4th JHPS International Symposium on Fluid Power*. 1999, pp. 631–636.
- [46] Itoh T., Cui Q., and Matsui T. "Neural network-based learning of human skill in hydraulic robots." In: *Proc of the 4th JHPS International Symposium on Fluid Power*. 1999, pp. 655–660.
- [47] Chang S. O. and Lee J. K. "A real-time adaptive learning control based on evolutionary algorithm of the application to an electrohydraulic servo system." In: *Proc of the 5th JFPS International Symposium on Fluid Power*. Vol. 2. Nov. 2002, pp. 573–578.
- [48] Ionescu F. and Vlad C. "Application of a neuro-fuzzy controller to an electrohydraulic axis." In: *Proc of the Sixth Scandinavian International Conference on Fluid Power*. Vol. 1. May 1999, pp. 1217–1224.
- [49] Boksenbom A. S. and Hood R. *General algebraic method applied to control analysis of complex engine types*. Tech. rep. NACA-TR-930, 1949.
- [50] Morgan B. S. "The synthesis of linear multivariable systems by state-variable feedback." In: *IEEE Trans on Automatic Control*. Vol. 9. 5. 1964, pp. 405–411.

Bibliography

- [51] Wang X. Z. et al. "A summary of multivariable decoupling methods." In: *Journal of Shenyang Architectural and Civil Engineering Institute* 16.2 (2000), pp. 143–145.
- [52] Rosenbrock H. H. "Distinctive problems in process control." In: *Chem Eng Prog.* 1962.
- [53] Rosenbrock H. H. "Design of multivariable control systems using the inverse Nyquist array." In: *Proc IEE.* Vol. 116. 1969, pp. 1929–1936.
- [54] Rosenbrock H. H. *Computer-aided control system design.* Academic Press, 1974.
- [55] Zhuang H. M., Bai F. Z., and Xue J. P. "Modeling, simulation, and control of an oil heater." In: *IEEE Control System Magazine.* Aug. 1987.
- [56] Gu X. H. and Zhou L. F. *Frequency Domain Method Linear Multi-variable System.* Shanghai Jiao Tong University Press, 1990.
- [57] Cheng P. *Multi-variable Linear Control System.* Beijing University of Aeronautics and Astronautics Press, 1990.
- [58] Singh R. P. and Narendra K. S. "Prior information in the design of multivariable adaptive controllers." In: *IEEE Trans on AC.* Vol. 29. 12. 1984, pp. 1108–1111.
- [59] Wittenmark R., Middleton R. H., and Goodwin G. C. "Adaptive decoupling of multivariable system." In: *Int J Control.* Vol. 44. 1. 1990, pp. 193–213.
- [60] Chai T. Y. "Direct adaptive decoupling control for general stochastic multivariable systems." In: *Int J Control.* Vol. 51. 4. 1990, pp. 885–909.
- [61] Mikles J. and Meszatos A. "A decoupling pole-placement controller for a class of multivariable systems." In: *Problem Control Inf Theory* 20.4 (1991), pp. 291–298.
- [62] Chen H. F. and Guo L. "Adaptive control with recursive identification for stochastic linear systems." In: *Advances in Control and Dynamic Systems* 26.2 (1987), pp. 112–116.

- [63] Wai R. J. and Liu W. K. "Nonlinear decoupled control for linear induction motor servo-drive using the sliding-mode technique." In: *IEE Proc-Control Theory Appl* 148.3 (2001), pp. 217–231.
- [64] Li G. S., Zhang W. W., and Wang H. Y. "Variable structure control for multi-variable temperature systems." In: *Journal of Ocean University of China* 27.4 (1997), pp. 583–588.
- [65] Chen S. P. and Sun Y. X. "Lower-order robust decoupler design." In: *Acta Automatica Sinica* 124.14 (1998), pp. 543–547.
- [66] Xue F. Z. "Multi-variable decoupling robust control based on genetic algorithm." In: *Journal of University of Science and Technology of China* 31.6 (2001), pp. 721–726.
- [67] Wang D. F., Wang J. D., and Han P. "New design of internal model decoupling control for multi-variable system." In: *Control Engineering of China* 10.5 (2003), pp. 463–465.
- [68] Zhang W. G. and Xiao S. D. "The application of an approximate decoupling method to the the flight control systems." In: *Acta Aeronautica ET Astronautica Sinica* 15.2 (1994), pp. 206–210.
- [69] Wang H. R. et al. "The design for decoupling robust controller with the state feedback." In: *Control and Decision* 9.4 (1994), pp. 12–16.
- [70] Sinha P. K. "A new condition for output feedback decoupling of multi-variable systems." In: *IEEE Trans on Automatic Control* 24.3 (1979), pp. 476–478.
- [71] Koumboulis F. N. and Skarpetis M. G. "Static controllers for magnetic suspension and balance systems." In: *IEE Proc-Control Theory Appl* 143.4 (1996), pp. 338–348.
- [72] Howze J. W. "Necessary and sufficient conditions for decoupling using output feedback." In: *IEEE Trans on Automatic Control* AC-18.1 (1973), pp. 44–46.
- [73] Wolovich W. A. "Output feedback decoupling." In: *IEEE Trans on Automatic Control* AC-20.1 (1975), pp. 148–149.
- [74] Wang S. H. and Dasison E. J. "Design of decoupled control systems: a frequency domain approach." In: *Int J Control* 21.4 (1975), pp. 529–536.

Bibliography

- [75] Mao W. J. and Chu J. "Input-output energy decoupling of linear time-invariant systems." In: *Control Theory and Applications* 19.1 (2002), pp. 146–148.
- [76] Mao W. J. and Chu J. "Delay-dependent conditions for input-output energy decoupling of linear delayed systems." In: *Control Theory and Applications* 19.4 (2002), pp. 532–536.
- [77] Mao W. J. "Observer-based energy decoupling of linear time-delay systems." In: *Journal of Zhejiang University (Engineering Science)* 37.5 (2003), pp. 499–503.
- [78] Mao W. J. and Chu J. "Input-output energy decoupling of linear time-delay systems." In: *Acta Automatica Sinica* 28.1 (2002), pp. 112–115.
- [79] Hazlerigg A. D. G. and Sinha P. K. "Noninteracting control by output feedback and dynamic compensation." In: *IEEE Trans on Automatic Control* AC-23.1 (1978), pp. 76–79.
- [80] Sahjendra N. and Sinha P. K. "Decoupling of invertible nonlinear systems with state feedback and precompensation." In: *IEEE Trans on Automatic Control* AC-25.6 (1980), pp. 1237–1239.
- [81] Deng Z. L. and Huang X. R. "Multi-variable decoupling pole assignment self-tuning feedforward controller." In: *IEE Proc-D* 138.1 (1991), pp. 85–88.
- [82] Xu Y. X. et al. "Neural network decoupling control of coupling of pressure and flow." In: *Journal of Henan University of Science & Technology (Natural Science)* 24.3 (2003), pp. 82–84.
- [83] Cong Y. Q., Xie J., and Zhang Y. "Study of multivariable nonlinear adaptive decoupling control system based on neural networks." In: *Control and Automation* 20.3 (2004), pp. 22–23.
- [84] Wang X., Yue H., and Chai T. Y. "Multivariable decoupling controller using multiple models for a non-minimum phase system." In: *Control and Decision* 18.1 (2003), pp. 7–12.
- [85] Wang X., Li S. Y., and Yue H. "Multiple models neural network decoupling controller for a nonlinear system." In: *Control and Decision* 19.4 (2004), pp. 424–428.

- [86] Chai T. Y. "Multivariable intelligent decoupling control and its application." In: *Proceedings of the Third World Congress on Intelligent Control and Automation*. 2000.
- [87] Czogalaand E. and Zimmermann H. J. "Some aspects of synthesis of probabilistic fuzzy controllers." In: *Fuzzy Sets and Systems* 13.2 (1984), pp. 169–178.
- [88] Walichiewicz L. "Decomposition of linguistic rule in the design of a multidimensional fuzzy control algorithm." In: *Cybernetics Syst Res* 2.3 (1984), pp. 185–193.
- [89] Gupta M. M., Kiszka J. B., and Trojan G. M. "Multivariable structure of fuzzy control system." In: *IEE Trans SMC* 16.5 (1986), pp. 638–656.
- [90] Kiszka J. B., Gupta M. M., and Trojan G. M. "Multivariable fuzzy controller under Godela implication." In: *Fuzzy Sets and Systems* 34.3 (1990), pp. 301–321.
- [91] Zhang W. G. et al. "The study on a fuzzy neural decoupled hybrid controller." In: *Computer Simulation* 20.8 (2003), pp. 52–54.
- [92] Li Y., Gao F., and Lin T. X. "A novel tracking strategy of a mobile robot with 3 degrees of freedom." In: *Journal of System Simulation* 16.3 (2004), pp. 585–588.
- [93] Huang R. "Research on human-simulated intelligent control of multi-variable hydraulic servo system of spring mill." MA thesis. Chongqing University, 1996.
- [94] Liu C. H. *Decoupling Theory of Multivariable Process Control System*. China Water Power Press, 1988.
- [95] Tochizawa M. and Edge K. A. "A comparison of some control strategies for a hydraulic manipulator." In: *Proceeding of American Control Conference*. 1999, pp. 744–748.
- [96] Wang Q. F. and Lu Y. X. "Decoupling control of electro-hydraulic multi-variable position system." In: *China Mechanical Engineering* 11.7 (1998), pp. 729–732.
- [97] Tian L. F., Pei Z. C., and Li S. Y. "Decoupling of hydraulic loading teststand with secondary regulation." In: *China Mechanical Engineering* 8.6 (1997), pp. 101–103.

Bibliography

- [98] Wang Z. L. "Compensating cross-linking disturbance and load change of multivariant electrohydraulic servo system." In: *Machine Tool and Hydraulics* 2 (1985), pp. 6–10.
- [99] Wang Y. Q. and Qi X. Y. "A study on the coupled load in rolling mill and the dissolution of interference – Part I. Theoretical analysis." In: *Journal of Northeast Heavy Machinery Institute* 1 (1987), pp. 31–35.
- [100] Wang H. and Li H. R. "Coupling influence and decoupling of the secondary regulation load simulation test equipment for the drive axle of heavy vehicle." In: *Chinese Journal of Mechanical Engineering* 140.6 (2004), pp. 19–22.
- [101] Mare P. J.-C. and Moulaire P. "The decoupling of position controlled electrohydraulic actuators mounted in tandem or in series." In: *Proc of the 7th Scandinavian International Conference on Fluid Power*. 2002, pp. 93–108.
- [102] Luo A. "Decoupling control of multi-variable electric-hydraulic servo system." In: *The Chinese Journal of Nonferrous Metals* 6.1 (1996), pp. 140–144.
- [103] Zhu Z. T. "Modeling and control of multi-DOF electro-hydraulic servo system." In: *Journal of Guangdong Mechanical Institute* 12.2 (1994), pp. 31–37.
- [104] Zhang Y. G., Zhang Z. H., and Xiong Y. F. "Adaptive decoupling control of nonlinear multivariable electrohydraulic servo system." In: *Journal of Shanghai Jiaotong University* 28.2 (1994), pp. 23–30.
- [105] Yu J. Y. et al. "Application of full-order sliding mode variable structure decoupling controller to hydraulic simulator design." In: *Acta Aeronautica Et Astronautica Sinica* 126.13 (2005), pp. 376–379.
- [106] Wang S. M. *Analysis and Design of Multivariable Control System*. China Electric Power Press, 1996.
- [107] Zhang H. et al. "Neural adaptive control of a MIMO electric-hydraulic servo system." In: *Proceedings of ASME Fluid Power Systems and Technology*. Vol. 63. 1997, pp. 7–12.
- [108] Shu H. L. "PID neural network for decoupling control of strong coupling multivariable time-delay systems." In: *Control Theory and Applications* 15.6 (1998), pp. 920–924.

- [109] Liu Y. J., Yi L. G., and Tong H. "A new method of multivariable control for electro-hydraulic servo testing system." In: *Transactions of China Electrotechnical Society* 18.6 (2003), pp. 48–52.
- [110] MTS. *Model 793.00 System Software*.
- [111] Instron. *Labtronic 8800 Controller*.
- [112] DTE. *Operator Manual of DTE 3500 Series*. 4.0. 2010.
- [113] Walter and Bai AG. *Closed-Loop Digital Controllers*.
- [114] Li L. J. and Thurner T. "Accurate modeling and identification for servo-hydraulic cylinder system in multi-axial test applications." In: *Ventil* 19.6 (2013), pp. 462–470.
- [115] Moog Inc. *G761 Series Servovalves*. East Aurora, NY, USA.
- [116] Sobe K. "Entwicklung eines Konzepts zur Regelung servohydraulischer Pruefzylinder." MA thesis. Graz University of Technology, 2011.
- [117] Ljung L. *System Identification Toolbox User's Guide*. R2011b. The MathWorks Inc. Sept. 2011.
- [118] Chen W. H. *An Introduction to Differentiable Manifold*. Higher Education Press, 2001.
- [119] Isidori A. *Nonlinear Control Systems*. Third. Springer, 1995.
- [120] Hu S.S. *Automatic Control Theory*. Fourth. Science Press, 2006.
- [121] Li D.P. *Theoretical Basis of Nonlinear Control System*. Harbin Engineering University Press, 2006.
- [122] He Y. Y. and Yan M. D. *Nonlinear Control Theory and Its Application*. Xidian University Press, 2007.
- [123] Gao W. B., Cheng M., and Xia X. H. "The development of nonlinear control system." In: *Acta Automatica Sinica* 17.5 (1995), pp. 513–523.
- [124] Gao W. B. *Introduction of Nonlinear Control System*. Science Press, 1988.
- [125] Li C. W. and Feng Y. K. *The inverse system method of multivariable nonlinear control*. Tsinghua University Press, 1991.
- [126] Brockett R. W. "Nonlinear systems and differential geometry." In: *Proc. of IEEE* 64.1 (1976), pp. 61–71.

Bibliography

- [127] Fliess M., Lamnabhi M., and Lagarrigue F. L. "An algebraic approach to nonlinear functional expansions." In: *IEEE Trans on Circuits and Systems* 30.8 (1983), pp. 554–570.
- [128] Cheng D. Z. *The Geometric Theory of Nonlinear System*. Science Press, 1991.
- [129] Cheng D. Z., Tarn T. J., and Isidori A. "Global external linearization of the nonlinear systems via feedback." In: *IEEE Trans on Automatic Control* 30.8 (1985), pp. 808–811.
- [130] Sampei M. and Furuta K. "On time scaling for nonlinear systems: application to linearization." In: *IEEE Trans on Automatic Control* AC-31.5 (1986), pp. 459–462.
- [131] Arapostathis A. et al. "The effect of sampling on linear equivalence and feedback linearization." In: *Systems and Control Letters* 13 (1989), pp. 373–381.
- [132] Nam K. "Linearization of discrete-time nonlinear systems and a canonical structure." In: *IEEE Trans on Automatic Control* 34.1 (1989), pp. 119–122.
- [133] Liu X. P. and Zhang S. Y. "Linearization of single input singular control systems." In: *Control and Decision* 5 (1992), pp. 372–376.
- [134] Liu X. P. and Zhang S. Y. "Nonlinearity of nonlinear singular system." In: *Information and Control* 4 (1993), pp. 209–214.
- [135] Lu Q. *Nonlinear Control of Electric Power System*. Science Press, 1993.
- [136] Meyer G., Su R., and Hunt L. R. "Application of nonlinear transformations to automatic flight control." In: *Automatica* 20.1 (1984), pp. 103–107.
- [137] Singh S. N. "Control of nearly singular decoupling systems and nonlinear aircraft maneuver." In: *IEEE Trans on Aerospace and Electronic Systems* 24.6 (1988), pp. 775–784.
- [138] Li. Y. H. et al. "Nonlinear control of hydraulic servo system." In: *Machine Tool and Hydraulics* 1 (1994), pp. 21–25.
- [139] Li. Y. H. et al. "Nonlinear optimal design of hydraulic servo system." In: *Machine Tool and Hydraulics* 5 (1994), pp. 255–260.

- [140] Jen Y. and Lee C. "Robust speed control of a pump-controlled motor system." In: *Control Theory and Applications, IEE Proceedings D* 139.6 (1992), pp. 503–510.
- [141] Yao B. "Adaptive robust motion control of single-rod hydraulic actuators: theory and experiments." In: *IEEE/ASME Transactions on Mechatronics* 5.1 (2000), pp. 79–91.
- [142] Xia X. H. and Gao W. B. *Control and Decoupling of Nonlinear System*. Science Press, 1997.
- [143] Chiasson J. "A new approach to dynamic feedback linearization control of an induction motor." In: *IEEE Trans on Automatic Control* 43.3 (1998), pp. 391–397.
- [144] Zhang C. P. et al. "Nonlinear control of asynchronous motor based on direct feedback linearization." In: *Proceedings of the Csee* 23.2 (2003), pp. 99–102.
- [145] Duan F. H. and Deng H. D. "Study on the DDPS of a linear time-delay system." In: *Automation and Instrumentation* 1.1 (2000), pp. 1–8.
- [146] Moog C. H. et al. "The disturbance decoupling problem for time-delay nonlinear systems." In: *IEEE Trans on Automatic Control* 45.2 (2000), pp. 305–309.
- [147] Xia X. and Moog C. H. "Disturbance decoupling by measurement feedback for SISO nonlinear systems." In: *IEEE Trans on Automatic Control* 44.7 (1999), pp. 1425–1429.
- [148] Velasco-Villa M., Alvarez J., and Castro-Linares R. "On the disturbance decoupling problem for a class of nonlinear time delay systems." In: *Proceedings of the 32nd Conference on Decision and Control*. 1993.
- [149] Marino R. and Tomei P. "Adaptive output feedback tracking with almost disturbance decoupling for a class of nonlinear systems." In: *Automatica* 36.12 (2000), pp. 1871–1877.
- [150] Marino R. and Tomei P. "Adaptive output feedback regulation with almost disturbance decoupling for nonlinear parameterized systems." In: *International Journal of Robust and Nonlinear Control* 10 (2000), pp. 655–669.

Bibliography

- [151] Wang X. P. and Cheng Z. L. "Robust almost disturbance decoupling of nonlinear systems with uncertain dynamic input." In: *Journal of Shandong University (Natural Science)* 38.4 (2003), pp. 13–18.
- [152] Bi W. P., Mu X. W., and Lin L. "Almost disturbance decoupling for a class of minimum- phase higher-order cascade nonlinear systems." In: *Applied Mathematics and Mechanics* 24.4 (2003), pp. 391–397.
- [153] Isidori A. and Astolfi A. "Disturbance attenuation and H infinity control via measurement feedback in nonlinear systems." In: *IEEE Trans on Automatic Control* 37.9 (1992), pp. 1283–1293.
- [154] Isidori A., Schwartz B., and Tarn T. J. "Semiglobal L2 performance bounds for disturbance attenuation in nonlinear systems." In: *IEEE Trans on Automatic Control* 44.8 (1999), pp. 1535–1545.
- [155] Ito H. and Jiang Z. P. "Output feedback disturbance attenuation with robustness to nonlinear uncertain dynamics via state-dependent scaling." In: *Proceedings of the 40th IEEE Conference on Decision and Control*. 2001.
- [156] Slotine J.-J. and Li W. P. *Applied Nonlinear Control*. Prentice Hall, 1991.
- [157] Hong Y. G. and Cheng D. Z. *Analysis and Control of the Nonlinear Systems*. Science Press, 2005.
- [158] Hu Y. M. *Nonlinear Control System Theory and Application*. National Defence Industrial Press, 2005.
- [159] Li Y. H., Shi W. X., and Lin T. Q. "Current situation and development of the control strategies of modern hydraulic servo system." In: *Hydraulics and Pneumatics* 1 (1995), pp. 3–6.
- [160] Li L. J. and Thurner T. "Modeling and simulation of servo-hydraulic cylinder systems for multi axis test control." In: *Advanced Materials Research* 711 (2013), pp. 416–421.
- [161] Chen Y. Q. and Wen C. Y. *Iterative Learning Control - Convergence, Robustness and Applications*. Springer, 1999.

- [162] Arimoto S., Kawamura S., and Miyazaki F. "Bettering operation of dynamic systems by learning: A new control theory for servomechanism or mechatronics systems." In: *Proceedings of 23rd Conference on Decision and Control*. Dec. 1984.
- [163] Arimoto S. et al. "Learning control theory for dynamical systems." In: *Proceedings of 24th Conference on Decision and Control*. Dec. 1985.
- [164] Arimoto S. "Learning control theory for robotic motion." In: *International Journal of Adaptive Control and Signal Processing* 4 (1990), pp. 543–564.
- [165] Chien C. J. and Liu J. S. "A P-type iterative learning controller for robust output tracking of nonlinear time-varying systems." In: *Proceedings of the American Control Conference*. 1994.
- [166] Shou J. X., Zhang Z. J., and Pi D. Y. "On the convergence of open-closed-loop D-type Iterative learning control for nonlinear systems." In: *IEEE International Symposium on Intelligent Control*. 2003.
- [167] Chen Y. Q. and Moore K. L. "PI-type iterative learning control revisited." In: *Proceedings of the American Control Conference*. 2002.
- [168] Feng Z. J., Zhang Z. J., and Pi D. Y. "Open-closed-loop PD-type iterative learning controller for nonlinear systems and its convergence." In: *Proceedings of the 5th World Congress on Intelligent Control*. 2004.
- [169] Ji G. and Luo Q. "An open-closed-loop PID-type iterative learning control algorithm for uncertain time-delay systems." In: *Proceedings of the 4th International Conference on Machine Learning and Cybernetics*. 2005.
- [170] Hu Y. M. and Xiao H. M. "Higher-order iterative learning control algorithm of nonlinear systems." In: *Mathematica Applicata* 4.7 (2008), pp. 382–389.
- [171] Heinzinger G. et al. "Robust learning control." In: *Proceedings of 28th Conference on Decision and Control*. Dec. 1989.
- [172] Arimoto S., Naniwa T., and Suzuki H. "Robustness of P-type learning control with a forgetting factor for robotic motions." In: *Proceedings of 29th Conference on Decision and Control*. Dec. 1990.

Bibliography

- [173] Pi D. Y. and Panaliappan K. "Robustness of discrete nonlinear systems with open-closed-loop iterative learning control." In: *Proceedings of 2002 International Conference on Machine Learning and Cybernetics*. Vol. 3. 2002, pp. 1263–1266.
- [174] Kim Y. T. et al. "Robust higher-order iterative learning control for a class of nonlinear discrete-time systems." In: *Proceedings of the IEEE International Conference on Systems, Man and Cybernetics*. Vol. 3. 2003, pp. 2219–2224.
- [175] Shao C., Gao F. R., and Yang Y. "Robust stability of optimal iterative learning control and application to injection molding machine." In: *Acta Automatica Sinica* 29.1 (2003), pp. 72–79.
- [176] Liu S. and Lin J. "Robust iterative learning control against disturbances and initialization errors for uncertain plants." In: *Proceedings of the 6th World Congress on Intelligent Control and Automation*. Vol. 1. 2006, pp. 3815–3819.
- [177] Xu J. X. and Viswanathan B. "Adaptive robust iterative learning control with dead zone scheme." In: *Automatica* 36.1 (2000), pp. 91–99.
- [178] Yang S. Y., Fan X. P., and Luo A. "Adaptive robust iterative learning control for uncertain robotic systems." In: *Proceedings of the 4th World Congress on Intelligent Control and Automation*. Vol. 2. 2002, pp. 964–968.
- [179] Tayebi A. and Zaremba M. B. "Internal model-based robust iterative learning control for uncertain LTI systems." In: *Proceedings of the 39th IEEE Conference on Decision and Control*. Vol. 4. Dec. 2000, pp. 3439–3444.
- [180] Yang X. J. and Li J. M. "Robust adaptive sliding mode iterative learning control based on the neural network." In: *Journal of Xidian University* 29.3 (2002), pp. 382–386.
- [181] Saab S. S., Vogt W. G., and Mickle M. H. "Learning control algorithms for tracking slowly varying trajectories." In: *IEEE Transactions on Systems, Man, and Cybernetics* 27.4 (1997), pp. 657–670.
- [182] Choi J. Y. and Park H. J. "Use of neural networks in iterative learning control systems." In: *International Journal of Systems Science* 31.10 (2000), pp. 1227–1239.

- [183] Liu S. "Design and application of iterative learning control system." PhD thesis. Zhejiang University, 2002.
- [184] French M. and Rogers E. "Nonlinear iterative learning by an adaptive Lyapunov technique." In: *Proceedings of the 37th IEEE Conference on Decision and Control*. Dec. 1998, pp. 175–180.
- [185] Xu J. X. and Tan Y. "A composite energy function-based learning control approach for nonlinear systems with time-varying parametric uncertainties." In: *IEEE Trans on Automatic Control* 47.11 (2002), pp. 1940–1945.
- [186] Park B. H., Kuc T. Y., and Lee J. S. "Adaptive learning control of uncertain robotic systems." In: *International Journal of Control* 65.5 (1996), pp. 725–744.
- [187] Choi J. Y. and Lee J. S. "Adaptive iterative learning control of uncertain robotic systems." In: *IEE Proceedings - Control Theory and Applications*. Vol. 147. 2. 2000, pp. 217–223.
- [188] Liu H. P. "Iterative learning control and adaptive neural network control of uncertain nonlinear system." MA thesis. Zhejiang University of Technology, 2005.
- [189] Furuta K., Yamakita M., and Sato Y. "Computation of quadratic optimal control for linear retarded system." In: *Proceedings of the 26th IEEE Conference on Decision and Control*. Vol. 26. 1. Dec. 1987, pp. 2162–2167.
- [190] Buchheit K. H., Pandit M., and Befort M. "Optimal iterative learning control of an extrusion plant." In: *Proceedings of IEE International Conference of Control*. Vol. 1. Mar. 1994, pp. 652–657.
- [191] Tao T. M., Kosut R. L., and Aral G. "Learning feedforward control." In: *Proceedings of American Control Conference*. Vol. 3. 1994, pp. 2575–2579.
- [192] Hatzikos V., Haetoenen J., and Owens D. H. "Genetic algorithms in norm-optimal linear and non-linear iterative learning control." In: *International Journal of Control* 77.2 (2004), pp. 188–197.
- [193] Oh S. R., Bien Z., and Suh I. H. "An iterative learning control method with application to robot manipulators." In: *IEEE Journal of Robotics and Automation* 4.5 (1988), pp. 508–514.

Bibliography

- [194] Bone G. M. "A novel iterative learning control formulation of generalized predictive control." In: *Automatica* 31.10 (1995), pp. 1483–1487.
- [195] Amann N., Owens D. H., and Rogers E. "Predictive optimal iterative learning control." In: *International Journal of Control* 69.2 (1998), pp. 203–226.
- [196] Lee J. H., Lee K. S., and Kim W. C. "Model-based iterative learning control with a quadratic criterion for time-varying linear systems." In: *Automatica* 36 (2000), pp. 641–657.
- [197] Kim W. C. et al. "Analysis and reduced-order design of quadratic criterion-based iterative learning control using singular value decomposition." In: *Computers and Chemical Engineering* 24.8 (2000), pp. 1815–1819.
- [198] Kuc T. Y., Lee J. S., and Nam K. "An iterative learning control theory for a class of nonlinear dynamic systems." In: *Automatica* 28.6 (1992), pp. 1215–1221.
- [199] Amann N. et al. "An H-infinity approach to linear iterative learning control design." In: *International Journal of Adaptive Control and Signal Processing* 10.6 (1996), pp. 767–781.
- [200] Hou Z. S. and Xu J. X. "A new feedback-feedforward configuration for the iterative learning control of a class of discrete-time systems." In: *Acta Automatica Sinica* 33.3 (2007), pp. 323–326.
- [201] Togai M. and Yamano O. "Learning control and its optimality: analysis and its application to controlling industrial robots." In: *Proceedings of the 1986 IEEE International Conference on Robotics and Automation*. 1986.
- [202] Bien Z. and Hub K. M. "Higher-order iterative learning control algorithm." In: *IEE Proceedings of Control Theory and Applications*. 1989.
- [203] Chien C. J. and Liu J. S. "A P-type iterative learning controller for robust output tracking of nonlinear time-varying systems." In: *Proceedings of the American Control Conference*. June 1994.
- [204] Xu S. X. and Yang F. W. "Synthesis of an iterative learning controller for uncertain linear systems." In: *Control Theory and Applications* 19.4 (2002), pp. 650–652.

- [205] Wang D. "Analysis of convergence rate of iterative learning control algorithm." MA thesis. Shenyang University of Technology, 2006.
- [206] Heinzinger G. et al. "Stability of learning control with disturbances and uncertain initial conditions." In: *IEEE Trans on Automatic Control* 37.1 (1992), pp. 110–114.
- [207] Chen Y. et al. "An iterative learning controller with initial state learning." In: *IEEE Trans on Automatic Control* 44.2 (1999), pp. 371–376.
- [208] Lee H. S. and Bien Z. "Study on robustness of iterative learning control with non-zero initial error." In: *International Journal of Control* 64.3 (1996), pp. 345–359.
- [209] Ren X. M. and Gao W. B. "Learning control with an arbitrary initial state." In: *Acta Automatica Sinica* 20.1 (1994), pp. 74–79.
- [210] Lee H. S. and Bien Z. "A note on convergence property of iterative learning controller with respect to sup norm." In: *Automatica* 33.8 (1997), pp. 1591–1593.
- [211] Sun M. X. and Wang D. W. "Sampled-data iterative learning control for nonlinear systems with arbitrary relative degree." In: *Automatica* 37.2 (2001), pp. 283–289.
- [212] Yao Z. S., Yang C. W., and Wang H. F. "A frequency-domain design method for iterative learning control in an arbitrary initial state." In: *Systems Engineering And Electronics* 25.2 (2003), pp. 214–215.
- [213] Geng Z., Carroll R., and Xie J. H. "Two-dimensional model and algorithm analysis for a class of iterative learning control systems." In: *International Journal of Control* 52.4 (1990), pp. 833–862.
- [214] Padieu F. and Su R. J. "An H-infinity approach to learning control systems." In: *International Journal of Adaptive Control and Signal Processing* 4.6 (1990), pp. 465–474.
- [215] Xie S. L., Tian S. P., and Xie Z. D. "Fast algorithm of iterative learning control based on geometric analysis." In: *Control Theory and Applications* 20.3 (2003), pp. 419–422.

Bibliography

- [216] Qu Z. H. et al. "A new learning control scheme for robots." In: *Proceedings of the 1991 IEEE International Conference on Robotics and Automation*. Apr. 1991.
- [217] Luca A. D. and Ulivi G. "Iterative learning control of robots with elastic joints." In: *Proceedings of the 1992 IEEE International Conference on Robotics and Automation*. May 1992.
- [218] Moon J. H., Doh T. Y., and Chung M. J. "An iterative learning control scheme for manipulators." In: *Proceedings of the 1997 IEEE/RSJ International Conference on Intelligent Robots and Systems*. 1997.
- [219] Pandit M. and Buchheit K. H. "Optimizing iterative learning control of cyclic production processes with application to extruders." In: *IEEE Trans on Control Systems Technology* 7.3 (1999), pp. 382–390.
- [220] Venugopal K. P., Sudhakar R., and Pandya A. S. "On-line learning control of autonomous underwater vehicles using feedforward neural networks." In: *IEEE Journal of Oceanic Engineering* 17.4 (1992), pp. 308–319.
- [221] Pang Z. X. and Li C. X. "Application of iterative PID controller in hydraulic system." In: *Chinese Journal of Mechanical Engineering* 37.4 (2001), pp. 103–105.
- [222] Yu S. J., Xu Z. Q., and Bai J. C. "Iterative learning compensation design for terminal voltage of power systems excitation controller." In: *Power System Protection and Control* 37.7 (2009), pp. 40–45.
- [223] Lee K. S., Bang S. H., and Chang K. S. "Feedback-assisted iterative learning control based on an inverse process model." In: *Journal of Process Control* 4.2 (1994), pp. 77–89.
- [224] Wu H. Y., Zhou Z. Y., and Xiong S. S. "D-type iterative learning control with application to FNS limb motion control system." In: *Control Theory and Applications* 13.3 (2001), pp. 410–413.
- [225] Yao Z. S. and Yang C. W. "The application of iterative learning control in ferment system of tobacco leaf." In: *Process Automation Instrumentation* 23.12 (2002), pp. 41–43.
- [226] Duan S. et al. "A closed-loop D-type iterative learning control for electro-hydraulic position servo systems with uncertainties." In: *ICROS-SICE International Joint Conference*. 2009.

- [227] Wang Y. L. et al. "Iterative learning control of electro-hydraulic position servo system." In: *International Conference on Systems and Informatics*. 2012.
- [228] Zheng J. M., Zhao S. D., and Wei S. G. "Iterative learning control for switched reluctance motor direct-drive electro-hydraulic position servo system." In: *International Conference on Computer and Automation Engineering*. 2009.
- [229] Grundelius M. and Bernhardsson B. "Constrained iterative learning control of liquid slosh in an industrial packaging machine." In: *Proceedings of the 39th IEEE Conference on Decision and Control*. Dec. 2000.
- [230] Lee T. H. et al. "Iterative learning control of permanent magnet linear motor with relay automatic tuning." In: *Mechatronics* 10 (2000), pp. 169–190.
- [231] Li X. Z., Jian L. K., and He Y. "Research and application of iterative learning control." In: *Machine Tool and Hydraulics* 6 (1997), pp. 3–5.
- [232] Lee K. S., Chin I. S., and Lee H. J. "Model predictive control technique combined with iterative learning for batch processes." In: *AIChE Journal* 45.10 (1999), pp. 2175–2187.
- [233] Lee J. J. and Lee J. W. "Design of iterative learning controller with VCR servo system." In: *IEEE Trans on Consumer Electronics* 39.1 (1993), pp. 13–24.
- [234] Yang D. R. et al. "Experimental application of a quadratic optimal iterative learning control method for control of wafer temperature uniformity in rapid thermal processing." In: *IEEE Transactions on Semiconductor Manufacturing* 16.1 (2003), pp. 36–44.
- [235] Zhang X. G. and Lin H. "Robustness analysis of open-closed-loop D-type iterative learning control algorithm for nonlinear systems with deviations on initial state." In: *IMACS Multiconference on Computational Engineering in Systems Applications*. Oct. 2006, pp. 1707–1711.
- [236] Yu S. J., Qi X. D., and Wu J. H. *Theory and Application of Iterative Learning Control*. China Machine Press, 2005.

Bibliography

- [237] Chen H. D. and Jiang P. "Adaptive iterative learning control for nonlinear systems with unknown high-frequency gain." In: *Control and Decision* 17 (2002), pp. 715–718.
- [238] Jiang P. and Chen H. D. "Iterative learning control of MIMO systems with less model knowledge." In: *Proceedings of the 2004 IEEE Conference on Robotics, Automation and Mechatronics*. Vol. 1. Dec. 2004, pp. 490–495.
- [239] Jiang P. and Chen H. D. "Nussbaum gain based iterative learning control for a class of multi-input multi-output nonlinear systems." In: *Proceedings of the 44th IEEE Conference on Decision and Control*. Dec. 2005, pp. 2439–2444.
- [240] Yu M., Wang J. S., and Xin H. H. and Qi D. L. "Output feedback adaptive iterative learning control for nonlinear discrete-time systems with unknown control directions." In: *51st IEEE Conference on Decision and Control*. Dec. 2012, pp. 4660–4665.
- [241] Wang W. "Inverse compensation and iterative learning control for nonlinear systems with hysteresis." MA thesis. Zhejiang Sci-Tech University, 2013.
- [242] Choi J. W. et al. "Control of ethanol concentration in a fed-batch cultivation of acinetobacter calcoaceticus RAG-1 using a feedback-assisted iterative learning algorithm." In: *Journal of Biotechnology* 49 (1996), pp. 29–43.
- [243] Li L. J., Poms U., and Thurner T. "Accurate position control of a servo-hydraulic test cylinder by iterative learning control technique." In: *Proceeding of 2014 UKSim-AMSS 8th European Modelling Symposium*. 2014, pp. 297–302.

Appendix

Appendix A.

Experimental Results of P-Type ILC Algorithm with Random Signal

In the experiment firstly the random signal is used as the setpoint signal directly so as to achieve the control results without ILC algorithm i.e. only an ordinary PI controller is used. Figure A.1 shows the experimental results which are the comparison between the desired output signal and the actual system output signal. Observing Figure A.1 one can find that the valve-controlled cylinder system with an ordinary PI controller reveals a significant difference between the desired output signal and the actual output signal which is not allowed in engineering.

Then the FDF-extended open-loop P-type ILC algorithm described by Eq. (6.39) is applied in the real world electro-hydraulic servo position control system with the learning parameters given by Eq. (7.1). The overall control structure is given by Figure 6.2. Moreover the cutoff frequency of the low-pass frequency domain filter is $f_c = 20$ Hz. Figure A.2 to Figure A.4 are the experimental results for it.

Figure A.2 shows the comparison of the desired output and actual output of the system after 20 iterations and Figure A.3 describes the relative error of the system output after 20 iterations. Observing Figure A.2 and Figure A.3 one can find that after 20 iterations the actual output curve of the system is almost coincident with the desired output one and the relative error of the system output is very small. Therefore with the FDF technology the convergence speed of the ILC algorithm remains satisfying. Moreover Figure A.4 proves the stability of the algorithm.

Appendix A. Experimental Results of P-Type ILC Algorithm with Random Signal

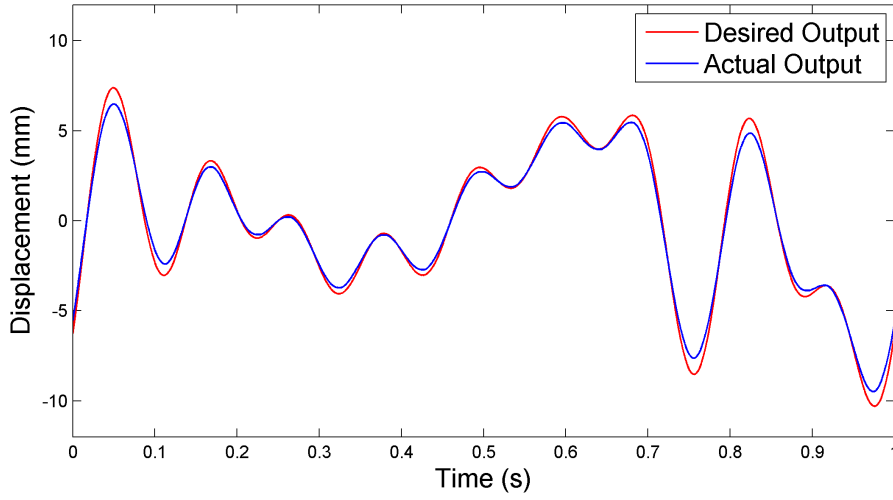


Figure A.1.: Comparison of the Desired Output and the Actual Output of the System without ILC Algorithm with Random Signal

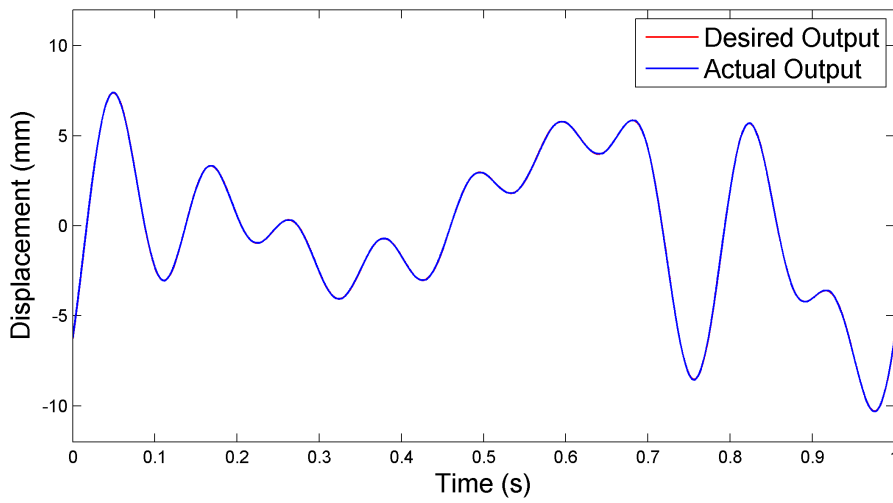


Figure A.2.: Comparison of the Desired Output and the Actual Output of the System with Open-Loop P-Type ILC Algorithm Based on FDF after 20 Iterations with Random Signal

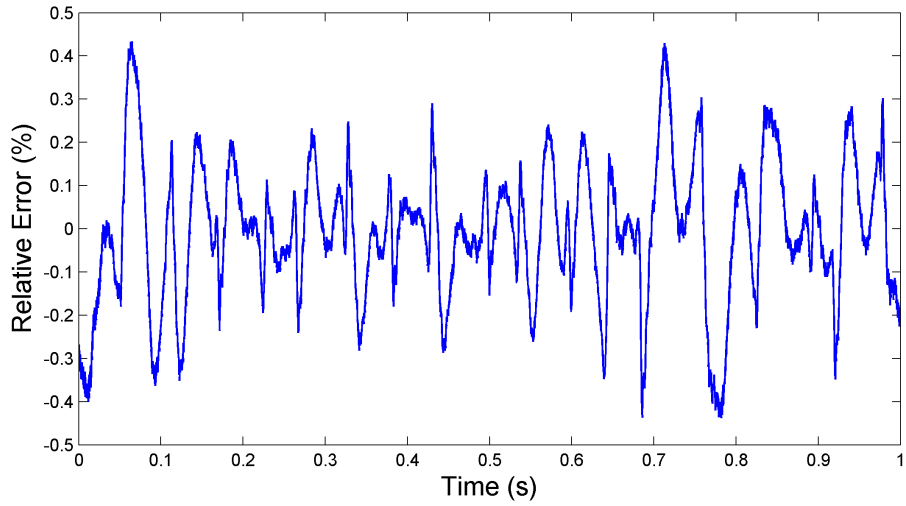


Figure A.3.: Relative Error of the System Output with Open-Loop P-Type ILC Algorithm Based on FDF after 20 Iterations with Random Signal

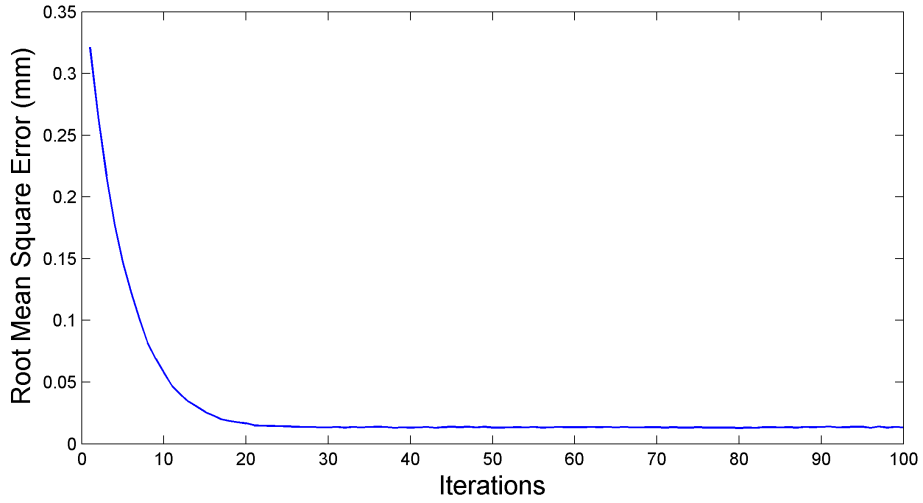


Figure A.4.: RMS Errors of the Control System Using Open-Loop P-Type ILC Algorithm Based on FDF with Random Signal

Appendix A. Experimental Results of P-Type ILC Algorithm with Random Signal

Appendix B.

Experimental Results of Adaptive ILC Algorithm with Random Signal

In the experiment firstly the random signal is used as the setpoint signal directly so as to achieve the control results without ILC algorithm i.e. only an ordinary PI controller is used. Figure B.1 shows the experimental results which are the comparison between the desired output signal and the actual system output signal. Observing Figure B.1 one can observe that the valve-controlled cylinder system with an ordinary PI controller reveals a significant difference between the desired output signal and the actual output signal which is not allowed in engineering.

Then the adaptive ILC algorithm with the Nussbaum type gain given by Eq. (6.47) to Eq. (6.49) is applied in the real world electro-hydraulic servo position control system. Figure 6.3 shows the overall control structure of the algorithm. Figure B.2 to Figure B.4 are the experimental results for it.

Figure B.2 represents the comparison of the desired output and actual output of the system after 20 iterations and Figure B.3 represents the relative error of the system output after 20 iterations. Note from Figure B.2 and Figure B.3 that after 20 iterations the actual output curve of the system is almost coincident with the desired output one and the relative error of the system output is very small. Hence the convergence speed of the adaptive ILC algorithm is satisfying. Furthermore Figure B.4 proves the stability of the algorithm.

Appendix B. Experimental Results of Adaptive ILC Algorithm with Random Signal

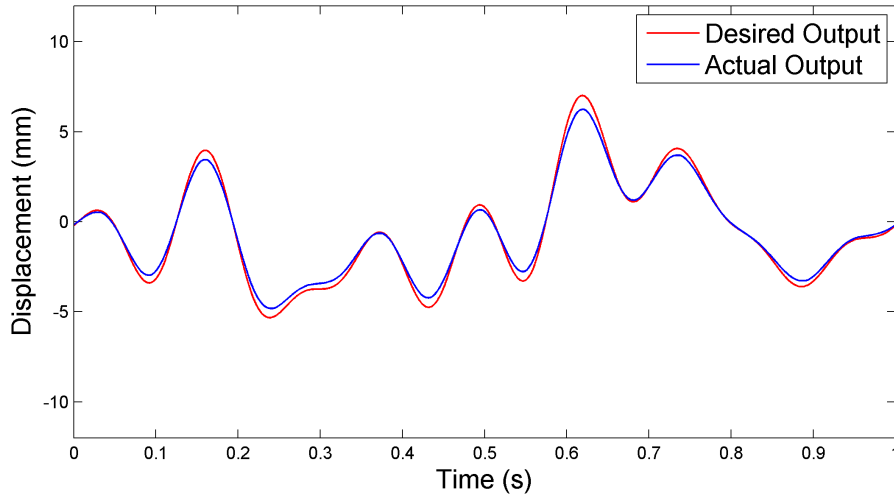


Figure B.1.: Comparison of the Desired Output and the Actual Output of the System without ILC Algorithm with Random Signal

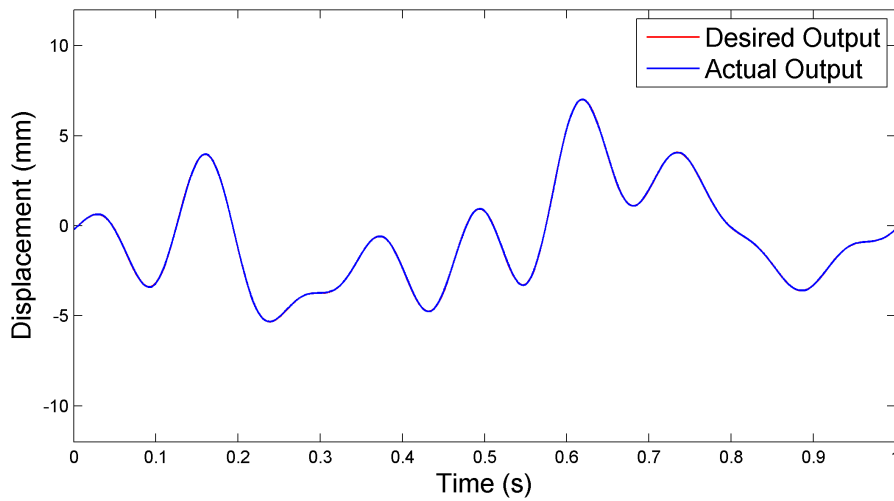


Figure B.2.: Comparison of the Desired Output and the Actual Output of the System with Adaptive ILC Algorithm after 20 Iterations with Random Signal

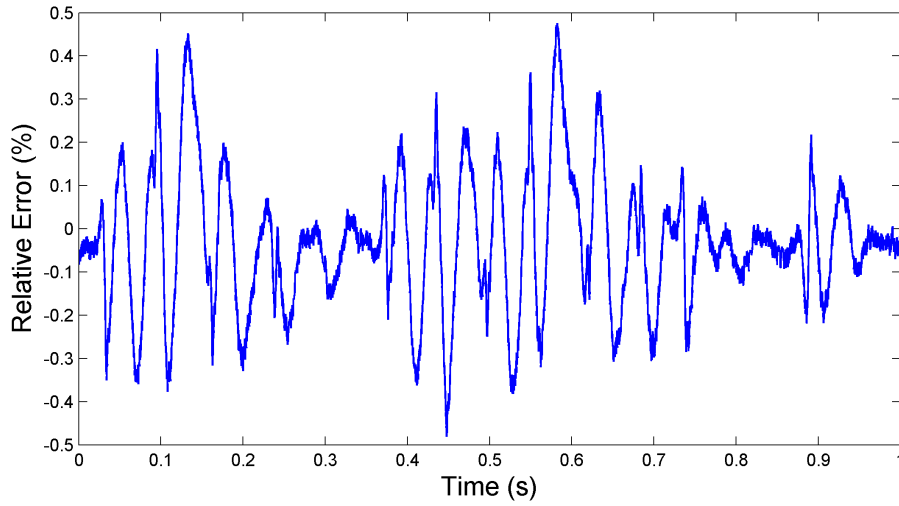


Figure B.3.: Relative Error of the System Output with Adaptive ILC Algorithm after 20 Iterations with Random Signal

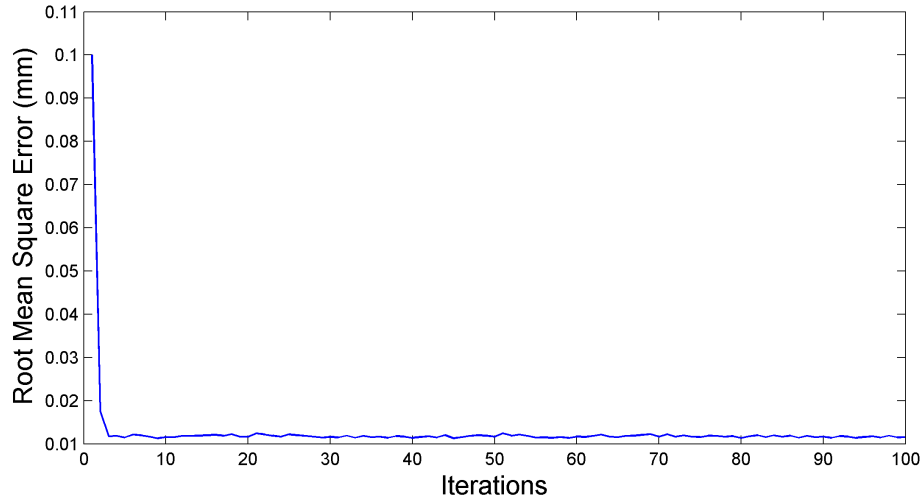


Figure B.4.: RMS Errors of the Control System Using Adaptive ILC Algorithm with Random Signal

Appendix B. Experimental Results of Adaptive ILC Algorithm with Random Signal

Appendix C.

Experimental Results of Inverse Model ILC Algorithm with Random Signal

In the experiment firstly the random signal is used as the setpoint signal directly so as to achieve the control results without ILC algorithm i.e. only an ordinary PI controller is used. Figure C.1 shows the experimental results which are the comparison between the desired output signal and the actual system output signal. Observing Figure C.1 one can observe that the valve-controlled cylinder system with an ordinary PI controller reveals a significant difference between the desired output signal and the actual output signal which is not allowed in engineering.

Then the inverse model ILC algorithm described by Eq. (6.65) is applied in the real world electro-hydraulic servo position control system. Figure 6.4 shows the overall control structure of the algorithm. Figure C.2 to Figure C.4 are the experimental results for it.

Figure C.2 shows the comparison of the desired output and actual output of the system after 20 iterations and Figure C.3 shows the relative error of the system output after 20 iterations. Observing Figure C.2 and Figure C.3 one can find that after 20 iterations the actual output curve of the system is almost coincident with the desired output one and the relative error of the system output becomes very small. Consequently the convergence rate of the inverse model ILC algorithm is good. Additionally Figure C.4 proves the stability of the algorithm.

Appendix C. Experimental Results of Inverse Model ILC Algorithm with Random Signal

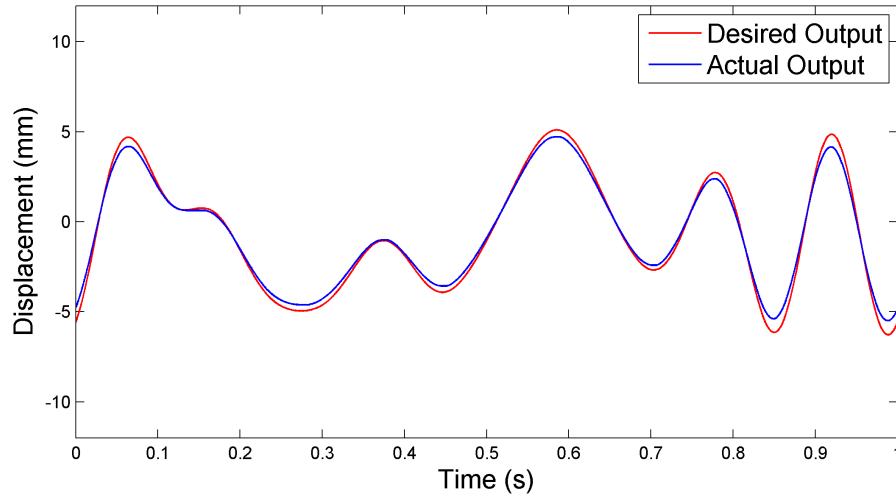


Figure C.1.: Comparison of the Desired Output and the Actual Output of the System without ILC Algorithm with Random Signal

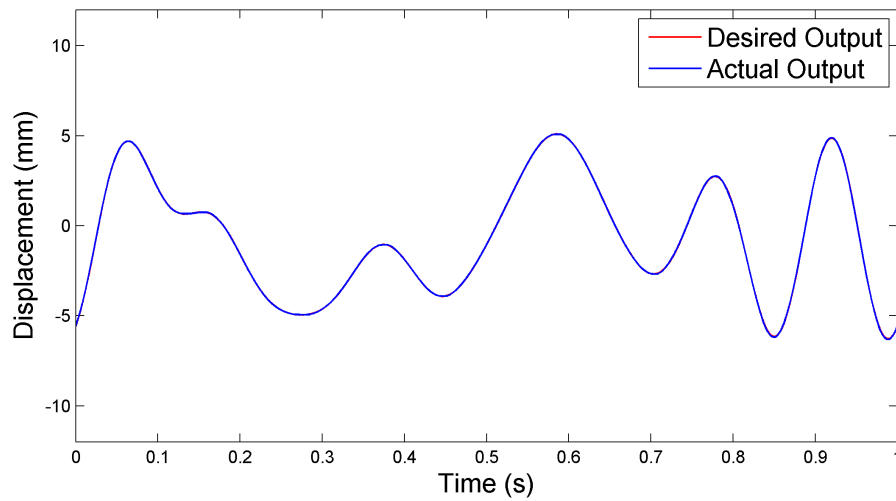


Figure C.2.: Comparison of the Desired Output and the Actual Output of the System with Inverse Model ILC Algorithm after 20 Iterations with Random Signal

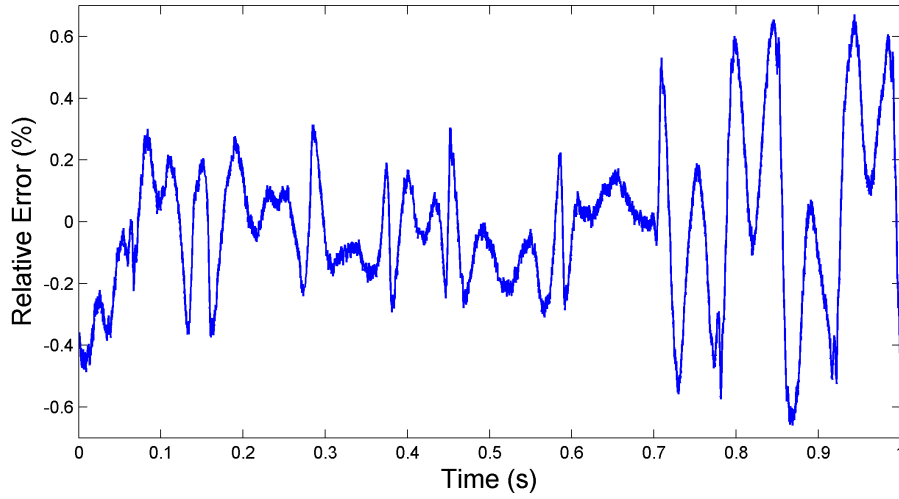


Figure C.3.: Relative Error of the System Output with Inverse Model ILC Algorithm after 20 Iterations with Random Signal

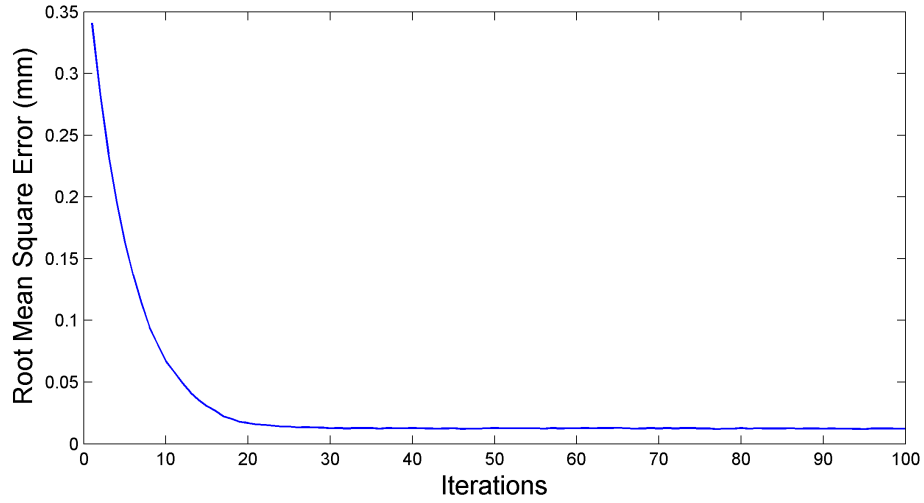


Figure C.4.: RMS Errors of the Control System Using Inverse Model ILC Algorithm with Random Signal